Vol. 268, No. 2, October 16, 1992
Completing Volume 268

ISSN 0003-2670

# ANALYTICA CHIMICA ACTA

An international journal devoted to all branches of analytical chemistry



ELSEVIER

# ANALYTICA CHIMICA ACTA

**Scope.** *Analytica Chimica Acta* publishes original papers, preliminary communications and reviews dealing with every aspect of modern analytical chemistry. Reviews are normally written by invitation of the editors, who welcome suggestions for subjects. Preliminary communications of important urgent work can be printed within four months of submission, if the authors are prepared to forego proofs.

**Submission of Papers**

*Americas*

Prof. Harry L. Pardue
Department of Chemistry
1393 BRWN Bldg, Purdue University
West Lafayette, IN 47907-1393
USA
Tel:(+1-317) 494 5320
Fax:(+1-317) 496 1200

*Computer Techniques*

Prof. J.T. Clerc
Universität Bern
Pharmazeutisches Institut
Baltzerstrasse 5, CH-3012 Bern
Switzerland
Tel:(+41-31) 654171
Fax:(+41-31) 654198

*Other Papers*

Prof. Alan Townshend
Department of Chemistry
The University
Hull HU6 7RX
Great Britain

Tel:(+44-482) 465027
Fax:(+44-482) 466410

Prof. Willem E. van der Linden
Laboratory for Chemical Analysis
Department of Chemical Technology
Twente University of Technology
P.O. Box 217, 7500 AE Enschede
The Netherlands
Tel:(+31-53) 892629
Fax:(+31-53) 356024

Prof. Paul Worsfold
Dept. of Environmental Sciences
University of Plymouth
Plymouth PL4 8AA
Great Britain

Tel:(+44-752) 233006
Fax:(+44-752) 233009

Submission of an article is understood to imply that the article is original and unpublished and is not being considered for publication elsewhere. *Anal. Chim. Acta* accepts papers in English only. There are no page charges. Manuscripts should conform in layout and style to the papers published in this issue. See inside back cover for "Information for Authors".

**Publication**. *Analytica Chimica Acta* appears in 14 volumes in 1993. The subscription price for 1993 (Vols. 267–280) is Dfl. 4214.00 plus Dfl. 462.00 (p.p.h.) (total approx. US$ 2817.00). *Vibrational Spectroscopy* appears in 2 volumes in 1993. The subscription price for *Vibrational Spectroscopy* (Vols. 4 and 5) is Dfl. 700.00 plus Dfl. 66.00 (p.p.h.) (total approx. US$ 461.50). The price of a combined subscription (*Anal. Chim. Acta* and *Vib. Spectrosc.*) is Dfl. 4592.00 plus Dfl. 528.00 (p.p.h.) (total approx. US$ 3084.25). All earlier volumes (Vols. 1–266) except Vols. 23 and 28 are available at Dfl. 259.50 (US$ 156.25), plus Dfl. 18.00 (US$ 11.00) p.p.h., per volume. The Dutch guilder price is definitive. The U.S. dollar price is subject to exchange-rate fluctuations and is given only as a guide. Subscriptions are accepted on a prepaid basis only, unless different terms have been previously agreed upon.
Our p.p.h. (postage, packing and handling) charge includes surface delivery of all issues, except to subscribers in the U.S.A., Canada, Australia, New Zealand, China, India, Israel, South Africa, Malaysia, Thailand, Singapore, South Korea, Taiwan, Pakistan, Hong Kong, Brazil, Argentina and Mexico, who receive all issues by air delivery (S.A.L.–Surface Air Lifted) at no extra cost. For Japan, air delivery requires 25% additional charge of the normal postage and handling charge; for all other countries airmail and S.A.L. charges are available upon request.

**Subscription orders**. Subscription orders can be entered only by calendar year and should be sent to: Elsevier Science Publishers B.V., Journals Department, P.O. Box 211, 1000 AE Amsterdam, The Netherlands. Tel: (+31-20) 5803 642, Telex: 18582, Telefax: (+31-20) 5803598, to which requests for sample copies can also be sent. Claims for issues not received should be made within three months of publication of the issues. If not they cannot be honoured free of charge. Readers in the U.S.A. and Canada can contact the following address: Elsevier Science Publishing Co. Inc., Journal Information Center, 655 Avenue of the Americas, New York, NY 10010, U.S.A. Tel: (+1-212) 6333750, Telefax: (+1-212) 6333990, for further information, or a free sample copy of this or any other Elsevier Science Publishers journal.
**Advertisements**. Advertisement rates are available from the publisher on request.

**Detailed "Instructions to Authors"** for *Analytica Chimica Acta* was published in Volume 256, No. 2, pp. 373–376. Free reprints of the "Instructions to Authors" of *Analytica Chimica Acta* and *Vibrational Spectroscopy* are available from the Editors or from: Elsevier Science Publishers B.V., P.O. Box 330, 1000 AH Amsterdam, The Netherlands. Telefax: (+31-20) 5862845.

**US mailing notice – Analytica Chimica Acta** (ISSN 0003-2670) is published biweekly by Elsevier Science Publishers (Molenwerf 1, Postbus 211, 1000 AE Amsterdam). Annual subscription price in the USA US$ 2555.25 (subject to change), including air speed delivery. Application to mail at second class postage rate is pending at Jamaica, NY 11431. *USA Postmasters*: Send address changes to Anal. Chim. Acta, Publications Expediting, Inc., 200 Meacham Av., Elmont, NY 11003. Airfreight and mailing in the USA by Publication Expediting.

# ANALYTICA CHIMICA ACTA

An international journal devoted to all branches of analytical chemistry

*(Full texts are incorporated in CJELSEVIER, a file in the Chemical Journals Online database available on STN International; Abstracted, indexed in: Aluminum Abstracts; Anal. Abstr.; Biol. Abstr.; BIOSIS; Chem. Abstr.; Curr. Contents Phys. Chem. Earth Sci.; Engineered Materials Abstracts; Excerpta Medica; Index Med.; Life Sci.; Mass Spectrom. Bull.; Material Business Alerts; Metals Abstracts; Sci. Citation Index)*

VOL. 268 NO. 2 CONTENTS OCTOBER 16, 1992



*(Continued overleaf)*

*Contents (continued)*

*Analytica Chimica Acta*, 268 (1992) 195–204
Elsevier Science Publishers B.V., Amsterdam



# Determination of atrazine and simazine in estuarine samples by high-resolution gas chromatography and nitrogen selective detection

M. Ahel

*Center for Marine Research Zagreb, Institute Rudjer Boskovic, P.O. Box 1016, Zagreb (Croatia); and Marine Organic Chemistry Group IRP3, Plymouth Marine Laboratory, PL1 3DH Plymouth (UK)*

K.M. Evans, T.W. Fileman and R.F.C. Mantoura

*Marine Organic Chemistry Group IRP3, Plymouth Marine Laboratory, PL1 3DH Plymouth (UK)*

(Received May 21st 1992)

**Abstract**

A method for the determination of ultra trace concentrations of triazine herbicides in natural water using silica $C_{18}$ solid-phase extraction (SPE) and high-resolution gas chromatography with nitrogen-selective detection (GC-NPD) has been developed and optimized for estuarine conditions. Recoveries of spiked dissolved simazine and atrazine at a concentration of 100 ng $l^{-1}$ were 82–85% and 87–97%, respectively and were only slightly affected by the range of salinities and pH encountered for estuarine samples. The sediment-bound (particulate) triazines were ultrasonically extracted with high recoveries (86–91%) using dichloromethane. The water sample extracts were analysed without any additional clean up whereas the sediment extracts were purified using miniature silica gel columns. Nitrogen selective detection provided interference-free detection of simazine and atrazine in the extracts. The detection limits for simazine and atrazine in water and sediment were 1 ng $l^{-1}$ for 1 l of water and 5 ng $g^{-1}$ 200 mg of suspended sediments. The reproducibility of the determination of atrazine and simazine in real water samples at low ng $l^{-1}$ concentrations as shown by %R.S.D., was better than 10%. A comparison of the GC-NPD determination with an alternative method using ion selective detection (GC-ITD) showed very good agreement and indicated superior (ca. 5 fold) sensitivity of the NPD. The method was applied to a study of triazine herbicides in estuarine waters of the Rivers Tamar, Thames and Mersey.

*Keywords:* Gas chromatography; Atrazine; Estuarine samples; Simazine

The *s*-triazines are a diverse family of herbicides which have been used in vast quantities ($> 34.5 \times 10^6$ and $0.7 \times 10^6$ kg year$^{-1}$ in US and UK respectively) as the principal agrochemical control of broadleaf and grassy weeds, in croplands, on roads and on railways [1–3]. As a consequence of their application and relatively high water solubility, the triazines are widely distributed in aquatic environments, including groundwater, rivers, lakes, estuaries and rain [4–8].

A wide variety of analytical methods have been developed for the determination of the triazine herbicides in various environmental samples [4–20]. Most of these methods represent a combination of an enrichment procedure, including either solvent extraction [5,7,9,15–17] or solid-phase ex-

*Correspondence to:* R.F.C. Mantoura, Plymouth Marine Laboratory, Prospect Place, Plymouth PL1 3DH (UK).

traction (SPE) [4,6,9–13], with subsequent chromatographic analysis. Several liquid chromatographic (LC) techniques have been proposed for the specific determination of different triazine herbicides [12–15]. However in the majority of publications on triazine herbicides in the aquatic environment, capillary gas chromatography (GC) seems to be the method of choice [4–7,9–11,16,17]. Both nitrogen selective (NPD) [7–11] and mass-selective detectors [4,5,16,17] provide sufficient selectivity and sensitivity for triazine determinations in the ng $l^{-1}$ range. Recently, relatively simple and elegant immunoassay methods [18–20] have also become available for the collective determination of triazine herbicides. These can be regarded as a tool for rapid screening if large samples sets are to be analysed.

Since estuaries feature steep gradients of both pollutant concentrations and physicochemical characteristics, such as salinity, turbidity, and pH, these must be carefully considered when developing methods of analysis for trace organic pollutants in estuarine samples. This is particularly true for partially ionizable species, like triazine herbicides, whose distribution in different environmental compartments could be significantly influenced by the estuarine master variables. This paper describes a method for the SPE extraction and GC-NPD analysis of trace concentrations (1–100 ng $l^{-1}$) of simazine and atrazine optimized for estuarine water and sediments.

## EXPERIMENTAL

### *Sample collection and storage*

Estuarine water samples were collected in February–August 1991 at several sites in the Tamar, Thames and Mersey estuaries. Sampling was performed using a special sampling device fitted with a 2.5-l glass bottle which allowed collection of samples at different depths. Samples were analysed either immediately upon return to the laboratory or were stored in a cold room for a maximum of 24 h. Sediment samples were collected manually on the mudflats in the Tamar estuary. The sediments were wrapped in aluminium foil and kept frozen (−20°C) until analysis. Before extraction, all sediments were freeze dried.

### *Chemicals*

Reference triazine compounds including atrazine, simazine, propazine, prometryn, terbutryn, ametryn and prometon were obtained from Supelco (triazines kit, cat. No. 4-9092; purity > 98%) (Saffron Walden). Terbuthylazine, desethyl- and deisopropylatrazine were obtained from Greyhound (Birkenhead). Stock solutions of 0.1–1 mg $ml^{-1}$ were prepared in toluene. A series of calibration solutions for GC-NPD and GC-ITD analyses in the range of 5 pg $\mu l^{-1}$ to 10 ng $\mu l^{-1}$ were prepared in ethyl acetate or dichloromethane (DCM) by diluting the stock solutions. All solvents used for the analyses (DCM, toluene, ethyl acetate, diethyl ether) were high purity grades such as glass distilled (Rathburn, Walkerburn) and Distol (Fisons, Loughborough). Anhydrous sodium sulphate and silica gel 40 were purchased from BDH Merck (Eastleigh). Distilled, deionized water for laboratory Model experiments was taken from a Milli-Q Water System (Millipore, Watford).

### *Sample preparation and analysis*

Prior to analysis, water samples were filtered through glass fibre filters (Whatman, GF/F). The filters were stored in scintillation vials (20 ml) and were kept deep-frozen until analysis. Further treatment of the particulate samples on filters was identical to that for sediment analysis.

The pH value of the filtrate was checked and, if necessary, adjusted to between 8.0 and 8.5 with potassium hydroxide. The dissolved triazine herbicides were enriched on Sep-Pak $C_{18}$ silica cartridges (0.3 g; part No. 51910, Waters, Milford, MA) as previously described by Hileman [6]. Sep-Pak cartridges were preconditioned with 5 ml DCM followed by 5 ml methanol. 1 l of filtered water sample was passed through the cartridge at a flow-rate of approximately 20 ml $min^{-1}$ under a positive nitrogen pressure. The analytes were desorbed from the cartridge into clean vials with 4 ml of DCM and the extract was dried by percolation through a DCM-prewashed column (2–3 g) of anhydrous sodium sulphate. After application

of the extract, the triazine herbicides were quantitatively recovered with up to 3 ml DCM and evaporated under a stream of $N_2$ to a 100–200 $\mu$l volume.

Freeze-dried estuarine sediments (typically 200–500 mg) and particulate matter collected on the filters were ultrasonically extracted twice by ultrasonication for 15 min in 5 ml of DCM. Before extraction, the glass fibre filters were macerated with a stainless-steel spatula in order to improve contact with the extracting solvent. Extraction of the filters was carried out in the vials previously used for their storage. The extraction vial contents were centrifuged at 1431 *g* using 15-ml glass tubes. The extract was separated from the sediment by Pasteur pipette and transferred into a clean vial. Further procedures were identical to that described for water extracts.

Prior to the GC analysis, an internal standard (terbuthylazine or prometryn) was added to the

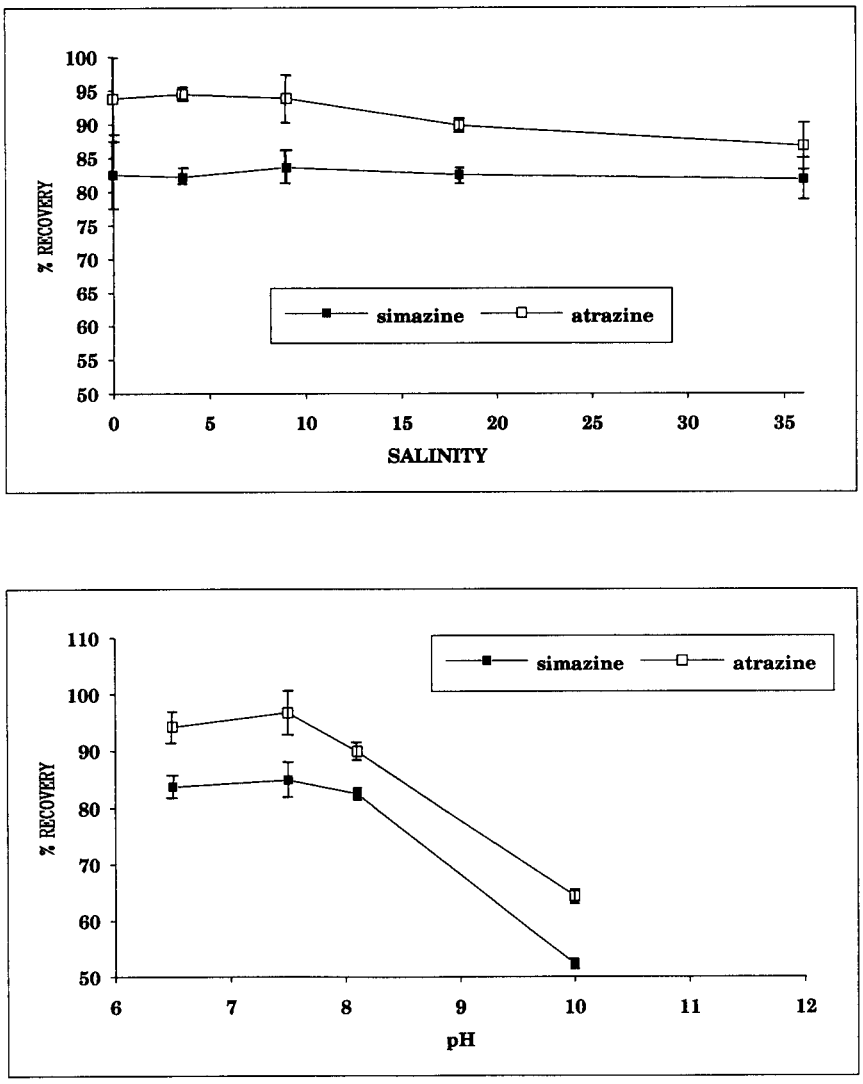


Fig. 1. The recovery and reproducibility of the determinations of simazine and atrazine in estuarine water in relation to salinity (‰) (pH 8.1) and pH (salinity 18‰).

extracts in a quantity corresponding to the expected analyte concentration.

*Extract purification*

An additional clean-up step was necessary for organically rich sediment extracts but was omitted for most of the water sample extracts. A modified procedure [1], using a silica minicolumn was applied. Briefly, 0.5 g of silica gel deactivated with 3% deionized water was put into a Pasteur pipette and pre-washed with DCM. The extract, contained in approximately 5 ml DCM, was introduced onto the adsorption column and the eluant discarded. The column was washed with 1 ml of *n*-hexane and this fraction was also discarded. The triazines were eluted with 4 ml diethyl ether or, alternatively, ethyl acetate. Prior to GC analysis the purified extracts were evaporated down to 100–200 $\mu$l under a stream of nitrogen.

*Equipment*

Triazine determinations were carried out using a Hewlett Packard 5890 gas chromatograph equipped with an on-column injector and thermionic detector. The gas chromatograph was fitted with a fused-silica capillary column (25 m $\times$ 0.32 mm i.d.) containing a 0.5-$\mu$m bonded phase of HP-5 (Hewlett Packard). Helium was used as a carrier gas at a linear velocity of 25–30 cm $s^{-1}$. Typically, 1-$\mu$l aliquots of the standard solutions or sample extracts were injected into the gas chromatograph. The column temperature was programmed from 70 to 250°C at 5°C $min^{-1}$ and the detector operated at 280°C. Throughout the study, standard solution at concentrations of 50 and 100 pg $\mu l^{-1}$ were analysed daily in order to check the instrument condition (response factors) and the chromatographic behaviour (retention times, peak shapes, and separation) of the triazine herbicides.

Structural identifications and confirmations were achieved using a Carlo Erba gas chromatograph (Mega HRGC) coupled to a Finnigan Mat 700 ion trap detector. The gas chromatographic column (25 m $\times$ 0.2 mm i.d., 0.17-$\mu$m bonded phase HP-5) was coupled directly to the ITD through a short (40 cm), straight transfer line (280°C). The gas chromatographic conditions were very similar to those described above for GC-NPD determinations.

Qualitative analyses were done by comparing retention times and the mass spectra of the analytes with those of authentic standards which had been run under the same GC-ITD conditions. Quantitative determinations of the triazine herbicides using GC-ITD were obtained from the chromatograms acquired in scan mode (mass range 45–300 daltons). However, reconstructed selected ion chromatograms were used to determine the peak areas of the analytes and of the internal standard (prometryn). The ions *m/e* 201, 200 and 241 were chosen for the quantitative determination of simazine, atrazine and prometryn, respectively.

## RESULTS AND DISCUSSION

*Recovery, reproducibility and determination limit*

The influence of salinity on the determination of simazine and atrazine at the trace concentration of 100 ng $l^{-1}$ is presented in Fig. 1. As can be seen, variation of salinity in the range of 0 to 36‰ has no significant influence on the recovery and reproducibility of the triazine herbicide determination. The recoveries of simazine and atrazine varied in the narrow ranges of 8.18–83.6% and 86.7–94.4%, respectively. The recoveries of dealkylated atrazine derivatives were lower than 20%, thus the applied enrichment procedure was not suitable for the determination of triazine degradation products. The lower recovery of the dealkylated atrazines and simazine compared to atrazine can be explained by their lower lipophilicities, i.e., lower breakthrough volumes. Indeed, Thurman et al. [4] have shown that the 10% breakthrough capacity of Sep-Pak $C_{18}$ cartridges for simazine (1200 ml) was significantly lower than that for atrazine (2000 ml). In addition, these breakthrough capacities were determined at a flow-rate of 4 ml $min^{-1}$, compared to approximately 20 ml $min^{-1}$ applied in our study. According to supplier's instructions obtained with the cartridges the breakthrough capacity is expected to decrease at higher flow-rates. This would explain the somewhat lower recoveries of

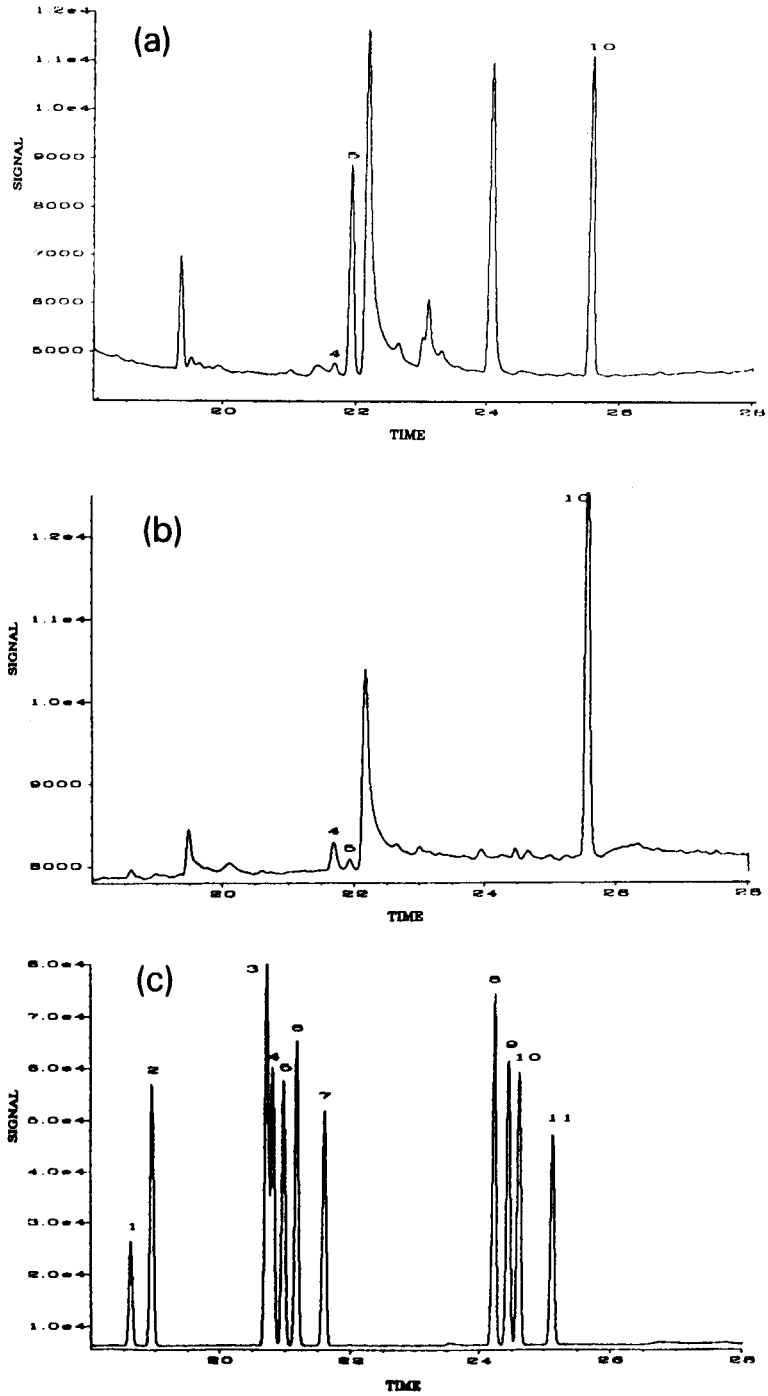


Fig. 2. Gas chromatograms of triazine herbicides: (a) dissolved triazines from the Tamar estuary, (b) particulate triazines from the Tamar estuary, (c) a standard solution containing 100 ng $ml^{-1}$ of each of the following compounds: desisopropyl atrazine (1), desethyl atrazine (2), prometon (3), simazine (4), atrazine (5), propazine (6), terbuthylazine (7), simetryn (8), ametryn (9), prometryn (10) (I.S.) and terbutryn (11).

triazines in our study obtained from 1-l samples compared to the Thurman's results obtained from the samples of 100 ml. This slightly lower recovery at a flow-rate of 20 ml $min^{-1}$ seems to be an acceptable disadvantage as the resulting benefit is a significant reduction of the time needed for extraction.

The influence of pH on the determination of the dissolved triazine herbicides was examined at a medium estuarine salinity of 18‰ (Fig. 1). The recoveries of simazine (82.5–84.9%) and atrazine (89.8–96.8%) were high and varied only slightly in the range of pH values expected in estuarine conditions (6.5–8.5). Therefore, the adjustment of the pH to 8–8.5 prior to percolation through the Sep-Pak $C_{18}$ cartridge could be omitted for estuarine water samples. However, recoveries were found to be significantly lower at pH 10 (52.3 and 64.4%, respectively).

Reproducibility of the triazine determination in model water samples (100 ng $l^{-1}$), expressed as the relative standard deviation (R.S.D.) of replicate analyses (Fig. 1), was better than 5%. Similarly, good reproducibilities (R.S.D. < 10%) were obtained for the replicate analyses of natural estuarine samples which contained trace concentrations of dissolved simazine (3.3–30.9 ng $l^{-1}$) and atrazine (14.1–229 ng $l^{-1}$) (Table 1). Although, as expected, better reproducibilities were achieved for the higher concentration range, the method proved to be satisfactorily precise for determinations in the lowest concentration range of 1–10 ng $l^{-1}$.

High recoveries (85.5 and 90.9%) were obtained when analysing sediment samples spiked with simazine and atrazine at trace concentrations (77 and 120 ng $g^{-1}$, respectively) (Table 1). Taking into account common problems with the preparation of a homogeneous model sediment sample, the achieved reproducibilities of 9.8 and 9.0% should be considered fairly good. All real sediment samples from the Tamar estuary examined so far contained no detectable concentrations (< ng $g^{-1}$) of simazine and atrazine. Therefore, the reproducibility of the triazine herbicide determination in real sediments is not presented.

Determination limits of the triazine herbicides, accepting a signal-to-noise ratio of 3, were 1 ng $l^{-1}$ and 5 ng $g^{-1}$ based on 1 l of water and 200 mg of sediment, respectively.

TABLE 1

Reproducibility of the determination of simazine and atrazine in estuarine samples at ultra trace concentrations and sediments [a]

| | | Simazine | Atrazine |
|---|---|---|---|
| Tamar, 23.9 km [b] | $X$ (ng $l^{-1}$) | 3.3 | 14.1 |
| | $S$ (ng $l^{-1}$) | 0.3 | 0.8 |
| | R.S.D. (%) | 9.3 | 5.9 |
| | $n$ | 4 | 4 |
| Tamar, 27.8 km [b] | $X$ (ng $l^{-1}$) | 16.8 | 229 |
| | $S$ (ng $l^{-1}$) | 0.9 | 2.8 |
| | R.S.D. (%) | 5.0 | 1.2 |
| | $n$ | 2 | 2 |
| Tamar, 3.6 km [b] | $X$ (ng $l^{-1}$) | 2.8 | 8.8 |
| | $S$ (ng $l^{-1}$) | 0.2 | 1.6 |
| | R.S.D. (%) | 7.1 | 18.1 |
| | $n$ | 3 | 3 |
| Tavy [c] | $X$ (ng $l^{-1}$) | 30.9 | 37.1 |
| | $S$ (ng $l^{-1}$) | 1.9 | 1.7 |
| | R.S.D. (%) | 6.1 | 4.6 |
| | $n$ | 3 | 3 |
| Sediment | $X$ (ng $l^{-1}$) | 65.8 | 109.1 |
| | $S$ (ng $l^{-1}$) | 6.5 | 9.8 |
| | R.S.D. (%) | 9.8 | 9.0 |
| | $n$ | 6 | 6 |
| | Recovery | 85.5 | 90.9 |

[a] Freeze-dried sediment (9 g) from the Tamar estuary was spiked with simazine and atrazine at the concentrations of 77 ng $g^{-1}$ and 120 ng $g^{-1}$, respectively; 200-mg aliquots of the spiked sediment sample were extracted using an ultrasonic bath. $X$ = Mean triazine concentration. $S$ = Standard deviation of triazine concentrations. [b] Figures in km denote distances from the weir for the stations where the water samples were collected; 1-l subsamples were analysed. [c] Water sample was collected on the station at Denham Bridge; 0.5-l subsamples were analysed.

*Separation and interferences*

The thermionic detector is widely accepted as a very suitable detector for the determination of nitrogen-rich triazine herbicides owing to its high sensitivity and selectivity for nitrogen [8–10,22] but it does not provide a structural identification of the analytes like mass spectrometry [4–6,16,17]. Therefore, one of the most important prerequisites for successful analysis using NPD is an efficient separation of the analytes from interfering

compounds, including other members of the same class of chemicals and other, chemically completely different, organic compounds. Fig. 2 presents the chromatograms of a triazine herbicide mixture (Fig. 2a), a water sample extract from the Tamar estuary (Fig. 2b), and a sediment extract from the Tamar estuary (Fig. 2c). As can be seen, almost baseline resolution can be achieved using a 25-m HP-5 fused-silica column (film thickness 0.5 $\mu$m) for most of the selected herbicides. The only overlapping peaks were prometon and simazine. However, real water sample extracts obtained for different UK rivers have shown that of many possible triazines only simazine and atrazine were present at detectable concentrations ($> 1$ ng $l^{-1}$). This observation was confirmed by examining selected extracts by GC-ITD. This fact reduced the problem of triazine herbicide determination to the two critical representatives. The applied quantities of simazine and atrazine, with annual consumption figures for UK being several hundred tons, exceed by far the quantity of any other triazine herbicide [23]. Therefore, simazine and atrazine are the only triazines on the UK red list of toxic compounds [24,25].

The chromatographic pattern of the samples obtained, for the investigated UK estuaries influenced our choice of internal standard (I.S.) Deuterated triazines, which appear to be ideal internal standards for GC-MS determinations [6,16], are not applicable for GC-NPD determinations because they co-elute with the normal triazines. The most convenient choice was therefore another triazine, which is not used in the area being investigated. For example, Perreira and Rostad [5] have used terbuthylazine as an I.S. At the beginning of our study we applied the same I.S., but an unidentified, partially co-eluting non-triazine peak observed in some extracts prevented accurate quantification. Prometryn was later found to elute in the part of chromatogram virtually free from interferences ($<$ ng $l^{-1}$) and this was adopted as our I.S.

As can be seen from the chromatogram of the water extract (Fig. 2b), several other peaks are apparent in addition to simazine and atrazine. Most of these peak were not ultimately identified, but it was shown that some of them came from the solvent. The most inconvenient contamination was that which co-eluted with propazine (equivalent concentration 20–50 ng $l^{-1}$). We were not able to positively identify this interference, but a comparison of its responses by NPD and MS (total ion current) detection suggested that it might contain nitrogen or phosphorus. No interference with simazine and atrazine at levels beyond 1 ng $l^{-1}$ was observed. Peaks which were positively identified in the extracts were phthalate esters, the most common laboratory contaminants.

Large unidentified peaks which appeared in the higher boiling point region of the chromatogram (not presented in Fig. 2) could be compounds which were hydrolytically released from the $C_{18}$ cartridges as suggested by Thurman et al. [4].

The extracts obtained during the enrichment procedure were virtually colourless indicating that triazine herbicides could be fairly selectively recovered from $C_{18}$ silica cartridges in the presence of other more polar materials, such as humics, using dichloromethane as an eluent. This allowed direct injection of such extracts onto the GC column without any additional clean-up. No significant deterioration of the GC column was observed as a consequence of injections of non-purified extracts, even after up to 100 injections. Distortion of the simazine and dealkylated atrazine peak shapes was used as an indicator of a deteriorating capillary column. Any problems of this kind were solved by occasionally cutting the first 30 cm of the fused-silica column.

*Comparison between GC-NPD and GC-ITD*

The comparison of GC-NPD and GC-ITD techniques for the determination of simazine and strazine in real samples proved that GC-NPD can be considered an accurate, interference-free analytical technique (Table 2). Relatively good agreement was obtained for determinations in the low and in the high concentration ranges. However, the sensitivity of NPD ($<$ 10 pg of the triazine injected) is more than five times higher than the sensitivity of ITD. Consequently, the determination of triazine herbicides in the lowest concen-

TABLE 2

Dissolved and particulate triazine herbicides in the Tamar and Thames estuaries [a]

| Station and date | Dissolved [b] | | Particulate [b] | |
|---|---|---|---|---|
| | Simazine | Atrazine | Simazine | Atrazine |
| Tamar, April 22, 1991 | | | | |
| 1 | 2.8 | 6.0 | < 0.5 | < 0.5 |
| 2 | 3.3 | 8.0 | < 0.5 | < 0.5 |
| 3 | 3.3 | 8.4 | < 0.5 | < 0.5 |
| 4 | 3.3 | 11.3 | < 0.5 | < 0.5 |
| 5 | 2.1 | 11.8 | < 0.5 | < 0.5 |
| 6 | 2.0 | 9.7 | < 0.5 | < 0.5 |
| Thames, June 26, 1991 | | | | |
| 1 | 42 | 22 | < 0.5 | < 0.5 |
| 2 | 270 | 150 | 1.0 | 0.5 |
| 3 | 400 | 260 | 1.0 | 0.5 |
| 4 | 590 | 410 | 1.2 | 0.6 |
| 5 | 910 | 560 | 2.0 | 0.9 |
| 6 | 1240 | 400 | 3.3 | 1.0 |
| 7 | 1250 | 460 | 3.7 | 1.0 |
| 8 | 1080 | 350 | 2.9 | 1.1 |
| 9 | 1210 | 380 | 3.2 | 0.9 |

[a] Determined by GC-NPD. [b] Concentration in ng $l^{-1}$.

tration range (1–5 ng $l^{-1}$) was possible only using NPD.

*Application*

The presented method is being successfully applied to the study of the estuarine behaviour of triazine herbicides with special emphasis on their partition between the dissolved and particulate phases. Some of the results obtained in the Tamar and Thames estuaries are presented in Table 2. As can be seen the concentrations of the dissolved triazines vary widely. The triazine concentrations in the Tamar were far below the suggested admissible limits for drinking water (100 ng $l^{-1}$) [26] but those in the Thames were up to 15 times higher. The concentrations of particle-bound triazines (expressed as concentration in the original water sample) were very low, from < 0.5 ng $l^{-1}$ in the Tamar to 3.7 ng $l^{-1}$ in the Thames. The relative contributions of particulate triazines (< 1% of the total) suggested that adsorption might play only a minor role in the distribution of these compounds throughout estuaries, even if the particle load is expected to be as high as several hundred mg $l^{-1}$ [21]. This fact allows an estimation of the input of triazine herbicides into coastal seas via river discharges by analysing the dissolved triazines only, as indicated previously by Pereira and Rostad [5], which reduces the necessary analytical effort in such studies. However, filtration of estuarine water sample is a necessary step in the analytical procedure using Sep-Pak $C_{18}$ enrichment, because 1 l of a non-filtered turbid sample cannot be easily passed through the cartridge.

Figure 3 shows typical axial concentration profiles of atrazine and simazine for the Tamar

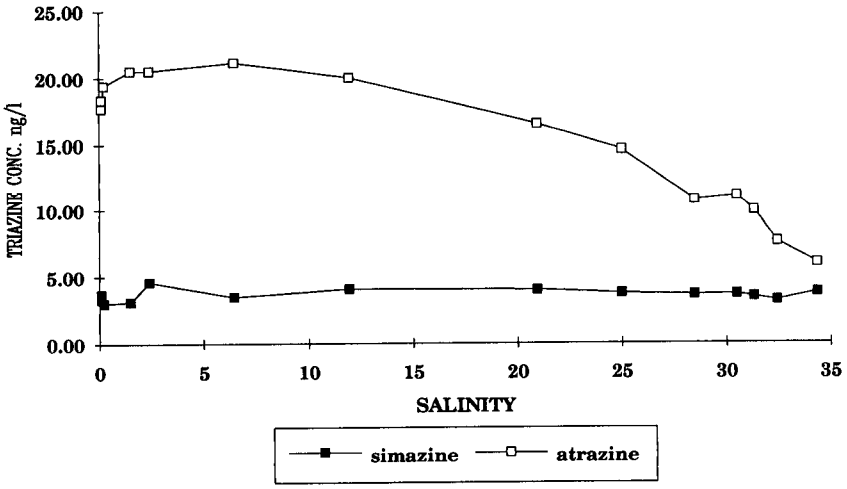


Fig. 3. Distributions of dissolved simazine and atrazine in the Tamar estuary, May 1991.

TABLE 3

Comparison of the determination of triazine herbicides in estuarine samples by GC-NPD and GC-ITD [a]

| Station and date [c] | GC-NPD [b] | | GC-ITD [b] | |
|---|---|---|---|---|
| | Simazine | Atrazine | Simazine | Atrazine |
| Tamar, June 13, 1991 | | | | |
| 31 km | 4 | 19 | < 5 | 15 |
| 8 km | 7 | 75 | < 5 | 68 |
| 6.7 km | 6 | 67 | < 5 | 70 |
| 3.8 km | 7 | 49 | < 5 | 55 |
| 2.5 km | 7 | 40 | 6 | 35 |
| 0 km | 8 | 45 | 9 | 53 |
| Tamar, June 20, 1991 | | | | |
| 31 km | 2 | 7 | < 5 | 9 |
| 28 km | 3 | 19 | < 5 | 12 |
| 23.9 km | 5 | 31 | < 5 | 32 |
| 18.4 km | 5 | 36 | < 5 | 44 |
| 12 km | 6 | 38 | 10 | 39 |
| Thames, June 26, 1991 | | | | |
| 1 | 42 | 22 | 33 | 22 |
| 2 | 270 | 150 | 220 | 160 |
| 3 | 400 | 260 | 350 | 310 |
| 4 | 590 | 410 | 590 | 500 |
| 5 | 910 | 560 | 770 | 490 |
| 6 | 1240 | 400 | 1090 | 380 |
| 7 | 1250 | 460 | 1160 | 550 |
| 8 | 1080 | 350 | 970 | 350 |
| 9 | 1210 | 380 | 1010 | 430 |
| Mersey, August 13, 1991 | | | | |
| 1 | 250 | 260 | 220 | 280 |
| 2 | 1040 | 930 | 1160 | 1110 |
| 3 | 66 | 55 | 74 | 49 |

[a] Determinations from the same sample extracts (ng $l^{-1}$). [b] Concentrations of the dissolved triazines in ng $l^{-1}$. [c] Distances in km denote positions of the sampling stations.

estuary. The distribution shows a characteristic maximum, the position of which depends upon seasonally variable inputs and hydrodynamic conditions (governed principally by the tidal regime and the river flow). The vertical distribution of atrazine and simazine shows, as expected, a decrease of triazine concentration with depth. The difference between the surface and bottom concentrations is, however, relatively small (35–26 ng $l^{-1}$ atrazine; 6–5 ng $l^{-1}$ simazine) which indicates efficient vertical mixing of the water column, even in the deepest part of the estuary. It should be pointed out that these concentration variations were observed at concentration levels below 10 ng $l^{-1}$, which suggests very good performance of the analytical method in the extremely low concentration range.

*Conclusion*

The method using enrichment on the Sep-Pak $C_{18}$ cartridges and gas chromatography with nitrogen-selective detection (GC-NPD) can be regarded as an attractive alternative to GC–MS based methods [4–6,16,17] for the determination of triazine herbicides in natural waters. The method is fairly precise and accurate in the low ng $l^{-1}$ range and shows superior sensitivity to GC–ITD. When analysing 1-l water samples, which allows determination down to 1 ng $l^{-1}$, the limiting factor for the sample throughput is the enrichment step (about 5–7 samples per day, per system). Consequently, the analysis time can be significantly reduced if the concentrations of the analytes in the particular environment are known to be in the higher ng $l^{-1}$ range by reducing the required sample volume accordingly. Another limitation of the proposed method is its inability to analyse the triazine degradation products concurrently with the parent compounds. The most promising alternative for such a purpose would be the mixed bed solid-phase extraction [12] or liquid–liquid extraction [15] coupled with reversed-phase liquid chromatography [12,15].

This work forms part of Plymouth Marine Laboratory's Project IRP3, funded by the National River Authority (contract (A4/107). We thank the staff at the NRA Northwest and Thames regions who assisted with sample collection from the Mersey and Thames estuaries. EC fellowship to Dr. M. Ahel is also gratefully acknowledged. We also thank Dr. M. Gough (NRA, Southern Region Labs., Waterlooville, Hampshire) in the early phase of this work.

REFERENCES

1 B. Hileman, Environ. Sci. Technol., 16 (1982) 645A–650A.
2 F. Frank and G.J. Sirons, Sci. Total Environ., 12 (1979) 223–239.

3 US Environmental Protection Agency, Report Nos. EPA/600/x-84/330 and EPA/600/x-84/233.
4 E.M. Thurman, M. Meyer, M. Pomes, C.A. Perry and A.P. Schwab, Anal. Chem., 62 (1990) 2043–2048.
5 W.E. Pereira and C.E. Rostad, Environ. Sci. Technol., 24 (1990) 1400–1406.
6 H.-R. Buser, Environ. Sci. Technol., 24 (1990) 1049–1058.
7 T.L. Wu, Water Air Soil Pollut., 15 (1981) 173–184.
8 R.P. Richards, J.W. Kramer, D.B. Baker and K.A. Krieger, Nature, 327 (1987) 129–131.
9 T.R. Steinheimer and M.G. Brooks, Int. J. Environ. Anal. Chem., 17 (1984) 97–111.
10 P.C. Bardalaye and W.B. Wheeler, Int. J. Environ. Anal. Chem., 25 (1986) 105–113.
11 T.G. Kreindl, H. Malissa and K. Winsauer, Mikrochim. Acta, I/1–2 (1986) 1–13.
12 M. Battista, A. Di Corcia and M. Marchetti, Anal. Chem., 61 (1989) 935–939.
13 K.A. Ramsteiner, J. Chromatogr., 465 (1989) 410–416.
14 J.N. Sieber, D.E. Glotfelty, A.D. Lucas, M.M. McChesney, J.C. Sagebiel and T.A. Wehner, Arch. Environ. Contam. Toxicol., 19 (1990) 583–592.
15 D. Barcelo, G. Durand and J. Albaiges, in G. Angeletti and A. Bjoerseth (Eds.), Organic Micropollutants in the Aquatic Environment, Kluwer, Dordrecht, 1991, pp. 132–141.
16 V. Lopez-Avila, P. Hirata, S. Kraska, M. Flanagan, J.H. Taylor, Jr. and S.C. Hern, Anal. Chem., 57 (1985) 2797–2801.
17 W.E. Pereira, C. Rostad and T.J. Leiker, Anal. Chim. Acta, 228 (1990) 69–75.
18 R.J. Bushaway, B. Perkins, S.A. Savage, S.J. Lekousi and B.S. Ferguson, Bull. Environ. Contam. Toxicol., 40 (1988) 647–654.
19 K.S. Goh, J. Hernandez, S.J. Powell and C.D. Greene, Bull. Environ. Contam. Toxicol., 45 (1990) 208–214.
20 L. Weil, R.J. Schneider, O. Schaefer, P. Ulrich, M. Weller, T. Rupert and R. Niessner, Fresenius' J. Anal. Chem., 339 (1991) 468–469.
21 A.W. Morris, R.F.C. Mantoura, A.J. Bale and R.J.M. Howland, Nature, 274 (1978) 678–680.
22 C.J. Miles, K. Yanagihara, S. Ogata, G. Van De Verg and R. Boesch, Bull. Environ. Contam. Toxicol., 44 (1990) 955–962.
23 M. Fielding, S. Gibby and K. Moore, in G. Angeletti and A. Bjoerseth (Eds.), Organic micropollutants in the aquatic environment, Kluwer, Dordrecht, 1991, pp. 142–162.
24 Commission of European Communities, Communication from the Commission to the Council on Dangerous Substances which might be included in the List 1 of the Council Directive 76/464/EEC, Official Journal C176, 14 July, 1982.
25 A.R. Agg and T.F. Zabel, J. Inst. Water Environ. Management, 4 (1990) 44–50.
26 EEC Drinking Water Guideline, 80/778/EEC, EEC No. L229/11-29, August 30th, 1980.

*Analytica Chimica Acta*, 268 (1992) 205–215
Elsevier Science Publishers B.V., Amsterdam



# Coupled column liquid chromatography for the trace determination of polar pesticides in water using direct large-volume injection: method development strategy applied to methyl isothiocyanate

E.A. Hogendoorn and C. Verschraagen

*Laboratory of Organic Analytical Chemistry, National Institute of Public Health and Environmental Protection (RIVM), P.O. Box 1, 3720 BA Bilthoven (Netherlands)*

U.A.Th. Brinkman

*Department of Analytical Chemistry, Free University, De Boelelaan 1083, 1081 HV Amsterdam (Netherlands)*

P. van Zoonen

*Laboratory of Organic Analytical Chemistry, National Institute of Public Health and Environmental Protection (RIVM), P.O. Box 1, 3720 BA Bilthoven (Netherlands)*

(Received 29th January 1992)

**Abstract**

The potential of coupled column liquid chromatography (LC) for the trace determination of a single polar compound by direct large-volume injection of aqueous samples was studied and a general approach to method development for this class of compound is discussed. As a new application, the determination of methyl isothiocyanate (MITC) by means of reversed-phase (RP) LC column switching and UV detection at 237 nm is reported. With direct injection of 770-$\mu$l samples, the detection limit is 1 $\mu g\, l^{-1}$ and the time of analysis is about 10 min. For a further increase in selectivity and detectability (down to a level of about 0.1 $\mu g\, l^{-1}$), a rapid liquid–liquid extraction followed by an organic–aqueous phase switch on a silica cartridge is required prior to RPLC. No residues of MITC were found in over 200 surface water samples investigated.

*Keywords:* Liquid chromatography; Methyl isothiocyanate; Pesticides; Waters

Reversed-phase column liquid chromatography (RPLC) can be used to determine small amounts of polar organic compounds in (environmental) water samples. An important advantage of RPLC in conjunction with aqueous samples is that the low eluotropic strength of water allows the injection of large sample volumes. However, when working with highly polar analytes, problems are encountered. Retention is small even on highly hydrophobic $C_{18}$-bonded silica phases and, as a result trace enrichment becomes difficult and only a limited separation capacity is available to separate the analyte(s) from early eluting interferences, which are always present in environmental samples.

*Correspondence to:* P. van Zoonen, Laboratory of Organic Analytical Chemistry, National Institute of Public Health and Environmental Protection (RIVM), P.O. Box 1, 3720 BA Bilthoven (Netherlands).

In recent papers, RPLC column switching with UV detection using two essentially equivalent separation columns was used for the sensitive and selective determination of the polar analytes chloroallyl alcohol [1] and ethylenethiourea [2] in ground water samples. With trial and error optimization, column-switching procedures were developed to assay the analytes at a level of 1 $\mu g\ l^{-1}$ in water samples by direct large-volume injection. The analysis time from sample introduction to chromatographic peak is less than 10 min, which makes this technique very attractive for screening purposes. The above column-switching RPLC procedure appears to have high potential for rapid trace analyses for individual polar analytes. Relevant aspects of column-switching optimization for the determination of moderately polar pesticides have been reviewed [3]. When dealing with a single polar analyte and the strongly varying polar matrix interferences of environmental samples, application of the rational column-switching optimization procedure with chromatogram simulation [4] does not appear to be suitable. However, on the basis of the experimental experience gained in previous studies [1,2], it should be possible to develop a generally applicable strategy. Therefore, it was the main aim of this study to summarize the most important column-switching parameters and to propose and test a procedure for method development.

To confirm the suitability of the proposed procedure, it was applied to the determination of methyl isothiocyanate (MITC) in ground and surface water samples. MITC is a soil fumigant, applied prior to planting crops; it controls soil fungi, nematodes, weed seeds and soil insects. Generally, a formulation of 30–50% aqueous solution of metam-Na (sodium methylcarbamodithioate) is used. In an aqueous environment the salt degrades rapidly to gaseous MITC, which possesses the pesticidal action. MITC is also the main metabolite (active compound) of the pesticide Dazomet (3,5-dimethyl-1,3,5-thiadiazinane-2-thione), which is also converted rapidly into MITC after application.

Because of the volatility of MITC (1733 Pa, 20°C), gas chromatography (GC) with flame photometric detection is often used for its determination [5–9]. The isolation and concentration of MITC can be performed (off-line) by means of extractive distillation into a small volume of ethyl acetate [5,6] or with a purge and trap capillary GC system either fully [7,8] or semi [9] on-line. MITC and metam-Na have been determined by means of RPLC with UV detection at 247 nm in pond water and sewage effluents [10], the limit of detection being claimed to be 1 $\mu g\ l^{-1}$ for MITC. Unfortunately, the recovery data and chromatograms in the quoted paper relate only to MITC levels $> 200\ \mu g\ l^{-1}$

## EXPERIMENTAL

### *Chemicals*

Methyl isothiocyanate (MITC; content > 99.5%) was obtained from Dr. S. Ehrenstorfer (Promochem, Wesel, Germany). A 1000 $\mu g\ ml^{-1}$ stock solution of MITC was prepared in acetonitrile. For LC analysis the stock solution was diluted in LC-grade water and kept in a refrigerator at 4°C. Acetone (Nanograde), acetonitrile (LC Grade S) and 2,2,4-trimethylpentane (isooctane; LC grade) were from Promochem, Rathburn (Walkburn, UK) and J.T. Baker (Deventer, Netherlands), respectively. Sodium chloride was from Merck (Darmstadt). LC-grade water was obtained by purifying demineralized water in a Milli-Q system (Millipore, Bedford, MA). Acetonitrile–water (40–45 + 60–55, v/v) was used as the first mobile phase (M-1) and acetonitrile–water (50 + 50, v/v) as the second mobile phase (M-2). Disposable 1-ml SPE cartridges containing 100 mg of silica gel (40 $\mu m$) were from J.T. Baker. The cartridges were conditioned before use with 1 ml of acetone followed by 3 ml of isooctane.

### *Equipment*

A Baker-10 system (J.T. Baker) was used for solid-phase extraction. For liquid–liquid extraction a shaking machine capable of handling simultaneously twenty 50-ml bottles with screw-caps and PTFE-laminated septa was used.

The LC system consisted of a Gilson (Villiers-le-Bel, France) Model 232 autosampler equipped

with two Type 7010 high-pressure switching valves from Rheodyne (Berkeley, CA) for injection and column switching, and two Model 305 isocratic pumps and a Model 116 variable-wavelength UV–visible detector from Gilson. A 50 × 4.6 mm i.d. column packed with 3-$\mu$m Microspher $C_{18}$ (Chrompack, Middelburg, Netherlands) or a 50 × 4.6 mm i.d. column packed with 7-$\mu$m Hypercarb (Shandon, Astmoor, UK) was used as the first (C-1) separation column. A 100 × 4.6 mm i.d. cartridge column packed with 3-$\mu$m Microspher $C_{18}$ was used as the second column (C-2). If a Microspher $C_{18}$ packed column was used as C-1, a 10 × 3 mm i.d. RP guard column (Chrompack) was placed in front of it and replaced weekly.

*Direct determination of MITC*

The mobile phases, M-1 (40% acetonitrile) and M-2 (50% acetonitrile), were both adjusted to a flow-rate of 1 ml/min. A 770-$\mu$l water sample was injected on to C-1 (packed with 3-$\mu$m Microspher $C_{18}$). After clean-up with 1.7 ml of M-1 (injection volume included), C-1 was switched on-line with C-2 for 24 s to transfer the MITC-containing fraction (with 0.40 ml of M-2) to C-2. The retention time of MITC on C-2 was about 2.4 min. Quantification of MITC was done by peak-height comparison with the UV response at 237 nm of an equal volume of MITC in LC-grade water.

*Determination of MITC after extraction and phase switching*

A 50-ml water sample was added to a screw-cap red bottle containing 18 g of sodium chloride. After the addition of 3.0 ml of isooctane the bottle was closed and shaken mechanically (horizontal position) for 15 min. The organic phase was poured over a small funnel containing anhydrous sodium sulphate and collected in a tube. A 1.0-ml volume of isooctane extract was pipetted on to a (preconditioned) 100-mg silica cartridge, the vacuum being released from the Baker-10 system when the liquid reached the top of the silica packing material. The procedure was repeated for another 1.0 ml of the same isooctane extract on a fresh cartridge. Next, 1.0 ml of water was brought on to each cartridge and passed through the cartridges into a tube by applying an over-pressure using a syringe placed on top of the cartridges. The combined aqueous solutions were filtered (0.45 $\mu$m) into an autosampler vial. After capping, a 1-ml loop injection from this solution was made on to C-1 (packed with 7-$\mu$m Hypercarb) with a mobile phase (M-1) of 45% acetonitrile (1 ml/min). The flow-rate of M-2 (50% acetonitrile) of the second column was set at 0.9 ml/min. After clean-up with 2.0 ml of M-1 (injection volume included), C-1 was switched on-line with C-2 for 30 s for the transfer of the MITC-containing fraction (with 0.45 ml of M-2) to C-2.

## RESULTS AND DISCUSSION

*General approach*

From previous studies [1,2], it appeared that the successful LC determination of a highly polar organic compound in an environmental aqueous sample requires sufficient preseparation between the analyte and the UV-absorbing ionic species, e.g., anions and humic acids, always present in relatively high concentrations, on C-1 (selectivity), and the introduction of a relatively large sample volume into the chromatographic system without causing unacceptable band broadening (sensitivity). The attainable selectivity and sensitivity of a column-switching LC procedure depends on the nature of the analyte and the selection of suitable conditions for a number of LC parameters. Based on the results acquired [1,2], a scheme of method development (Fig. 1) was derived consisting of a number of steps which will be discussed below.

*Step 1.* The applicable UV absorption [wavelength ($\lambda$) and molar absorbtivity ($\epsilon$)] and the retention of the analyte from pure water on to the $C_{18}$-type stationary phase largely determine the sensitivity and selectivity that can be obtained. In our experience (also see below), with insufficient UV–visible absorption and selectivity ($\epsilon \lesssim 1000$ l mol$^{-1}$ cm$^{-1}$ and $\lambda < 200$ nm) and/or an essential absence of retention on a $C_{18}$-bonded phase ($k' \lesssim 1$), the successful development of a column-switching LC procedure for trace-level analysis becomes highly unlikely.

*Step 2.* Column C-1 must provide sufficient

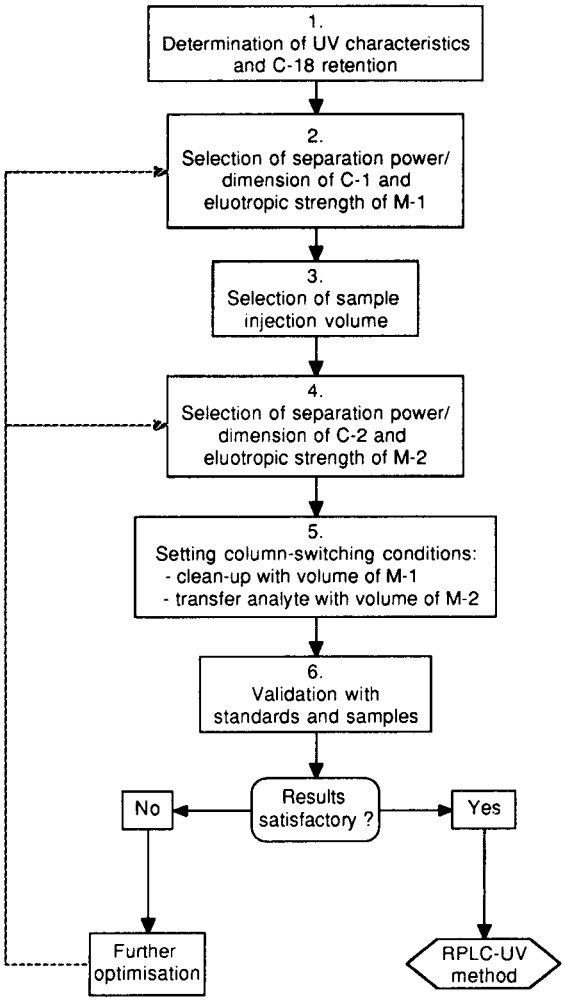


Fig. 1. Scheme of column-switching RPLC method development.

separation to remove a major part of the abundantly available early-eluting ionic matrix constituents prior to elution of the analyte. Therefore, a column with relatively high separation power will usually be necessary. In order to optimize both sensitivity (sample load) and selectivity (separation power) the use of 4.6 mm i.d. columns packed with small particles ($d_p < 10$ $\mu$m) is favourable. An unnecessary increase in separation power and dimensions of the column must be avoided; the peak elution volume, which is inversely proportional to the sensitivity of detection of the analyte, should be kept as low as possible. An increase in the column dimensions will also increase the reconditioning time (if necessary) of column C-1 between analyses.

In order to suppress the band broadening of the analyte on C-1 during injection of large volumes of water samples, the eluotropic strength of the mobile phase (M-1) should be high. In general, an eluotropic strength of M-1 should be selected such that the capacity factor of the analyte is in the range of 1–3, rendering a clean-up volume of at least twice the dead volume of the column ($V_0$) to remove a large part of the excess of early-eluting interferences.

Step 2 should also be used to improve the selectivity by selecting the proper column packing material, organic modifier and/or buffer.

*Step 3.* Having adjusted the separation power of C-1 and, even more important, the eluotropic strength of M-1, the maximum allowable sample injection volume is determined. Owing to the small $C_{18}$ retention of a polar compound, focusing of the analyte at the top of the column is impossible, and band broadening rapidly starts to increase with increasing injection volume.

In general, the start of peak deformation of the analyte on injection on to C-1 is selected as a criterion for the maximum allowable injection volume.

*Step 4.* It is preferable to select a column C-2 possessing a higher separation power than C-1. This will provide some flexibility when optimizing the eluotropic strength of M-2 in order to reach a proper compromise between the required separation efficiency on the second column and the desired peak compression (sensitivity of detection). Actually, there will probably be a limited choice because of the expected poor retention of the analyte of interest.

*Step 5.* With the selected parameter values, the final column-switching conditions are easily found by connecting C-1 directly with the UV detector. With M-1 as mobile phase, the volumes to be used for clean-up and transfer can be read from the chromatogram obtained on injecting a standard solution. The volume of M-1 emerging from C-1 until the analyte starts to elute is the maximum volume that can be used for clean-up; the peak volume of the analyte (as recorded at the

baseline), in principle, is the minimum volume to be used for transferring the analyte from C-1 to C-2.

*Step 6.* Finally, the overall procedure is used to analyse real water samples. Of course, depending on the type of water sample and the site of sampling, the concentration and nature of the ionic and/or highly polar interferences can vary considerably. Such problems have indeed been encountered, viz., in the determination of ethylenethiourea (ETU) in various types of ground water [2]. In such a case, the parameters of step(s) 2 and/or 4 must be re-adjusted. In our experience, increasing the separation power of column C-1 is most efficient.

*RPLC column-switching method for MITC*

In order to test the applicability of the above strategy, the trace-level determination of MITC in ground and surface water samples was studied.

*Step 1.* On 5-$\mu$m Hypersil ODS and with pure water as the mobile phase, MITC has $k' = 20$. The UV absorption spectrum of MITC shows maxima at 205 nm ($\epsilon = 4500$ l mol$^{-1}$ cm$^{-1}$) and 237 nm ($\epsilon = 3000$ l mol$^{-1}$ cm$^{-1}$). As generally detection selectivity is improved at higher UV wavelengths, 237 nm was selected for detection. The low UV absorbance of MITC indicates a main problem, lack of sensitivity. Therefore, the selection of the next parameters will be focused on maximizing the sensitivity.

*Step 2.* The high retention of MITC on $C_{18}$-bonded silica will provide sufficient preseparation between the analyte and the early-eluting interferences. Hence, the selection of a column with a low separation power as C-1 looks attractive from the point of view of the speed of analysis (clean-up on and reconditioning of C-1). However, a column with a high separation power in combination with a mobile phase of higher eluotropic strength allows the injection of larger volumes of water samples.

In order to study the elution behaviour of MITC, 50–60 mm × 4.6 mm i.d. columns packed with highly hydrophobic packing materials ($C_{18}$-bonded silica or porous graphitic carbon) were used. Acetonitrile was preferred to methanol as modifier, because with the same capacity factors of MITC, the peak volumes of the analyte turned out to be smaller. Based on the test results summarized in Table 1, a 50 × 4.6 mm i.d. 3-$\mu$m Microspher column was selected as C-1 because of the high analyte retention. A mobile phase of acetonitrile–water (40 + 60, v/v) was chosen as M-1 providing an adequate retention of about $k' = 2.5$. The potential of a Hypercarb column, which had been successfully applied to the determination of ETU [11], was also studied. Hypercarb, which has a higher hydrophobicity than (and a different retention behaviour to) $C_{18}$-bonded silicas, is an attractive material when selectivity has to be improved.

TABLE 1

Retention of MITC on various highly hydrophobic columns [a]

| Packing material | Column length (mm) | $d_p$ ($\mu$m) | $k'$ | Number of plates ($N$) |
|---|---|---|---|---|
| Hypersil ODS | 60 | 5 | 2.6 | 1900 |
| Hypersil ODS | 60 | 3 | 2.6 | 2400 |
| Microspher $C_{18}$ | 50 | 3 | 2.8 | 2200 |
| Hypercarb | 50 | 7 | 2.1 | 1350 |

[a] Injection volume, 540 $\mu$l; mobile phase, acetonitrile–water (40+60, v/v) at 1 ml min$^{-1}$; column i.d. 4.6 mm in all instances.

*Step 3.* In earlier work, 200-$\mu$l sample injections resulted in detection limits of 1 $\mu$g l$^{-1}$ for both ETU ($\epsilon = 18000$ l mol$^{-1}$ cm$^{-1}$ detected at 233 nm) and chloroallyl alcohol (CAAL) ($\epsilon =$ 10000 l mol$^{-1}$ cm$^{-1}$ detected at 205 nm) in water samples. Considering the low $\epsilon$ value of MITC, about a fivefold higher injection volume is required to obtain the same sensitivity here. To determine the maximum allowable injection volume, sample volumes ranging between 100 and 2000 $\mu$l and containing 920 ng of MITC were injected on to a 50 × 4.6 mm I.D. column packed with 3-$\mu$m Microspher or 7-$\mu$m Hypercarb using acetonitrile–water (40 + 60, v/v) as the mobile phase. The results in Table 2 show that on increasing the sample volume on Microspher the MITC peak height starts to decrease rapidly while the peak volume increases. Volumes above about 700–800 $\mu$l causes excessive band broadening, as illustrated in Fig. 2. On Hypercarb the peak volume remains constant up to an injection vol-

ume of about 600 μl, while 1000 μl of sample can be loaded on this material without excessive band broadening of the MITC peak. The results indicate that using the selected parameter values for C-1 and M-1 (see above), about 750 μl is the maximum allowable injection volume.

*Steps 4 and 5.* In order to achieve some peak compression on C-2, a 100 × 4.6 mm i.d. column packed with 3-μm Microspher $C_{18}$ was selected as C-2, with acetonitrile–water (50:50, v/v) as M-2. Connecting C-1 with the UV detector volumes of 1.7 (M-1) and 0.40 ml (M-2) were measured for clean-up and transfer, respectively.

*Step 6.* The procedure (for final conditions, see Experimental) was validated with standard solutions and real samples. A linear response ($r$ = 0.99999) was obtained for the determination of MITC in water for concentrations (five data points) between 7 and 700 μg $l^{-1}$. The relative standard deviations (R.S.D.) of the MITC peak height and retention time were 4.4% and 0.4% (7 μg $l^{-1}$; $n$ = 7), respectively. For spiked surface and ground water samples (7 μg $l^{-1}$; $n$ = 10) a limit of detection (signal-to-noise ratio = 3) of 1 μg $l^{-1}$ was determined. The relatively high eluotropic strength of M-1 (40% acetonitrile in water) makes flushing of C-1 with a strong eluent, e.g., pure acetonitrile, between runs superfluous. Consequently, the total time of analysis is only about 10 min.

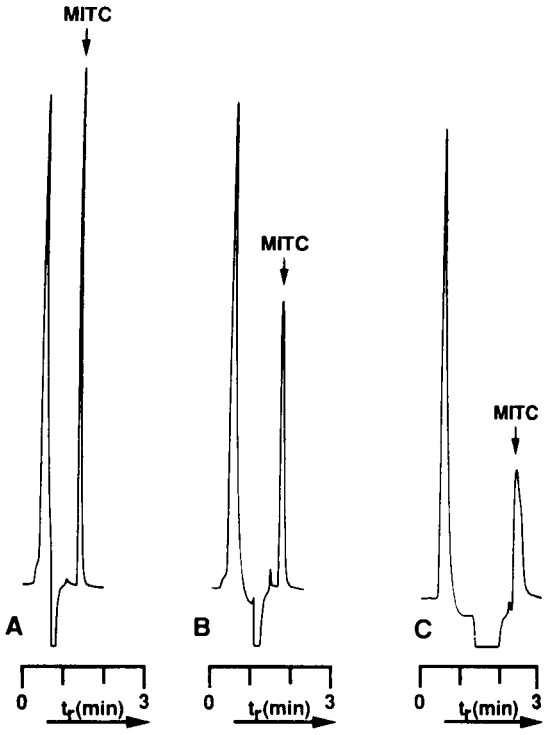


Fig. 2. Influence of the sample injection volume on peak shape of MITC. Injections of 920 ng of MITC on a 50×4.6 mm i.d. 3-μm Microspher column in water. Sample volume: (A) 270, (B) 770 or (C) 1540 μl. Mobile phase, acetonitrile–water (40+60, v/v) at 1 ml $min^{-1}$; UV detection at 237 nm (0.16 a.u.f.s.).

TABLE 2

Influence of sample (water) volume on peak volume (4σ) and peak height of MITC [a]

| Injection volume (μl) | 3-μm Microspher $C_{18}$ | | 7-μm Hypercarb | |
|---|---|---|---|---|
| | Peak height (mm) | Peak volume (μl) | Peak height (mm) | Peak volume (μl) |
| 105 | 335 | 120 | 210 | 220 |
| 270 | 285 | 140 | 210 | 220 |
| 540 | 227 | 180 | 210 | 220 |
| 770 | 179 | 240 | 175 | 240 |
| 1050 | 139 | 320 | 147 | 290 |
| 1540 | 99 | 480 | 110 | 400 |
| 2040 | 70 | 670 | 75 | 600 |

[a] 920 ng of MITC injected on to two different 50×4.6 mm i.d. columns. Mobile phase, acetonitrile–water (40+60, v/v) at 1 ml $min^{-1}$, UV detection at 237 nm (0.05 a.u.f.s.).

The mean recovery of MITC at a level of 7 μg $l^{-1}$ was 95% (R.S.D. = 7%; $n$ = 5) for spiked ground water and 92% (R.S.D. = 5%, $n$ = 5) for spiked surface water. A typical RPLC–UV trace is shown in Fig. 3A, which convincingly demonstrates the advantages of the multi-dimensional approach. In order to investigate the potential of the Hypercarb material, the same spiked surface sample was analysed on a Hypercarb column as C-1 with conditions as mentioned for Fig. 3B. As a volume of 1000 μl can now be used (see step 3), it causes a certain increase in sensitivity with Hypercarb as compared with Microspher. However, the separation between the analyte and the early-eluting interferences is less efficient than when Microspher is used as C-1.

*Extraction, concentration and RPLC procedure*

In order to comply with the EC directive for drinking water (0.1 $\mu$g $l^{-1}$ for a single contaminant), an attempt was made to include a simple extration and concentration step in the procedure. In principle, tenfold concentration should be sufficient to obtain the required sensitivity. Because of the high volatility of MITC, a liquid–liquid extraction as used in the determination of CAAL [1] or ETU [2] cannot be applied. As regards solid-phase extraction (SPE), 10 ml of water can be loaded on to a 500 mg $C_{18}$ cartridge before MITC breaks through. A small volume of strong eluent has to be used to desorb MITC: 400 $\mu$l of acetonitrile elute 90% of MITC from the cartridge. However, when using the present RPLC procedure (injection volume ca. 0.7–1.0 ml), while maintaining the required tenfold concentration (10 ml of sample to 1 ml of SPE extract), the 400-$\mu$l MITC-containing acetonitrile can only be brought up to a final solution in acetonitrile–water (40:60). The disastrous effect of such a high modifier content on the system performance is illustrated in Fig. 4. In other words, to maintain sensitivity, only purely aqueous solutions can be used for injection. SPE on a $C_{18}$ cartridge is not a viable approach.

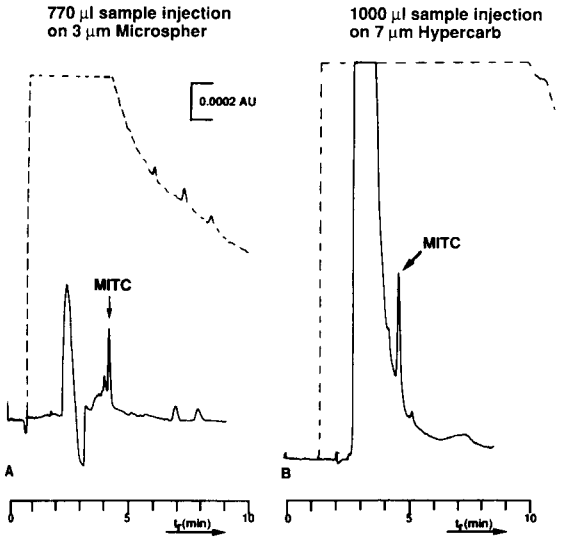


Fig. 3. Column-switching RPLC with direct sample injection of a blank surface water spiked with 7 $\mu$g $l^{-1}$ of MITC using different 50×4.6 mm i.d. columns as C-1 and UV detection at 237 nm. Solid lines, chromatogram obtained using the column-switching procedure. Dashed lines, chromatogram obtained using the two columns connected in series without column-switching (mobile phase M-2). RPLC conditions: see Experimental; M-1, acetonitrile–water (45+55, v/v) at 1 ml $min^{-1}$, M-2, acetonitrile–water (50+50, v/v) at 0.9 ml $min^{-1}$, C-2, 100×4.6 mm i.d. 3-$\mu$m Microspher; clean-up volume, 2.0 ml of M-1; transfer volume, 0.45 ml of M-2.

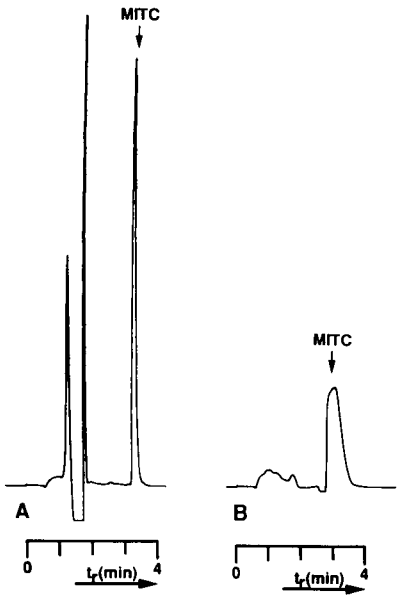


Fig. 4. Influence of modifier content of the sample solution on the peak shape of MITC. Injection of a 500-$\mu$l aqueous sample containing 475 ng of MITC and (A) 0% or (B) 40% of acetonitrile on a 100×4.6 mm i.d. 3-$\mu$m Microspher column. Mobile phase, acetonitrile–water (40+60, v/v) at 1 ml $min^{-1}$, UV detection, 237 nm (0.05 a.u.f.s.).

A more adequate concentration procedure, presented schematically in Fig. 5, was obtained by combining a single liquid–liquid extraction with a solvent-phase switch from isooctane to water on a 100-mg, 40-$\mu$m silica cartridge. Experiments showed that liquid–liquid extraction (50 ml of water per 3 ml of isooctane) yields an MITC recovery of about 50%. The 100-mg silica cartridge retains 95% of MITC on a loading of 1 ml of isooctane solution (dried over sodium sulphate), and 1 ml of pure water desorbs 70% of MITC from the silica cartridge. This means that the whole procedure provides a recovery of about 35%. After SPE and filtration, 1 ml of water sample solution yields a volume of about 800 $\mu$l, of which a maximum of 600 $\mu$l can be used for

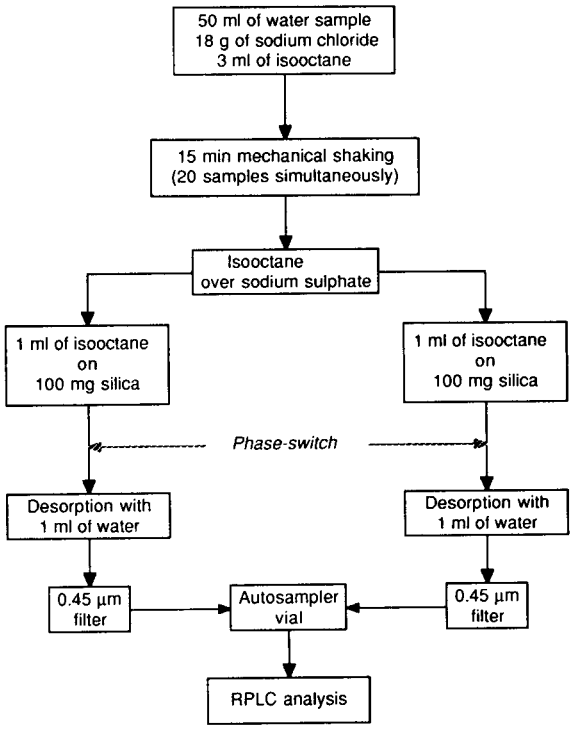


Fig. 5. Scheme of the RPLC determination of MITC in water samples using liquid–liquid extraction and SPE on silica for sample pretreatment.

accurate loop injection. Compared with the 770-$\mu$l direct analysis (detection limit 1 $\mu$g $l^{-1}$), the present 50-ml sample extraction and phase-switching procedure gives about a sixfold increase in the sensitivity, which is insufficient to obtain a limit of detection (LOD) of 0.1 $\mu$g $l^{-1}$. A means of increasing the sensitivity further is to increase the injection volume. The maximum allowable injection volume on the Microspher column is about 750 $\mu$l. To obtain the required sensitivity, the Hypercarb column was now selected as C-1, making it possible to inject a sample volume of at least 1 ml. In order to collect such an injection volume, SPE of the isooctane extract was carried out in duplicate with $2 \times 1$ ml of extract and using two silica cartridges in parallel (see Fig. 5).

*Results.* The method was validated by analysing surface water samples spiked with MITC at different levels. The repeatability and reproducibility data are listed in Table 3. The RPLC analysis of an extract of surface water spiked with 0.46 $\mu$g $l^{-1}$ of MITC is shown in Fig. 6. The phase switching on silica resulted in a considerable increase of the selectivity: for the ca. 200 surface water samples investigated with this method, all chromatograms showed only (identical) background signals originating from the reagent blank (dotted line in Fig. 6). Therefore, immediately after elution of MITC a new sample (extract) can be injected, keeping the time of RPLC analysis to less than 5 min. Partly as a result of the good reproducibility of the chromatographic pattern, the limit of detection was found to be 0.1 $\mu$g $l^{-1}$. No MITC was detected in any of the water samples analysed.

TABLE 3

MITC recovery from spiked surface water determined by means of extraction–phase switching RPLC with UV detection

| Parameter | Spiking level ($\mu$g $l^{-1}$) | |
|---|---|---|
| | 0.4–1.0 | 5–10 |
| Number of experiments | 34 | 29 |
| Overall recovery (%) | 36 | 35 |
| Repeatability (%) | 1.6 | 2.1 |
| Reproducibility (%) | 2.5 | 2.8 |

*Discussion of the multi-dimensional behaviour*

The chromatograms in Fig. 3 illustrate well the different retention behaviours of early-eluting

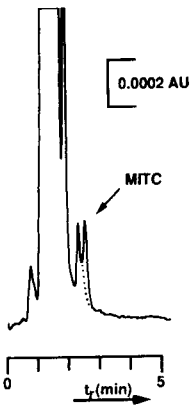


Fig. 6. RPLC of a blank surface water spiked with 0.46 $\mu$g $l^{-1}$ of MITC after extraction with isooctane and phase switching on silica. UV detection at 237 nm. Dotted line: chromatogram of blank sample (identical with reagent blank). RPLC conditions: see Experimental.

ionic or polar interferents and the analyte of interest, when using the same chromatographic conditions (stationary and mobile phase) with and without column switching. The results, which fully agree with earlier experience with the trace-level determination of ETU and CAAL [1,2], can be explained as follows.

Ionic solutes are known [12] to show a concentration-dependent retention behaviour on $C_{18}$-bonded silica with aqueous eluents. Probably, at low concentrations, ionic compounds cannot penetrate the pores of the alkyl-bonded silica because of the negative charges (residual silanol groups) on their surface ($k' < 0$). An increase in the salt concentration will diminish the ion exclusion effect, owing to increased interaction with the cations of the salt, and the retention will increase to equal that of an unretained compound ($k' = 0$). The phenomenon of concentration-dependent retention behaviour was investigated in this study by injecting aqueous potassium bromide solutions of widely different concentrations on to a 50 × 4.6 mm i.d. Microspher column (Fig. 7). Admittedly, the overall effect is small ($\Delta k' = 0.34$; $\Delta t_r = 0.2$ min); however, with a total analysis time of less than 5 min, even such a shift

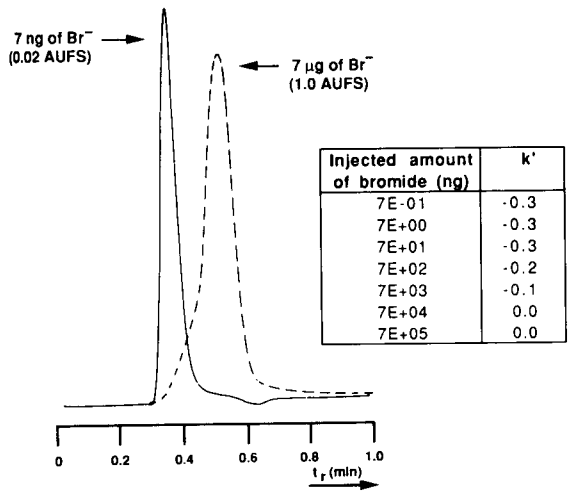


Fig. 7. Concentration-dependent behaviour of a potassium bromide solution (2.4 µl) injected on to a 50×4.6 mm i.d. 3-µm Microspher column with a mobile phase of methanol–water (5 + 95, v/v) at 1 ml min$^{-1}$. UV detection of bromide at 210 nm. For further details, see text.

in the early part of the chromatogram can play an important role. Obviously, on injecting a real water sample, the interfering ions, present in high concentrations, will migrate with a speed essentially identical with that of an unretained solute. As the analyte of interest displays a distinct, albeit low, retention, the bulk of the interferences will be removed from C-1 just before transfer of the analyte-containing fraction to C-2. The remaining, much lower, concentration of co-eluted anions will migrate faster ($k' < 0$) on C-2, rendering a considerable increase in separation between the polar analyte and the ionic compounds. The effect will, of course, be essentially absent when the columns are simply connected in series without any intermediate switching procedure.

*Conclusions*

A systematic approach to column-switching RPLC method development has been used to develop a procedure for the trace-level determination of MITC that allows screening the analyte at the 1 µg l$^{-1}$ level in environmental water samples using UV detection at 237 nm. The limit of detection of MITC can be improved to 0.1 µg l$^{-1}$ by including a simple pretreatment which involves extraction with isooctane and a subsequent isooctane-to-water phase switch on a disposable silica cartridge.

Considering the scope of coupled-column RPLC for the rapid screening of polar analytes in water using large-volume injections, the parameters that primarily determine the sensitivity and selectivity of a method in column-switching RPLC are summarized in Fig. 8. The experimental results obtained so far are presented in Table 4. As regards the analyte studied, the capacity factor, the wavelength selected for detection and the corresponding molar absorptivity are of most interest. It is clear from the data in Table 4 that 1 µg l$^{-1}$ detection limits can be obtained by simple direct large-volume injection, provided that two of the main characteristics are adequate. Recently a previous method for bentazone [13] was reconsidered. The method consisted in a manual liquid–liquid extraction–concentration step followed by RPLC column switching. From Table 4, it can be seen that all the relevant properties of

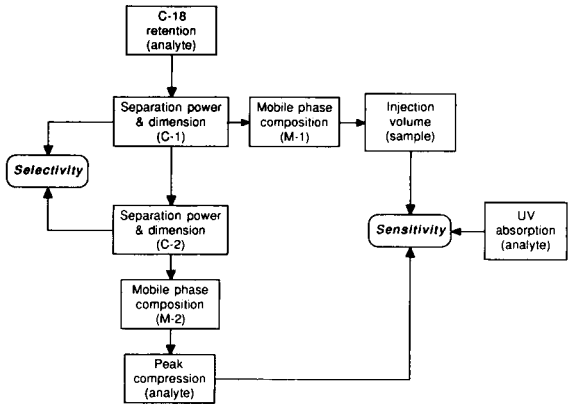


Fig. 8. Column-switching RPLC parameters influencing sensitivity and selectivity.

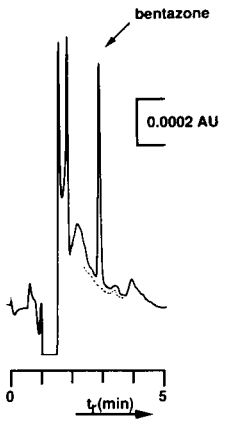


Fig. 9. Column-switching RPLC with direct sample injection (2 ml) of a blank drinking water containing 0.1% of phosphoric acid and spiked with 1.0 $\mu g\ l^{-1}$ of bentazone. LC conditions: C-1, 50×4.6 mm i.d. 3-$\mu$m Microspher; C-2, 100×4.6 mm i.d. 3-$\mu$m Microspher; M-1, methanol–0.1% phosphoric acid (50+50, v/v); M-2, methanol–0.1% phosphoric acid (60+40, v/v); clean-up volume, 4.7 ml of M-1; transfer volume, 0.5 ml of M-2; flow-rates, 1 ml $min^{-1}$; UV detection, 220 nm. Dotted line: chromatogram of blank sample.

bentazone are more favourable than those of ETU, CAAL and MITC. Accordingly, better results can therefore be expected. Experiments [14] indeed showed that because of the relatively high retention on $C_{18}$-bonded silica, up to at least a 2-ml sample could be injected without additional band broadening compared with a 100-$\mu$l injection. Figure 9 shows a typical RPLC–UV trace for a 1 $\mu g\ l^{-1}$ spiked and a blank water sample. The detection limit is calculated to be about 0.1 $\mu g\ l^{-1}$.

From our experience so far, it can be concluded that LODs of ca. 1 $\mu g\ l^{-1}$ with direct injection of water samples are feasible for polar compounds with moderately favourable properties (see Table 4 and Fig. 8). For compounds with even more favourable properties, such as bentazone, direct large-volume injection can yield LODs of 0.1 $\mu g\ l^{-1}$.

TABLE 4

Details of polar compounds analysed by means of large-volume-injection column-switching RPLC with UV detection

| Parameter | Ethylenethiourea (ETU) | Chloroallyl alcohol (CAAL) | Methyl isothiocyanate (MITC) | Bentazone |
|---|---|---|---|---|
| Formula | 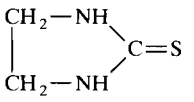 | 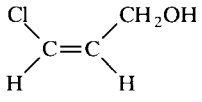 | 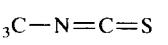 | 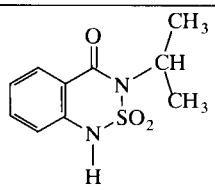 |
| Water solubility ($g\ l^{-1}$) | 20 | infinite | 8 | 0.5 |
| $k'$ [a] | 1.5 | 7.0 | 20 | > 100 |
| $\lambda$ (nm) | 233 | 205 | 237 | 220 |
| $\epsilon$ ($l\ mol^{-1}\ cm^{-1}$) | 18 000 | 10 000 | 3000 | 25 000 |
| Sample volume ($\mu$l) | 200 | 200 | 750 | 2000 |
| LOD ($\mu g\ l^{-1}$) [b] | 1 | 1 | 1 | 0.1 |

[a] On 5-$\mu$m Hypersil ODS; mobile phase, pure water for ETU, CAAL and MITC and 0.1% phosphoric acid for bentazone.
[b] Detection limit without any sample pretreatment and concentration.

REFERENCES

1 E.A. Hogendoorn, A.P.J.M. de Jong, P. van Zoonen and U.A.Th. Brinkman, J. Chromatogr., 511 (1990) 243.
2 E.A. Hogendoorn, P. van Zoonen and U.A.Th. Brinkman, Chromatographia, 31 (1991) 285.
3 E.A. Hogendoorn, C.E. Goewie and P. van Zoonen, Fresenius' J. Anal. Chem. 339 (1991) 348.
4 E.A. Hogendoorn, R. Hoogerbrugge, C.E. Goewie, P. van Zoonen and P.J. Schoenmakers, J. Chromatogr., 552 (1991) 113.
5 M. Ottnad, N.A. Jenny and C.H. Röder, in G. Zweig and J. Sherma (Eds.), Analytical Methods for Pesticides and Plant Growth Regulations, Vol. 10, Academic, New York, 1978, p. 563.
6 P.A. Greve and E.A. Hogendoorn, in P.A. Greve (Ed.), Analytical Methods for Residues of Pesticides in Foodstuffs, Part II, SDU, The Hague, 5th edn., 1988, p. 134.
7 H.T. Badings, C. de Jong and R.P.M. Dooper, J. High Resolut. Chromatogr. Chromatogr. Commun., 8 (1985) 755.
8 H.J. Scheuremann, in M. Blacha-Puller and J. Siebers (Eds.), Rückstandsanalysemethoden, Part I, Biologische Bundesanstalt für Land- und Fortwirtschaft, Braunschweig, 2nd edn., 1989, p. 243.
9 T.H.M. Noy and G. Krijgsman, in P. Sandra (Ed.), Proceedings of the 10th International Symposium on Capillary Chromatography, Vol. 1, Hüthig, Heidelberg, 1989 P. 376.
10 F.G.P. Mullins and G.F. Kirkbright, Analyst, 112 (1987) 701.
11 R.T. Krause, J. Assoc. Off. Anal. Chem., 72 (1989) 975.
12 M.J.M. Wells and C.R. Clark, Anal. Chem., 53 (1981) 1341.
13 E.A. Hogendoorn and C.E. Goewie, J. Chromatogr., 475 (1989) 432.
14 E.A. Hogendoorn and P. van Zoonen, Fresenius' J. Anal. Chem., 343 (1992) 73.

*Analytica Chimica Acta*, 268 (1992) 217–223
Elsevier Science Publishers B.V., Amsterdam



# Determination of diquat in real samples by electron spin resonance spectrometry

Angela Sánchez-Palacios

*Department of Chemistry (Applied Physical Chemistry), Faculty of Sciences, Universidad Autónoma de Madrid, 28049 Madrid (Spain)*

Tomás Pérez-Ruiz and Carmen Martínez-Lozano

*Department of Analytical Chemistry, Faculty of Sciences, Universidad de Murcia, 30071 Murcia (Spain)*

(Received 15th November 1991; revised manuscript received 2nd April 1992)

**Abstract**

A simple, selective and sensitive method for the determination of the herbicide diquat in different materials is described. The diquat radical generated by its reduction with alkaline sodium dithionite can be detected by electron spin resonance (ESR) spectrometry at room temperature. There is a linear relationship between diquat concentration and the intensity of the central line of the ESR spectrum over the range 1–100 $\mu$g ml$^{-1}$. The method has been successfully applied to the determination of diquat in different matrices.

*Keywords:* Electron spin resonance spectrometry; Diquat; Herbicides; Pesticides; Soils; Waters; Urine

Diquat [6,7-dihydrodipyrido(1,2-*a* : 2′,1′-*c*)pyrazinediium dibromide] is a very potent herbicide [1] which is widely employed throughout the world and its toxicity has been investigated by many workers [2]. Its herbicidal activity appears to depend, in part, on the ease of one-electron reduction to form a stable but air-sensitive cation radical.

Diquat can be reversibly reduced to a green monocation radical by electrochemical [3], chemical [4] and photochemical [5] procedures. The planarity of the heterocyclic nuclei permits the easy generation of the radical and its stability is due to the great delocalization of its odd electron over the whole molecule.

The determination of diquat in herbicide formulations, water, blood, urine and agricultural products has been reported. These methods include ultraviolet absorptiometry [6], spectrometry of the reduced form obtained with alkaline sodium dithionite [7,8] or L-cysteine [9,10], spectrofluorimetry [11,12], polarography [13,14], gas chromatography [15] and liquid chromatography [16,17]. Other methods include direct potentiometry with ion-selective electrodes based on crown ethers [18,19], flow-injection analysis [12] and a photokinetic method [20].

Electron spin resonance (ESR) spectrometry detects only paramagnetic species. The presence of other radicals does not interfere with the measurement if they do not have the same $g$ factor. For this reason, the clean-up process required in other methods can be omitted in the ESR method. In addition, ESR spectrometry is fairly sensitive; concentrations of radicals of the order of $10^{-7}$ M can be detected.

The ESR spectrum of the diquat radical has been obtained after reduction with zinc in trifluo-

*Correspondence to:* T. Pérez-Ruiz, Department of Analytical Chemistry, Faculty of Sciences, Universidad de Murcia, 30071 Murcia (Spain).

roacetic acid [21] and in methanol [22] media and its hyperfine coupling constants have been also determined. However, there is no report of the ESR spectrum of this radical generated by sodium dithionite in alkaline medium.

This paper describes the ESR spectrum of the diquat radical using sodium dithionite as reductor. This radical shows a very complex hyperfine structure which permits the identification and determination of diquat. Further, ESR spectrometry has been investigated as a suitable method for the determination of this herbicide in real samples without prior separation or concentration.

## EXPERIMENTAL

### *ESR spectrometry*

A Varian E-12 ESR spectrometer operating at 100 kHz field modulation was employed. Measurements were made using low microwave power (2–5 mW) and a modulation amplitude of either 0.05 or 0.5 G. The $g$ factor was determined by means of a high-precision frequency meter and gaussmeter.

The relative intensities of the ESR signals were calculated from the following equation, which can be deduced from [23]:

$$I \propto \frac{Y \Delta H_{pp}^2}{SM}$$

where $I$ is proportional to the spin concentration of the paramagnetic species, $Y$ is half the peak-to-peak amplitude of the first-derivative line, $\Delta H_{pp}$ is the peak-to-peak line width, $S$ is the gain of the amplifier and $M$ is the modulation amplitude in gauss.

The central line of the spectrum of diquat radical (denoted line 10) was used for the quantification. The gain was $4 \times 10^2$–$1 \times 10^4$ depending on the concentration of the radical; $\Delta H_{pp}$ was 1.2 G for concentrations of diquat $< 0.2$ g $l^{-1}$.

### *Reagents*

All chemicals were of analytical-reagent grade and doubly distilled water was used throughout. An aqueous 400 $\mu$g ml$^{-1}$ diquat stock solution was prepared from the pure chemical supplied by Dr. S. Ehrenstorfer and less concentrated solutions were prepared by suitable dilution. Sodium dithionite solutions were prepared in 0.2 M phosphate buffer just before use.

### *Procedure*

Mix equal volumes of the solutions of diquat and sodium dithionite in 0.2 M phosphate buffer (pH 8). The final concentration of sodium dithionite must be 0.2% (w/v) for samples containing between 100 and 40 $\mu$g ml$^{-1}$ of diquat and 0.05% (w/v) for samples containing between 40 and 1 $\mu$g ml$^{-1}$ of diquat. Transfer the mixed solution into a thin, flat, ESR cell, wait 3 min and record the spectrum with a scan rate of 10 G min$^{-1}$ at room temperature. Construct a calibration graph of the intensity of the central line (line 10) of the ESR spectrum versus diquat concentration.

### *Sample pretreatment*

Commercial herbicides, waters and urine were analysed following the general procedure after dilution of the sample with doubly distilled water to obtain a suitable concentration level.

The procedure used for the extraction of diquat from potatoes has been described previously [12]. The herbicide was determined directly in the solution obtained from the treatment of the sample.

## RESULTS AND DISCUSSION

Diquat ($DQ^{2+}$) is reduced by sodium dithionite to a stable green cation radical at room tem-

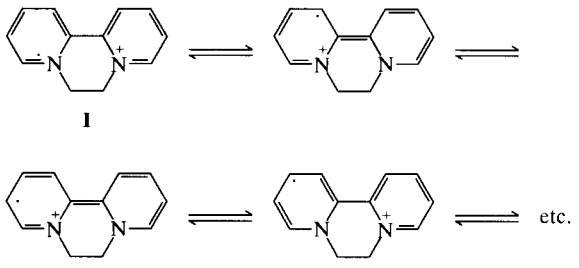


Fig. 1. Canonical structures of diquat radical.

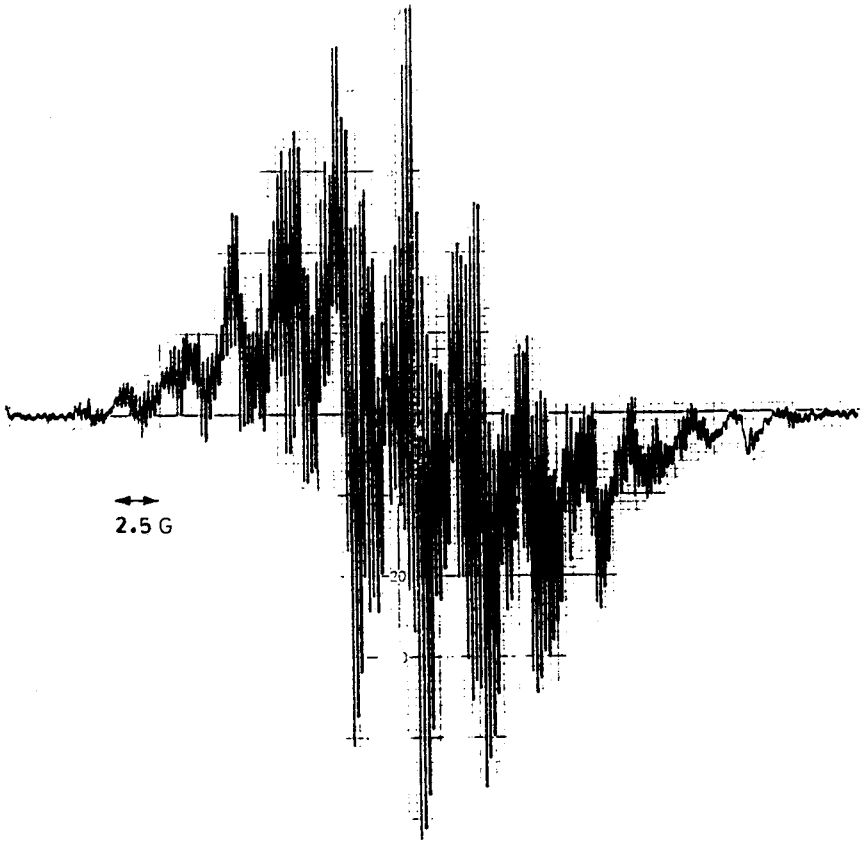


Fig. 2. ESR spectrum of diquat radical. Modulation width 0.05 G; scan range 2.5 G $cm^{-1}$; gain $5 \times 10^3$; diquat 90 $\mu g\ ml^{-1}$; sodium dithionite 0.2%; 0.1 M phosphate buffer (pH 8).

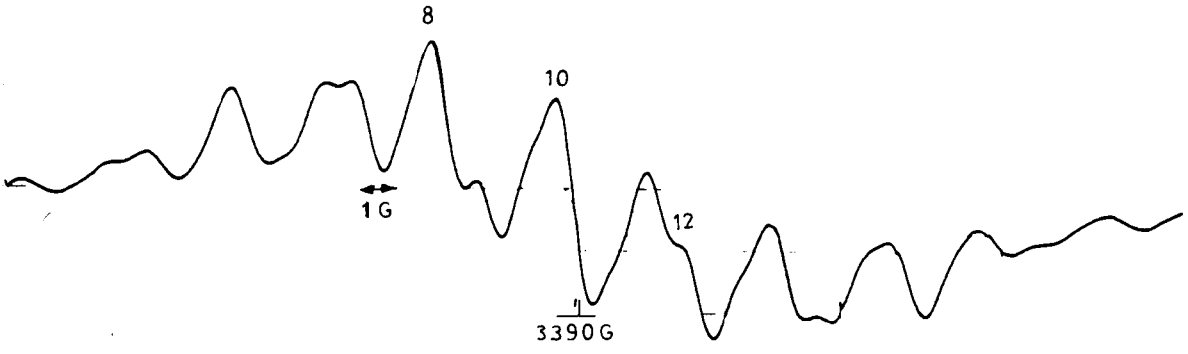


Fig. 3. ESR spectrum of diquat radical. Modulation width 0.5 G; scan range 1 G $cm^{-1}$; gain $10^3$; diquat 40 $\mu g\ ml^{-1}$; sodium dithionite 0.2%; 0.1 M phosphate buffer (pH 8).

perature. Further reduction gives a neutral product, 1,1′-ethylene-2,2′-dihydropyridine:

$$DQ^{2+} + 1e^- \rightleftharpoons DQ^{+\cdot}$$

$$DQ^{+\cdot} + 1e^- \rightleftharpoons DQ$$

Based on the canonical structures shown in Fig. 1, we should have several splittings due to the protons in positions not equivalent of spin $\frac{1}{2}$ and to the two equivalent nitrogens of spin 1 with the odd electron. Consequently, a maximum number of $5^2 \times 3^4$ lines should be expected. Therefore, the ESR spectrum of this radical should be very complicated in dilute solution.

When a mixture of diquat and sodium dithionite in phosphate buffer (pH 8) at room temperature was placed in the cavity of the ESR spectrometer, the development of an intense ESR signal was observed at the minimum operating (recording) time, i.e., about 3 min after the reactants had been mixed. At a small modulation width (0.05 G) and a low concentration of diquat (90 $\mu$g ml$^{-1}$), the spectrum consists of ca. 155 equally spaced lines with a line width of 0.15 G and a complex and well resolved hyperfine structure (Fig. 2). An increase in the modulation width from 0.05 to 0.5 G yields a spectrum of only 19 lines (Fig. 3), but the ESR signal intensity is increased tenfold. The measured value of the $g$ factor of the radical is 2.00274.

Figure 3 indicates that lines 8 and 12 have different heights, because sodium dithionite generates the $SO_2^{-\cdot}$ radical anion, which is always present in equilibrium with dithionite [24,25]. This is emphasized in Fig. 4, where the ESR spectrum of 2 $\mu$g ml$^{-1}$ diquat was obtained under the same conditions as in Fig. 3 but using a gain ten times higher. The $SO_2^{-\cdot}$ radical was also formed without diquat and its singlet has a $g$ factor of 2.0053 with a width of 1.2 G.

The amount of diquat radical formed (measured by the intensity of line 10) was not affected in the presence of oxygen, but the ESR spectrum obtained in desgassed solution showed that lines 8 and 12 were of the same height.

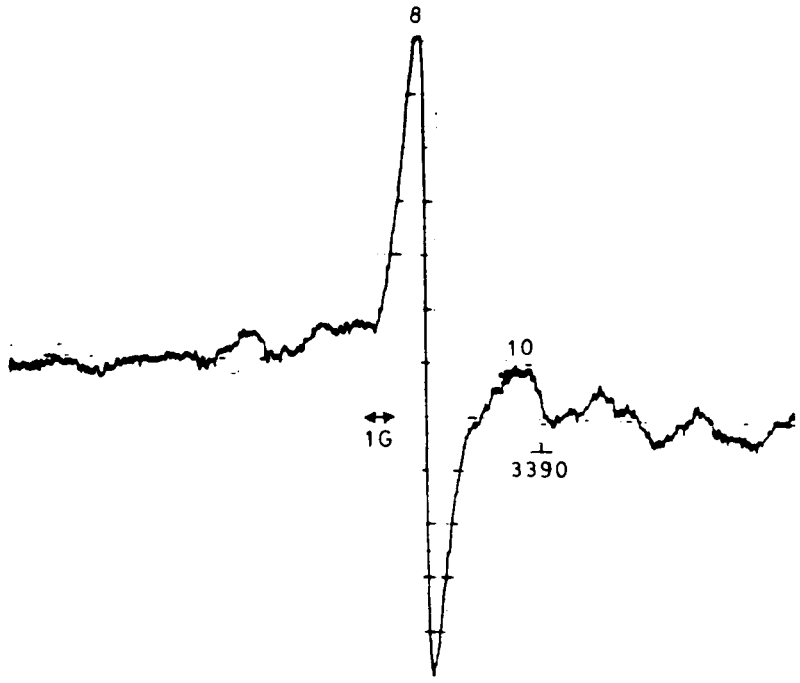


Fig. 4. ESR spectrum of diquat radical at the lowest concentration of diquat tested (2 $\mu$g ml$^{-1}$). Gain $10^4$; sodium dithionite 0.03; other conditions as in Fig. 3.

The diquat radical was found to be stable to light. After exposure to room light for 1 h, no appreciable decay was observed.

In order to achieve good sensitivity, the instrumental conditions used in Fig. 3 were selected for use. The relative intensity of the central line (line 10) was used for the quantification of diquat.

*Optimization of reaction conditions*

To establish the optimum conditions for the ESR signal, the relative intensity of line 10 ($I_{10}$) as a function of the main variables were studied. These variables were optimized using the univariate method.

The influence of pH on the stability of the reduced diquat using phosphate buffer solutions was examined over the range 7.0–11.0 (Fig. 5). The diquat radical was the most stable at pH 8. Varying the buffer concentration in the range 0.05–0.2 M did not affect affect the ESR signal.

In the same way, the effect of pH on the stability of the $SO_2^{-\cdot}$ radical was studied using solutions containing 0.3% (w/v) dithionite. The greater ESR signal was obtained at pH 8. It is important to emphasize that the ESR signal of $SO_2^{-\cdot}$ is strongly decreased in the presence of

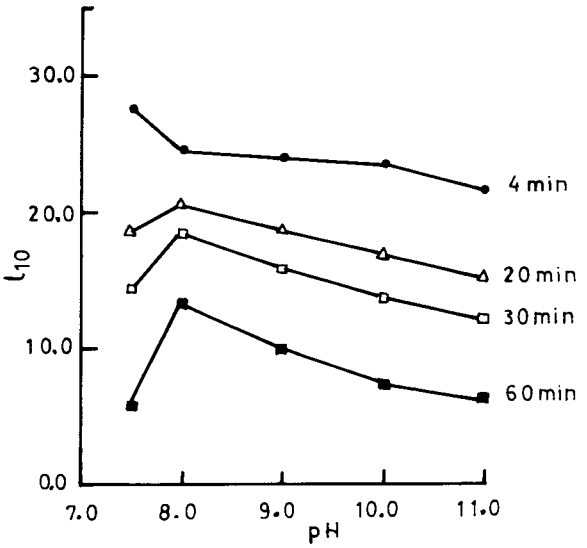


Fig. 5. Effect of pH on the stability of diquat radical at different times. Instrumental parameters as in Fig. 2; diquat 50 $\mu$g ml$^{-1}$; sodium dithionite 0.2%; 0.1 M phosphate buffer (pH 8).

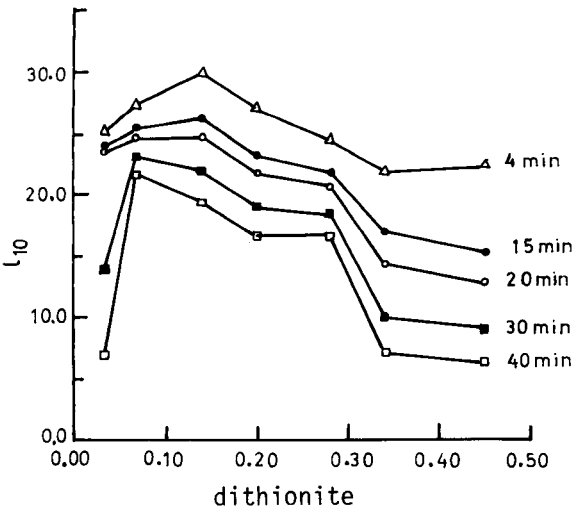


Fig. 6. Influence of sodium dithionite on the stability of diquat radical over different time periods. Instrumental parameters as in Fig. 2; diquat 50 $\mu$g ml$^{-1}$; 0.1 M phosphate buffer (pH 8).

diquat (50 $\mu$g ml$^{-1}$ diquat produces a decrease of 85%).

The effect of the concentration of sodium dithionite on the stability of diquat radical in 0.1 M phosphate buffer (pH 8) is shown in Fig. 6. Maximum and more stable values of $I_{10}$ were reached at about 0.2% sodium dithionite. However, for samples with low levels of diquat (< 30 $\mu$g ml$^{-1}$), a 0.05% sodium dithionite concentration is recommended in order to minimize the contribution of the $SO_2^{-\cdot}$ radical to the analytical signal.

As temperature changes in the range 20–40°C had little effect on the intensity of line 10 of diquat radical, subsequent experiments were performed at room temperature.

To summarize, the optimum conditions for the determination of diquat are modulation width 0.5 G, scan range 1 G cm$^{-1}$, gain $10^3$–$10^4$, pH 8 (0.1 M phosphate buffer) and 0.2% sodium dithionite for samples over the range 40–100 $\mu$g ml$^{-1}$ and 0.05% sodium dithionite for those containing between 1 and 40 $\mu$g ml$^{-1}$.

*Determination of diquat*

Under the recommended conditions, there was a linear relationship between diquat concentra-

tion and the intensity of line 10 over the range 1–100 $\mu$g ml$^{-1}$. The relative standard deviations ($n$ = 10) were 3.33% for the range 1–30 $\mu$g ml$^{-1}$ and 2.32% for the range 30–100 $\mu$g ml$^{-1}$.

*Interferences*

An extensive interference study, aimed at the determination of diquat in real samples, was performed. The maximum amount of a substance causing an error of less than ±3% in the determination of 10 $\mu$g ml$^{-1}$ diquat was taken as the tolerance limit. The results showed that large concentrations of foreign substances did not interfere; there were no effects from 500-fold (w/w) amounts of $Na^+$, $K^+$, $NH_4^+$, $NO_3^-$, $Cl^-$ and $SO_4^{2-}$. Those metal ions which form hydroxides or insoluble phosphates ($Fe^{3+}$, $Al^{3+}$, $Cu^{2+}$, $Zn^{2+}$, etc.) interfered owing to precipitation in the basic solution; this can be prevented by the addition of EDTA. There were also no effects from surfactants such as sodium dodecyl sulphonate or cetylpyridinium chloride, which may be found in natural waters, or from organophosphates and other herbidides or pesticides such as (2,4-dichlorophenoxy)acetic acid (2,4-D), (2,4,5-trichlorophenoxy)acetic acid (2,4,5-T), 1,1,1-trichloro-2,2-bis(4-chlorophenyl) ethane (DDT) and difenzoquat at similar concentrations to diquat. However, it is necessary to emphasize that paraquat was not tolerated at all, because it was reduced by alkaline sodium dithionite to paraquat radical, which also showed a strong ESR signal.

*Applications*

The ESR method reported here is sensitive and very selective and therefore has great potential for the determination of diquat in different samples. This is confirmed by the results obtained in analyses of commercial herbicides, waters, potatoes, soils and synthetic urine.

The commercial herbicides were analysed directly if paraquat was not present. The results obtained for diquat in waters, potatoes, soils and urine were in good agreement with the amount added in the preparation of synthetic samples. The results are summarized in Table 1.

*Conclusions*

This work clearly demonstrates the suitability of measuring the ESR signal of reduced diquat for the determination of the herbicide. A comparison between the ESR method and the other

TABLE 1

Determination of diquat added to real samples

| Sample | Diquat added | Diquat found | |
|---|---|---|---|
| | | ESR method [a] | Photometric method [b] |
| *Commercial herbicide* | | | |
| Reglone | 200.0 mg ml$^{-1}$ | 200.7 ± 0.1 mg ml$^{-1}$ | 200.3 mg ml$^{-1}$ |
| *Waters* | | | |
| Sample 1 | 5.0 $\mu$g ml$^{-1}$ | 4.86 ± 0.08 $\mu$g ml$^{-1}$ | 4.92 $\mu$g ml$^{-1}$ |
| Sample 2 | 10.0 $\mu$g ml$^{-1}$ | 9.91 ± 0.09 $\mu$g ml$^{-1}$ | 9.96 $\mu$g ml$^{-1}$ |
| *Soils* | | | |
| Sample 1 | 4.0 $\mu$g ml$^{-1}$ | 4.12 ± 0.04 $\mu$g ml$^{-1}$ | 4.16 $\mu$g ml$^{-1}$ |
| Sample 2 | 20.0 $\mu$g ml$^{-1}$ | 19.86 ± 0.03 $\mu$g ml$^{-1}$ | 20.18 $\mu$g ml$^{-1}$ |
| *Synthetic urine* | | | |
| Sample 1 | 6.0 $\mu$g ml$^{-1}$ | 6.14 ± 0.06 $\mu$g ml$^{-1}$ | 5.98 $\mu$g ml$^{-1}$ |
| Sample 2 | 10.0 $\mu$g ml$^{-1}$ | 9.68 ± 0.04 $\mu$g ml$^{-1}$ | 10.14 $\mu$g ml$^{-1}$ |
| *Potatoes* | | | |
| Sample 1 | 2.0 $\mu$g g$^{-1}$ | 1.94 ± 0.06 $\mu$g g$^{-1}$ | 1.92 $\mu$g g$^{-1}$ |
| Sample 2 | 12.0 $\mu$g g$^{-1}$ | 12.24 ± 0.09 $\mu$g g$^{-1}$ | 11.90 $\mu$g g$^{-1}$ |

[a] Average ± S.D. for five separate determinations. [b] Average of two separate determinations.

methods indicates that the former has the advantage of excellent selectivity because paraquat is the only interferent among many associated foreign species.

The authors express their gratitude to the DGICYT for financial support (projects 84-392 and PB90-0008).

REFERENCES

1 L.A. Summers, The Bipyridinium Herbicides, Academic, London, 1980.
2 T.J. Haley, Clin. Toxicol., 1 (1979) 14.
3 L. Pospisil, J. Kuta and J. Volke, J. Electroanal. Chem., 58 (1975) 217.
4 P.C. Kearney and D.D. Kaufman, Herbicides, Vol. 2, Dekker, New York, 1976, pp. 504–505.
5 A. Harriman and M.A. West, Photogeneration of Hydrogen, Academic, London, 1982.
6 S.D. Faust and N.E. Hunter, J. Am. Water Works Assoc., 57 (1965) 1028.
7 A. Calderbank and S.H. Yuen, Analyst, 91 (1966) 625.
8 S.H. Yuen, J.E. Bagness and D. Myles, Analyst, 92 (1967) 375.
9 K. Minakata, O. Suzuki and M. Asano, Forensic Sci. Int., 42 (1989) 231.
10 K. Minakata, O. Suzuki and M. Asano, Forensic Sci. Int., 44 (1990) 27.
11 V.H. Freed and R.E. Hughes, Weeds, 7 (1959) 364.
12 T. Perez-Ruiz, C. Martinez-Lozano and V. Tomas, Anal. Chim. Acta, 244 (1991) 99.
13 J. Volke and V. Volka, Collect. Czech. Chem. Commun., 34 (1969) 2037.
14 J. Polak and J. Volke, Chem. Listy, 77 (1983) 1190.
15 S. Kawase, S. Kanno and S. Ukai, J. Chromatogr., 283 (1984) 231.
16 R. Gill, S.C. Qua and A.C. Moffat, J. Chomatogr., 255 (1983) 483.
17 J. Hajslova, P. Cuhra, T. Davidek and J. Davidek, J. Chromatogr., 479 (1989) 243.
18 G.J. Moody, R.K. Owusu and J.D.R. Thomas, Analyst, 112 (1987) 121.
19 G.J. Moody, R.K. Owusu and J.D.R. Thomas, Analyst, 113 (1988) 65 and 1653.
20 T. Perez-Ruiz, M.C. Martinez-Lozano, V. Tomas and E. Yagüe, Analyst, 115 (1990) 783.
21 P.D. Sullivan and M.L. Williams, J. Am. Chem. Soc., 98 (1976) 1711.
22 A.L. Rieger and P.H. Rieger, J. Phys. Chem., 88 (1984) 5845.
23 J.E. Wertz and J.R. Bolton, Electron Spin Resonance. Elementary Theory and Practical Applications, McGraw-Hill, New York, 1972.
24 R.G. Rinker, T.P. Gordon, D.M. Mason and W.H. Corcoran, J. Phys. Chem., 63 (1959) 302.
25 O. Lambeth and G. Palmer, J. Biol. Chem., 248 (1973) 6095.

*Analytica Chimica Acta*, 268 (1992) 225–233
Elsevier Science Publishers B.V., Amsterdam



# Flow analysis for trace amounts of copper by ion-exchanger phase absorptiometry with 4,7-diphenyl-2,9-dimethyl-1,10-phenanthroline disulphonate and its application to the study of karst groundwater storm runoff

Kazuhisa Yoshimura and Shiro Matsuoka

*Chemistry Laboratory, College of General Education, Kyushu University, Ropponmatsu, Chuo-ku, Fukuoka 810 (Japan)*

Youji Inokura

*Miyazaki Forest Research Institute, Faculty of Agriculture, Kyushu University, Shiiba, Miyazaki 883-04 (Japan)*

Ushio Hase

*Resources and Environment Protection Research Laboratories, NEC Corporation, Miyazaki, Miyamae-ku, Kawasaki 216 (Japan)*

(Received 24th February 1992; revised manuscript received 26th May 1992)

**Abstract**

Ion-exchanger phase absorptiometry was applied to flow analysis for trace amounts of copper in water. The increase in the absorbance of the coloured complex with 4,7-diphenyl-2,9-dimethyl-1,10-phenanthroline disulphonate, which was concentrated on-line on to an ion exchanger packed in a flow-through cell, could be measured continuously with a spectrophotometer at 484 nm. The detection limit was 0.08 ng $cm^{-3}$ with 8.3 $cm^3$ of sample solution. The proposed method permitted a highly sensitive, selective determination of copper in karst groundwater samples without any preconcentration. By measuring the copper concentration response in water after a storm, the infiltration rate of rain water from the soil zone to the underground river of a karst groundwater system could be evaluated to be about 10–20 m $day^{-1}$.

*Keywords:* Flow system; Ion exchange; Ion exchanger; UV–Visible spectrophotometry; Absorptiometry; Copper; Waters

To estimate, plan and manage water resources, it is essential to characterize a water basin (i.e., to clarify thickness, lateral extent, rock type and water-transmitting properties of rock formations capable of retaining large volumes of water) and to know the direction of groundwater movement. Discharge variations at a spring and among different springs are often accompanied by changes in water quality, especially in the contents of trace elements [1], which can give important information on drainage basins and groundwater flow directions.

The Akiyoshi-do groundwater system, whose drainage basin covers some contact metasomatic deposits of copper, is characterized by a higher

*Correspondence to:* K. Yoshimura, Chemistry Laboratory, College of General Education, Kyushu University, Ropponmatsu, Chuo-ku, Fukuoka 810 (Japan).

content of copper (about 1 ng $cm^{-3}$) than other groundwaters (below 0.1 ng $cm^{-3}$) [2]. In a previous experiment, a porphyrin with a molar absorptivity of the Soret band of the order of $10^5$ $mol^{-1}$ $dm^3$ $cm^{-1}$ was employed as a colouring agent for ion-exchanger phase absorptiometry for copper [3] and applied to the determination of copper contents in groundwaters in the Akiyoshi-dai karst area [2]. Although this ion-exchanger phase absorptiometric method, based on the direct measurement of the degree of light absorption by a cation-exchange resin phase which has sorbed a copper complex of porphyrin, is very sensitive, the method requires 200-$cm^3$ water samples with copper contents below ng $cm^{-3}$ levels. A more rapid, simple and sensitive approach is to use a flow-through cell packed with a much smaller amount of ion exchanger.

Many attempts to apply ion-exchanger phase absorptiometry to flow analysis have been made since the first report [4–11]. Lazaro et al. [12] reported that a PAN-immobilized Dowex 50W resin packed in the flow cell can be used for the determination of copper(II). Although more than 50 samples with copper contents at mg $dm^{-3}$ levels can be measured within 1 h, it requires a preconcentration procedure for samples containing less than 1 $\mu$g $dm^{-3}$ levels of copper and it cannot be used for the determination of copper in natural samples because of its poor selectivity. The porphyrin has high selectivity towards copper [3], but it is not suitable for the flow method of ion-exchanger phase absorptiometry because the coloured complex could not be desorbed from the ion-exchange resin packed in the flow-through cell.

It is well known that 4,7-diphenyl-2,9-dimethyl-1,10-phenanthroline disulphonate (PMPS) (bathocuproine disulphonate) has high selectivity towards copper [13]. Ohzeki et al. [14] tried to enrich trace amounts of copper by complexing it with sixteen different chelating agents, and found PMPS to be the most effective for the rapid enrichment of copper into an anion exchanger from large-volume samples. The copper–PMPS complex could be easily desorbed from the anion exchanger. In this work, ion-exchanger phase absorptiometry was developed for flow analysis for trace amounts of copper in water with PMPS and applied to investigate storm runoff of karst groundwater. This method could also be applied to the determination of copper in rock samples.

## EXPERIMENTAL

### *Chemicals*

All chemicals were of analytical-reagent grade. Water, purified with a Milli-Q SP reagent water system (Millipore), was used for the dilution of samples and reagents.

All solutions were thoroughly filtered through a 0.45-$\mu$m membrane filter beforehand. BL-9EX, a non-ionic surfactant (nonaoxyethylene dodecyl ether) was purchased from Nikko Chemicals.

*Standard copper solution, 1000 mg Cu $dm^{-3}$.* This was prepared by dissolving copper(II) chloride dihydrate in dilute nitric acid. The concentration was standardized by EDTA titration with 1-(2-pyridylazo)-2-naphthol as indicator.

*Carrier solution and colouring agent solution.* A reducing agent–buffer solution was prepared by dissolving 50 g of hydroxylammonium chloride and 200 g of citric acid in about 500 $cm^3$ of water, mixing it with 10 $cm^3$ of 4% (w/v) BL-9EX solution, adjusting the pH of the solution to 6.0 with ammonia, filtering it through a 0.22-$\mu$m membrane filter, passing it through a polypropylene column (10 cm × 1 cm i.d.) packed with Bio-Rad Chelex 100 (100–200 mesh) in the ammonium form and then diluting it with water to a total volume of 1 $dm^3$.

For procedure 1, a carrier solution was prepared by diluting the solution mentioned above by adding nine volumes of water. A colouring agent solution was prepared by dissolving 0.02 g of the sodium salt of PMPS obtained from Dojindo (Kumamoto) in 200 $cm^3$ of the reducing agent–buffer solution.

For procedure 2, a carrier solution for the colouring agent was prepared by diluting with water 200 $cm^3$ of the reducing agent–buffer solution described above to 1 $dm^3$. Colouring agent solution was prepared by dissolving 0.01 g of the reagent in 200 $cm^3$ of the carrier solution. The other carrier solution for the sample was pre-

pared by diluting with water 10 $cm^3$ of hydrochloric acid to 1 $dm^3$.

*Desorbing agent solution.* This was prepared by diluting with water 50 $cm^3$ of concentrated nitric acid to 500 $cm^3$.

*Anion exchanger.* QAE Sephadex A-25 (Pharmacia) in the chloride form was used.

*Apparatus*

A flow-through cell was supplied by Nippon Quartz Glass; it was black-sided, and had a path length of 10 mm and a diameter of 1.5 mm. The cell was blocked with a polypropylene filter tip to prevent outflow of the ion exchanger and the filter tip was placed in such a position that the light path was not blocked [4]. Only 3–5 mm of the light-path portion was filled with the ion exchanger.

Light measurements were made with a Nippon Bunko UVIDEC-320 double-beam spectrophotometer. The spectrophotometer was mounted vertically so that the top layer of the ion-exchanger beads in the flow-through cell were levelled horizontally. An internally mirrored tube (40 mm × 12 mm i.d.) was placed between the cell holder and the light-detector window to recover partly the light scattered form the cell. A perforated metal plate of attenuance 2 (attenuance = log $I_0/I$, for the example in which light is scattered in addition to being absorbed by the system) was placed in a reference beam to balance the light intensities.

The carrier solutions were pumped with Sanuki DM2M-1024 medium-pressure pumps.

*Procedure for collecting and storing water samples*

Fresh water was filtered through a 0.45-$\mu$m cellulose nitrate membrane filter with a disposable syringe filter unit (Advantec, DISMIC-25) at the site where the water sample was collected. After filtration, the pH values of the filtered samples were adjusted to about 1 by adding 0.5 $cm^3$ of hydrochloric acid and the solution stored in a 50-$cm^3$ polyethylene container; under these conditions the loss of copper is negligible [15]. The acidified sample solution was directly introduced and neutralized on-line by mixing it with citrate buffer solution (procedure 2). The hydrochloric acid concentration in the sample solutions should be kept constant at $0.10 \pm 0.02$ mol $dm^{-3}$.

*Procedure for decomposing rock samples*

For decomposition of rock samples, a microwave acid digestion method was applied. In a microwave acid digestion bomb (Sanplatec N-25), a 100-mg sample was decomposed by heating twice for 60 s with 1 $cm^3$ of concentrated nitric acid and 0.7 $cm^3$ of concentrated hydrofluoric acid [16]. The solution was then evaporated and the dry residue was dissolved in a mixture of 20 $cm^3$ of water and 0.5 $cm^3$ of hydrochloric acid. After dilution with water to 50 $cm^3$, the solution was stored in a polyethylene vessel.

*Procedure for the determination of copper in water (colour development as in the batch method, procedure 1)*

The flow diagram is shown in Fig. 1a. To a water sample containing 4–200 ng of copper in a 20-$cm^3$ volumetric flask were added 2 $cm^3$ of the colouring agent solution. The solution was diluted with water to 20 $cm^3$ and mixed, then 8.3

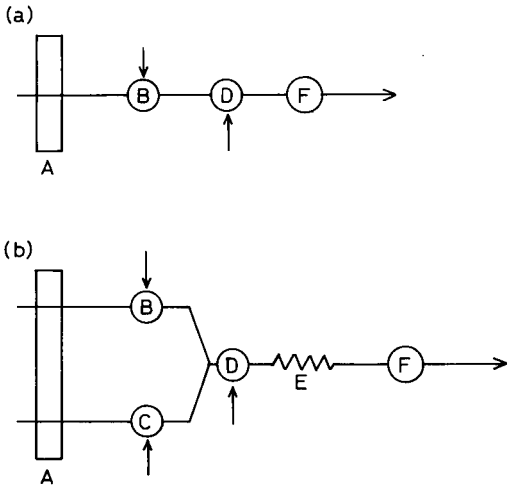


Fig. 1. (a) Schematic single-line flow analysis diagram. (b) Manifold for FIA. (A) Pump; (B) six-way rotary valve for sample introduction with 8.3-$cm^3$ PTFE tube loop; (C) six-way rotary valve for introduction of a colouring agent solution with 2.1-$cm^3$ PTFE tube loop; (D) six-way rotary valve for desorbing agent introduction; (E) mixing and reaction tube (1 m of PTFE tubing of 1 mm i.d.); (F) absorptiometric detector packed with ion exchanger.

$cm^3$ of the sample were introduced into the stream. The flow-rate was kept constant at 1.1 $cm^3$ $min^{-1}$. All tubing was made of PTFE (1 mm i.d.). The increase in absorbance was continuously monitored at 484 nm and recorded on a strip-chart recorder set at 0.5 absorbance full-scale. A solution for desorbing the copper complex from the ion-exchanger phase was introduced into the stream by means of another PTFE six-way rotary valve with a sample loop (ca. 1 $cm^3$).

*Procedure for the determination of copper in water (on-line colour development, procedure 2)*

Sample solution (8.3 $cm^3$) containing 0.8–80 ng of copper and the colouring agent solution (2.1 $cm^3$) were introduced simultaneously into the stream by means of six-way rotary valves. The carrier solutions for the sample and the colouring agent were pumped at flow-rates of 0.8 and 0.2 $cm^3$ $min^{-1}$, respectively. The absorbance was monitored continuously and recorded in the same way as in procedure 1. A schematic diagram of the flow analysis system is shown in Fig. 1b.

## RESULTS AND DISCUSSION

*Absorption spectrum of copper–PMPS complex*

In solution, the copper(I)–PMPS complex shows a maximum absorption at 481 nm where the molar absorptivity is 13 200 $mol^{-1}$ $dm^3$ $cm^{-1}$. Because of its high negative charge of −3, the complex species is easily sorbed in an anion ex-

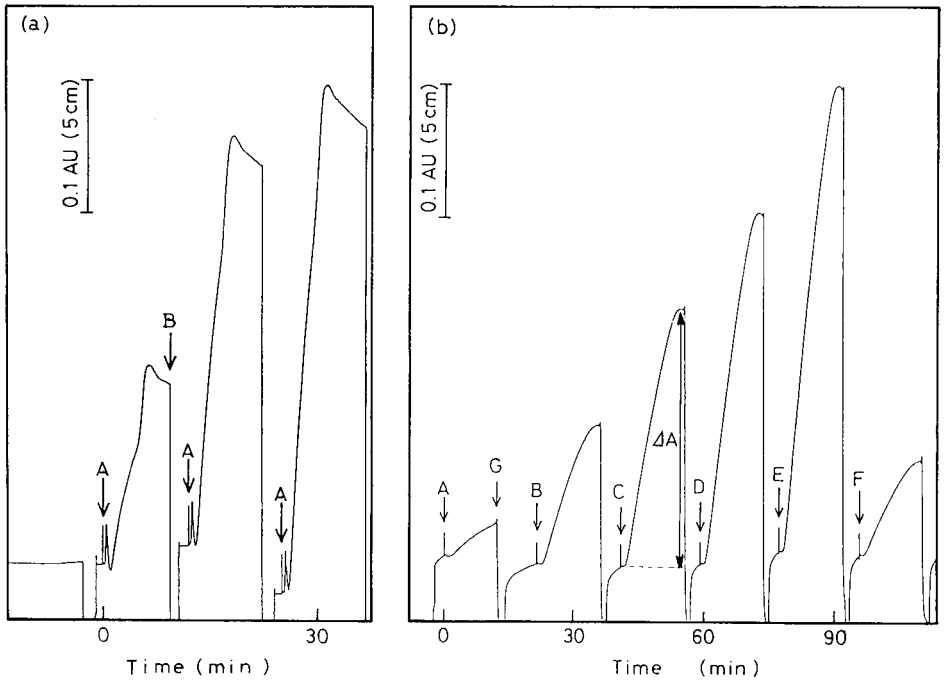


Fig. 2. (a) Colour development profiles of copper using the flow system (procedure 1) without the surfactant. (A) Sample introduction (40 ng of Cu, 4 $cm^3$); (B) desorbing agent introduction. Ion exchanger, QAE-Sephadex A-25; flow-through cell, 1.5 mm diameter; flow-rate, 1.1 $cm^3$ $min^{-1}$; wavelength, 484 nm. (b) FIA profiles obtained with the flow system (procedure 2). Sample volume, 8.3 $cm^3$. (A) Blank; (B) 20.8; (C) 41.5; (D) 62.3; (E) 83.0 ng of Cu; (F) groundwater; (G) desorbing agent (1.4 mol $dm^{-3}$ $HNO_3$). Carrier solution, 0.12 mol $dm^{-3}$ HCl; flow-rate, 0.8 $cm^3$ $min^{-1}$. PMPS solution volume, 2.1 $cm^3$ [0.005% (w/v) PMPS, 2.5% (w/v) hydroxylammonium chloride, 0.02% (w/v) BL-9EX, 0.2 mol $dm^{-3}$ citrate, pH 5.5]; carrier solution, 2.5% (w/v) hydroxylammonium chloride, 0.02% (w/v) BL-9EX, 0.2 mol $dm^{-3}$ citrate, pH 5.5; flow-rate, 0.2 $cm^3$ $min^{-3}$. Ion exchanger, QAE-Sephadex A-25; flow-through cell, 1.5 mm diameter; wavelength, 484 nm.

changer, QAE-Sephadex A-25, showing a maximum absorption at 484 nm; the wavelength was fixed at 484 nm for the flow analysis of copper. The composition of any complex formed by copper and PMPS in the ion-exchanger phase was studied by the molar ratio method. The reagent-to-metal molar ratio of the complex was 2:1, the same as in the solution.

*Application of ion exchanger phase absorptiometry to flow analysis (procedure 1)*

*Effect of pH of solution on colour development.* The quantitative complex formation of copper(I)–PMPS was achieved within the pH range 4–10 [17]. The solution was kept at a pH of 5–6 with citrate.

*Concentrations of PMPS and reducing agent.* An amount of reagent greater than that required by stoichiometry (Cu : PMPS = 1 : 2) is needed for complete colour development. The concentration of PMPS in the range examined (0.0001–0.002%, w/v) was sufficient for complete colour development; higher concentrations resulted in higher reagent blanks. The final concentration of PMPS was fixed at 0.001% (w/v), i.e., $2 \times 10^{-5}$ mol $dm^{-3}$.

The presence of 0.5% (w/v) of hydroxylammonium chloride was sufficient for complete reduction of copper. A content larger than 0.5% (w/v) resulted in lower absorbances both for the coloured complex and the reagent blank because of their decreased distribution ratios.

The colour development was almost complete within 3 min and the net absorbance was constant even after 2 h.

*Adsorption of the copper–PMPS complex on the wall of the PTFE tube.* The copper–PMPS complex species easily adsorbs on the wall of the PTFE tube, probably owing to hydrophobic interaction between the surface moiety of PTFE and the solute. This effect resulted in low reproducibility of measurements, as shown in Fig. 2a. The addition of a non-ionic surfactant, BL-9EX, to both the sample solution and the carrier solution was very effective in overcoming this problem. However, its concentration should not be higher than the critical micellar concentration of $1 \times 10^{-4}$ mol $dm^{-3}$ [18], otherwise the sensitivity decreases. In the present system, the final surfactant concentration was maintained at 0.004% (w/v), i.e., about $7 \times 10^{-5}$ mol $dm^{-3}$.

*Flow-rate.* At a constant flow-rate, there was a strictly linear relationship between measured absorbance and copper concentration. However, high flow-rates gave rise to an increase in pressure drop. Therefore, the total flow-rate was maintained constant in the range 0.9–1.1 $cm^3$ $min^{-1}$. Probably because of slow diffusion of the coloured species into the resin particles, a change in flow-rate from 1.0 to 1.5 $cm^3$ $min^{-1}$ led to a decrease in sensitivity of 80%.

*Calibration and detection limit.* The increase in absorbance of the background just after the sample injection, $\Delta A$, could be measured on the chart. The coloured copper species in the ion-exchanger phase were easily desorbed with 1.4 mol $dm^{-3}$ nitric acid. The cell could be used repeatedly for measurements of four water samples per hour. The calibration graph obtained was linear from 0.5 to 10 ng $cm^{-3}$ of copper and could be expressed as

$$\Delta A = 0.0288C + 0.0686 \quad (1)$$

where $C$ is the sample concentration in ng $cm^{-3}$. Procedural blanks were determined and subtracted from the sample concentration.

*Sensitivity.* The distribution ratio of the copper(I)–PMPS complex, defined by the equation

$$D = \frac{(\text{mol of copper sorbed})/(\text{dm}^3 \text{ of swollen ion exchanger})}{(\text{mol of copper})/(\text{dm}^3 \text{ of solution})} \quad (2)$$

can be a measure of the copper retention in the flow-through cell. The colour development profile of the complex species can be explained according to the plate theory [11]. As already shown in a previous paper [4], in a high distribution ratio system with $D$ higher than $5 \times 10^4$, almost all the sample species was retained after the passage of at least 20 $cm^3$ of a carrier solution, whereas the sample species introduced was eluted from the cell in a fairly short time for low-$D$ systems. For the present system, the $D$ value was $1.1 \times 10^5$, suggesting quantitative retention of the copper(I)–PMPS complex in the flow-through cell and that a higher sensitivity can be obtained by

TABLE 1

Effects of foreign ions on the determination of copper [a]

| Foreign ion | Concentration ($\mu g\ cm^{-3}$) | Cu found ($ng\ cm^{-3}$) | Error (%) |
|---|---|---|---|
| Mg | 10 | 10.0 | 0 |
| Ca | 100 | 10.2 | +2 |
| Fe(III) | 1 | 9.9 | −1 |
| Co | 0.01 | 10.0 | 0 |
| Ni | 0.01 | 10.0 | 0 |
| Zn | 0.01 | 10.0 | 0 |

[a] Sample volume introduced: 8.3 $cm^3$ (10.0 ng $cm^{-3}$).

introducing larger sample volumes. Probably because of its low distribution ratio, the sorption of the free colouring agent on the ion exchanger reached a steady state after the introduction of the sample solution into the flow system [11]. The greater the volume of the sample introduced, the greater the signal-to-blank ratio will be.

The ratio of the two absorbances for sample solutions in the same copper concentration, *SR*, can be measured to compare the sensitivity of the present method and the corresponding solution absorptiometry sensitivity. In the system with complete sorption of the coloured species in the ion exchanger, *SR* is closely related to:

$$SR = (\bar{\epsilon}V)/(\epsilon lS) \quad (3)$$

where $\epsilon$ and $\bar{\epsilon}$ are the molar absorptivities of the coloured species in solution and in the solid phase, respectively, $l$ the light path length for solution absorptiometry, $V$ the volume of sample solution introduced and $S$ the cross-sectional area (normal to the light beam) of the flow-through cell packed with the ion exchanger. The ratio is a function of both the diameter of the flow-through cell and the sample volume, which are very important factors for obtaining high sensitivity [4]. At a fixed sample volume (8.3 $cm^3$), the *SR* value obtained (140) was lower than the value expected (470) if $l = 1$ cm. The low diffusion rate of the coloured species into the ion exchanger may lower the sensitivity (see above).

*Precision.* The precision was measured with 8.3-$cm^3$ sample solutions containing 42 ng of copper. For five determinations, the absorbances obtained were $0.151 \pm 0.002_8$. The relative standard deviation was 1.9%.

*Effects of concomitant ions.* There are few metal ion interferences in the corresponding conventional absorptiometry when PMPS is used [13,14,17]. The effect of foreign ions is shown in Table 1. The amounts of coexisting ions normally present in natural waters are tolerable. As described later, magnesium, aluminium, calcium, titanium, iron and manganese in a rock sample did

TABLE 2

Determination of copper in groundwater and rock samples

| Sample | Cu added (ng) | Net absorbance [b] | Cu found (ng) | Cu recovered (ng) |
|---|---|---|---|---|
| Groundwater [a] | 0 | 0.0216 | 4.90 | – |
| | 8.3 | 0.0589 | 13.4 | 8.5 |
| | 16.6 | 0.0926 | 21.0 | 16.1 |
| | 24.9 | 0.131 | 29.7 | 24.8 |
| **Sample** | **Sample introduced [d] (mg)** | **Net absorbance [b]** | **Cu found (ng)** | **Cu content ($\mu g\ g^{-1}$)** |
| JB-1 [c] | 0.199 | 0.0493 | 11.2 | 56.3 |
| | 0.398 | 0.110 | 25.1 | 63.1 |
| | 0.598 | 0.171 | 38.8 | 64.9 |
| | 0.996 | 0.236 | 53.6 | 53.8 |
| | 1.20 | 0.298 | 67.8 | 56.7 |
| | 1.39 | 0.343 | 78.0 | 56.0 |

[a] Groundwater issuing from Akiyoshi-do Cave in the Akiyoshi-dai karst area; 8.3 $cm^3$ of sample solution (0.1 mol $dm^{-3}$ HCl) were introduced into the system. [b] $\Delta A - \Delta A$(for the blank). [c] Reference material (a basalt sample from the Geological Survey of Japan); sample solution introduced = 8.3 $cm^3$. [d] 0.120 g of JB-1 were decomposed with HF and $HNO_3$ and dissolved in 100 $cm^3$ with 0.12 mol $dm^{-3}$ HCl. Further dilution was effected with the HCl solution.

not affect the copper determination when present at levels of 830, 1400, 1200, 140, 1100 and 20 times the concentration of copper (as weight ratio), respectively.

The presence of sodium chloride as background electrolyte resulted in lower absorbances for the sample and reagent blank. It is recommended that a calibration graph prepared at the same concentration of background electrolyte as that in the sample solution is used, particularly when the electrolyte concentration is high.

*Application to flow injection (procedure 2)*

*Colour development profile and calibration.* Figure 2b shows a typical colour development profile. After introduction of the sample and a colouring agent, the absorbance increased because of the sorption of the copper(I)–PMPS complex on the ion exchanger packed in the flow-through cell. The calibration graph has a positive blank due to the PMPS solution, but gives a linear plot that can be expressed by the equation

$$\Delta A = 0.0387C + 0.0530 \quad (4)$$

Copper concentrations at 0.1–10 ng $cm^{-3}$ levels could be determined for three water samples within 1 h. A recovery test was done for a karst groundwater sample. As shown in Table 2, the recovery of the copper added was quantitative.

*Determination of copper in a reference rock.* The proposed method was applied to the determination of copper in a reference rock sample JB-1 (a basalt sample from the Geological Survey of Japan). For six determinations, the values obtained were $58.5 \pm 4.4$ $\mu g\ g^{-1}$ (Table 2), which compared favourably with the certified value of 56.3 $\mu g\ g^{-1}$ [19].

*Concentration variation of copper concentration in groundwater issuing from Akiyoshi-do Cave after storm*

The changes in spring water chemistry after a storm have a pattern composed of sequential and sometimes superimposed pulses of water of different quality and amount from different stores and tributary inputs [1]. The Akiyoshi-do Cave catchment basin occupies about half of the Akiyoshi-dai Plateau (Yamaguchi Prefecture), 18.5 $km^2$, including 16.5 $km^2$ of a limestone area. Akiyoshi-dai Plateau, most of which is a Quasi-National Park in Yamaguchi Prefecture, Western Japan, is one of the biggest karst plateaus in Japan, and Akiyoshi-do Cave is located at the

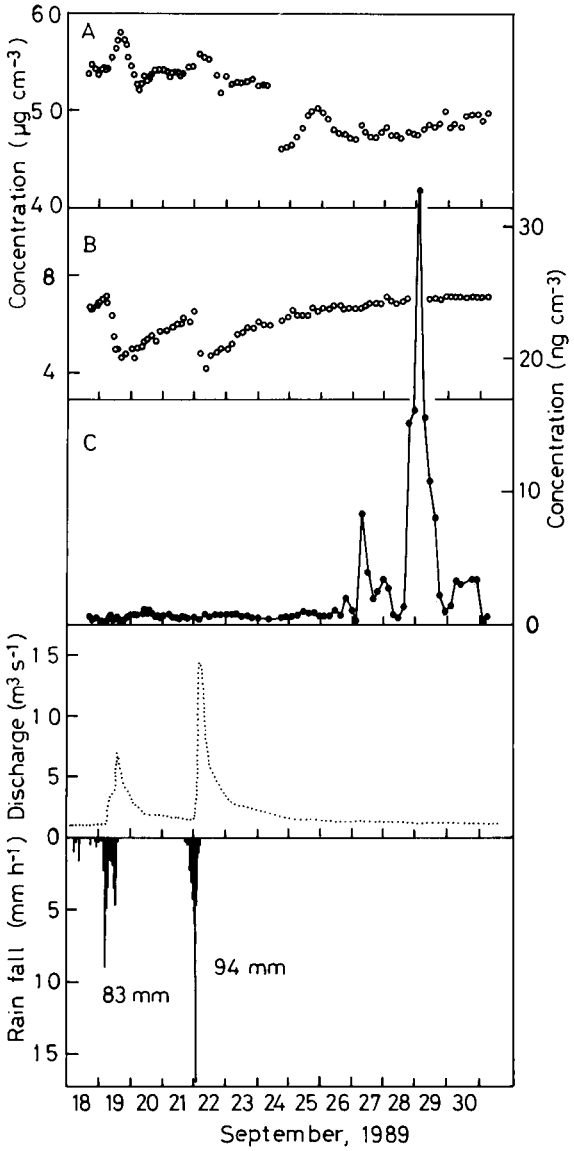


Fig. 3. Concentrations and water discharge as a function of time for groundwater during a flood event. Concentrations of (A) calcium, (B) chloride and (C) copper. Analytical method: (A) AAS; (B) ion chromatography; (C) the proposed method.

TABLE 3

Comparison of sensitivities and limits of detection of different methods

| Method | Amount of sample taken ($cm^3$) | Sensitivity [a] ($ng\ cm^{-3}$) | Detection limit ($ng\ cm^{-3}$) | Ref. |
|---|---|---|---|---|
| Absorptiometry [b]: | | | | |
| T(4-MPy)P [c] | – | 29 | – | 23 |
| PMPS | – | 530 | – | 16 |
| Ion-exchange phase absorptiometry: | | | | |
| T(4-MPy)P | 200 | 1.3 | 0.44 | 2 |
| | 1000 | 0.32 | 0.072 | 2 |
| PMPS: | | | | |
| Procedure 1 | 8.3 | 3.5 | 0.10 | This work |
| Procedure 2 | 8.3 | 2.6 | 0.08 | This work |
| FAAS [d] | – | 30 [g] | 5 | 24 |
| ETAAS [e] | 0.01 | 1.3 [g] | 0.2 | 24 |
| ICP-AES [f] | – | – | 0.5 | 25 |

[a] Copper concentration giving a final absorbance of 0.1. [b] 1-cm cell. [c] T(4-MPy)P = $\alpha,\beta,\gamma,\delta$-tetrakis(4-*N*-methylpyridyl)porphine. [d] FAAS = flame atomic absorption spectrometry. [e] ETAAS = electrothermal atomic absorption spectrometry. [f] ICP-AES = inductively coupled plasma atomic emission spectrometry. [g] 1% absorption.

southern foot of the plateau. In this area, the average annual precipitation is 1974 mm, the average runoff from Akiyoshi-do Cave is 955 mm and the mean solutional denudation rate in the basin is 0.051 mm per year [20]. For the underground river issuing from Akiyoshi-do Cave, the changes after a storm in discharge and in the contents of calcium, chloride and copper are shown in Fig. 3.

The runoff response is similar to that for a surface stream, except for the longer time lag between the runoff peak and the storm peak. Of the major components, calcium and hydrogencarbonate are supplied by the dissolution of Akiyoshi limestone in the presence of dissolved carbon dioxide, whereas chloride is supplied by wet and dry deposits mainly in the form of sea salt. The increase in calcium concentration and the decrease in chloride concentration at the start of the flood are due to the flushing out of water with a long residence time in the deeper phreatic zone and the subcutaneous zone beneath the soil zone. Although detailed assignments of the changes in spring water chemistry were not the aim of this study, it is noteworthy that the copper concentration in groundwater issuing from Akiyoshi-do Cave showed peaks 8 days after storms. Such a high concentration of copper in karst groundwater cannot be accounted for on the basis of solubility of copper minerals: the groundwater in contact with limestone is supersaturated with respect to minerals such as malachite [21]. The copper may be supplied by oxidation of sulphide ores with the aid of sulphur-oxidizing bacteria [22] in the non-calcareous soil zone in the contact metasomatic ore area of the Akiyoshi-do Cave drainage basin. In this area, the depth of the groundwater table from the surface is 50–100 m, and a 2.5-km connection between a sink hole and Akiyoshi-do Cave has been confirmed by dye tracing with sodium fluorescein; the coloured water was observed at Akiyoshi-do Cave 52 h after the injection into the sink hole [3]. The infiltration rate of rain water during a flood period from the soil zone to the underground river of the Akiyoshi-do Cave groundwater system could be evaluated for the first time to be about 10–20 m $day^{-1}$.

*Conclusion*

A comparison of the sensitivities of various analytical methods for the determination of copper is shown in Table 3. The proposed method has several advantages especially for the determination of copper in karst spring water; it is a highly sensitive and selective method for water

samples with high contents of calcium and magnesium to which acid has been added for preservation.

Measurements of trace amounts of copper in karst groundwater after storms made it possible to evaluate the infiltration rate of rain water from the soil zone to the underground river.

This work was partially supported by a Grant-in-Aid for Scientific Research (C), Nos. 01540486 and 03640497, from the Ministry of Education, Science and Culture, Japan. The authors express their thanks to Dr. K. Matsumi, Dr. T. Yuasa and Dr. T. Okuda for helpful discussions and encouragement throughout this work.

REFERENCES

1 D. Ford and P. Williams, Karst Geomorphology and Hydrology, Unwin Hyman, London, 1989.
2 K. Yoshimura, M. Ota and T. Tarutani, Bull. Akiyoshi-dai Mus. Nat. Hist., 18 (1983) 21.
3 K. Yoshimura, S. Nigo and T. Tarutani, Talanta, 29 (1982) 176.
4 K. Yoshimura, Anal. Chem., 59 (1987) 2922.
5 K. Yoshimura, Bunseki Kagaku, 36 (1987) 656.
6 K. Yoshimura, Analyst, 113 (1988) 471.
7 K. Yoshimura, S. Matsuoka and H. Waki, Anal. Chim. Acta, 225 (1989) 313.
8 F. Lazaro, M.D. Luque de Castro and M. Valcarcel, Anal. Chim. Acta, 225 (1989) 231.
9 K. Yoshimura, S. Nawata and G. Kura, Analyst, 115 (1990) 843.
10 N. Lacy, G.D. Christian and J. Ruzicka, Anal. Chem., 62 (1990) 1482.
11 K. Yoshimura and U. Hase, Analyst, 116 (1991) 835.
12 F. Lazaro, M.D. Luque de Castro and M. Valcarcel, Anal. Chim. Acta, 214 (1988) 217.
13 D. Blair and H. Diehl, Talanta, 7 (1961) 163.
14 K. Ohzeki, M. Minorikawa, F. Yokota, I. Nukatsuka and R. Ishida, Analyst, 115 (1990) 23.
15 K.S. Subramanian, C.L. Chakrabarti, J.E. Sueiras and I.S. Maines, Anal. Chem., 50 (1978) 444.
16 T. Suzuki and M. Sensui, Anal. Chim. Acta, 245 (1991) 43.
17 Y. Kikuchi, K. Satoh, K. Sawada and T. Suzuki, Bunseki Kagaku, 39 (1990) 301.
18 H. Lange, Kolloid-Z., 201 (1965) 131.
19 A. Ando, S. Omori and S. Terashima, in T. Hanya (Ed.), Proceedings of the Annual Meeting of the Geochemical Society of Japan, Geochemical Society of Japan, Tokyo, 1983, pp. 168.
20 Y. Inokura, K. Yoshimura, A. Sugimura and T. Haikawa, J. Speleol. Soc. Jpn., 14 (1989) 51.
21 R.M. Garrels and C.L. Christ, Solutions, Minerals, and Equilibria, Freeman and Cooper, San Francisco, 1965.
22 W. Stumm and J.J. Morgan, Aquatic Chemistry, Wiley, New York, 1970.
23 H. Ishii and H. Koh, Bunseki Kagaku, 28 (1979) 473.
24 M. Suzuki, Atomic Absorption Spectrophotometry, Kyoritsu, Tokyo, 1984.
25 H. Haraguchi, ICP Atomic Emission Spectroscopy, Kodansha, Tokyo, 1989.

*Analytica Chimica Acta*, 268 (1992) 235–246
Elsevier Science Publishers B.V., Amsterdam



# Equilibrium dialysis–ligand exchange: a novel method for determining conditional stability constants of radionuclide–humic acid complexes

L.R. Van Loon and S. Granacher

*Paul Scherrer Institute, Würenlingen and Villigen, CH-5232 Villigen PSI (Switzerland)*

H. Harduf

*University of Haifa, Oranim (Israel)*

(Received 24th March 1992; revised manuscript received 11th May 1992)

**Abstract**

The equilibrium dialysis–ligand exchange technique (EDLE) is a combination of two classical techniques and is designed to measure the conditional stability constants of radionuclide–humic acid complexes over broad pH and ionic strength ranges. The use of a reference ligand hinders the hydrolysis of the radionuclide and enables the stability constant to be determined under neutral and alkaline conditions. By measuring the distribution of the radionuclide between the reference ligand and the humic acid, the conditional stability constant can be calculated. The technique was tested with $^{60}Co^{2+}$ and a commercial humic acid (HA) (Aldrich). It was possible to measure the conditional stability constants for the Co–HA complex for pH values between 5 and 10 in an ionic strength range between 0.02 and 0.2 M. The conditional stability constant increases non-linearly with increasing pH and decreases with increasing ionic strength.

*Keywords:* Ion exchange; Equilibrium dialysis; Humic acids; Ligand exchange; Radionuclides; Stability constants

The influence of natural organic acids [humic acids (HA) and fulvic acids (FA)] on radionuclide migration through the geo- and biosphere is still a source of uncertainty in radioactive waste management. HA and FA can complex radionuclides and trace metals and increase their solubility [1–4]. In addition, natural organic matter may decrease the adsorption of radionuclides on the surface of water bearing fissures and reduce the retardation effect of matrix diffusion, both of which result in enhanced transport through the geosphere. An assessment of the influence of natural organic acids is therefore necessary. However, the availability of appropriate stability constant data for radionuclide–HA complexes is a prerequisite for such an assessment.

Most data reported in the literature have been determined under conditions that are irrelevant for most safety assessment studies, i.e., low pH (2–5), high ionic strength and high metal to HA ratio [5–13]. The main reason for this is that, at low pH, the hydrolysis of the metal is negligible. Under these conditions, precipitation of the nuclide is avoided and mainly two species are present in solution: the metal–HA complex and the free metal. The concentration of the free metal is relatively high and can be measured accurately. A wide variety of techniques are available to deter-

*Correspondence to:* L.R. Van Loon, Paul Scherrer Institute, Würenlingen and Villigen, CH-5232 Villigen PSI (Switzerland).

mine the stability constant under such conditions [4].

The conditional (effective) stability constants of metal–HA complexes depend strongly on pH and ionic strength and may vary by several orders of magnitude in the pH range 5–10. Applying these conditional constants determined at low pH values to conditions of higher pH values is therefore basically wrong. Also, the common practice of linearly extrapolating conditional stability constant data obtained at low pH values to slightly alkaline conditions typical of most groundwaters is generally inappropriate because of the lack of information on the evolution of the conditional stability constants with pH and can lead to incorrect conclusions regarding the extent of radionuclide complex formation with HA and FA.

The determination of stability constants under neutral and alkaline conditions is often a problem because of the extensive hydrolysis of most of the radionuclides of interest under these conditions and because the free metal concentration is very low and difficult to determine. New techniques have to be developed to overcome these difficulties. Maes et al. [14] developed a modified ion-exchange technique and were able to measure conditional stability constants of Eu- and Am–HA complexes at pH ≈ 9. The technique, however, can hardly be applied at low (< 0.02 M) or high ionic strength values (> 0.15 M). In this paper, a method is proposed which is a combination of ligand exchange and equilibrium dialysis (EDLE) as a potential technique for determining conditional stability constants of radionuclide–HA complexes over a broad pH range. This combination of two classical techniques represents a means of solving the earlier mentioned problems. For pH values below 8, the EDLE results were compared with those obtained by an ion-exchange method.

## THEORY OF THE EDLE TECHNIQUE

Basically, the EDLE technique measures the stability constant of the radionuclide–HA complex relative to a reference radionuclide–ligand (L) complex of known stability. From the distribution of the radionuclide (M) between the humic acid (HA) and the reference ligand (L), the stability constant of the radionuclide–HA complex can be calculated. The concentration and type of reference ligand has to be chosen with care and in such a way that the hydrolysis of the radionuclide (at the desired pH) is reduced to levels which can be ignored in comparison with the concentrations of the other species in the system.

Consider the following competing reactions taking place:

$$M + HA \rightleftharpoons MHA \quad (1)$$

$$M + nL \rightleftharpoons ML_n \quad (2)$$

The stability constants of these reactions are defined as

$$K_{MHA} = \frac{[MHA]}{[M][HA]} \quad (3)$$

$$K_{ML} = \frac{[ML_n]}{[M][L]^n} \quad (4)$$

From Eqns. 3 and 4, the stability constant of the MHA complex can be derived as

$$K_{MHA} = \frac{[MHA]K_{ML}[L]^n}{[ML_n][HA]} \quad (5)$$

where

$K_{MHA}$ = stability constant of the MHA complex (l $eq^{-1}$);
$K_{ML}$ = stability constant of the $ML_n$ complex ($M^{-n}$);
[HA] = concentration of the free HA (eq $l^{-1}$);
[L] = concentration of the free reference ligand (M);
[MHA] = concentration of the radionuclide–HA complex (M);
$[ML_n]$ = concentration of the radionuclide–reference ligand complex (M).

The concentration of humic acids is expressed as equivalents of dissociated functional groups. As will be seen later, the trace metal concentration is many times lower than the ligand concentration, so that the free ligand concentration (L and HA) equals the total ligand concentration.

The ligand exchange technique has been used in the past in combination with spectrophotome-

try [15,16]. The amount of metal complexed by the competing ligand is determined spectrophotometrically. One of the main difficulties with this method is the selection of the competing ligand L, which not only must have the appropriate properties with respect to complexation but also the $ML_n$ complex formed must have favourable spectroscopic properties. Alternatively, the ligand exchange method has been used in combination with a separation technique [17]. The two complexes formed (ML and MHA) are separated and the concentration of the two species can be determined by measuring the metal concentration in both fractions. This increases the choice of the reference ligand compared with the spectroscopic technique because the $ML_n$ complex formed need not have spectroscopic properties. However, only those $ML_n$ complexes which are stable enough and do not dissociate during the separation can be selected.

In the EDLE technique proposed here, equilibrium dialysis is used to distinguish between the metal bound on the reference ligand and the metal bound to the HA. Equilibrium dialysis has been used previously to determine the complexation capacity of humic acids [18,19]. The distribution of a radionuclide between the humic acid and the reference ligand can be measured by equilibrium dialysis provided that the membrane is impermeable to the MHA complex and permeable to the $ML_n$ complex. Basically, there are two compartments separated by a semi-permeable membrane. Compartment 1 contains the HA and the reference ligand and compartment 2 contains only the reference ligand. When a metal is introduced into this system, it will be distributed between the two compartments. At equilibrium, the total concentration of metal M in compartment 1 is

$$C_1 = [MHA] + [ML] + [M] \quad (6)$$

and the total concentration in compartment 2 is

$$C_2 = [ML] + [M] \quad (7)$$

When the concentration of the reference ligand is high enough, the concentration of the free metal, [M], is negligibly small, so that

$$C_1 = [MHA] + [ML] \quad (8)$$

and

$$C_2 = [ML] \quad (9)$$

The concentration of metal bound to the humic acid can be calculated from the difference in concentration:

$$[MHA] = C_1 - C_2 \quad (10)$$

The concentration of metal bound to the reference ligand L is

$$[ML] = C_2 \quad (11)$$

The EDLE method has several advantages. The hydrolysis of the metal is avoided and the stability constants can be measured at higher pH values. The free metal concentration does not need to be measured as in most of the classical techniques for determining stability constants. Depending on pH, ionic strength and the stability of the complex, the free metal concentration can be very small and difficult to measure, introducing relatively large errors. The method is applicable to many metals at very low M/HA ratios. This is important for complexation studies with radionuclides where in many instances their concentrations are low in natural systems.

## EXPERIMENTAL

### *Materials*

A commercial humic acid (Aldrich) was used. The humic acid was first purified by a slightly modified procedure [20]. A 5-g amount of the humic acid was dissolved in 500 ml of solution containing 0.01 M NaOH and 0.048 M NaF. After shaking the suspension for 24 h, the humic acids were precipitated by acidifying the solution to pH 1 with concentrated HCl. The suspension was centrifuged at 10000 *g* for 15 min and the pellet was dissolved in 0.01 M NaOH–0.048 M NaF. The whole procedure was repeated three times. After the last acidification and centrifugation step, the humic acids (in the protonated form) were dialysed against distilled water until

no further $Cl^-$ could be detected by $AgNO_3$, then freeze-dried. After grinding in a PTFE mortar, the HA were stored in a glass vial in a desiccator.

The charge of the humic substances as a function of the pH was estimated from $Co(NH_3)_6^{3+}$ adsorption measurements as described by Maes et al. [21]. A 5-mg amount of the humic acids was mixed in centrifuge tubes with 30 ml of solution of various $Co(NH_3)_6^{3+}$ concentrations, labelled with $^{60}Co$. The pH of all samples was first adjusted to 2.5 with 0.1 M $HClO_4$ to obtain the same pH history over the total pH range for each sample. After this pretreatment, the pH was slowly adjusted to the desired value (3–11) with 0.1 M NaOH. The tubes were closed and shaken end-over-end overnight at room temperature. All manipulations were carried out under a nitrogen atmosphere. At equilibrium, the samples were centrifuged and the supernatant was assayed for $Co(NH_3)_6^{3+}$, organic matter and pH. The amount of adsorbed $Co(NH_3)_6^{3+}$ was calculated from the difference in concentration before and after equilibrium. The major impurities (Si, Fe, Mg, Al, Sr, Ca, Na, Cr) were determined by inductively coupled plasma atomic emission spectrometry (ICP-AES), after digesting the HA sample with $HNO_3$–$H_2O_2$.

*Ion-exchange method*

In the ion-exchange method, the stability constant of an MHA complex is determined by measuring the distribution of the metal between an ion-exchange resin and a solution in presence and absence of the HA. The theory of the ion-exchange method has been extensively described [3,4,22]. The working equation of the ion-exchange method can be expressed as

$$\log\left(\frac{K_d^o}{K_d} - 1\right) = \log K_{MHA} + n \log[HA] - \log A \qquad (12)$$

where

$K_d^o$ = partition coefficient of the metal M in absence of HA (ml $g^{-1}$);

$K_d$ = partition coefficient of the metal M in presence of HA (ml $g^{-1}$);

TABLE 1

Composition of the solutions used in the ion-exchange method at different pH values

| pH | Buffer [a] | HA (mg $l^{-1}$) |
|---|---|---|
| 5 | $AcO^-$–HOAc | 0; 6.25; 12.5; 25; 50; 100 |
| 6 | MES | 0; 6.25; 12.5; 25; 50; 100 |
| 7 | $H_2PO_4^-$–$HPO_4^{2-}$ | 0; 6.25; 12.5; 25; 50; 100 |
| 8 | Tris | 0; 6.25; 12.5; 25; 50; 100 |

[a] See Table 2 for abbreviations.

$K_{MHA}$ = stability constant of the MHA complex ( eq $l^{-1}$);

[HA] = concentration of HA (eq $l^{-1}$);

$n$ = number of ligands per metal atom;

$A$ = $1 + K_{MB}[B]$ = correction term when a buffer B, with complexing properties, has been used; [B] is the concentration of the buffer and $K_{MB}$ is the stability constant of the metal–buffer complex.

A 100-mg amount of a cation-exchange resin (Dowex 50W-X4) in the $Na^+$ form was placed in a centrifuge tube and 20 ml of a solution containing a buffer, $NaClO_4$ and different concentrations of HA were added. The compositions of the solutions used in the ion-exchange method are summarized in Table 1. The volume was made up to 25 ml by adding 5 ml of solution of the same composition but without HA and spiked with $^{60}Co$. The final concentration of Co in the tubes was ca. $10^{-8}$ M. The tubes were shaken end-over-end overnight at room temperature. At equilibrium, the centrifuge tubes were left standing in a vertical position to let the ion-exchange resin settle. The pH was measured and the $^{60}Co$ activity in solution was determined with a sodium iodide gamma counter (Packard, Minaxi $\gamma$, autogamma 5000 series). From the difference in radioactivity before and after equilibrium, the distribution coefficients could be calculated. The stability constants of the Co–HA complex was determined by applying Eqn. 12. The coefficient $n$ was set at 1 (it was assumed that a 1 : 1 complex between the Co and the HA had been formed).

*Selection of the reference ligand*

A crucial factor in the EDLE technique is the choice of the right type and concentration of

reference ligand (L). On the one hand, the radionuclide must show a measurable distribution between L and HA. On the other, in absence of the HA, the metal must be present mainly as the ML complex. Roughly one can say that the ML complex must have about the same stability constant ($\pm 1$ log $K$-unit) as the MHA complex. Under these conditions, the same concentration of HA and L in the system leads to an equal distribution of the radionuclide between L and HA. Published data on MHA stability constants are therefore helpful in choosing the right reference ligand.

After the right reference ligand L has been selected, its concentration has to be calculated. The minimum concentration required can be determined by considering the situation without HA. Here the concentration of L must be chosen so that the radionuclide M is mainly present as the ML complex ($[ML]/[M] \geqslant 0.98$). Geochemical codes such as PHREEQE or MINEQL are very useful for these purposes, especially when the hydrolysis of the radionuclide becomes important. The exact concentration of L depends on the concentration of HA used in the experiments. When no data on the stability constants are available, realistic estimates have to be made. For each pH value, this procedure has to be repeated. It is often a matter of trial and error to choose the right type and concentration of reference ligand. As an example, the case for $Co^{2+}$ at pH 6 and $I = 0.1$ M will be analysed here.

The stability constant (log $K$) of the Co–HA complex at pH 6 and $I = 0.1$ M as determined by an ion-exchange method [23] is ca. 5 ($K = 10^5$ l eq$^{-1}$). The stability constant (log $K$) of the reference ligand should therefore have a value between 4 and 6. Log $K$ for the Co–oxalate complex is 3.9 at $I = 0.1$ M so that oxalate can be selected as a suitable reference ligand. As hydrolysis does not play a significant role at pH 6, the minimum concentration of oxalate required can be calculated as

$$[Ox] = \frac{[CoOx]}{[Co^{2+}] \times 10^{3.9}} \qquad (13)$$

On fixing the ratio $[CoOx]:[Co^{2+}]$ at 40 (97.5% of Co is present as CoOx), the concentration of oxalate is 0.005 M. When an equal distribution of the Co between oxalate and HA is desired, the concentration of the HA in the system has to be

$$[HA] = 1 \times \frac{0.005 \times 10^{3.9}}{10^5} = 0.4 \text{ meq l}^{-1} \qquad (14)$$

With a functional group density of 4 meq g$^{-1}$, the concentration of HA is ca. 100 mg l$^{-1}$. The composition of the solutions used in the complexation studies with Co are summarized in Table 2. Basically, the solutions contain a pH buffer, a reference ligand, humic acids and a neutral salt for ionic strength adjustment. Buffer compounds with no or very low complexing capacities have been selected [24].

TABLE 2

Composition of the solutions used in the EDLE method at different pH values

| pH | Buffer [a] | Reference ligand [a] | HA (mg l$^{-1}$) |
|---|---|---|---|
| 5 | $AcO^-$–HOAc | Oxalate | 0; 20; 50; 100 |
| 6 | MES | Oxalate | 0; 20; 50; 100 |
| 7 | MOPS | Oxalate | 0; 20; 50; 100 |
| 7 | MOPS | IDA | 0; 20; 50; 100 |
| 8 | Tris | IDA | 0; 20; 50; 100 |
| 9.5 | CHES | IDA | 0; 20; 50; 100 |
| 9.5 | $CO_3^-$–$HCO_3^-$ | $CO_3^{2-}$ | 0; 20; 50; 100 |
| 10 | CAPS | IDA | 0; 20; 50; 100 |
| 10 | $CO_3^{2-}$–$HCO_3^-$ | $CO_3^{2-}$ | 0; 20; 50; 100 |

[a] MES = 2-(*N*-morpholino)ethanesulphonic acid; MOPS = 3-(*N*-morpholino)propanesulphonic acid; Tris = tris(hydroxymethyl)aminomethane; CHES = 3-(cyclohexylamino)ethanesulphonic acid; IDA = iminodiacetic acid; CAPS = 3-(cyclohexylamino)propanesulphonic acid; $AcO^-$–HOAc = acetate–acetic acid.

*Equipment*

Figure 1 shows a schematic view of the dialysis cell used. The cell consists of a 50-ml centrifuge tube (Oak Ridge Type, polysulphonate) of which the open end is covered by a dialysis membrane (Dialysis Tubing-Visking, Medicell, London; MW cut-off 10000–14000). The membrane is held firmly in position via a cap, with a circular hole (diameter 18 mm), which is screwed down on the body of the tube. The tube is placed upside down in a 50-ml polyethylene bottle. The inner (centrifuge tube) and outer (bottle) solutions are separated by the membrane.

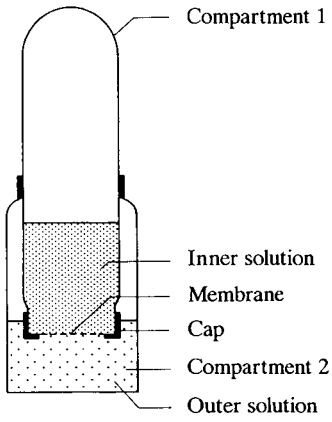


Fig. 1. Schematic diagram of the dialysis cell used for the experiments.

*Measurement of stability constants*

Before the measurements of the conditional stability constants were started, some preliminary experiments to determine the time required to obtain diffusion equilibrium were carried out. For this purpose, a series of diffusion cells were set up as follows. Both the centrifuge tube and the 50-ml bottle were filled with 10 ml of a solution containing 0.01 M $NH_4OAc$ and 0.04 M $NaClO_4$ at pH 7. The solution in the centrifuge tube was spiked with 20 $\mu$l of $^{60}Co$ (634 kBq $ml^{-1}$) solution. The open end of the centrifuge tube was covered by a membrane which was fixed by a cap. The centrifuge tube was placed upside down in the bottle and the cells were shaken gently at a constant temperature of 20°C. At different time intervals, single dialysis cells were opened and 2 ml of both solutions were sampled. The activity of the $^{60}Co$ was determined by gamma counting.

For the determination of the stability constants, 10 ml of the solution designed for the desired conditions of pH and ionic strength (Table 2) were placed in the centrifuge tube and spiked with 20 $\mu$l of $^{60}Co^{2+}$ (634 kBq $ml^{-1}$) solution. The total concentration of $Co^{2+}$ in the solution was ca. $10^{-8}$ M. The 50-ml bottle was filled with 10 ml of the same solution containing no HA. The same sampling and analysis procedures as described earlier were used. At the end of each experiment, the pH of the solutions was measured and the concentration of HA in both compartments was determined by UV measurements at 254 nm (Model 260 optic spectrophotometer, Guided Wave, Inc.). The equipment was calibrated with solutions of the same pH and composition, containing known concentrations of humic acids.

## RESULTS AND DISCUSSION

Table 3 shows the major impurities in the purified and unpurified sample. As can be seen, the purification procedure is effective for removing the major impurities. The ash contents calculated from these levels of impurities are 8.4% for the untreated sample and 0.13% for the purified sample. Kim et al. [20] found analogue ash contents of 10.4% for the untreated Aldrich humic acid sample and 0.07% for the purified sample. The Co content of the sample was not analysed. Kim et al. [20], however, found values of 2.5 mg $kg^{-1}$ for the unpurified sample and 0.33 mg $kg^{-1}$ for the purified sample as determined by neutron activation analysis. Assuming that the same levels of Co are present in our samples of Aldrich HA, the solutions containing the highest HA concentration (100 mg $l^{-1}$) had a concentration of stable Co of $5.6 \times 10^{-10}$ M. This is much lower than the concentration of $^{60}Co$ used in the experiments. Kim et al. [20] also reported that the concentrations of most of the trace elements in the purified sample were lower than 1 mg $kg^{-1}$.

Figure 2 shows the results of the preliminary experiments. The ratio of the concentrations of

TABLE 3

Analysis of the major impurities of a purified and an unpurified Aldrich HA sample by ICP-AES

| Element | Unpurified (mg $kg^{-1}$) | Purified (mg $kg^{-1}$) |
|---|---|---|
| Si | 672 | 89 |
| Fe | 10236 | 633 |
| Mg | 321 | 13 |
| Al | 1809 | 29 |
| Sr | 23 | 1.8 |
| Ca | 4463 | 267 |
| Na | 66330 | 238 |
| Cr | 18 | 26 |

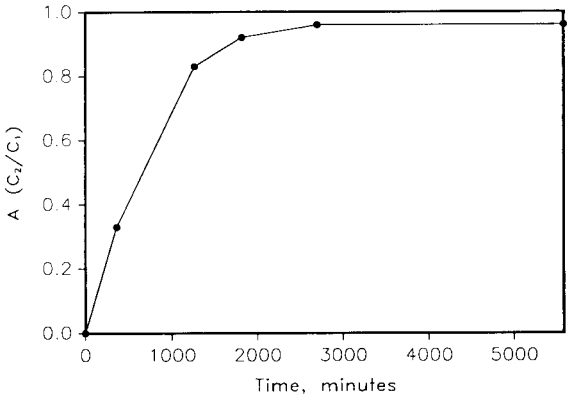


Fig. 2. Evolution of the concentration ratio $A$ as a function of time in a blank experiment.

$^{60}$Co in the two solutions is plotted as a function of the equilibration time. At diffusion equilibrium, the ratio should be exactly 1. As can be seen, the ratio reaches a maximum value of 0.96 after 2 days. The system therefore does not reach complete diffusion equilibrium. Based on these preliminary experiments, an equilibration time of 4 days was chosen for all subsequent experiments. As was seen in later experiments, this time was sufficiently long to obtain equilibrium for the complexation process.

In the experiments with HA, the difference in concentration in the two compartments is caused by two facts: part of the Co is bound to the HA and the diffusion on the CoL complex has not yet reached equilibrium. The degree of non-equilibrium is always determined by running blank experiments, in which the same solutions are used but without HA. The following procedure was applied to correct for the non-equilibrium state. From the blank experiments, the degree of equilibrium ($A$) can be derived as

$$A = C_2^b / C_1^b \quad (15)$$

where $C_1^b$ and $C_2^b$ represent the concentration of Co in the first and the second compartment for the blank experiments. To determine the amount of radionuclide bound on the humic acid, the measured concentrations have to be corrected, or the concentration of radionuclide in both compartments at real diffusion equilibrium has to be calculated. Assume that the measured concentration of the radionuclide is $C_1$ in compartment 1 and $C_2$ in the second compartment. The nuclide in the second compartment is present as the reference complex, its concentration being a fraction $A$ of the reference complex concentration in compartment 1. The equilibrium concentration of the reference complex in compartment 2 ($C_2^{eq}$) can be calculated as

$$C_2^{eq} = (C_2 + C_2/A)/2 \quad (16)$$

The equilibrium concentration of the nuclide in the first compartment ($C_1^{eq}$) is

$$C_1^{eq} = C_1 - (C_2^{eq} - C_2) \quad (17)$$

where $C_2^{eq}$ and $C_1^{eq}$ are the concentrations of the radionuclide that can be expected at real diffusion equilibrium. From these corrected concentrations, the amount of the radionuclide bound on the humic acid can be calculated as the difference in corrected concentrations between the two compartments. Generally, the corrections to be made are low. After 4 days equilibrium time, the concentration ratio $A$ in the blank experiments usually reaches values between 0.9 and 1.0.

The relative amounts of humic acids which actually passed through the membrane during the

TABLE 4

Overview of the amount of humic acid diffused through the membrane during the experiments (percentage of total % $\pm \sigma$, $n = 9$)

| $I$ (M) | pH 5 | pH 6 | pH 7 | pH 8 | pH 8.8 | pH 10 |
|---|---|---|---|---|---|---|
| 0.02 | 8.2 ± 3.5 | 7.2 ± 2.3 | 13.7 ± 6.9 | 8.4 ± 1.8 | 7.7 ± 3.3 | 5.8 ± 1.1 |
| 0.05 | 6.9 ± 3.9 | 6.5 ± 3.0 | 10.9 ± 3.4 | 10.1 ± 1.8 | 10.1 ± 5.0 | 10.1 ± 4.9 |
| 0.1 | 8.6 ± 3.9 | 8.4 ± 3.8 | 10.5 ± 1.2 | 7.0 ± 2.9 | 11.9 ± 2.2 | 8.9 ± 2.8 |
| 0.2 | 10.4 ± 2.9 | 12.6 ± 3.6 | 9.4 ± 2.1 | 14.2 ± 2.3 | 12.4 ± 3.8 | 11.4 ± 2.3 |

course of the experiments (4 days) are summarized in Table 4. Depending on the pH and the ionic strength, up to a maximum of 15% of the HA present in compartment 1 diffuses through the membrane. This process causes a decrease in the HA concentration in compartment 1 and an increase in compartment 2. Formally, this means that Eqn. 10 is no longer valid as the presence of humic acids in the second compartment may change the speciation of the radionuclide. However, in practice, the concentration of the reference ligand is high compared with the HA concentration in this compartment, and the speciation of the radionuclide will be predominantly determined by the reference ligand. It was calculated that if up to 10% of the Co concentration in the second compartment is present as HA complexes, then this leads to an error of ca. 2% in the stability constants (log $K$) calculated from Eqn. 10. Hence we conclude that the diffusion of small amounts of HA through the membrane is acceptable and does not significantly interfere with the measurements, provided that the experimental conditions are correctly chosen.

Figures 3 and 4 show the distribution of $^{60}Co$ between HA and reference ligands, oxalate and $CO_3^{2-}$, respectively, at different pH values as obtained by the dialysis technique. There is a clearly defined distributrion between the HA and the reference ligand. As the concentration of HA is increased, there is a proportional shift in the

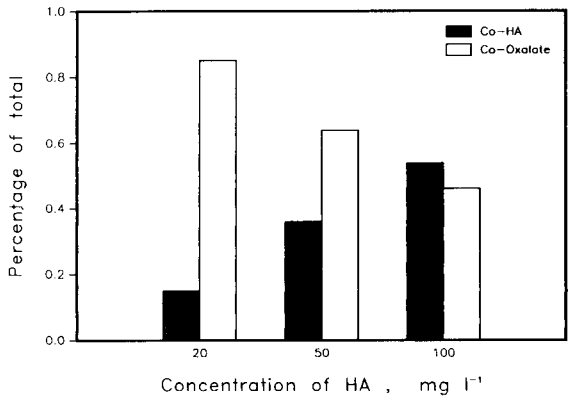


Fig. 3. Distribution of $^{60}Co^{2+}$ between oxalate and HA at pH 6 and $I$ = 0.02 M ([oxalate] = 5 mM).

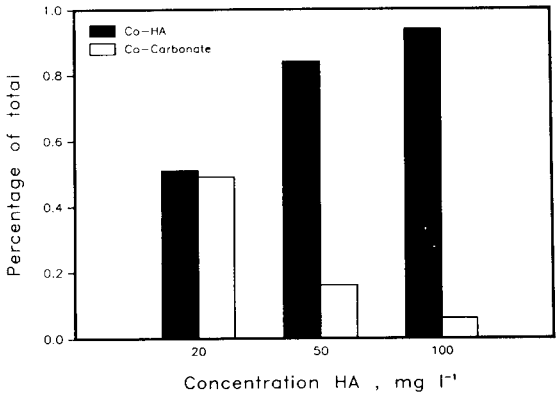


Fig. 4. Distribution of $^{60}Co^{2+}$ between carbonate and HA at pH 9.94 and $I$ = 0.02 M ([carbonate] = 4.5 mM).

speciation from the reference ligand to the HA, i.e., doubling the concentration of HA causes a doubling of the MHA/ML ratio. This is in agreement with what would be expected from Eqn. 5.

In order to optimize the accuracy of the measurements, it is desirable to choose the experimental conditions such that an MHA/ML ratio between 0.2 and 5 will be achieved. Below or above these ratios, the radionuclide is mainly present as the reference complex or HA complex. Ratios lying beyond this range can still be used, but may result in larger errors.

Clearly, the accuracy of the measured stability constant depends strongly on the accuracy of the constants used for the reference complexes. Therefore, these constants have to be selected carefully from the literature or have to be measured. Table 5 gives an overview of some selected data on stability constants of the Co complexes

TABLE 5

Overview of the stability constants of different Co–reference ligand complexes used for estimating Co–HA stabilities.

| Reference ligand | Log $K_1$ | Log $\beta_2$ | Ref. |
|---|---|---|---|
| Oxalate | 4.69 | 7.15 | 26, 27 |
| | 4.75 | 6.91 | 26, 27 |
| | 4.66 | | 25 |
| | 4.64 | | 26, 27 |
| IDA | 7.90 | 13.51 | 23 |
| | 7.81 | 13.15 | 26, 27 |
| $CO_3^{2-}$ | 6.56 | 9.91 | Estimated |

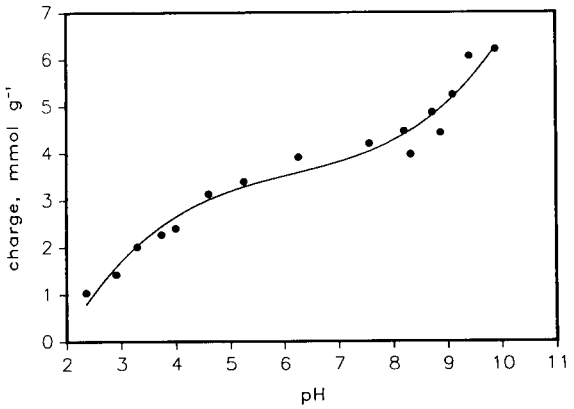


Fig. 5. Change in the surface charge of HA as a function of pH as determined by the adsorption of $Co(NH_3)_6^{3+}$.

for the ligands used in the experiments. Some of the constants were determined by ourselves using the ion-exchange method [23,25] and are in excellent agreement with values reported in the literature [26,27]. The values for the Co–carbonate complexes were estimated from the stability constants for Ni–carbonate [28] by applying a linear correlation between the stability constants of Co–carboxylic acid complexes and Ni–carboxylic acid complexes.

The Co–HA complexes were assumed to be 1:1 and the stability constant was calculated by applying Eqn. 5. As the molecular weight of the humic acid was unknown, its concentration was expressed in mmol $l^{-1}$ (or meq $l^{-1}$) of deprotonated functional groups. This concentration depends on the pH and to a lesser extent on the ionic strength of the solution. Figure 5 shows the variation of the surface charge of the HA as a function of the pH as determined with $Co(NH_3)_6^{3+}$. As discussed by Maes et al. [21], this corresponds to the amount of deprotonated groups on the HA molecule. At pH 7, the deprotonation curve reaches a plateau level of ca. 3.5–4 mmol $g^{-1}$. At this stage, all the carboxylic groups have been deprotonated. Beyond pH 8, weaker acidic groups such as phenolic groups ($pK_H \approx 9.5$) start to deprotonate and cause a further increase in the charge. For each pH value, one can deduce from this curve the amount of deprotonated groups and consequently the concentration of HA that has to be used in Eqn. 5. Between pH 5 and 10, the amount of deprotonated functional groups ranges from 3 to 6 mmol

TABLE 6

Conditional stability constants of the Co–HA complex between pH 5 and 10 and ionic strength values between 0.02 and 0.2 M

| Method [a] | $I = 0.02$ M | | $I = 0.05$ M | | $I = 0.1$ M | | $I = 0.2$ M | |
|---|---|---|---|---|---|---|---|---|
| | pH ($\pm\sigma$ [b]) | Log $K$ ($\pm\sigma$ [b]) | pH ($\pm\sigma$ [b]) | Log $K$ ($\pm\sigma$ [b]) | pH ($\pm\sigma$ [b]) | Log $K$ ($\pm\sigma$ [b]) | pH ($\pm\sigma$ [b]) | Log $K$ ($\pm\sigma$ [b]) |
| A | 5.09 ± 0.01 | 4.97 ± 0.15 | 5.10 ± 0.02 | 4.53 ± 0.14 | 5.04 ± 0.01 | 3.95 ± 0.20 | 5.02 ± 0.01 | 3.53 ± 0.14 |
| | 6.02 ± 0.01 | 5.36 ± 0.25 | 5.99 ± 0.01 | 4.89 ± 0.29 | 6.00 ± 0.01 | 4.65 ± 0.24 | 6.00 ± 0.01 | 4.25 ± 0.29 |
| | 7.37 ± 0.01 | 6.20 ± 0.21 | 7.27 ± 0.01 | 5.79 ± 0.26 | 7.23 ± 0.01 | 5.28 ± 0.22 | 7.07 ± 0.01 | 4.94 ± 0.15 |
| | 8.10 ± 0.01 | 6.31 ± 0.26 | 8.02 ± 0.01 | 6.00 ± 0.23 | 8.01 ± 0.01 | 5.79 ± 0.31 | 8.00 ± 0.01 | 5.51 ± 0.32 |
| B | 5.06 ± 0.02 | 5.03 ± 0.13 | 5.00 ± 0.01 | 4.90 ± 0.08 | 5.11 ± 0.02 | 4.40 ± 0.05 | 5.03 ± 0.04 | 4.17 ± 0.16 |
| | 6.08 ± 0.01 | 5.63 ± 0.10 | 6.01 ± 0.01 | 5.23 ± 0.09 | 5.99 ± 0.01 | 5.00 ± 0.10 | 6.02 ± 0.01 | 4.93 ± 0.08 |
| | 6.92 ± 0.02 | 5.70 ± 0.16 | 6.94 ± 0.02 | 5.50 ± 0.13 | 6.95 ± 0.01 | 5.32 ± 0.12 | 7.08 ± 0.01 | 5.09 ± 0.09 |
| C | 6.01 ± 0.01 | 5.02 ± 0.12 | 5.96 ± 0.01 | 4.90 ± 0.11 | 5.94 ± 0.01 | 4.76 ± 0.11 | 5.96 ± 0.01 | 4.59 ± 0.15 |
| | 6.83 ± 0.02 | 5.79 ± 0.15 | 6.92 ± 0.02 | 5.51 ± 0.24 | 6.90 ± 0.04 | 5.62 ± 0.16 | 6.84 ± 0.01 | 5.28 ± 0.22 |
| | 7.95 ± 0.01 | 6.80 ± 0.16 | 7.96 ± 0.01 | 6.70 ± 0.12 | 7.95 ± 0.01 | 6.34 ± 0.09 | 8.03 ± 0.02 | 6.20 ± 0.06 |
| | 8.84 ± 0.07 | 7.36 ± 0.13 | 8.86 ± 0.05 | 7.13 ± 0.44 | 8.75 ± 0.10 | 7.04 ± 0.09 | 8.73 ± 0.09 | 7.08 ± 0.07 |
| | 8.87 ± 0.05 | 7.66 ± 0.26 | 8.87 ± 0.06 | 7.13 ± 0.13 | 8.83 ± 0.13 | 7.07 ± 0.16 | 8.83 ± 0.14 | 6.83 ± 0.07 |
| | 9.42 ± 0.12 | 8.39 ± 0.34 | 9.39 ± 0.09 | 8.51 ± 0.40 | 9.69 ± 0.12 | 7.99 ± 0.18 | 9.56 ± 0.12 | 7.61 ± 0.08 |
| | 9.73 ± 0.13 | 8.28 ± 0.12 | 9.77 ± 0.09 | 8.40 ± 0.14 | 9.81 ± 0.08 | 8.08 ± 0.23 | | |
| D | 8.82 ± 0.19 | 7.38 ± 0.24 | | | | | 8.87 ± 0.05 | 6.67 ± 0.19 |
| | 9.91 ± 0.04 | 9.13 ± 0.26 | 9.84 ± 0.05 | 8.55 ± 0.20 | 9.78 ± 0.04 | 8.31 ± 0.27 | 9.89 ± 0.02 | 8.69 ± 0.27 |
| | 9.94 ± 0.04 | 8.81 ± 0.21 | | | | | 9.90 ± 0.03 | 8.40 ± 0.14 |

[a] (A) Ion-exchange method; (B) EDLE (oxalate); (C) EDLE (IDA); (D) EDLE ($CO_3^{2-}$). [b] $n = 9$.

$g^{-1}$. For simplicity, we used a constant value of 4 mmol $g^{-1}$. This causes an error in the calculation which is maximum at the boundary values of the pH range used in the experiments, i.e., 5 and 10, respectively. At pH 10, the conditional stability constants have been overestimated by 0.17 log $K$ and at pH 5 the effective stability constants have been underestimated by 0.12 log $K$. For pH values between 5 and 10, lower errors have a risen. The use of a pH-independent concentration of HA therefore introduces only small errors in the log $K$ values.

Table 6 summarizes the measured conditional stability constants at different pH and ionic strength values. The values are the mean values of nine measurements. As can be seen, the two methods produce comparable results. The ion-exchange method, however, always gives lower values than the EDLE technique. Also, the use of different reference complexes under nearly the same pH and ionic strength conditions results in comparable stability constants. As already mentioned, the value of the stability constant for the reference complex used in the calculations is very important and determines the accuracy of the stability constant of the MHA complex.

Figure 6 shows a graphical representation of the pH dependence of the stability constants ($I$ = 0.1 M) of the Co–HA complex at trace concentrations of $Co^{2+}$ ([Co] $\approx 10^{-8}$ M). Each point on the curve represents the mean value of nine measurements. The conditional stability constant (log $K_1$) of the Co–HA complex increases nonlinearly with pH, mainly because of the progressive deprotonation of the functional groups on the HA macromolecule with increasing pH. A quantitative explanation of the observed phenomena requires models that take into account bonding site heterogeneity (chemical term) and also electrostatic effects [29,30–32]. Because this would be outsite the scope of this paper, the discussion will be restricted to a qualitative interpretation of the observed phenomena, i.e., to explain roughly the pH dependence observed for the conditional stability constants.

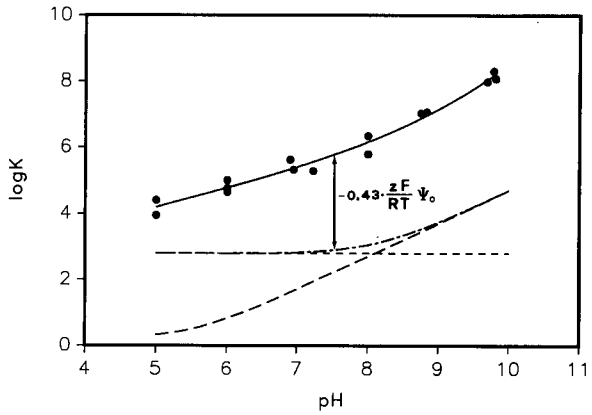


Fig. 6. Change in the overall conditional stability constant ($K_{ov}$, $I = 0.1$ M) and the intrinsic stability constant ($K^{int}_{CoHA}$) of the Co–HA complex as a function of pH. •, Experimental points (log $K_{ov}$); ------, $SO_1^{2-}$ only; — — —, $SO_2^{2-}$ only; –·–·–, $SO_1^{2-} + SO_2^{2-}$.

According to Gamble et al. [33] and Tipping et al. [34], phthalic acid ($SO_1^{2-}$) and salicylic acid ($SO_2^{2-}$) types of sites are present in the HA molecule and are responsible for the binding of metals on the HA. The overall binding of $Co^{2+}$ with the humic acid can be written as

$$Co + HA \rightleftharpoons CoHA \tag{18}$$

This reaction can also be written in terms of the different groups responsible for the bonding:

$$SO_1^{2-} + Co^{2+} \rightleftharpoons SO_1Co \quad K_{CoSO_1} = 2.8 \tag{19}$$

$$SO_2^{2-} + Co^{2+} \rightleftharpoons SO_2Co \quad K_{CoSO_2} = 7.7 \tag{20}$$

The overall intrinsic stability constant is defined as

$$K^{int}_{CoHA} = \frac{[CoHA]}{[Co^{2+}][HA]} \tag{21}$$

$$K^{int}_{CoHA} = \frac{[CoSO_1] + [CoSO_2]}{[Co^{2+}]([SO_1^{2-}] + [SO_2^{2-}])} \tag{22}$$

$$K^{int}_{CoHA} = K_{CoSO_1} \cdot \frac{[SO_1^{2-}]}{[SO_1^{2-}] + [SO_2^{2-}]} + K_{CoSO_2} \cdot \frac{[SO_2^{2-}]}{[SO_1^{2-}] + [SO_2^{2-}]} \tag{23}$$

The amount of $SO_1^{2-}$ and $SO_2^{2-}$ depends on the

pH and can be evaluated according the following reactions:

$$SO_1^{2-} + H^+ \rightleftharpoons SO_1H^- \quad K^1_{H1} = 5.5 \tag{24}$$

$$SO_1H^- + H^+ \rightleftharpoons SO_1H_2 \quad K^1_{H2} = 2.9 \tag{25}$$

and

$$SO_2^{2-} + H^+ \rightleftharpoons SO_2H^- \quad K^2_{H1} = 13 \tag{26}$$

$$SO_2H^- + H^+ \rightleftharpoons SO_2H_2 \quad K^2_{H2} = 2.9 \tag{27}$$

Combination of Eqns. 23 and 24–27 gives an expression for the overall stability constant of the Co–HA complex as a function of pH. Figure 6 is a graphical representation of this expression for the cases where only $SO_1^{2-}$, $SO_2^{2-}$ or both groups are involved in the binding process. The case where both groups are involved gives the most satisfactory results. At low pH, the cobalt is mainly associated with the $SO_1^{2-}$ groups and at high pH $Co^{2+}$ prefers to bind at the $SO_2^{2-}$ sites. The predicted values, however, are always lower than the experimental values, the difference being smaller at low pH values and becoming larger with increasing pH. This difference can be explained by an electrostatic term.

The observable change in Gibbs free energy related to the complexation process is split into two terms according to

$$\Delta G_{compl} = \Delta G_{int} + \Delta G_{coulombic} \tag{28}$$

where

$$\Delta G_{compl} = -2.3RT \log K_{ov} \tag{29}$$

and

$$\Delta G_{int} = -2.3RT \log K^{int}_{CoHA} \tag{30}$$

$\Delta G_{coul}$ is the energy required to bring a $Co^{2+}$ ion from the bulk of the solution to a surface site ($SO_1^{2-}$ and/or $SO_2^{2-}$) at potential $\Psi_0$ [35]. Hence

$$\Delta G_{coul} = zF\Psi_0 \tag{31}$$

where $z$ is the charge number of the ion under consideration ($z = 2$ for $Co^{2+}$). The combination of Eqns. 28–31 results in

$$\log K_{ov} = K^{int}_{CoHA} - \frac{zF}{2.3RT}.\Psi_0 \tag{32}$$

The overall conditional stability constant ($K_{ov}$) is the sum of an intrinsic constant and an electrostatic term. Since the surface charge and consequently also the surface potential of the humic acid increases with pH, the electrostatic term will increase with increasing pH. This explains the increasing difference between the predicted ($K^{int}_{CoHA}$) and observed ($K_{ov}$) data in Fig. 6. The contribution of the electrostatic term to the overall conditional stability constant is important and can be as large as the chemical term. For the evaluation of the electrostatic term, different models are available [30–32]. However, this is beyond the scope of this paper and will be treated elsewhere.

*Conclusions*

The combination of two classical techniques, equilibrium dialysis and ligand exchange, seems to be a promising method for the determination of stability constants of radionuclide–HA complexes over broad pH and ionic strength ranges. The main advantage of the technique is that the stability constant can be determined under neutral and slightly alkaline conditions, typical of many environmental systems of interest for safety assessment studies. The method is applicable to any radioisotope and/or metal that can be determined by atomic absorption spectrometry or inductively coupled plasma mass spectrometry, provided that suitable reference complexes for these metals are available.

The evolution of the conditional stability constant as a function of pH and ionic strength must be explained by assuming a site heterogeneity and probably electrostatic effects.

This work was supported financially by the Swiss National Cooperative for the Storage of Radioactive Wastes, NAGRA. The authors thank A. Dierckx and Dr. A. Maes (Catholic University Leuven, Belgium) for the surface charge measurements and Dr. R. Grauer and Dr. M. Bradbury (Paul Scherrer Institute) for their comments on the manuscript.

REFERENCES

1 S. Boggs, Jr., D. Livermore and M.G. Seitz, Humic Substances in Natural Waters and their complexation with

Trace Metals and Radionuclides: a Review, ANL-84-78 Argonne National Laboratory, Argonne, IL, 1985.
2 R.A. Saar and J.H. Weber, Environ. Sci. Technol., 16 (1982) 510A.
3 F.J. Stevenson, Humus Chemistry: Genesis, Composition, Reactions, Wiley, New York, 1982, Chap. 13.
4 J. Buffle, Complexation Reactions in Aquatic Systems: an Analytical Approach, Horwood, Chichester, 1988, Chap. 5.
5 V. Moulin, P. Robouch and P. Vitorge, Inorg. Chim. Acta, 140 (1987) 303.
6 J.I. Kim, H. Wimmer and R. Klenze, Radiochim. Acta, 54 (1991) 35.
7 J.I. Kim, G. Buckau, E. Bryant and R. Klenze, Radiochim. Acta, 48 (1989) 135.
8 R.A. Torres and G.R. Choppin, Radiochim. Acta, 35 (1984) 143.
9 E.L. Bertha and G.R. Choppin, J. Inorg. Nucl. Chem., 40 (1978) 655.
10 V. Moulin, P. Robouch, P. Vitorge and B. Allard, Radiochim. Acta, 44/45 (1988) 33.
11 K.L. Nash and G.R. Choppin, J. Inorg. Nucl. Chem., 42 (1980) 1045.
12 M. Caceci, Radiochim. Acta, 39 (1985) 51.
13 P.M. Shanbag and G.R. Choppin, J. Inorg. Nucl. Chem., 43 (1981) 3369.
14 A. Maes, J. De Brabandere and A. Cremers, Radiochim. Acta, 44/45 (1988) 51.
15 J.R. Tuschall, Jr., and P.L. Brezonik, Anal. Chim. Acta, 149 (1983) 47.
16 R.B. Fulton and B. Kratochvil, Anal. Chem., 52 (1980) 546.
17 K. Hirose, Y. Doliya and Y. Sugimura, Mar. Chem., 11 (1982) 343.
18 R.E. Truitt and J.H. Weber, Anal. Chem., 53 (1981) 337.
19 W.C. Li, D.M. Victor and C.L. Chakrabarti, Anal. Chem., 52 (1980) 520.
20 J.I. Kim, G. Buckau, G.H. Li, H. Duschner and N. Psarros, Fresenius' J. Anal. Chem., 338 (1990) 245.
21 A. Maes, F. Van Elewijck, J. Vancluysen, J. Tits and A. Cremers, in B. Allard, H. Borén and A. Grimvall (Eds.), Lecture Notes in Earth Sciences, Vol 33, Springer, Berlin, 1991, p. 85.
22 F. Van Elewijck, Humic Acid Chemistry of Cadmium in Podzol $B_h$ and Boom Clay, Dissertationes de Agricultura No. 187, Department of Agriculture, Catholic University of Louvain, Louvain, 1990.
23 L.R. Van Loon, unpublished results, 1991.
24 D.D. Perrin and B. Dempsey, Buffers for pH and Metal Ion Control, Chapman and Hall, London, 1974, p. 176.
25 L.R. Van Loon and Z. Kopajtic, Radiochim. Acta, 54 (1991) 193.
26 L.G. Sillen and A.E. Martell, Stability Constants of Metal-Ion Complexes, Special Publication 25, Chemical Society, London, 1971.
27 S. Kotrly and L. Sucha, Handbook of Chemical Equilibria in Analytical Chemistry, Horwood, Chichester, 1985, p. 414.
28 B. Baeyens and M.G. McKinley, A PHREEQE Database for Pd, Ni and Se, PSI Report 34 and NAGRA NTB 88–28, Paul Scherrer Institute, Villigen, 1989.
29 F.R.M.J. Cleven, PhD Thesis, Agricultural University, Wageningen, 1984.
30 J.C.M. de Wit, W.H. van Riemsdijk, M.M. Nederlof, D.G. Kinniburgh and L.K. Koopal, Anal. Chim. Acta, 232 (1990) 189.
31 J.C.M. de Wit, M.M. Nederlof, W.H. van Riemsdijk and L.K. Koopal, Water Air Soil Pollut. 57–58 (1991) 339.
32 B.M. Bartschat, S.E. Cabaniss and F.M.M. Morel, Environ Sci. Technol., 26 (1992) 284.
33 D.S. Gamble, A.W. Underdown and C.H. Langford, Anal. Chem., 52 (1980) 1901.
34 E. Tipping, C.A. Backes and M.A. Hurley, Water Res., 22 (1988) 597.
35 P.W. Schindler and W. Stumm, in W. Stumm (Ed.), Aquatic Surface Chemistry: Chemical Processes at the Particle-Water Interface, Wiley, New York, 1987, p. 83.

*Analytica Chimica Acta*, 268 (1992) 247–254
Elsevier Science Publishers B.V., Amsterdam



# Relationships between the reversed-phase liquid chromatographic retention characteristics and physico-chemical parameters of some β-casomorphin peptides

Franka Kálmán

*Bioorganic Chemistry, Martin-Luther University, Halle-Wittenberg (Germany)*

Tibor Cserháti and Klára Valkó

*Central Research Institute for Chemistry, Hungarian Academy of Sciences, P.O. Box 17, H-1525 Budapest (Hungary)*

Klaus Neubert

*Bioorganic Chemistry, Martin-Luther University, Halle-Wittenberg (Germany)*

(Received 24th March 1992; revised manuscript received 21st May 1992)

**Abstract**

Log $k'_w$ and slope values for ten β-casomorphin peptides were calculated in ten different reversed-phase liquid chromatographic systems using methanol as organic modifier. The differences between the retention behaviours of $C_8$, $C_{18}$ and $C_{30}$ columns were fairly small the eluent composition had a greater impact than the length of the hydrophobic ligand on the retention of peptides. A quaternary amino column showed considerably different retention characteristics. The results suggest that each substructure in the peptides makes a similar contribution to the overall retention of the peptide. The retention parameters of peptides mainly correlated with their electronic and steric characteristics. This finding emphasizes the importance of the electrostatic interactions between the free silanol groups on the surface of the reversed-phase support and the polar substructures of peptides.

*Keywords:* Liquid chromatography; Casomorphin peptides; Peptides

In recent years, reversed-phase liquid chromatography (RPLC) has been widely used as a rapid, precise means for determining physico-chemical properties of organic molecules, which are correlated with the biological activity [1,2]. Reversed-phase, size-exclusion, ion-exchange and affinity LC are available for separations of peptides [3]. The retention in RPLC is governed mostly by hydrophobic interactions, and the method is therefore applicable to the determination of the lipophilicity of the molecules. In RPLC the retention of a solute generally decreases linearly with increasing concentration of the organic component of the eluent. To increase the accuracy of the determination of lipophilicity, linear correlations between the retention values and the concentration of the organic component of the eluent have been calculated. The retention value extrapolated to zero organic component concentration is regarded as the most accurate estimate of lipophilicity [4].

*Correspondence to:* T. Cserháti, Central Institute for Chemistry, Hungarian Academy of Sciences, P.O. Box 17, H-1525 Budapest (Hungary).

The application of multivariate mathematical–statistical methods to interpret large data sets is one of the major advances in chromatography in recent years. The retention of a solute depends on many factors such as the support characteristics (specific surface area, specific pore volume, average pore diameter [5], surface pH value [6,7], etc.), eluent characteristics (dipole moment, dielectric constant, molar refractivity of the solvents [6], etc.) and the characteristics of the solute or its substituents (lipophilicity, polarity, specific hydrophilic [9] and hydrophobic surface areas [10], etc.). Stepwise regression analysis [11] is suitable for selecting the chromatographic and/or solute characteristics that significantly influence the retention behaviour. Principal component analysis (PCA) [2] takes the retention strength and selectivity simultaneously into consideration. PCA situates the eluents or solutes in a multi-dimensional space whose dimensions correspond to the number of principal components. As the human brain cannot think in multi-dimensional space, the non-linear mapping technique [13] reduces the dimensions to two in such a manner that the distances between the points (eluents or solutes) on the two-dimensional surface correspond to their distances in the multi-dimensional space. The resulting maps reveal the solutes or eluent systems clustered according to the retention strength and selectivity. The coordinates of the non-linear map have no concrete physico-chemical meaning, they only indicate the distribution of the eluent systems or solutes in the two-dimensional surface.

The advantage of PCA in chromatography has been discussed recently [14,15]. Sometimes it is desirable to separate the eluent strength from eluent selectivity or, for solutes, the retention strength from the selectivity of the retention. With the help of the technique of spectral mapping [16] it is possible to calculate first the order of eluent strength (called potency in the spectral mapping technique) and then the eluent selectivity (called: spectra). The calculation can be carried out not only for the eluents but also for the solutes, where the potency refers to the retention strength and the spectra to the selectivity of retention [17,18].

The β-casomorphins, representing a fragment of bovine milk protein, are distinguished by their opioid properties [19]. The amino acid sequence and the enzymatic stability of β-casomorphins are different from those of other opioid peptides, such as enkephalins, endorphins, dynorphins and dermorphins. The pentapeptide Tyr–Pro–Phe–Pro–Gly (β-casomorphin-5) is the most potent compound of this new group of opiate peptides. Structural modifications by substitution of D-amino acids and other amino acid residues in different positions of the β-casomorphin sequence result in remarkable differences in their opiate activity. Studies of the physico-chemical parameters of β-casomorphin analogues may make some contributions to the structure–activity relationships of these compounds.

The objectives of these investigations were to determine the retention parameters of some structurally modified β-casomorphin peptides in RPLC under various conditions, to classify the LC systems according to their retention characteristics and to find correlations between the retention properties and physico-chemical parameters of the investigated peptides.

## EXPERIMENTAL

The chromatographic system consisted of a Merck–Hitachi L-6200 LC pump, and L-4000 UV detector, an AS-2000 autosampler and a D-2500 chromato-integrator. The detection wavelength was set at 220 nm and the flow-rate was 0.8 ml $min^{-1}$. All of the measurements were carried out

TABLE 1

Parameters of the columns used in the experiments [a]

| No. | Ligand type | Batch | Carbon loading (%) | Nitrogen (loading (%) |
|---|---|---|---|---|
| 1 | $C_8$ | 31088 | 8.91 | 0 |
| 2 | $C_{18}$ | 15105 | 14.80 | 0 |
| 3 | $C_{30}$ | 17019 | 14.19 | 0 |
| 4 | $C/N_{14}$ | 06030 | 15.8 | 1.05 |

[a] Each column was purchased from Serva and had the dimensions 250×4.6 mm i.d., and was packed with stationary phase of 5-μm particle size and 100-Å pore size.

TABLE 2

Reversed-phase LC systems used for studying the retention behaviour of peptides

| No. of system | Column | Eluent composition | | pH |
|---|---|---|---|---|
| | | Aqueous component [a] | Organic component | |
| 1 | $C_8$ | 0.02 M $CH_3COONa$ 0.06% TFA | 44–52% methanol | 3.55 |
| 2 | $C_8$ | 0.02 M $CH_3COONa$ 0.06% TFA | 40–52% methanol 0.25% *n*-octanol | 3.55 |
| 3 | $C_8$ | 0.02 M $KH_2PO_4$ | 40–50% methanol | 3.00 |
| 4 | $C_8$ | 0.02 M $KH_2PO_4$ | 35–55% methanol | 4.50 |
| 5 | $C_8$ | 0.02 M $KH_2PO_4$ | 42–55% methanol | 6.50 |
| 6 | $C_8$ | 0.02 M $KH_2PO_4$ | 42–50% methanol | 7.20 |
| 7 | $C_{18}$ | 0.02 M $CH_3COONa$ 0.06% TFA | 40–52% methanol | 3.55 |
| 8 | $C_{18}$ | 0.02 M $CH_3COONa$ 0.06% TFA | 42–50% methanol 0.25% *n*-octanol | 3.55 |
| 9 | $C/N_{14}$ | 0.02 M $CH_3COONa$ 0.06% TFA | 29–35% methanol | 3.55 |
| 10 | $C_{30}$ | 0.02 M $CH_3COONa$ 0.06% TFA | 40–52% methanol 0.25% *n*-octanol | 3.55 |

[a] TFA = trifluoroacetric acid.

at 25°C. The samples were dissolved in the eluent at about 1 mg $ml^{-1}$ concentration and 20 $\mu$l of solution were injected. The column dead time was determined from the retention of sodium nitrate. The parameters of the prepacked reversed-phase columns used in this study are summarized in Table 1 and the RPLC conditions are given in Table 2. The $\beta$-casomorphin peptides were synthesized by step-by-step elongation from the *C*-terminal end [19]. The structures of the peptides are shown in Table 3.

TABLE 3

Structures of some $\beta$-casomorphin peptides

| No. of peptide | Structure |
|---|---|
| I | H-Tyr-Pro-Phe-Pro-Gly-Pro-Ile-OH |
| II | H-Tyr-Pro-Phe-Pro-Gly-OH |
| III | H-Tyr-D-Pro-Phe-Pro-Gly-OH |
| IV | H-Tyr-Pro-D-Phe-Pro-Gly-OH |
| V | H-Tyr-Pro-Phe-D-Pro-Gly-OH |
| VI | H-Tyr-D-Ala-Phe-Pro-Gly-OH |
| VII | H-Tyr-D-Ala-Phe-D-Pro-Gly-OH |
| VIII | H-D-Tyr-Pro-D-Phe-Pro-Gly-OH |
| IX | H-Phe-Pro-Phe-D-Pro-Gly-OH |
| X | H-Phe-Pro-D-Phe-Pro-Gly-OH |

*Mathematical methods*

Linear correlations were calculated between the log $k'$ values and the organic phase concentration ($C$, vol. %) in the eluent separately for each peptide in each LC system (total 100 equations):

$$\log k' = \log k'_w - SC \quad (1)$$

where $S$ is the slope. The parameters of Eqn. 1 (slope and intercept values) were correlated with each other in order to reveal structural similarities of the investigated peptides regarding their partition behaviour in the RPLC systems [20]. The spectral mapping technique was applied to separate the retention strengths (potencies) and retention selectivities (spectra) of peptides taking into consideration simultaneously the intercept and slope values. The ten LC systems and the parameters of Eqn. 1 were the variables and the observations of the data matrix, respectively. The transversed data matrix served to separate the retention strengths and selectivities of the LC systems. The non-linear selectivity maps were calculated in both instances.

PCA was was used to determine the similarities and dissimilarities of peptides and LC sys-

tems taking into consideration simultaneously the retention strength and selectivity. PCA was carried out separately for the intercept and slope values of Eqn. 1. To avoid possible information loss caused by the normalization, the calculations were carried out on the covariance and not on the correlation matrix. The non-linear map of PC loadings and PC components was calculated in both instances.

To find the relationships between the retention behaviour of peptides and their physicochemical parameters, stepwise regression was applied. The parameters of Eqn. 1, the coordinates of the spectral map and the non-linear PC maps were taken as dependent variables. The hydrophobicity ($z_1$), side-chain bulk ($z_2$) and electronic properties ($z_3$) of peptides were calculated by summarizing the corresponding published values of the individual amino acid side-chains [21] and were considered as independent variables. To avoid speculative and unrestricted conclusions due to the small number of observations, the

TABLE 4

Parameters of linear correlations between the log $k'$ values of $\beta$-casomorphin peptides and the concentration ($C$) of the organic component in the eluent: log $k' = \log k'_w - SC$

| No of peptide [a] | Parameter | No. of HPLC system [a] | | | | | | | | | |
|---|---|---|---|---|---|---|---|---|---|---|---|
| | | 1 | 2 | 3 | 4 | 5 | 6 | 7 | 8 | 9 | 10 |
| I | Log $k'_w$ | 3.703 | 2.370 | 3.655 | 3.446 | 2.854 | 2.935 | 3.580 | 1.945 | 3.977 | 3.788 |
| | $S \times 10^2$ | −6.394 | −4.252 | −6.529 | −6.250 | −5.196 | −5.429 | −6.249 | −3.607 | −9.999 | −6.756 |
| | $r$ | 0.9995 | 0.9910 | 0.9997 | 0.9975 | 0.9938 | 0.9792 | 0.9984 | 0.9964 | 0.9999 | 0.9994 |
| II | Log $k'_w$ | 2.092 | 1.430 | 2.253 | 2.282 | 1.873 | 1.706 | 2.229 | 1.236 | 2.818 | 2.153 |
| | $S \times 10^2$ | −4.444 | −3.599 | −5.090 | −5.133 | −4.230 | −3.874 | −4.868 | −3.352 | −8.149 | −4.734 |
| | $r$ | 0.9972 | 0.9971 | 0.9999 | 0.9973 | 0.9976 | 0.9689 | 0.9974 | 0.9983 | 0.9964 | 0.9924 |
| II | Log $k'_w$ | 2.388 | 1.579 | 2.405 | 2.528 | 2.174 | 2.065 | 2.434 | 1.203 | 3.132 | 2.362 |
| | $S \times 10^2$ | −4.862 | −3.702 | −5.202 | −5.474 | −4.705 | −4.451 | −5.070 | −3.095 | −8.916 | −4.975 |
| | $r$ | 0.9927 | 0.9921 | 0.9999 | 0.9980 | 0.9928 | 0.9892 | 0.9982 | 0.9941 | 0.9962 | 0.9988 |
| IV | Log $k'_w$ | 2.951 | 1.845 | 2.702 | 2.854 | 2.524 | 2.266 | 2.959 | 1.332 | 3.281 | 2.849 |
| | $S \times 10^2$ | −5.735 | −3.887 | −5.426 | −5.629 | −4.935 | −4.385 | −5.763 | −3.012 | −8.856 | −5.610 |
| | $r$ | 0.9971 | 0.9981 | 0.9998 | 0.9979 | 0.9974 | 0.9895 | 0.9984 | 0.9990 | 0.9960 | 0.9978 |
| V | Log $k'_w$ | 2.510 | 1.733 | 2.372 | 2.480 | 2.248 | 1.868 | 2.280 | 1.189 | 3.429 | 2.362 |
| | $S \times 10^2$ | −5.142 | −3.809 | −5.167 | −5.297 | −4.775 | −3.914 | −4.751 | −3.090 | −9.719 | −5.060 |
| | $r$ | 0.9989 | 0.9970 | 0.9998 | 0.9981 | 0.9957 | 0.9514 | 0.9980 | 0.9917 | 0.9940 | 0.9963 |
| VI | Log $k'_w$ | 2.370 | 1.541 | 2.246 | 2.377 | 2.080 | 1.790 | 2.416 | 1.123 | 3.372 | 2.089 |
| | $S \times 10^2$ | −4.897 | −3.675 | −4.944 | −5.110 | −4.485 | −3.902 | −5.068 | −2.965 | −9.913 | −4.560 |
| | $r$ | 0.9976 | 0.9965 | 0.9996 | 0.9982 | 0.9967 | 0.9654 | 0.9975 | 0.9941 | 0.9990 | 0.9977 |
| VII | Log $k'_w$ | 2.702 | 1.629 | 2.488 | 2.654 | 2.419 | 2.071 | 2.715 | 1.320 | 3.118 | 2.474 |
| | $S \times 10^2$ | −5.331 | −3.736 | −5.169 | −5.292 | −4.797 | −4.076 | −5.553 | −3.195 | −8.642 | −5.065 |
| | $r$ | 0.9985 | 0.9945 | 0.9996 | 0.9982 | 0.9971 | 0.9879 | 0.9996 | 0.9926 | 0.9935 | 0.9977 |
| VIII | Log $k'_w$ | 2.722 | 1.603 | 2.604 | 2.714 | 2.370 | 2.154 | 2.635 | 1.272 | 3.291 | 2.438 |
| | $S \times 10^2$ | −5.367 | −3.719 | −5.428 | −5.446 | −4.693 | −4.215 | −5.281 | −3.080 | −9.030 | −4.987 |
| | $r$ | 0.9981 | 0.9935 | 0.9906 | 0.9985 | 0.9924 | 0.9925 | 0.9946 | 0.9859 | 0.9942 | 0.9994 |
| IX | Log $k'_w$ | 3.307 | 2.028 | 3.297 | 3.123 | 2.975 | 2.811 | 3.173 | 1.726 | 3.651 | 3.189 |
| | $S \times 10^2$ | −5.394 | −3.997 | −6.191 | −5.695 | −5.339 | −4.937 | −5.872 | −3.506 | −9.630 | −5.991 |
| | $r$ | 0.9995 | 0.9998 | 0.9971 | 0.9985 | 0.9963 | 0.9780 | 0.9997 | 0.9986 | 0.9950 | 0.9944 |
| X | Log $k'_w$ | 3.515 | 2.170 | 3.269 | 3.383 | 3.294 | 2.943 | 3.612 | 1.984 | 3.866 | 3.375 |
| | $S \times 10^2$ | −6.013 | −3.867 | −5.776 | −5.822 | −5.623 | −4.857 | −6.344 | −3.715 | −9.778 | −5.950 |
| | $r$ | 0.9973 | 0.9996 | 0.9991 | 0.9988 | 0.9978 | 0.9785 | 0.9975 | 0.9970 | 0.9954 | 0.9984 |

[a] See Tables 2 and 3.

number of accepted independent variables was limited to one and the acceptance limit was set at the 95% significance level.

## RESULTS AND DISCUSSION

*Dependence of capacity factor on eluent composition*

The reproducibility of retention time measurements was better than 1.7% ($n = 12$). The parameters of Eqn. 1. are given in Table 4. The linear equations fit the experimental data well, the significance level being over 95% in each instance. The log $k'$ value decreased linearly with increasing concentration of the organic component of the eluent. This observation lends support to the assumption that the peptides do not show a silanophilic effect, the retention probably being governed by the molecular characteristics. The retention parameters of peptides differ considerably according to the LC systems and peptides concerned, indicating that the peptide structure, column type and eluent composition have similar effects on the retention. In most instances a significant linear relationship was found between the log $k'_w$ (intercept) and $S$ (slope) values of Eqn. 1. The values of the regression coefficient were 0.9741, 0.9377, 0.9831, 0.9440, 0.7568, 0.9192, 0.8686 and 0.9900 for LC systems 3, 4, 5, 6, 7, 8, 9 and 10, respectively. This result shows that the compounds can be regarded as structurally similar with respect to their chromatographic behaviour.

*Retention strength and retention selectivity*

The retention strengths (potency values) of the LC systems are given in Table 5. The retention strength of the RP-8 column for peptides decreases with increasing pH (compare LC systems 3–6) of the eluent and the effect does not depend linearly on the pH, as can be seen in Fig. 1. This finding emphasizes the importance of eluent pH in the retention of ionizable compounds such as peptides. The retention strength increased with increasing length of the covalently bonded alkyl chain (compare LC systems 1, 7 and 10). The effect of octanol was not clear; it increased the retention on an $C_8$ but decreased it on an $C_{18}$ column (compare LC systems 1–2 and 7–8). For a better understanding of the role of octanol more investigations are needed. The $C/N_{14}$ phase is electrostatically shielded by the quaternary amino groups. An outstanding by high retention was obtained owing to a "mixed-mode" retention mechanism.

The peptides do not form separate clusters according to their chemical structure on the two-dimensional non-linear spectral map (Fig. 2). This finding indicates that each substructure in the peptides may make a similar contribution to the

TABLE 5

Retention strength (potency) of LC systems

| No. of LC system [a] | Retention strength (potency) | No. of LC system [a] | Retention strength (potency) |
|---|---|---|---|
| 1 | 4.32 | 6 | 4.79 |
| 2 | 4.61 | 7 | 5.22 |
| 3 | 6.18 | 8 | 4.09 |
| 4 | 6.11 | 9 | 13.10 |
| 5 | 5.35 | 10 | 5.95 |

[a] See Table 2.

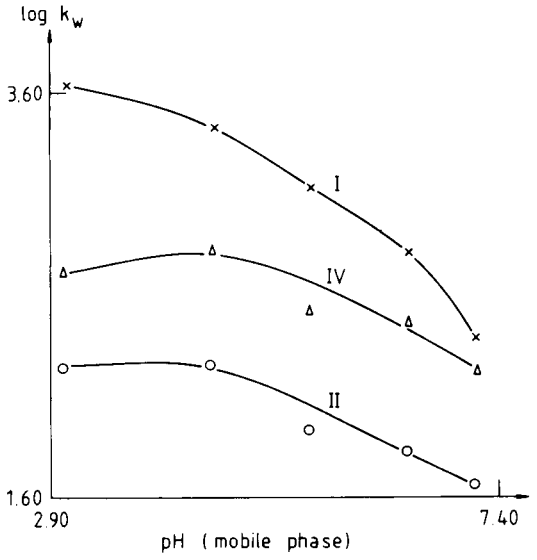


Fig. 1. Dependence of the log $k'_w$ values of some $\beta$-casomorphin peptides. Numbers refer to peptides in Table 3. LC systems 3–6 (Table 2).

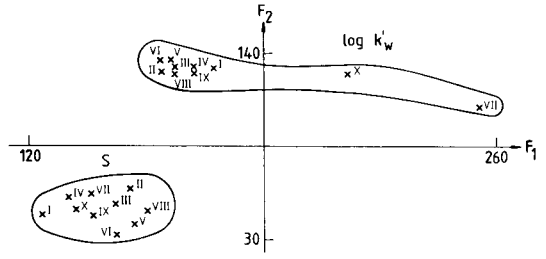


Fig. 2. Two-dimensional non-linear selectivity (spectral) map of peptides. Numbers refer to peptides in Table 3. No. of iterations: 130, Maximum error: $7.05 \times 10^{-3}$.

TABLE 6

Results of PCA

| No. of PC | $PCA_A$ [a] | | $PCA_B$ [a] | |
|---|---|---|---|---|
| | Eigenvalue | Variance explained (%) | Eigenvalue | Variance explained (%) |
| 1 | 8.04 | 80.44 | 1.98 | 76.96 |
| 2 | 1.02 | 10.23 | 0.29 | 11.34 |
| 3 | 0.54 | 5.41 | 0.13 | 5.16 |

[a] $PCA_A$ = PCA carried out on the log $k'_w$ (intercept) data matrix; $PCA_B$ = PCA carried out on the $S$ (slope) data matrix.

overall retention of the peptides. The peptides form clusters according to the retention parameters, that is, the underlying retention mechanism is probably similar for each peptide.

The LC systems form three distinct clusters on the two-dimensional non-linear spectral map (Fig. 3). The results suggest that the eluent composition has a greater effect than the length of the alkyl chain covalently bonded to the silica surface on the retention characteristics. The unique separation behaviour of the quaternary amino column is manifested in the separate position of point 9. The conclusions drawn from Fig. 3 (eluents with different pH forms one cluster) are in apparent contradiction with the results in Fig. 1 showing the pH dependence of the retention. This contradiction can be explained by the supposition that the importance of other chromatographic parameters overshadows that of the eluent pH.

*Comparison of LC systems*

The results of PCA are given in Table 6. Both calculations showed similar results. The first component explains most of the variance. This indi-

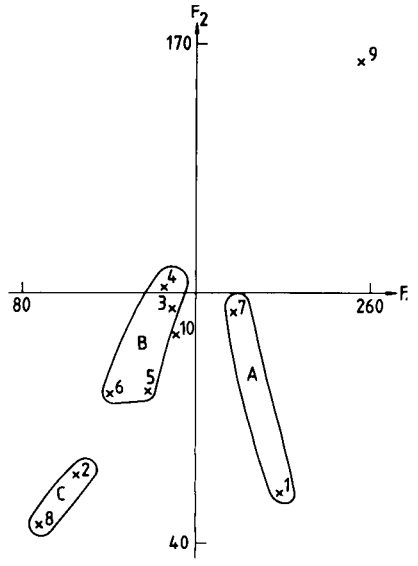


Fig. 3. Two-dimensional non-linear selectivity (spectral) map of LC systems. Numbers refer to LC systems in Table 2. No. of iterations: 349, Maximum error: $7.83 \times 10^{-3}$. A = $C_8$ and $C_{18}$ column, TFA in the eluent; B = $C_8$ column, buffered eluents; C = $C_8$ and $C_{18}$ column, *n*-octanol in the eluent.

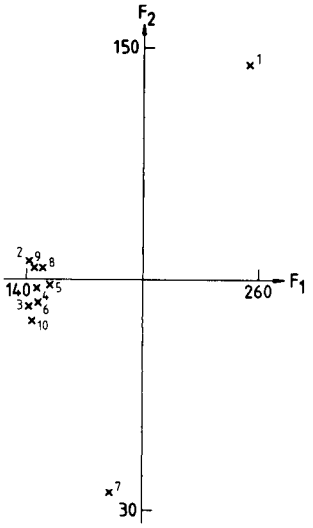


Fig. 4. Two-dimensional non-linear map of principal component loadings. Log $k'_w$ data matrix. No. of iterations: 159. Maximum error: $1.25 \times 10^{-3}$. Numbers refer to LC systems in Table 2.

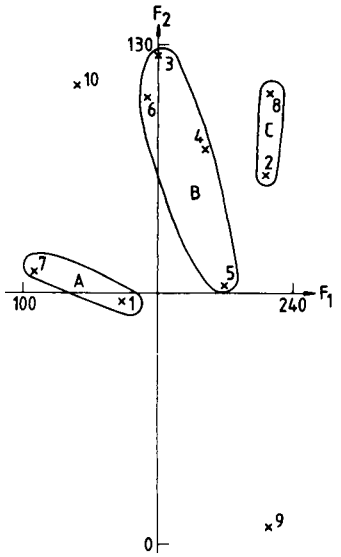


Fig. 5. Two-dimensional non-linear map of principal component loadings. Slope ($S$) data matrix. No. of iterations: 82. Maximum error: $2.77 \times 10^{-2}$. Numbers refer to LC systems in Table 2. A = $C_8$ and $C_{18}$ column, TFA in the eluent; B = $C_8$ column, buffered eluent; C = $C_8$ and $C_{18}$ column, $n$-octanol in the eluent.

cates that the LC systems are fairly similar and the differences between their retention characteristics are low.

The two-dimensional non-linear map of PCA loadings calculated from the log $k'_w$ values (Fig. 4) differentiate between the LC systems to a lesser extent than the map calculated from the slope ($S$) values (Fig. 5); however, the log $k'_w$ and $S$ values are highly correlated. This result indicates that both the log $k'_w$ and $S$ values have to be taken into consideration in the evaluation of the retention behaviour of an RPLC column.

*Dependence of the retention of peptides on physico-chemical characteristics*

The results of stepwise regression analysis are given in Tables 7 and 8. Non-significant correlations were excluded from both tables. It is surprising that in most instances the electronic properties of the peptides have the greatest impact on their individual retention parameters (Table 7); however, the LC system is a typical reversed-phase one and no anomalous retention behaviour was observed. It is assumed that the peptides may interact with the free silanol groups even in the LC systems used and the interaction is of electrostatic character. As the strength of electrostatic interactions also decreases with decreasing dielectric constant (higher methanol content) of the eluent, the resulting retention behaviour is simi-

TABLE 7

Parameters of significant linear correlations between the retention parameters of peptides derived from Eqn. 1 and their hydrophobicity ($z_1$). side-chain bulk ($z_2$) and electronic properties ($z_3$) [results of stepwise regression analysis, $n = 10$ ($r_{95\%} = 0.6319$)]: $Y = a + bX$

| $Y$ | $X$ | $a$ | $b$ | $r$ |
|---|---|---|---|---|
| Log $k'_w$ of LC system 1 | $z_2$ | 3.67 | −1.88 | 0.8919 |
| Log $k'_w$ of LC system 2 | $z_3$ | 0.53 | 0.18 | 0.7902 |
| Log $k'_w$ of LC system 3 | $z_3$ | 0.44 | 0.33 | 0.8507 |
| Log $k'_w$ of LC system 4 | $z_3$ | 1.01 | 0.25 | 0.7950 |
| Log $k'_w$ of LC system 5 | $z_3$ | 0.74 | 0.25 | 0.7357 |
| Log $k'_w$ of LC system 6 | $z_3$ | 0.12 | 0.31 | 0.8364 |
| Log $k'_w$ of LC system 8 | $z_3$ | −0.06 | 0.21 | 0.8459 |
| Log $k'_w$ of LC system 9 | $z_3$ | 1.92 | 0.21 | 0.7658 |
| Log $k'_w$ of LC system 10 | $z_3$ | 0.17 | 0.36 | 0.8171 |
| $S$ value of LC system 3 | $z_3$ | −3.10 | −0.34 | 0.8468 |
| $S$ value of LC system 4 | $z_3$ | −4.02 | −0.21 | 0.7868 |
| $S$ value of LC system 5 | $z_3$ | −3.31 | −0.22 | 0.7094 |
| $S$ value of LC system 6 | $z_3$ | −2.04 | −0.34 | 0.8305 |
| $S$ value of LC system 8 | $z_3$ | −2.10 | −0.17 | 0.7979 |
| $S$ value of LC system 9 | $z_1$ | −7.69 | 0.30 | 0.6394 |
| $S$ value of LC system 10 | $z_3$ | −2.36 | −0.43 | 0.8031 |

TABLE 8

Parameters of significant linear correlations between the retention parameters of peptides derived from spectral map and PCA and their hydrophobicity ($z_1$), side-chain bulk ($z_2$) and electronic properties ($z_3$) [results of stepwise regression analysis, $n = 10$ ($r_{95\%} = 0.6319$)]: $Y = a + bX$

| $Y$ | $X$ | $a$ | $b$ | $r$ |
|---|---|---|---|---|
| Retention strength | $z_3$ | −10.8 | −0.85 | 0.8160 |
| First coordinate of selectivity (spectral) map | $z_2$ | 181.8 | −26.4 | 0.7831 |
| Second coordinate of selectivity (spectral) map | $z_2$ | 128.0 | 6.50 | 0.7446 |
| First coordinate of $PCA_A$ map | $z_2$ | 164.6 | −35.97 | 0.8511 |
| Second coordinate of $PCA_A$ map | $z_3$ | 225.0 | −19.60 | 0.8475 |
| First coordinate of $PCA_B$ map | $z_2$ | 164.4 | −34.68 | 0.7335 |

lar to that of the real reversed-phase separation mode in that the retention also decreases with increasing concentration of the organic component in the eluent. We should stress again that the conclusions mentioned above are valid only for these peptide–support pairs and they cannot be generalized owing to the small number of solutes considered. The variables derived from spectral mapping and PCA are also correlated with the steric and electronic parameters of peptides but not with their hydrophobicity (Table 8). This finding lends support to the hypothesis outlined above.

*Conclusions*

The retention behaviour of ten β-casomorphin peptides were similar on $C_8$, $C_{18}$ and $C_{30}$ LC columns and differed strongly on a quaternary amino column. The results indicate that each substructure of the peptides influences their retention and that the electronic and steric parameters of the amino acid side-chains have the greatest impact on the retention.

This work was supported in part by grant OTKA 2670 of the Hungarian Academy of Sciences.

REFERENCES

1 K. Valkó, Trends Anal. Chem., 6 (1987) 214.
2 R. Kaliszan, Quantitative Structure Retention Relation ships, Wiley, New York, 1987.
3 J. Pick, in G. Szepesi (Ed.), HPLC in Pharmaceutical Analysis, Vol. 2, CRC, Boca Raton, FL, 1990, Chap. I, pp. 3–55.
4 J. Draffehn, B. Schönecker and K. Ponsold, J. Chromatogr., 205 (1980) 113.
5 S.T. Weber and W.G. Tramposch, Anal. Chem., 55 (1983) 1771.
6 O.H. Gupta and K.P. Mishra, J. Chromatogr., 219 (1981) 101.
7 H. Engelhardt and H. Müller, J. Chromatogr., 218 (1981) 395.
8 L.R. Snyder and J.J. Kirkland, Introduction to Modern Liquid Chromatography, Wiley, New York, 2nd edn., 1979, p. 253.
9 Z. Perzina, M. Sarsunová, K. Schmidt and J. Krepelka, Pharmazie, 41 (1986) 236.
10 Cs. Horváth, W. Melander and I. Molnár, J. Chromatogr., 125 (1976) 129.
11 H. Mager, Moderne Regressionsanalyse, Salle, Sauerlander, Frankfurt am Main, 1982, p. 135.
12 K.V. Mardia, J.T. Kent and J.M. Bibby, Multivariate Analysis, Academic, London, New York, 1979, p. 213.
13 J.W. Sammon, Jr., IEEE Trans. Comput., C18 (1969) 401.
14 P.J.M. Coenegracht, A.K. Smilde, H. Benak, C.H.P. Bruins, H.J. Metting, H. De Vries and D.A. Doornbos, J. Chromatogr., 550 (1991) 397.
15 T. Cserháti and Z. Illés, J. Pharm. Biomed. Anal., 9 (1991) 693.
16 P.J. Lewi, Arzneim.-Forsch., 26 (1976) 1295.
17 T. Cserháti, B. Bordás and M. Szögyi, J. Chromatogr. Sci., 24 (1986) 302.
18 T. Cserháti, J. Chromatogr. Sci., 29 (1991) 210.
19 K. Neubert, B. Hatrodt, I. Born, A. Barth, H.L. Ruethrich, G. Grecksch, U. Schrader and K. Liebmann, in F. Nyberg and V. Brante (Eds.), β-Casomorphins and Related Peptides, Fyris-Tryck, Uppsala, 1990, pp. 15–20.
20 K. Valkó, J. Liq. Chromatogr., 10 (1987) 1663.
21 J. Jonsson, L. Eriksson, S. Hellberg, M. Sjöström and A. Wold, Quant. Struct. Act. Relat., 8 (1989) 204.

*Analytica Chimica Acta*, 268 (1992) 255–260
Elsevier Science Publishers B.V., Amsterdam



# Determination of betamethasone and dexamethasone by derivatization and liquid chromatography [1]

Shou-Mei Wu, Su-Hwei Chen and Hsin-Lung Wu

*Graduate Institute of Pharmaceutical Sciences, Kaohsiung Medical College, Kaohsiung 807 (Taiwan)*

(Received 20th January 1992; revised manuscript received 29th April 1992)

**Abstract**

A derivatization method followed by liquid chromatography (LC) is described for the determination of the glucocorticoid epimers of betamethasone and dexamethasone. The method is based on the derivatization of the epimers with 1-ethoxy-4-(dichloro-*s*-triazinyl)naphthalene in acetonitrile, using potassium carbonate as a base catalyst. The resulting derivatives were readily separated by normal-phase LC. Several parameters that affect the derivatization are discussed. The method is feasible for the determination of betamethasone and dexamethasone in tablets.

*Keywords:* Liquid chromatography; Sample preparation; Betamethasone; Dexamethasone; Pharmaceuticals

Betamethasone (BXM; 9$\alpha$-fluoro-16$\beta$-methyl-11$\beta$,17$\alpha$,21-trihydroxypregna-1,4-diene-3,20-dione) and dexamethasone (DXM; 9$\alpha$-fluoro-16$\alpha$-methyl-11$\beta$,17$\alpha$,21-trihydroxypregna-1,4-diene-3,20-dione) (Fig. 1) are potent synthetic glucocorticoids that are widely used in the treatment of inflammation and other symptoms related to glucocorticoid deficiency [1]. Because of the close structural resemblance of these epimers (BXM and DXM), their direct determination is difficult; available liquid chromatography (LC) methods [2–7] are suitable only for the determination of the individual epimers (BXM or DXM) and related compounds and no simultaneous determination of both epimers has been reported. In previous work [8], an LC method was developed for the determination of BXM and DXM by derivatization of the epimers with a homochiral reagent, *N*-carbobenzoxyl-L-phenylalanine and using *N*,*N*′-dicyclohexylcarbodiimide as an activating agent.

In this study, a simple and improved method was established involving derivatization of BXM and DXM with 1-ethoxy-4-(dichloro-*s*-triazinyl)-naphthalene (EDTN) [9]. The EDTN derivatives of BXM and DXM offer a potential approach for the trace analysis of these epimers in various samples, because EDTN is a fluorophore and its derivatives are highly sensitive when monitored by a fluorescence detector. The proposed method was preliminarily applied to the determination of BXM and DXM in tablets and proved to be satisfactory. Further development of the method for the determination of traces of BXM and DXM in biological specimens is suggested.

*Correspondence to:* Hsin-Lung Wu, Graduate Institute of Pharmaceutical Sciences, Kaohsiung Medical College, Kaohsiung 807 (Taiwan).

[1] This work was presented in part at the annual meeting of the Pharmaceutical Society of the ROC, Taipei, 14th December 1991.

## EXPERIMENTAL

### *Reagents and solutions*

BXM, DXM and acetophenetidin (Sigma, St. Louis, MO), EDTN (Aldrich, Milwaukee, WI),

dichloromethane, hexane and isopropanol (Fisher, Fair Lawn, NJ), acetonitrile and potassium carbonate (Merck, Darmstadt) were used without further purification. All other chemicals were of analytical-reagent grade. Solutions of BXM, DXM, EDTN and acetophenetidin were prepared by dissolving the appropriate amounts of the respective compounds in acetonitrile.

*Liquid chromatography*

A Waters–Millipore LC system with a U6K injector, a Model 510 pump and a Model 486 UV–visible detector was used. A Nova-Pak silica column (150 × 3.9 mm i.d.; particle size 4 μm) with a Guard-Pak of Resolve Si (dead volume 60–75 μl; particle size 5 μm) (Waters–Millipore) and a mixed solvent of hexane–dichloromethane–propan-2-ol (100 + 100 + 4, v/v/v) at a flow-rate of 0.7 ml $min^{-1}$ were used. The column eluate was monitored at 254 nm. The solvents were pretreated with a vacuum filter for degassing.

*Mass spectrometry*

A JEOL JMS-HX 110 mass spectrometer was used with fast atom bombardment (FAB) with xenon as ionizing gas and an acceleration energy of 10 kV.

*Sample preparation*

Ten tablets of BXM or DXM were accurately weighed and pulverized. A suitable amount of the fine powder, equivalent to about 0.39 mg of BXM or DXM, was accurately weighed and transferred into a 20-ml volumetric flask. The volume was made up with acetonitrile and the mixture was sonicated at 40°C for 20 min. After cooling, a 7.0-ml aliquot of the suspension was transferred into a glass-stoppered test-tube and centrifuged at 250 *g* for 20 min. The clear supernatant as sample solution was derivatized as described below.

*Derivatization procedure*

A 0.4-ml aliquot of the respective epimer or sample solution was placed in a 10-ml glass-stoppered test-tube containing about 120 mg of potassium carbonate, then 0.4 ml of EDTN solution (5 mM) and 0.2 ml of acetophenetidin solution (0.15 mM) were added. The reaction mixture was shaken for 1.5 h at 70°C in a thermostated water-bath. At the end of the reaction, 10 μl of the final solution were injected into LC system.

## RESULTS AND DISCUSSION

Several parameters affecting the derivatization of BXM or DXM, including reaction solvent, amount of derivatizing reagent, reaction temperature, reaction time and catalyst, were studied in order to optimize the conditions for the derivatization of the respective epimers at the 20-nmol level. The effects of the parameters on the derivatization of BXM and DXM were evaluated by measuring the peak-area ratio of the derivative with respect to acetophenetidin (internal stan-

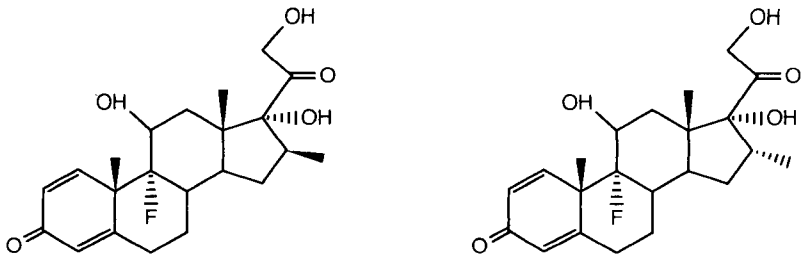


Fig. 1. Structures of (A) betamethasone and (B) dexamethasone.

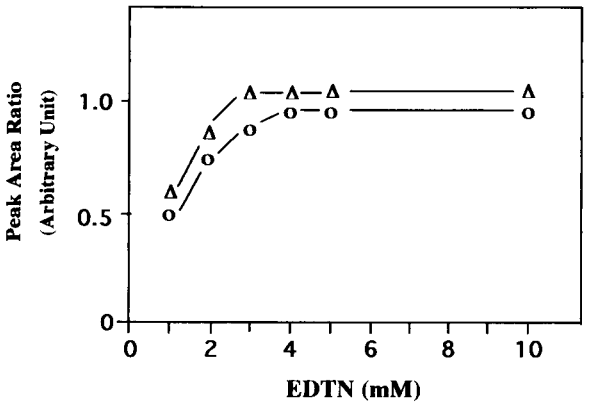


Fig. 2. Effect of the amount of EDTN on the formation of derivatives of (○) BXM and (△) DXM. See text for conditions.

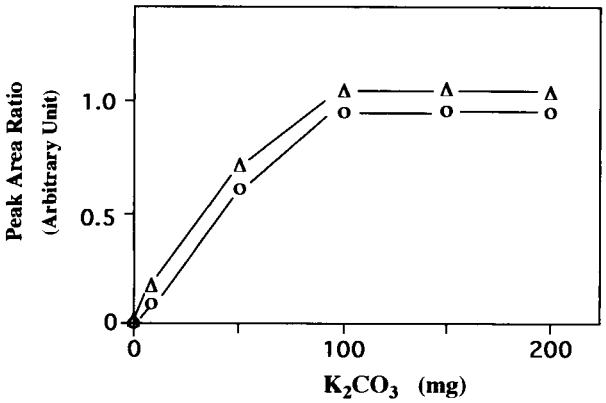


Fig. 3. Effect of the base catalyst on the formation of derivatives of (○) BXM and (△) DXM. See text for conditions.

dard, I.S.); the I.S. used was shown to be stable under the present derivatization conditions based on a simple study of the peak-area ratio of I.S. to caffeine versus reaction time from 0.5 to 1.5 h at 70°C; this resulted in no significant change in the peak-area ratio of the I.S. to caffeine.

*Effect of organic solvent*

The effects of various organic solvents on the derivatization of BXM and DXM were studied according to the derivatization procedure but at different temperatures in order to prevent the solvents from boiling. The solvents tested included acetonitrile, dioxane and isobutyl methyl ketone at 70°C, acetone at 45°C and dichloromethane at room temperature. Acetonitrile was found to be the best solvent for the derivatization of BXM and DXM.

*Effect of amount of derivatizing agent*

The amount of EDTN required for the derivatization of BXM and DXM to a plateau formation of the derivative is shown in Fig. 2. For the derivatization of 20 nmol of BXM, 1.6 μmol of EDTN was needed, equivalent to 0.4 ml of 4 mM EDTN solution. For the derivatization of DXM, 1.2 μmol of EDTN was required, but an excess of EDTN solution (2.0 μmol) was used to cover the additional consumption of the reagent by the matrix in analyses for BXM and DXM in real samples.

*Effect of amount of catalyst*

The effect of the amount of potassium carbonate (30–50 mesh) is shown in Fig. 3. In the absence of the base catalyst in the reaction system, no derivatives were detected. A suitable amount of potassium carbonate (about 120 mg) was selected for the derivatization of BXM and DXM. After derivatization, the excess of the solid base was separated in situ by centrifugation and the resulting clear solution was introduced into the LC system. This will be favourable when

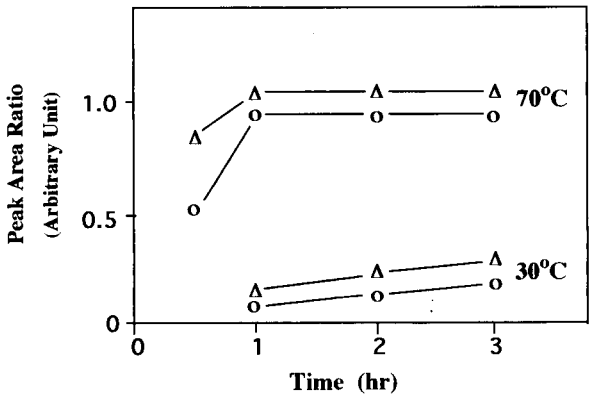


Fig. 4. Effect of reaction temperature and reaction time on the formation of derivatives of (○) BXM and (△) DXM. See text for conditions.

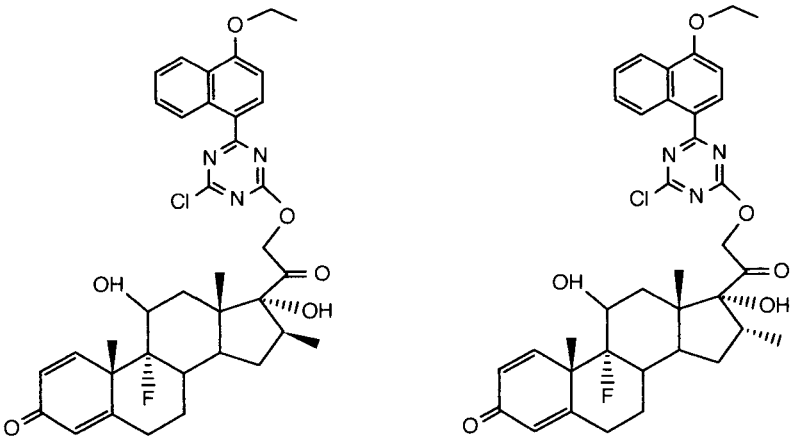


Fig. 5. Assumed derivatives of (A) betamethasone and (B) dexamethasone from EDTN.

normal-phase LC is used, because excess of base, especially strong base, could be inappropriate for a silica stationary phase.

*Effect of reaction temperature and reaction time*

The reaction temperature and reaction time required to reach an equilibrium for the derivatives are shown in Fig. 4. For derivatization at 70°C, 1 h was needed for BXM and DXM; with reaction at room temperature, plateau formation of the derivatives was not attainable in 3 h and resulted in lower yields as compared with reaction at 70°C.

*Mass spectral analysis of derivatives*

The structures of the derivatives of BXM and DXM were identified by FAB mass spectrometry with thioglycerin as a matrix. The quasi-molecular ions of the derivatives of BXM and DXM were found at $m/z = 676$, $[M + H]^+$; another ion common to both derivatives was at $m/z = 658$, corresponding to $[M + H]^+ - H_2O$, and a diagnostic ion at $m/z = 342$ was found with the BXM derivative, corresponding to $M^+$ minus a BXM moiety from cleavage of its carbonyl side-chain at $C_{17}$. No higher mass peaks of the derivatives from multiple derivatization of BXM and DXM were observed, and the use of EDTN for the derivatization of primary alcohols has been reported [9]. Therefore, the derivatives of BXM and DXM are speculated to result from the derivatization of the primary alcohol group at $C_{21}$ by EDTN, as illustrated in Fig. 5.

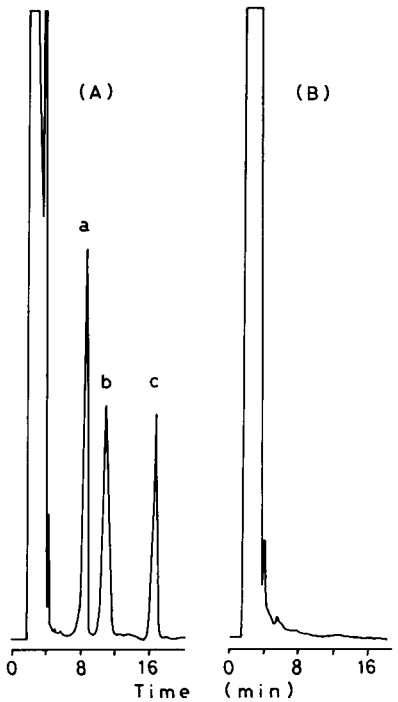


Fig. 6. Typical chromatograms for (A) the determination of betamethasone and dexamethasone in tablets and (B) reagent blank. Peaks: a = derivative of dexamethasone; b = derivative of betamethasone; c = acetophenetidin (I.S.).

*Calibration*

To evaluate the quantitative applicability of the method, four different amounts of each of BXM and DXM in the range 2–20 nmol were analysed and the linearity between the peak-area ratios ($y$) and sample weights ($x$, nmol) was examined. The linear regression equations obtained were $y = (0.05354 \pm 0.0044)x - (0.04025 \pm 0.00088)$ ($n = 3$), $r = 0.9997$, for BXM and $y = (0.05235 \pm 0.00032)x - (0.04008 \pm 0.00042)$ ($n = 3$), $r = 0.9993$, for DXM, indicating good linearity of the method. The detection limits (signal-to-noise ratio = 5) of BXM and DXM were 20 and 10 pmol per injection, respectively.

*Reproducibility and selectivity*

The precision (relative standard deviation) of the proposed method based on the peak-area ratios for ten replicate analyses of 10 nmol of BXM and DXM was 2.65% and 2.35%, respectively. The specificity of the method was studied by spiking samples of BXM and DXM with cortisone, hydrocortisone, prednisone, prednisolone, 6$\alpha$-methylprednisolone and triamcinolone. The derivatives of BXM and DXM could be resolved from those of the other glucocorticoids, indicating that the LC analysis of BXM and DXM is not interfered with by the other glucocorticoids tested; more importantly, with modification of the method it could be applied to the trace determination of the related glucocorticoids.

This study was centred on the derivatization of BXM and DXM with EDTN and the resulting derivatives were monitored by UV detection at 254 nm for simple operation. For more sensitive determinations of BXM and DXM at trace levels, the fluorescent derivatives from EDTN and an internal standard of a suitable glucocorticoid also labelled with EDTN can be detected fluorimetrically.

*Application*

The method was applied to the determination of BXM and DXM and their test mixture in commercial tablets. The results are shown in Table 1 and for both BXM and DXM they fall within the range of 90–110% required by the current USP [10]. Typical chromatograms are illustrated in Fig. 6. Obviously, the method can be used for the determination of BXM and DXM in bulk or in pharmaceutical preparations. Further application of the method to highly sensitive determinations of BXM and DXM in biological specimens is being investigated.

TABLE 1

Assay results for BXM and DXM tablets obtained from two commercial sources

| Sample | Percentage of claimed content [a] | |
|---|---|---|
| | BXM | DXM |
| *BXM tablet* | | |
| $B_1$ | 93.60 | |
| $B_2$ | 92.80 | |
| $B_3$ | 93.83 | |
| $B_4$ | 97.22 | |
| $B_5$ | 93.97 | |
| Mean | 94.28 | |
| S.D. | 1.70 | |
| *DXM tablet* | | |
| $D_1$ | | 102.62 |
| $D_2$ | | 102.10 |
| $D_3$ | | 100.28 |
| $D_4$ | | 102.90 |
| $D_5$ | | 98.72 |
| Mean | | 101.32 |
| S.D. | | 1.77 |
| *Test mixture* [b] | | |
| $M_1$ | 92.56 | 101.89 |
| $M_2$ | 93.83 | 100.94 |
| $M_3$ | 91.06 | 96.88 |
| Mean | 92.48 | 99.90 |
| S.D. | 1.38 | 2.66 |

[a] Labelled amount of BXM or DXM in each tablet is 0.5 mg.
[b] Test mixtures were formulated as various proportions of pulverized tablets of BXM and DXM in mg of labelled amount: $M_1$ (BXM 0.294 mg + DXM 0.098 mg); $M_2$ (BXM 0.196 mg + DXM 0.196 mg); and $M_3$ (BXM 0.098 mg + DXM 0.294 mg).

The authors are grateful to the National Science Council of the ROC for financial support of part of the work.

REFERENCES

1 H. Kalant and W.H.E. Roschlau, Principles of Medical Pharmacology, B.C. Decker, Toronto, Philadelphia, PA, 1989, p. 479.

2 Ph. Gaignage, G. Lognay, M. Marlier, M. Severin and Ph. Dreze, Chromatographia, 28 (1989) 623.
3 A. Shalaby and M. Shahjahan, J. Liq. Chromatogr., 14 (1991) 1267.
4 P.M. Plezia and P.L. Berens, Clin. Chem., 31 (1985) 1870.
5 D. Lamiable, R. Vistelle, H. Millart, V. Sulmont, R. Fay, J. Caron and H. Choisy, J. Chromatogr., 378 (1986) 486.
6 D. Lamiable, R. Vistelle, M. Nguyen-Khac and H. Millart, J. Chromatogr., 434 (1988) 315.
7 L.G. McLaughlin and J.D. Henion, J. Chromatogr., 529 (1990) 1.
8 S.H. Chen, S.M. Wu and H.L. Wu, J. Chromatogr., 595 (1992) 203.
9 R. Chayen, S. Gould, A. Harell and C.V. Stead, Anal. Biochem., 39 (1971) 533.
10 US Pharmacopeia XXII Revision, United States Pharmacopeial Convention, Rockville, MD, 1990, pp. 158 and 393.

*Analytica Chimica Acta*, 268 (1992) 261–274
Elsevier Science Publishers B.V., Amsterdam



# Induced reactant adsorption in metal–polyelectrolyte systems: pulse polarographic study

Jaume Puy

*Escola Tècnica Superior d'Enginyeria Agrària, Universitat Politècnica de Catalunya (UPC), Av. Rovira Roure 177, E-25006 Lleida (Spain)*

Francesc Mas

*Departament de Química Física, Universitat de Barcelona (UB), C / Martí i Franquès 1, E-08028 Barcelona (Spain)*

José M. Díaz-Cruz, Miquel Esteban and Enric Casassas

*Departament de Química Analítica, Universitat de Barcelona (UB), C / Martí i Franquès 1, E-08028 Barcelona (Spain)*

(Received 26th February 1992; revised manuscript received 26th May 1992)

**Abstract**

A theoretical model is developed for describing the reduction, by normal-pulse polarography, of a metal ion in the presence of a macromolecular ligand, including both the ligand adsorption and the induced adsorption of the metal ion. The following basic assumptions are made: reversible charge transfer at a stationary planar electrode (static mercury drop electrode); labile complex; large excess of ligand compared with the total metal concentration; Langmuirian adsorption for both the ligand and complex species; and diffusion coefficients for ligand and complex species very different from that of the free metal. The mathematical approach is based on transforming the system of differential equations with their boundary conditions into an integral equation which has been solved numerically. A simple procedure to obtain stability constants and adsorption parameters simultaneously from the experimental data is described. This model has been used to reproduce some experimental data from the Cd(II)–polymethacrylate system.

*Keywords:* Polarography; Induced reactant adsorption; Metal–polyelectrolyte systems

Voltammetric techniques are widely applied to the determination and speciation of trace metals in natural aquatic systems [1]. In the case of simple (monomeric) ligands, if the electrodic adsorption is absent, methods such as those of Lingane or DeFord–Hume have been used to evaluate the stability constants of labile metal complexes by means of the analysis of half-wave potential shifts [2]. However, in many instances experimental evidence is available for the adsorption of the ligand and the induced adsorption of the metal ion, with the formation of the metal complex in the adsorbed phase [3]. In these instances, theoretical efforts have been made to interpret the experimental results but a wider study is needed. A currently, but not unanimously, accepted conclusion of these studies is that the apparent stability constants determined by voltammetric means, using the equations suitable for the case without adsorption, are higher than the potentiometric values [4–9]. However, a general methodology for the determination of

*Correspondence to:* M. Esteban, Departament de Química Analítica, Universitat de Barcelona (UB), C/Martí i Franquès 1, E-08028 Barcelona (Spain).

stability constants from experimental values in the presence of adsorption has not been reported. Tur'yan [6] and Montemayor and Fatas [7,8] proposed expressions, based on the diffusion-layer approximation [9], involving adsorption. The treatment proposed by Lovrić and coworkers [10,11] is more rigorous, but it is devoted to d.c. polarography and restricted to ligands with diffusion coefficients equal to those of the metal ions. Other treatments [12,13] consider schemes limited by the charge-transfer process at the electrode. Several techniques have been used to elucidate adsorption complications. Normal-pulse polarography (NPP) is an excellent tool for studying electrochemical processes coupled with chemical reactions and involving reactant adsorption. This technique yields maxima in the response function (polarograms) as a consequence of reactant adsorption [14–16]. Several papers [17–24] concerning adsorption in NPP have been published, but in no instance was induced adsorption taken into account.

In addition to adsorption phenomena, another limiting feature of the classical voltammetric methods for the study of metal solution equilibria is the size of the ligand. Only recently has the 1 : 1 metal complexation process been rigorously analysed [25–27], the analysis involving the simultaneous effects of finite (or infinite) association/dissociation rates and of different diffusion coefficients for the various metal species, but without considering any adsorption phenomena. An extremely useful feature of this approach is its suitability for the study of metal speciation in the presence of large ligands (especially natural polyelectrolytes), since the diffusion coefficients of such ligands differ substantially from those of the free metal. However, the rigorous use of such an approach is only possible under experimental conditions in which adsorption is negligible. Experimental results [3,15,16] confirm the validity of the model when techniques minimizing adsorption [e.g., reversed-pulse polarography (RPP)] are applied.

Although the study of systems with natural polyelectrolytic ligands, which play a great biological and environmental role, is of great interest, some homofunctional synthetic polyacids have been used as ligands in order to verify the validity of the theoretical models developed, as the organic ligands occurring in nature are not homogeneous with respect either to the thermodynamics or to the kinetics of metal binding. Accordingly, ligands such as polyacrylic acid (PAA) and polymethacrylic acid (PMA) have been intensively discussed [28] as models for polyelectrolytic ligands. In particular, the Cd(II)–PMA system has been studied by different polarographic techniques [3], NPP showing the presence of induced Cd(II) adsorption.

In this paper, an extension of the above-mentioned model [25–27] restricted to the labile case, but including both ligand adsorption and metal-induced adsorption, is reported. The model proposed is solved rigorously using a mathematical procedure previously developed for pulse polarography [24,29–32]. Its validity was tested through the Cd(II)–PMA system, which was studied by NPP, with the main aim of simultaneously obtaining information about complexation and adsorption.

## MODELLING AND MATHEMATICAL FORMULATION

Consider the simple scheme of an electroactive metal ion M which may be reduced to the metal $M^0$, and a ligand L with which M may form the electroinactive complex ML. Both L and ML can be adsorbed on the electrode surface:

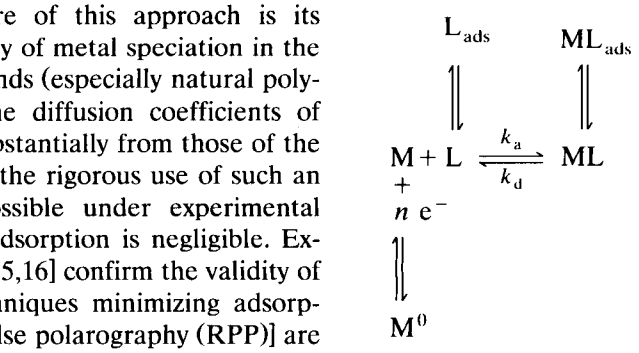


(1)

where charges of ionic species are omitted for the sake of simplicity. The following basic assumptions have been made: (a) the ligand is in a large excess over the total metal ion concentration, hence it can be assumed that $c_L(x, t) = c_L^*$; (b)

the electron transfer reaction is sufficiently fast to render the system electrochemically reversible; (c) the association/dissociation kinetics for the complex forming reaction are sufficiently fast to keep the metal and complex concentrations related through the equilibrium constant, over the whole system—this situation is referred to as the labile case; (d) a semi-infinite planar diffusion is assumed, for the sake of simplicity, although a static mercury drop electrode (SMDE) is used.

These restrictions allow the mathematical problem to be transformed into one of separable variables, which can be solved using the Laplace transformation method. In fact, condition (a) is only a first approximation for cases with ligand adsorption, although there is an excess of ligand. Work is in progress to overcome this limitation [33].

The mathematical formulation of this scheme corresponds to the following system of differential equations:

$$\frac{\partial c_{M^0}}{\partial t} = D_{M^0} \cdot \frac{\partial^2 c_{M^0}}{\partial x^2} \tag{2a}$$

$$\frac{\partial c_M}{\partial t} = D_M \cdot \frac{\partial^2 c_M}{\partial x^2} + k_d c_{ML} - k_a c_M c_L \tag{2b}$$

$$\frac{\partial c_{ML}}{\partial t} = D_{ML} \cdot \frac{\partial^2 c_{ML}}{\partial x^2} + k_a c_M c_L - k_d c_{ML} \tag{2c}$$

with initial conditions

$$t = 0,\ \forall x > 0;\ c_M = c_M^*;\ c_L = c_L^*;\ c_{ML} = c_{ML}^*;$$

$$c_{M^0} = 0 \tag{3a}$$

$$t = 0,\ \Gamma_{ML} = \Gamma_L = 0 \tag{3b}$$

and boundary conditions

$$x \to \infty$$

$$c_M = c_M^*;\ c_L = c_L^*;\ c_{ML} = c_{ML}^*;\ c_{M^0} = 0;\ \forall t \tag{4a}$$

$$x \to -\infty$$

$$c_{M^0} = 0;\ \forall t \tag{4b}$$

$$x \to 0$$

$$\frac{c_M(0,t)}{c_{M^0}(0,t)} = \exp\left\{\frac{nF}{RT}[E(t) - E_0]\right\} \tag{5}$$

$$D_M\left(\frac{\partial c_M}{\partial x}\right)_{x=0} + D_{M^0}\left(\frac{\partial c_{M^0}}{\partial x}\right)_{x=0} = 0 \tag{6a}$$

$$D_{ML}\left(\frac{\partial c_{ML}}{\partial x}\right)_{x=0} = \frac{d\Gamma_{ML}}{dt} \tag{6b}$$

$$\Gamma_{ML}(t) = f[c_{ML}(0,t),\ c_L^*] \tag{7a}$$

$$\Gamma_L(t) = f[c_{ML}(0,t),\ c_L^*] \tag{7b}$$

where $c_i$ and $c_i^*$ are the concentration and the bulk concentration in solution respectively, $D_i$ is the diffusion coefficient and $\Gamma_i(t)$ the adsorbed concentration of species $i$ on the electrode surface at time $t$.

Equation 2a arises from the diffusion of $M^0$ into the Hg electrode, which is also assumed to be semi-infinite and planar. Equations 7 represent a general kind of adsorption isotherm. It should be noted that the theoretical treatment is independent of the particular adsorption isotherm considered, and includes the possibility of assuming some of the more usual isotherms (Henry, Langmuir).

The restriction to labile systems (condition c) yields

$$K' \equiv Kc_L^* = \frac{c_{ML}(x,t)}{c_M(x,t)} \forall x,t \tag{8}$$

where $K$ is the stability constant of the complex and $c_L(x,t)$ has been replaced by $c_L^*$ according to the restriction to the case of an excess of ligand L [condition (a)] which allows the transport of L to be ignored.

Thus, the system of differential Eqns. 2 for $c_M$ and $c_{ML}$ can be uncoupled. Using the definition $c_T = c_M + c_{ML}$, the system is transformed into [25]

$$\frac{\partial c_{M^0}}{\partial t} = D_{M^0} \cdot \frac{\partial^2 c_{M^0}}{\partial x^2} \tag{9a}$$

$$\frac{\partial c_T}{\partial t} = D_T \cdot \frac{\partial^2 c_T}{\partial x^2} \tag{9b}$$

where $D_T$ is the mean diffusion coefficient for the present system, which is given by

$$D_T \equiv \frac{D_M c_M + D_{ML} c_{ML}}{c_M + c_{ML}} = \frac{D_M + D_{ML} K'}{1 + K'} \tag{10}$$

The boundary conditions (Eqns. 5 and 6) can be replaced by

$$\frac{c_T(0,t)}{c_{M^0}(0,t)} = (1+K')\exp\left\{\frac{nF}{RT}[E(t)-E_0]\right\} \tag{11}$$

and

$$D_T\left(\frac{\partial c_T(x,t)}{\partial x}\right)_{x=0} + D_{M^0}\left(\frac{\partial c_{M^0}(x,t)}{\partial x}\right)_{x=0} = \frac{d\Gamma_{ML}}{dt} \tag{12}$$

where Eqn. 12 is generated by the addition of Eqns. 6a and 6b.

The present system (Eqns. 9–12) is formally identical with that in which reactant adsorption is present but complexation is absent, to which the general theoretical treatment of pulse polarographic techniques can be applied [22–24].

The general expression for the response function of NPP can be written, following the mathematical treatment outlined in the Appendix:

$$I_{NPP} = nFA\left(\frac{\delta}{1+\delta}\right)\left\{\sqrt{\frac{D_T}{\pi}}\left[\frac{c_T^*}{\sqrt{t_d}} + \frac{c_T(0,t_0)}{\sqrt{t_p}} - \int_0^{t_0^-}\frac{c_T'(0,\tau)}{\sqrt{t_d-\tau}}d\tau\right] - \Gamma_{ML}(t_d)\right\} \tag{13}$$

where the prime means the time derivative of the function, and $t_d$ and $t_p$ are the drop time and the pulse time, respectively; $t_0$ is defined as the prepulse time ($t_0 = t_d - t_p$), the origin of time being considered to be at the beginning of each drop; $\delta$ is a function of potential defined as (Eqn. A5)

$$\delta(t) \equiv \sqrt{\frac{D_{M^0}}{D_T}}\frac{1}{(1+K')} \times \exp\left\{-\frac{nF}{RT}[E(t)-E_0]\right\} \tag{14}$$

and $c_T(0,t_0)$ is the total metal concentration ($c_M + c_{ML}$) near to the electrode surface, satisfying the following integral equation (Eqn. A4):

$$\Gamma_{ML}(t) = \left(2\sqrt{\frac{D_T}{\pi}}\right)\left\{c_T^*\sqrt{t} - \frac{1}{2}\int_0^t \frac{[1+\delta(\tau)]c_T(0,\tau)}{\sqrt{t-\tau}}d\tau\right\} \tag{15}$$

Equation 15 is the integral form of the mass balance around the electrode (Eqn. 12). The flux terms in Eqn. 12 have been written using the convolution theorem applied to obtain the inverse Laplace transform of the solution for diffusion Eqns. 9a and b, as outlined in the Appendix.

In order to solve the integral Eqn. 15, a particular adsorption isotherm must be considered. The Langmuir adsorption isotherm for both the ligand L and the complex ML is assumed, because in this isotherm only a small number of parameters has to be specified, and the qualitative conclusions so obtained can be extended to other experimental isotherms. Then, Eqn. 7 is written as

$$\Theta_L(t) = \frac{K_L c_L^*}{1 + K_L c_L^* + K_{ML} c_{ML}(0,t)} \tag{16a}$$

$$\Theta_{ML}(t) = \frac{K_{ML} c_{ML}(0,t)}{1 + K_L c_L^* + K_{ML} c_{ML}(0,t)} \tag{16b}$$

where $\Theta_i(t) = \Gamma_i(t)/\Gamma_m$ is the coverage of species $i$ (L and ML) and $\Gamma_m$ is the maximum surface concentration averaged for both species, for the sake of simplicity. $K_L$ and $K_{ML}$ are the adsorption coefficients of L and ML, respectively, and these constants are assumed to be independent of the applied potential.

Equation 16b implies that $c_{ML}(0,t=0^+) = 0$ at the electrode, because the drop is generated as a clean surface at the starting time ($t = 0^+$), and diffusion is the limiting step. The lability condition indicates that $c_M(0,0^+)$ and $c_T(0,0^+)$ are also zero, which is consistent with the reversibility condition (Eqn. 5) at $t = 0^+$ because no product is present at the beginning of the drop.

Since Eqn. 15 depends on $c_T(0,t)$, a relationship between $\Gamma_{ML}$ and $c_T(0,t)$ may be written. Using the condition $c_T = c_M + c_{ML}$ and the equi-

librium constant for the labile hypothesis (Eqn. 8), Eqn. 16b becomes

$$\Theta_{ML}(t) \equiv \frac{\Gamma_{ML}(t)}{\Gamma_m} = \frac{\tilde{K}_{ML} c_T(x=0,t)}{1 + \tilde{K}_{ML} c_T(x=0,t) + K_L c_L^*} \quad (17)$$

where

$$\tilde{K}_{ML} \equiv K_{ML} \cdot \frac{K'}{1+K'} \quad (18)$$

Then, Eqn. 15 coupled to Eqn. 17 forms a non-linear integral equation for the $c_T(0,t)$ function, which can be solved using numerical procedures [22,24,29–34] analogously to the case of reactant adsorption in NPP.

A special remark must be made about the kind of ligand adsorption. Although the ligand concentration has neither spatial nor temporal dependence, as there is an excess of ligand, $\Theta_L$ is time dependent as a consequence of its dependence on $c_{ML}(0,t)$ (Eqn. 16a). Moreover, the total coverage $\Theta_t$ ($\Theta_t = \Theta_L + \Theta_{ML}$) may be different from 1, the maximum value. The model described here is, in this respect, more general than that of Lovrić [10], in which it is assumed that the electrode surface is totally covered by the adsorbed species. Thus, the results obtained by Lovrić can be reproduced as a particular case of the present model.

An interesting limiting case to be analysed is that in which adsorption is absent. The solution of Eqn. 15 is then

$$c_T(0,t) = \begin{cases} 0 & t = 0^+ \\ c_T^* & t > 0 \end{cases} \quad (19)$$

as can be seen by putting Eqn. 19 into Eqn. 15 for $\Gamma_{ML} = 0$.

In order to deduce an expression for the current, Eqn. 19 must be introduced into Eqn. 13 and, taking into account that

$$\int_0^{t_0^-} \frac{c_T'(0,\tau)}{\sqrt{(t_d - \tau)}} \cdot d\tau = \frac{c_T^*}{\sqrt{t_d}} \quad (20)$$

since $c_T'(0,t) = c_T^* \delta_D(0)$ is a Dirac delta-function, Eqn. 13 becomes

$$I_{NPP} = \frac{\delta}{1+\delta}\left(nFA \cdot \frac{c_T^* \sqrt{D_T}}{\sqrt{\pi t_p}}\right) \quad (21)$$

Equation 21 is similar to that obtained by de Jong and van Leeuwen (Eqn. 31 in [27]), which yields the well known Cottrell equation when $\delta \to \infty$.

If an expression for the half-wave potential shifts is required, the condition $i = i_{lim}/2$ yields

$$\delta_{1/2} = \delta(E_{1/2}) = 1 \quad (22)$$

Introducing Eqn. 22 into Eqn. 14, and after rearrangement, the Guidelli–Cozzi equation [35] is obtained:

$$\frac{nF}{RT} \cdot \Delta E_{1/2} = -\frac{1}{2}\ln\left(\frac{D_T}{D_M}\right) - \ln(1+K') \quad (23)$$

which, for the case when $D_T \approx D_M \approx D_L$, yields the well known DeFord–Hume equation [2].

## EXPERIMENTAL

### *Reagents and apparatus*

Analytical reagent grade polymethacrylic acid (PMA) solutions obtained from BDH (average molecular mass 26 000 g mol$^{-1}$ according to BDH) were used to prepare stock solutions in water of ca. 0.1 mol l$^{-1}$ (in monomer). The total number of carboxylic groups was determined by conductimetric acid–base titration. The diffusion coefficient of PMA, as calculated from the literature data [3], is ca. $1.7 \times 10^{-7}$ cm$^2$ s$^{-1}$ for the molecular mass version used.

All other reagents were of analytical-reagent grade. $CO_2$-free KOH was used for the partial neutralization of the PMA solutions. $KNO_3$ was applied as supporting inert electrolyte. Solutions of $Cd(NO_3)_2$ were used at a concentration of $1 \times 10^{-4}$ mol l$^{-1}$. The diffusion coefficient of uncomplexed $Cd^{2+}$, at 25°C and in 0.1 mol l$^{-1}$ $KNO_3$ medium, is $0.73 \times 10^{-5}$ cm$^2$ s$^{-1}$ [36], whereas that of Cd in the mercury of the electrode, at 25°C is $2 \times 10^{-5}$ cm$^2$ s$^{-1}$ [37]. Ultrapure filtered water (Culligan water purification system) with a conductivity (after degassing traces of $CO_2$)

lower than 0.5 $\mu$S cm$^{-1}$ was used in all experiments. The Autolab system (Ecochemie, Utrecht, Netherlands) attached to a Model 663 VA stand (Metrohm) and to an Olivetti Model 290 personal computer by means of the electrochemical software package GPES2 (Ecochemie) was used. The reference electrode, the counter electrode and the working electrode were Ag/AgCl, KCl(sat.), glassy carbon and static mercury drop (SMDE) electrodes, respectively. Measurements were made at 25.0 ± 0.5°C. Purified nitrogen was used for deaeration and blanketing of the sample solutions. Acid–base conductimetric titrations of PMA stock solutions were performed with an Orion cell ($k$ = 1.03 cm$^{-1}$) attached to an Orion 120 microprocessor conductivity meter. pH measurements were made with an Orion SA 720 pH meter.

All calculations were carried out on an IBM 3090 computer (in FORTRAN-77) and the graphics were drawn on a Benson plotter connected to it.

## RESULTS AND DISCUSSION

### *Analysis of limiting current*

In order to facilitate the practical application of the theory developed here, experimental data are first analysed in terms of limiting current.

For the case without adsorption and for a labile complex, the linear plot of $I_{lim}$ vs. $t_p^{-1/2}$ (Cottrell dependence, $I_{lim} = nFAc_T^* D_T^{1/2} \pi^{-1/2} t_p^{-1/2}$) allows the $D_T$ value to be determined if $n$, $A$ and $c_T^*$ are known. Further, from Eqns. 8 and 10, the stability constant $K$ of the complex can be determined from this $D_T$ value when $D_M$ and $D_{ML}$ ($\approx D_L$) are known.

Under the same assumptions, another experimental procedure involving measurements of the current, at fixed $t_p$ values, in the absence and in the presence of ligand, is available. In this procedure, a normalized limiting current $\Phi$ is defined, which is related to the stability constant through [25–27]

$$\Phi \equiv \frac{I_{lim}(\text{with ligand})}{I_{lim}(\text{without ligand})} = \left( \frac{1 + \epsilon K c_L^*}{1 + K c_L^*} \right)^{1/2} \quad (24)$$

where $\epsilon = D_{ML}/D_M$ and $D_{ML} \approx D_L$. Hence it is possible to obtain the value of the stability constant, either from a particular experimental measurement of ($\Phi$, $c_L^*$) or, better, by fitting Eqn. 24 to experimental sets of $\Phi$ vs. $c_L^*$ values, obtained from a metal ion solution after successive additions of ligand [15,16].

The presence of adsorption prevents the use of these procedures in the simple way described. Figures 1 and 2 show that the effect of complexa-

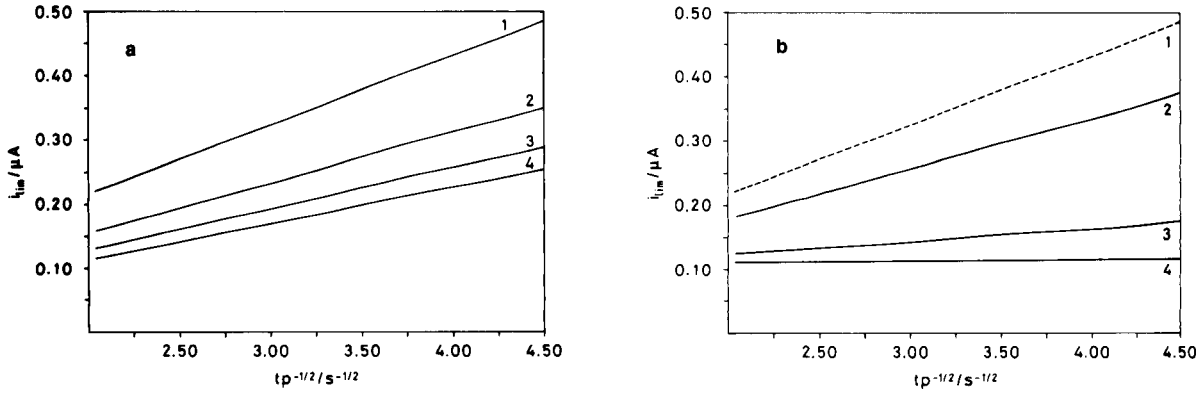


Fig. 1. Simulated curves of $i_{lim}$ vs. $t_p^{-1/2}$ (Cottrell plots). (a) Effect of the variation of the stability constant ($K$) for $K_{ML}$ = 10 l mol$^{-1}$: K = (1) 1 × 10$^3$; (2) 3 × 10$^3$; (3) 5 × 10$^3$; (4) 7 × 10$^3$ l mol$^{-1}$. (b) Effect of the variation of the adsorption coefficient of the complex ($K_{ML}$) for $K$ = 1 × 10$^3$ l mol$^{-1}$ and $K_{ML}$ = (1) 0 (limiting case without adsorption, dashed line), (2) 1 × 10$^3$, (3) 1 × 10$^4$ and (4) 1 × 10$^5$ l mol$^{-1}$. The parameters used are $n$ = 2, $T$ = 298.15 K, $A$ = 0.52 × 10$^{-6}$ cm$^2$, $c_M^*$ = 1 × 10$^{-4}$ M, $c_L^*$ = 1 × 10$^{-3}$ M, $D_{M^{n+}}$ = 7.3 × 10$^{-10}$ m$^2$ s$^{-1}$, $D_{M^0(Hg)}$ = 20 × 10$^{-10}$ m$^2$ s$^{-1}$, $D_L \approx D_{ML}$ = 0.168 × 10$^{-10}$ m$^2$ s$^{-1}$, $K_L$ = 0, and $\Gamma_m$ = 2 × 10$^{-5}$ mol m$^{-2}$, $E^0$ [Cd$^{2+}$/Cd(Hg)] = −0.3521 V. $I_{lim}$ and $t_p$ are given in $\mu$A and s, respectively.

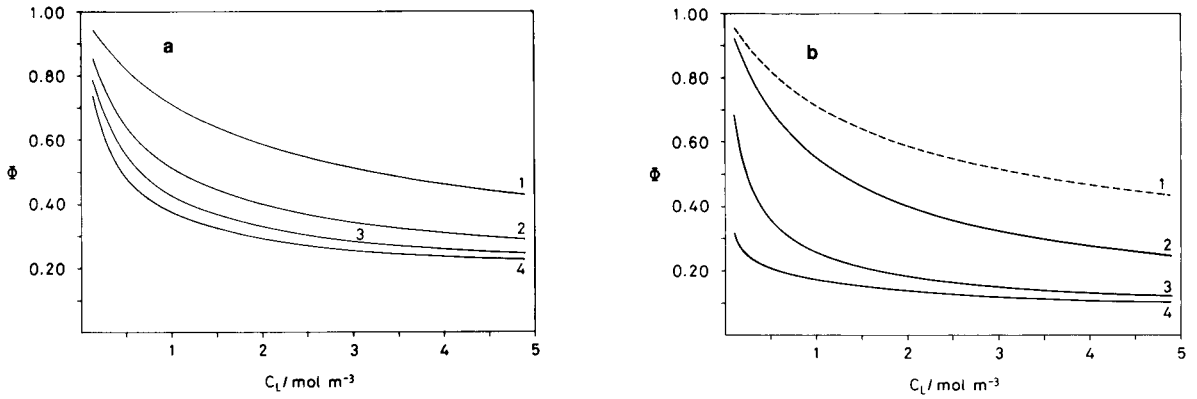


Fig. 2. Simulated curves of the normalized limiting current ($\Phi$) vs. $c_L^*$ for the same values of the parameters as in Fig. 1 and $t_p = 50$ ms. (a) Effect of the variation of the stability constant ($K$) for the same $K_{ML}$ and $K$ values as in Fig. 1a. (b) Effect of the variation of the adsorption coefficient of the complex ($K_{ML}$) for the same $K$ and $K_{ML}$ values as in Fig. 1b (the dashed line represents the case without adsorption). $c_L^*$ are given in mol $m^{-3}$.

tion and the effect of adsorption are similar in such plots. On the Cottrell-like plots (Figs. 1a and 2a) both effects decrease the limiting current without a loss of linearity, and a lower slope value is obtained. Therefore, in the presence of adsorption, the value of the stability constant $K$ obtained using the $D_T$ value given by the Cottrell-like plot is higher than that obtained if the adsorption is taken into account. Analogously, following the procedure using the normalized limiting current ($\Phi$), the same discrepancy is qualitatively found when $K$ values are evaluated from Eqn. 24 (Figs. 1b and 2b).

It is interesting that induced reactant adsorption yields an intercept in the Cottrell plot unlike that in the absence of adsorption, although the plot remains linear [38].

As the effects of complexation ($K$) and adsorption ($K_{ML}$) on the experimental behaviour are so similar, it follows that a non-linear fit of

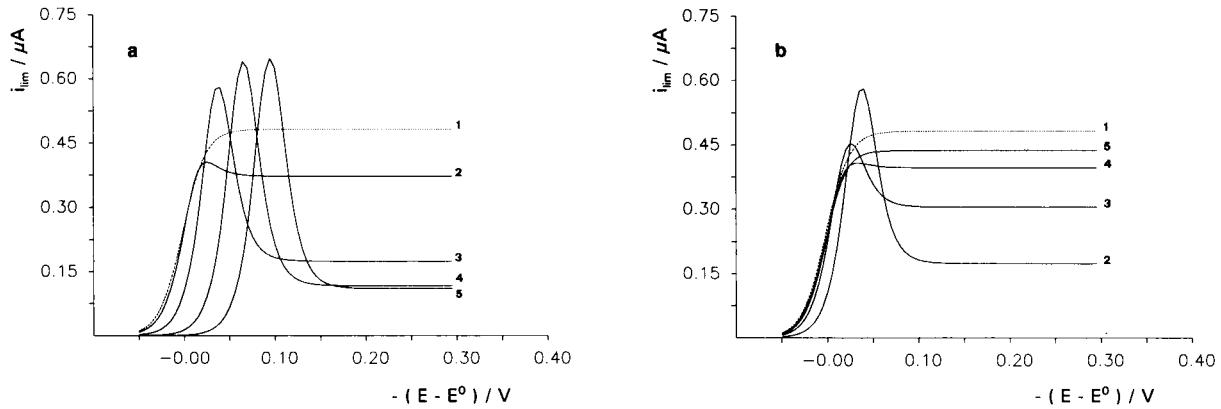


Fig. 3. Simulated curves of the NPP full wave for the same values of the parameters as in Fig. 1. (a) Effect of the variation of the adsorption coefficient of the complex ($K_{ML}$) for $t_p = 50$ ms and $\Gamma_m = 2 \times 10^{-9}$ mol $m^{-2}$: $K_{ML}$ = (1) 0 (limiting case without adsorption, dashed dotted line), (2) $1 \times 10^3$, (3) $1 \times 10^4$, (4) $1 \times 10^5$ and (5) $1 \times 10^6$ l $mol^{-1}$. (b) Effect of the variation of the averaged maximum coverage ($\Gamma_m$), of both the ligand L and the metal ion complex ML, for $t_p = 50$ ms: (1) $K_{ML} = 0$ and $\Gamma_m = 0$ (dashed line represents the case without adsorption); and (2–5) $K_{ML} = 1 \times 10^4$ l $mol^{-1}$ with $\Gamma_m$ = (2) $2 \times 10^{-5}$, (3) $5 \times 10^{-6}$, (4) $2 \times 10^{-6}$ and (5) $1 \times 10^{-6}$ mol $m^{-2}$.

the general Eqn. 13 to experimental limiting current values could be cumbersome and ambiguous. Then, for a set of experimental $I_{lim}$ vs. $c_M$, $c_L^*$ and/or $t_p$ data, it is possible to find different pairs of $K$ and $K_{ML}$ values, as desired, which minimize the standard deviation in the fitting process, with $\chi^2$ values of the same order of magnitude. The a priori unsuccessful fitting procedure mentioned above has been applied to several sets of limiting current data for the Cd–PMA system. This analysis confirms that a unique and unequivocal set of fitted parameters cannot be achieved.

The above discussion leads to the conclusion that the use of only limiting current data is unreliable when simultaneous processes of complexation and adsorption are involved.

*Analysis of the full wave*

In order to attain unambiguous results, a simulation study of the parametric dependence of the full NPP wave must be carried out. As has been mentioned, the influence of the reactant adsorption of the NPP response is characterized as follows [17–24]: the limiting current is decreased; $E_{1/2}$ is shifted; and a peak appears in the current response. These events have been explained in terms of the concentration profile of the species [14,18,22].

In the more complex case of induced reactant adsorption, the above-mentioned effects are also observed. Thus, simulated curves show that when either $K_{ML}$ or $\Gamma_M$ increases (Fig. 3a and b, respectively) the effects produced are the following: the peak height is increased, $I_{lim}$ is decreased and the whole response wave is shifted towards more negative potentials. Further, the present model introduces some new features to be considered.

The influence of the adsorption coefficient of the ligand, $K_L$, in the NPP response is illustrated in Fig. 4, which shows that inverse effects are produced when $K_L$ increases: the peak height is decreased, $I_{lim}$ is increased and the wave is shifted towards more positive potentials (for the case of a reduction process). This is easily understood since as $K_L$ increases $\Theta_{ML}$ decreases for a fixed value of $c_T(0,t)$, considerably reducing the effects

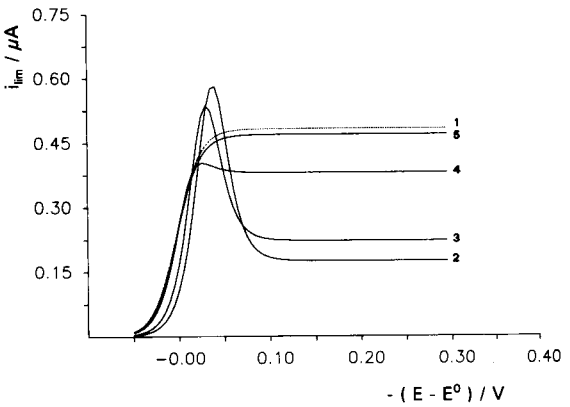


Fig. 4. Simulated curves of the NPP full wave, showing the effect of the variation of the adsorption coefficient of the ligand $K_L$ for the same values of the parameters as in Fig. 1, and for $t_p = 50$ ms, $K = 1 \times 10^3$ l mol$^{-1}$; (1) $K_{ML} = 0$ and $K_L = 0$ (dashed line represents the case without adsorption); (2–5) $K_{ML} = 1 \times 10^4$ l mol$^{-1}$ and $K_L =$ (2) 1; (3) $1 \times 10^2$, (4) $1 \times 10^4$ and (5) $1 \times 10^5$ l mol$^{-1}$.

due to the adsorption of the complex. In the limiting case of $K_L \gg K_{ML}$ (i.e., $\Theta_{ML} \to 0$), the NPP response tends to the case without adsorption, as a consequence of the adsorption competition between L and ML species.

The effect of varying the stability constant of the complex on the simulated response curve is shown in Fig. 5. In general terms, the effect of varying $K$ is more significant in the rising part of

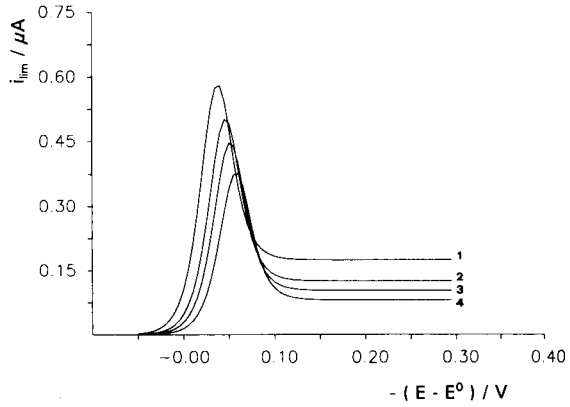


Fig. 5. Simulated curves of the NPP full wave, showing the effect of the variation of the stability constant $K$, for the same values of the parameters as in Fig. 1, and for $t_p = 50$ ms, $K_{ML} = 1 \times 10^4$ l mol$^{-1}$: $K =$ (1) $1 \times 10^3$; (2) $2 \times 10^3$; (3) $3 \times 10^3$; (4) $5 \times 10^3$ l mol$^{-1}$.

the peak (which is decreased and shifted to less negative potentials when $K$ increases) than on the limiting current (which decreases when $K$ increases). It is interesting that all the curves approximately converge somewhere in the decreasing part of the peak, independently of the final limiting current value.

The variation of the complex stability constant affects the full response wave in a very different manner from the variation of the adsorption coefficient of the complex: the peak height decreases as the $K$ values increase and the $K_{ML}$ values decrease, and the limiting current value decreases when either $K$ and/or $K_{ML}$ increase. Hence, this different behaviour suggests that a non-linear fitting procedure for the experimental values to the general system of Eqns. 13, 15 and 17 would be successful in obtaining the best values for the four parameters $K$, $K_{ML}$, $K_L$ and $\Gamma_m$.

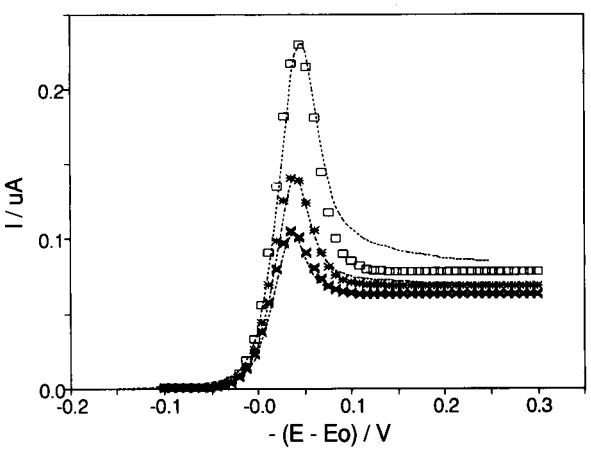


Fig. 6. Curves of the NPP full wave for the Cd(II)–PMA system. Experimental results are drawn as dashed lines, showing curves obtained at different $t_p$ values, for the same values of the experimental parameters as in Fig. 1 and for $c_M^* = 5.0 \times 10^{-5}$ M and $c_L^* = 1.0 \times 10^{-3}$ M. Symbols represent the simulated curves calculated with the model parameters shown in Table 1. $t_p$ = (□) 50, (*) 75 and (×) 100 ms.

*Experimental results for the Cd–PMA system*

In order to test the model developed here, Figs. 6 and 7 compare some experimental NPP waves obtained for the Cd(II)–PMA system with some waves calculated by numerical solution of the present model. In all instances, the values of the stability constant ($K$) necessary to reproduce the experimental waves satisfactorily are lower than those obtained from the experimental limiting currents applying the procedures described under *Analysis of the limiting current*, which are only suitable for the case without adsorption. Thus, the mean $K$ value obtained by applying Eqn. 21 to experimental limiting currents shown in Figs. 6 and 7 is $\log[K\ (\text{l mol}^{-1})] = 4.3 \pm 0.2$, while $\log[K\ (\text{l mol}^{-1})] = 4.2 \pm 0.2$ is obtained when Eqn. 24 is applied, whereas a value of $\log[K\ (\text{l mol}^{-1})] = 3.4 \pm 0.1.4$ (one order of magnitude lower than former values) is calculated from the set of numerical parameters (see Table 1) used in Figs. 6 and 7 (to reproduce the experimental full waves) by applying the treatment developed in this paper, which takes into account the adsorption effect. Table 1 summarizes the values of the parameters used in the theoretical waves and the $\chi_r^2$ values (reduced $\chi^2$, defined as $\chi^2/\phi$, where $\phi$ is the number of degrees of freedom) obtained in the fitting procedure. The mean fitted values for a fixed $K_L$ $\{\log[K_L\ (\text{l mol}^{-1})] = 1.7\}$ are $\log[K(\text{l mol}^{-1})] = 3.4 \pm 0.1$, $\log[K_{ML}\ (\text{l mol}^{-1})] = 4.9 \pm 0.2$ and $\Gamma_m = (1.7 \pm 0.3) \times 10^{-6}$ mol m$^{-2}$.

TABLE 1

Values of $\chi_r^2$ for the fitted curves of the experimental waves obtained for the Cd(II)–PMA system (Figs. 6 and 7)

| $c_T^*$ (M) | $c_L^*$ (M) | $t_p$ (ms) | $K$ (l mol$^{-1}$) | $K_{ML}$ (l mol$^{-1}$) | $\Gamma_m$ (mol m$^{-2}$) | $\chi_r^2$ ($=\chi^2/\phi$) [a] |
|---|---|---|---|---|---|---|
| $5.0 \times 10^{-5}$ | $1.0 \times 10^{-3}$ | 100 | 3130 | $4.99 \times 10^4$ | $1.43 \times 10^{-6}$ | $0.10 \times 10^{-4}$ |
| | | 75 | 2700 | $7.0 \times 10^4$ | | $0.16 \times 10^{-4}$ |
| | | 50 | 2000 | $1.3 \times 10^5$ | | $1.54 \times 10^{-4}$ |
| $1.0 \times 10^{-4}$ | $1.0 \times 10^{-3}$ | 100 | 2600 | $8.0 \times 10^4$ | $2.0 \times 10^{-6}$ | $0.64 \times 10^{-4}$ |
| | | 75 | 2400 | $1.0 \times 10^5$ | | $1.30 \times 10^{-4}$ |
| | | 50 | 1400 | $3.5 \times 10^5$ | | $3.21 \times 10^{-4}$ |

[a] $\phi$ = Number of degrees of freedom.

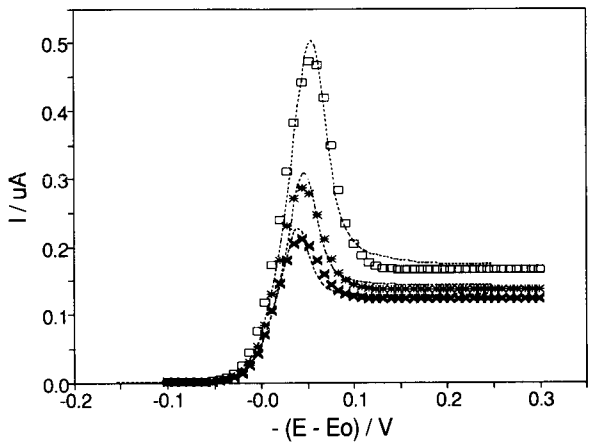


Fig. 7. As Fig. 6 for $c_M^* = 1.0 \times 10^{-4}$ M and $c_L^* = 1.0 \times 10^{-3}$ M.

In order to improve the fitting of the numerical results to experimental data avoiding a too cumbersome and computationally expensive optimization process, a systematic approach is required because of the large number of parameters (four) to be fitted. It is of great interest, especially for experimentalists, to facilitate the fitting process. This is achieved reasonably well when criteria about the main influence of every parameter over the full NPP wave are known. As a consequence of the small influence of $K$ on the decreasing part of the peak (Fig. 5), the fit in this region can be used to evaluate $K_{ML}$ under optimum conditions. Then, with the value found for $K_{ML}$, the fit of the rising part of the wave will be used to evaluate $K$, without perceptible changes in the decreasing part of the wave. Finally, with the $K$ and $K_{ML}$ values found, $K_L$ and $\Gamma_m$ can be evaluated from a more accurate fit of the limiting current zone and the peak maximum. After the full fitting sequence, some small modifications to the parameters can be observed. Usually, a second iterative process in the same sequence yields improved and satisfactory parameters. This simple process has proved to be the more successful.

Although fitting procedures based on the minimization of the sum of least squares by non-linear regression could improve the agreement between experimental results and numerical results, these methods are forbidden because of the large number of parameters to be fitted and the complexity of the set of integral equations, which must be numerically solved, and because they require more cumbersome criteria than that based on the least-squares minimization.

In order to improve the agreement between experimental and simulated data and to explain the systematic variation of $K$ and $K_{ML}$ with pulse time, some shortcomings of the present treatment can be outlined. As previous experimental results for the Cd(II)–PMA system demonstrated [3], the adsorptive behaviour of this system depends on the potential, not only on the initial value of the base potential (constant in NPP) but also on the final value in each pulse. The treatment proposed is restricted to the case of a constant adsorptive parameter (which would coincide with some average parameter). This approximation would be the more valid the narrower the potential range scanned. This range is easily minimized by choosing an initial potential close to the onset of the wave ($E_i = -0.5$ V vs. Ag/AgCl, in the present instance). Experimental results obtained at values of $E_i$ between $-0.5$ and 0 V yield increasing discrepancies when subjected to the present treatment because of the potential dependence of the adsorption parameters [39]. In order to treat experimental results obtained with such potential values ($-0.4$ V $< E_i < 0$ V), the theoretical model should include an explicit dependence of the adsorption parameters on the potential [40].

Another source of possible discrepancies between experimental results and simulated curves may be the assumption of Langmuirian adsorption. The model created to solve the problem under study allows us to consider other isotherms different from the Langmuirian one, with the pertinent changes in the numerical treatment. However, such isotherms (Frumkin, for instance) introduce additional parameters to be fitted. Then, the Langmuirian choice appears to be the most convenient at the present stage of development of the scheme created. A different choice of the adsorption isotherm would mainly affect the current around the peak in the curve, since the peak appearance is a typical adsorption feature. In the limiting region, the influence of the ad-

sorption is much lower because all reactant reaching the electrode is reduced, whereas at intermediate potentials (around the peak potential) the reduction and the adsorption processes take place simultaneously. It could be interesting to utilize the dependence of the observed behaviour on the reactant concentration as a valuable tool to verify the correct interpretation of the adsorption effects and the nature of the isotherms assumed. This will be discussed elsewhere [39].

Finally, the hypothesis of excess of ligand should be reconsidered in the following situations: in experimental systems with macromolecular ligands ($D_L \ll D_M$), where the transport of L can be low; and in cases with ligand adsorption, where the transport of ligand cannot be negligible. In both instances, the homogeneity $c_L(x,t) = c_L^*$ could not be reached. Efforts in this direction are in progress [33].

*Conclusions*

A new model for the voltammetry of metal–polyelectrolyte complex systems is proposed, considering both the adsorption of the polyelectrolyte and the induced adsorption of the metal ion. This model has been rigorously solved for the NPP reduction of a metal ion in the presence of a macromolecule such as PMA. The main advantages of the model are that it reproduces the main features of the NPP response satisfactorily, at least for the Cd(II)–PMA system, and it allows the analysis of the full NPP wave by taking into account the adsorption phenomena.

The authors are grateful to the Centre d'Informàtica de la Universitat de Barcelona and CESCA (Centre de Supercomputació de Catalunya) for providing with computation facilities. They also thank H.P. van Leeuwen (Wageningen Agricultural University, Wageningen, Netherlands) for his critical comments on the manuscript. The authors gratefully acknowledge support of this research by the Spanish Ministry of Education and Science (DGICYT: Project PB 90-0821) and the European Community (Programme Science); J. Puy and F. Mas also acknowledge support by the Spanish Ministry of Education and Science (DGICYT: Project PB 90-0455). A personal FPI grant from the Spanish Government to J.M. Díaz-Cruz is also gratefully acknowledged.

## APPENDIX

According to the scheme assumed in Eqn. 1, the faradaic current $I(t)$ is proportional to the flux of metal ion, M, or metal product, $M^0$, at the electrode surface. Moreover, if the electrode is stationary and semi-infinite planar diffusion is assumed, the current can be written as

$$I(t) = nFA\left\{ \begin{array}{l} +D_M\left(\dfrac{\partial c_M(x,t)}{\partial x}\right)_{x=0} \\ -D_M^0\left(\dfrac{\partial c_{M^0}(x,t)}{\partial x}\right)_{x=0} \end{array} \right. \quad \text{(A1)}$$

or, in terms of $c_T = c_M + c_{ML}$, as

$$I(t) = nFA\left\{ -D_T\left(\frac{\partial c_T(x,t)}{\partial x}\right)_{x=0} + \frac{d\Gamma_{ML}(t)}{dt} \right\} \quad \text{(A2)}$$

The flux terms $(\partial c_i(x,t)/\partial x)_{x=0}$, $i = M, M^0$, ML and T are obtained from the resolution of the transport problem. Using the Laplace transformation method and the convolution theorem [24,29–32], the integral flux terms can be written as

$$D_i\int_0^t\left(\frac{\partial c_i(x,\tau)}{\partial x}\right)_{x=0} d\tau = -\sqrt{\frac{D_i}{\pi}}\int_0^t \frac{c_i(0,\tau) - c_i^*}{\sqrt{t-\tau}} \cdot d\tau \quad \text{(A3)}$$

The problem is now to obtain $c_i(0,t)$, which can be obtained from the boundary conditions at $x = 0$.

*Integral equation for $\Gamma_{ML}(t)$*

Using Eqn. A3, the integral of the boundary

condition 12 can be written as

$$\Gamma_{ML}(t) - \Gamma_{ML}(t=0) = \left(2\sqrt{\frac{D_T}{\pi}}\right) \times \left\{c_T^* \sqrt{t} - \frac{1}{2}\int_0^t \frac{[1+\delta(\tau)]c_T(0,\tau)}{\sqrt{t-\tau}} \cdot d\tau\right\} \quad (A4)$$

where

$$\delta(t) \equiv \sqrt{\frac{D_{M^0}}{D_T}} \frac{1}{(1+K')} \times \exp\left\{-\frac{nF}{RT}[E(t) - E_0]\right\} \quad (A5)$$

and the reversibility condition 11 has been used to relate $c_{M^0}(0,\tau)$ and $c_T(0,\tau)$.

Equation A4 and the adsorption isotherm Eqn. 7a form an implicit integral equation in $\Gamma_{ML}(t)$, which can be solved numerically. $\Gamma_{ML}(t=0)$ has been taken to be zero according to the initial condition 3b.

*Integro-differential equation for $\Gamma_{ML}(t)$*

The use of the Leibnitz derivation rule under the integral sign in Eqn. A3 allows us to write the flux term as

$$D_i\left(\frac{\partial c_i(x,t)}{\partial x}\right)_{x=0} = +\sqrt{\frac{D_i}{\pi}}\left\{\frac{[c_i^* - c_i(0,0^+)]}{\sqrt{t}} - \int_0^t \frac{1}{\sqrt{t-\tau}}\left(\frac{dc_i(0,\tau')}{d\tau'}\right)_{\tau'=\tau} d\tau\right\} \quad (A6)$$

where $c_i(0,0^+)$, $i$ = ML, T, are zero.

Using Eqn. A6 and the reversibility condition 11, the boundary condition 12 can be written as

$$\Gamma'_{ML}(t) = \sqrt{\frac{D_T}{\pi}}\left\{\frac{c_T^*}{\sqrt{t}} - \int_0^t \frac{[(1+\delta(\tau))c_T(0,\tau)]'}{\sqrt{t-\tau}} \cdot d\tau\right\} \quad (A7)$$

where the prime represents the time derivative of the function. Equation A7 together with Eqn. 7a forms an integro-differential equation in $\Gamma_{ML}(t)$.

*Equation for $I_{NPP}$*

The NPP technique records the current at the dropping time, $t_d$, when the pulse potential has been applied at $t_0$, $I_{NPP} \equiv I(t_d)$. Thus, using Eqn. A5, Eqn. A2 becomes

$$I_{NPP} = nFA\left\{\sqrt{\frac{D_T}{\pi}}\left[\frac{c_T^*}{\sqrt{t_d}} - \int_0^{t_d} \frac{c'_T(0,\tau)}{\sqrt{t_d - \tau}} \cdot d\tau\right] + \Gamma'_{ML}(t_d)\right\} \quad (A8)$$

The time dependence of the potential applied to the drop in NPP can be written as

$$E(t) = E_B - EH(t - t_0) \quad (A9)$$

where $H(t-t_0)$ is the step function

$$H(t) \equiv \begin{cases} 0 & t < 0 \\ 1 & t > 0 \end{cases} \quad (A10)$$

and $E_B$ is the base potential, which is chosen so that no faradaic reaction occurs ($E_B \to \infty$, describes a reduction process). In terms of the dimensionless potential function defined in Eqn. A5, Eqn. A9 becomes

$$\delta(t) = \delta H(t - t_0) \quad (A11)$$

because $\delta_B \to 0$.

In order to simplify the integral term appearing in Eqn. A8, the integro-differential Eqn. A7 could be used. However, the integral term appearing in Eqn. A7 has a discontinuity due to the derivative of the dimensionless potential function $\delta(t)$ (Eqn. A11). Then, the integral term in Eqn. A7,

$$Y(t) = \int_0^t \frac{[(1+\delta(\tau))c_T(0,\tau)]'}{\sqrt{t_d - \tau}} \cdot d\tau \quad (A12)$$

contains the $\delta'(\tau)$ and $c'_T(0,\tau)$ functions. From Eqn. A11 the $\delta'(t)$ function can be written as

$$\delta'(t) = \delta H'(t - t_0) = \delta\delta_D(t - t_0) \quad (A13)$$

where $\delta_D$ is the Dirac delta function with the

important property

$$\int_{t_1}^{t_2} f(t)\delta_D(t-t_0)\,dt \equiv \begin{cases} 0 & t_0 \notin [t_1,t_2] \\ f(t_0) & t_0 \in [t_1,t_2] \end{cases} \quad \text{(A14)}$$

and the $c'_T(0,t)$ function is straightforward because $c_T(0,t)$ is a continuous function only for the reactant adsorption process (see Appendix A in [31]). Equation A12 then becomes

$$Y(t) = \frac{\delta c_T(0,t_0)}{\sqrt{t-t_0}} + Y(t_0^-) + Y(t_0^+) \quad t > t_0 \quad \text{(A15)}$$

with

$$Y(t_0^-) = \int_0^{t_0^-} \frac{c'_T(0,\tau)}{\sqrt{t_d-\tau}} \cdot d\tau \quad \text{(A16a)}$$

and

$$Y(t_0^+) = (1+\delta)\int_{t_0^+}^{t} \frac{c'_T(0,\tau)}{\sqrt{t_d-\tau}} \cdot d\tau \quad \text{(A16b)}$$

where $t_0^-$ and $t_0^+$ mean the limit value $t \to t_0$, if $t < t_0$ and if $t > t_0$, respectively, which are different due to the discontinuity in $\delta(t)$ at $t = t_0$.

To eliminate one of the integral terms in Eqn. A17, the integro-differential Eqn. A7 must be considered. If the term $Y(t_0^+)$ is isolated from the integro-differential Eqn. A7 and introduced into Eqn. A15, the integral term A12 becomes

$$Y(t) = \frac{1}{1+\delta}\left\{ -\sqrt{\frac{\pi}{D_T}}\,\Gamma'_{ML}(t) - \frac{\delta c_T(0,t_0)}{\sqrt{t-t_0}} - \int_0^{t_0^-} \frac{c'_T(0,\tau)}{\sqrt{t_d-\tau}} \cdot d\tau \right\} \quad \text{(A17)}$$

and then the NPP current Eqn. A8 becomes

$$I_{NPP} = nFA\left(\frac{\delta}{1+\delta}\right)\left\{\sqrt{\frac{D_T}{\pi}}\left[\frac{c_T^*}{\sqrt{t_d}} + \frac{c_T(0,t_0)}{\sqrt{t_p}} - \int_0^{t_0^-} \frac{c'_T(0,\tau)}{\sqrt{t_d-\tau}} \cdot d\tau\right] - \Gamma'_{ML}(t_d)\right\} \quad \text{(A18)}$$

This equation does not have an explicit analytical solution for the most frequently used adsorption isotherms, but a numerical solution can always be found.

## REFERENCES


1 J. Buffle, Complexation Reactions in Aquatic Systems. An Analytical Approach, Horwood, Chichester, 1988, Chap. 9.
2 D.R. Crow, Polarography of Metal Complexes, Academic, London, 1969.
3 M. Esteban, E. Casassas, H.G. de Jong and H.P. van Leeuwen, Anal. Chim. Acta, 229 (1990) 93.
4 A.M. Bond and G. Hefter, J. Electroanal. Chem., 68 (1976) 203.
5 E. Casassas and C. Ariño, J. Electroanal. Chem., 213 (1986) 235.
6 Y.I. Tur'yan, Zh. Obshch. Khim., 53 (1983) 2314.
7 M.C. Montemayor and E. Fatas, J. Electroanal. Chem., 246 (1988) 271.
8 M.C. Montemayor and E. Fatas, Electrochim. Acta, 33 (1988) 655.
9 M. Sluyters-Rehbach and J. Sluyters, J. Electroanal. Chem., 75 (1977) 371.
10 M. Lovrić, Anal. Chim. Acta, 218 (1989) 7.
11 S. Komorsky-Lovrić, M. Lovrić and M. Branica, J. Electroanal. Chem., 266 (1989) 185.
12 J. Gálvez, J. Zapata and C. Serna, J. Electroanal. Chem., 205 (1986) 21.
13 J. Gálvez and Su-Moon Park, J. Electroanal. Chem., 243 (1988) 263.
14 J. Buffle, A.M. Mota and M.L.S. Simoes Gonçalves, J. Electroanal. Chem., 223 (1987) 235.
15 J.M. Díaz-Cruz, C. Ariño, M. Esteban and E. Casassas, Electroanalysis, 3 (1991) 299.
16 A.M. Nadal, C. Ariño, M. Esteban and E. Casassas, Electroanalysis, 3 (1991) 309.
17 J.B. Flanagan, K. Takahashi and F.C. Anson, J. Electroanal. Chem., 85 (1977) 261.
18 H.P. van Leeuwen, J. Electroanal. Chem., 133 (1982) 201.
19 H.P. van Leeuwen, J. Electroanal. Chem., 162 (1984) 67.
20 H.P. van Leeuwen, M. Sluyters-Rehbach and K. Holub, J. Electroanal. Chem., 135 (1982) 13.
21 K. Holub and H.P. van Leeuwen, J. Electroanal. Chem., 162 (1984) 55.
22 M. Lovrić, J. Electroanal. Chem., 170 (1984) 143; 175 (1984) 33; 223 (1987) 271.
23 S. Komorsky-Lovrić and M. Lovrić, J. Electroanal. Chem., 190 (1985) 1.
24 F. Mas, J. Puy, F. Sanz and J. Virgili, J. Electroanal. Chem., 183 (1985) 73.
25 H.G. de Jong, H.P. van Leeuwen and K. Holub, J. Electroanal. Chem., 234 (1987) 1.
26 H.G. de Jong and H.P. van Leeuwen, J. Electroanal. Chem., 234 (1987) 17.
27 H.G. de Jong and H.P. van Leeuwen, J. Electroanal. Chem., 235 (1987) 1.

28 H.P. van Leeuwen, R. Cleven and J. Buffle, Pure Appl. Chem., 61 (1989) 255.
29 F. Mas, J. Puy, F. Sanz and J. Virgili, J. Electroanal. Chem., 158 (1983) 217.
30 J. Puy, F. Mas, F. Sanz and J. Virgili, J. Electroanal. Chem., 183 (1985) 27.
31 F. Mas, J. Puy, F. Sanz and J. Virgili, J. Electroanal. Chem., 183 (1985) 41.
32 E. Guaus, F. Mas, J. Puy and F. Sanz, J. Electroanal. Chem., 224 (1987) 1.
33 J. Puy, J. Galceran, J. Cecília, J. Salvador, F. Mas and M. Esteban, J. Electroanal. Chem., submitted for publication.
34 R.S. Nicholson and M.L. Olmstead, in J.S. Mattson, H.B. Mark, Jr., and H.C. MacDonald, Jr. (Eds.), Electrochemistry, Calculations, Simulation and Instrumentation, Part I; Dekker, New York, 1972, Chap. 5.
35 R. Guidelli and D. Cozzi, J. Phys. Chem., 71 (1967) 3027.
36 R.N. Adams, Electrochemistry at Solid Electrodes, Dekker, New York, 1969.
37 F. Vydra, K. Stulik and E. Juláková, Electrochemical Stripping Analysis, Wiley, London, 1976.
38 H.P. van Leeuwen, J. Buffle and M. Lovrić, Pure Appl. Chem., 64 (1992) 1015.
39 J.M. Díaz-Cruz, M. Esteban, E. Casassas, F. Mas and J. Puy, to be published.
40 J. Puy, F. Mas, J.M. Díaz-Cruz, M. Esteban and E. Casassas, J. Electroanal. Chem., 328 (1992) 271–285.

*Analytica Chimica Acta*, 268 (1992) 275–284
Elsevier Science Publishers B.V., Amsterdam



# Influence of anion-induced adsorption on the polarographic/voltammetric determination of stability constants

Marina Zelić and Marko Branica

*Center for Marine Research Zagreb, Rudjer Bošković Institute, P.O.B. 1016, 41001 Zagreb (Croatia)*

(Received 21st January 1992; revised manuscript received 15th May 1992)

**Abstract**

The polarographic/voltammetric determination of complexation constants, influenced by ligand-induced adsorption of metal ions, was studied. The factors affecting the final results, such as the "speed" of the applied technique, metal concentration, ionic strength and data treatment were examined, taking lead(II) and cadmium(II) in halide solutions as model systems. A comparison was made of the observations with existing theoretical predictions.

*Keywords:* Polarography; Voltammetry; Adsorption; Cadmium; Lead; Stability constants

Since the early 1950s when DeFord and Hume [1] published a method for the polarographic determination of stability constants, many metal–ligand systems have been studied in this way [2,3]. However, in three papers dealing with halide complexes of lead(II) and cadmium(II), Bond and Hefter [4–6] demonstrated the inequivalence of polarographic and potentiometric values, the former being much higher. The effect was ascribed to previously [7] observed anion-induced adsorption, i.e., "extraction" of dissolved metal from solutions of a surface-active ligand to mercury electrodes. Subsequently it became generally accepted that potentiometric results are not affected by adsorption whereas polarographic results are.

The earlier experiments [4–6] attracted great attention, resulting in numerous theoretical papers [8–14]. Attempts were made to understand the phenomenon and to predict optimum experimental conditions or data treatment. However, it is surprising that during the last 15 years few new measurements of a similar type have been made. Especially results corresponding to high electrolyte concentrations are lacking. Perhaps the most important experiments were those described by Fatas-Lahoz et al. [15], who clearly indicated that the dramatically increased half-wave potential shift obtained in an iodide solution (0.1 mol $l^{-1}$) of cadmium(II) was mainly caused by the measuring conditions. In other words, the effect can be significantly reduced by proper experimental design. It was therefore decided to examine the influence of different factors such as the polarographic/voltammetric technique used, time of electrolysis, metal concentration, ionic strength and data treatment, on the half-wave or peak potential shifts and the resulting values of stability constants. The observations were compared with existing theoretical predictions.

*Correspondence to:* M. Zelić, Center for Marine Research Zagreb, Rudjer Bošković Institute, P.O.B. 1016, 41001 Zagreb (Croatia).

## EXPERIMENTAL

For the preparation of solutions, analytical-reagent grade $Pb(NO_3)_2$, $Cd(NO_3)_2$, $NaClO_4 \cdot H_2O$, $LiClO_4 \cdot 3H_2O$, LiCl, NaBr, NaI and 70% $HClO_4$ (Merck, Ventron and Kemika) were used, together with redistilled or deionized water.

Polarographic/voltammetric measurements were performed using an EG&G Princeton Applied Research (PAR) Model 384B polarographic analyser connected to a PAR 303A static mercury drop electrode and a Houston Instrument Model DMP-40 digital plotter. Only the dependence of the half-wave potential on the drop lifetime was investigated using a BAS 100A electrochemical analyser (Bioanalytical Systems, West Lafayette, IN). Potentials were referred to a saturated Ag/AgCl(NaCl) electrode and a platinum wire was used as a counter electrode. Square-wave voltammetric (SWV) measurements were performed at a frequency ($f$) of 100 $s^{-1}$. In differential-pulse polarography (DPP), a drop lifetime of 1 s was chosen. The scan increment was 2 mV in both instances.

A titration procedure at a constant ionic strength ($I$), maintained with $NaClO_4$ or $LiClO_4$, was adopted. Dissolved metal was also kept at a constant level in each series of measurements except those in which the role of metal concentration was studied. All experiments were performed at a constant acidity (pH = 2 or 3) from solutions previously deaerated with high-purity nitrogen.

Because of some technical problems, the small polarographic cell that belongs to the PAR 303A static mercury drop electrode could not be thermostated but the experiments were performed at nearly 25°C.

## RESULTS AND DISCUSSION

### *Role of measuring conditions*

According to d.c. polarographic results obtained by Bond and Hefter [5], half-wave potential shifts measured in bromide solutions of lead(II) are much higher than expected from potentiometrically determined stability constants. At

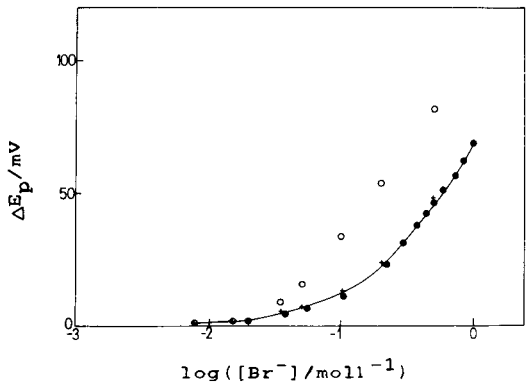


Fig. 1. Dependence of lead(II) half-wave potential shift on bromide concentration. The present results (●) are shown together with values published by (+) Kivalo [17] and (○) Bond and Hefter [5]. Full line indicates expected shifts, based on critical values [16] of formation constants of all $PbBr_p$ complexes.

$[Br^-] = 0.5$ mol $l^{-1}$ and $I = 1$ mol $l^{-1}$, the difference between the two values is 34 mV. As the "correct" shift should be only 48 mV, this result is surprising. Therefore, corresponding sampled d.c. polarographic measurements were performed at the same ionic strength using a static mercury drop electrode. The resulting values, measured at a relatively low metal concentration ($5 \times 10^{-5}$ mol $l^{-1}$), are given in Fig. 1.

It can be seen that our experimental points are located on the "theoretical" [16] curve together with Kivalo's [17] results, obtained at a high level of dissolved lead (1 mmol $l^{-1}$) in the presence of gelatine. The dependence of the half-wave potential shift ($\Delta E_{1/2}$) on the ligand concentration, based on Bond's polarographic experiments, is completely different (Fig. 1). As the main difference between the two sets of measurements is the drop lifetime ($t_d$), it seems that too high potential shifts were caused by the fast dropping ($t_d = 0.16$ s) used in the mentioned experiments [5]. For this reason the influence of $t_d$ on the polarographic results was investigated at $I = 4$ mol $l^{-1}$.

At such a high electrolyte concentration the adsorption effects should be more pronounced because of the decreased water activity [18,19]. It was confirmed that the fast dropping really causes the increased half-wave potential shifts (Fig. 2) in bromide but not in pure perchlorate solutions of

lead(II). The waves obtained at $t_d = 0.250$ s, depending on the bromide concentration, are shifted cathodically up to 26 mV in comparison with the signals recorded at $t_d = 1$ s. The difference between rapid and "normal" polarography was predicted [8,14] although not observed by Bond and Hefter [5].

Similar effects, i.e., dependence of the peak potential shift on the characteristic time variable, should be expected in other voltammetric techniques such as DPP [20] and SWV [21]. Additionally, different techniques are expected not to give the same $\Delta E_p$ values when applied to a given system, because of their different sensitivities to adsorption. This problem was studied using, in comparison with $PbBr_p$, more adsorbable $CdI_p$ complexes at $I = 1$ mol $l^{-1}$.

In Fig. 3a new results obtained by SWV are presented together with the literature values [6] (a.c., d.c. and expected) measured at similar metal concentrations of $4 \times 10^{-5}$–$5 \times 10^{-5}$ mol $l^{-1}$. On going towards more sensitive techniques, the

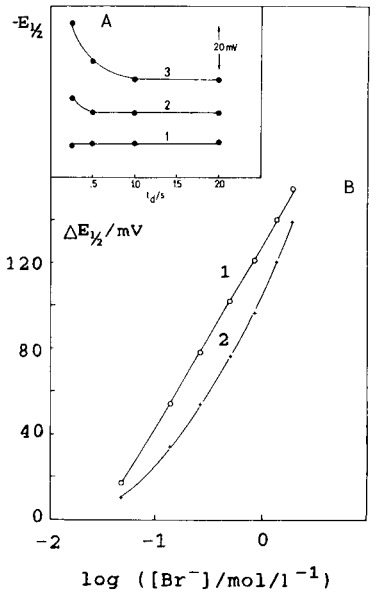


Fig. 2. (A) Dependence of the half-wave potential on the drop lifetime. $[Pb]_t = 5 \times 10^{-5}$ mol $l^{-1}$. $[Br^-] = (1)$ 0, (2) 0.047 and (3) 0.511 mol $l^{-1}$. $I = 4$ mol $l^{-1}$. $[HClO_4] = 0.01$ mol $l^{-1}$. (B) Dependence of the half-wave potential shift on bromide concentration. $t_d = (1)$ 0.250 and (2) 1.000 s. Other conditions as in (A).

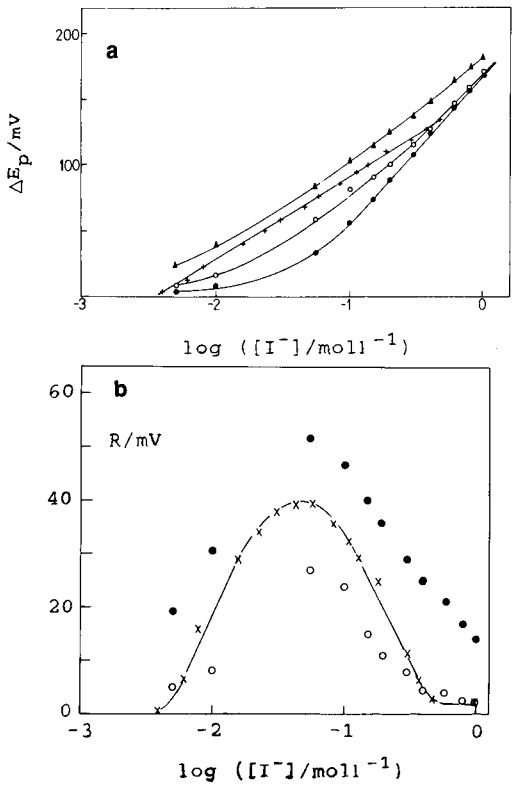


Fig. 3. (a) Shifts of the half-wave or peak potential in iodide solutions of cadmium(II) at $I = 1$ mol $l^{-1}$. Expected values, based on potentiometric data (●) [16], are given together with published [6] (○) d.c. ($t_d = 1$ s) and (▲) a.c. ($f = 300$ $s^{-1}$) polarographic and (×) our SWV ($f = 100$ $s^{-1}$) results. (b) Results from (a) presented as the difference ($R$) between measured and expected shifts of (○) d.c., (×) SWV and (●) a.c. signals.

curve in the $\Delta E_p$ (or $\Delta E_{1/2}$) vs. log [$I^-$] diagrams that can be described by a polynomial of the fourth order gradually becomes a straight line. If the same data are presented in another form, i.e., as the difference ($R$) between measured and expected [16] potential shifts at increasing ligand concentration (Fig. 3b), it becomes obvious that the highest values are connected with a.c. polarography (frequency 300 $s^{-1}$). The whole effect appears in the iodide concentration range in which the surface-active complex $CdI_2$ forms a significant fraction of the total dissolved metal (Fig. 4), as predicted previously [14]. Moreover, there is a nearly linear relationship between $R$ and this fraction.

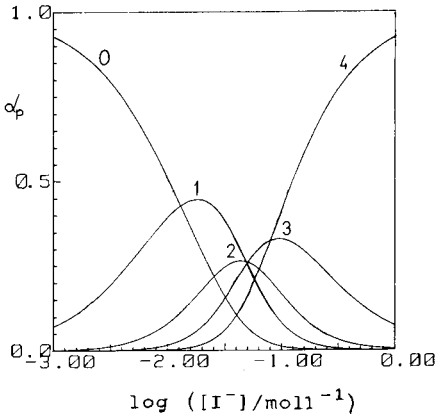


Fig. 4. Fractions of dissolved cadmium(II) bound in different iodide complexes at $I = 1$ mol $l^{-1}$. Numbers on the curves denote $p$ values of the corresponding $CdI_p$ species (log $\beta_1$ = 1.89, log $\beta_2$ = 3.2, log $\beta_3$ = 4.5, log $\beta_4$ = 5.6).

The influence of the applied polarographic/voltammetric technique on the measured half-wave or peak potential shifts has already been studied by Casassas and Ariño [22]. Their results, obtained at a higher metal concentration, could not be compared with those presented in Fig. 3, because they did not give details of their measuring procedure (drop time in d.c. polarography, frequency in a.c. polarography, etc.).

Although the experiments with weak, kinetically labile complexes are always performed at a large excess of the total ligand ($L_t$), different metal (M) concentrations can satisfy the condition $[L]_t \gg [M]_t$. However, if the metal concentration is gradually increased at a constant level of dissolved halide, the content of the surface-active complex species in the solution also increases, together with the coverage of the electrode surface. In other words, the shift of the polarographic/voltammetric signal is expected to depend on $[M]_t$ chosen for the experiment. The situation for $Pb^{2+}$–$Br^-$, $Cd^{2+}$–$Br^-$ and $Cd^{2+}$–$I^-$ systems is presented in Fig. 5a, b and c, respectively; the results obtained in chloride solutions of lead(II) have already been published [23]. In each instance a concentration of the total ligand was chosen than leads to a high percentage of the metal bound in the surface-active complex, taking into account previously obtained results [24,25] and/or literature data [26].

Three main types of peak potential shift with increasing total metal concentration could be distinguished. The first is characterized by a continuous increase in $\Delta E_p$ with increasing $[M]_t$, accompanied by a broadening of the signal, as demonstrated in the case of lead(II) adsorption from a chloride solution ($[Cl^-] = 2$ mol $l^{-1}$, $I = 4$ mol $l^{-1}$) [23]. The two other types are characterized by a gradual decrease in $\Delta E_p$ with increasing metal concentration, which finally reaches a constant value with (Fig. 6) or without obvious splitting of the reduction signal. (In each instance the observed behaviour is mainly governed by the type and parameters of the corresponding adsorption isotherm [27].) Consequently, the complexation constants determined by the same method in a given system at two different metal concentrations could also differ. This type of experiment could not be performed in iodide solutions of lead(II) because $PbI_2$ is sparingly soluble [16].

According to some recommendations [12], if the ligand is surface active, polarographic determination of complexation constants should be performed at as high as possible metal concentrations in order to obtain the main wave (or peak) instead of the post-wave. In practice, however, it is not easy to follow this principle. At a high level of dissolved metal the formation of a solid phase can occur. Additionally, it is not possible to fulfil the requirement $[L]_t \gg [M]_t$ at low ligand concentrations, which could be important in some systems, Polarograms of lead(II) recorded from bromide–perchlorate mixtures ($I = 4$ mol $l^{-1}$) at high levels of dissolved metal ($5 \times 10^{-4}$, $1 \times 10^{-3}$ and $2.5 \times 10^{-3}$ mol $l^{-1}$) [28] could not be used for the determination of stability constants.

In addition to the problems mentioned above, the main wave was poorly defined at low relative concentrations of $PbBr_2$ and/or separated from the post-wave by a minimum at high concentrations. Hence the accurate determination of its half-wave potential could not be performed. In some other systems, such as $Cd^{2+}$–$Br^-$, splitting of the signal does not occur at real concentrations of dissolved cadmium (up to $2.5 \times 10^{-3}$ mol $l^{-1}$).

Taking into account that the wave or peak shifts with increasing metal concentration in dif-

ferent ways on going from one system to another (and from one technique to another), it is obvious that the recommendation concerning the optimum $[M]_t$ cannot be taken literally. In the cadmium(II)–iodide system (Fig. 5C), the decease in the measured $\Delta E_p$ with increasing metal concentration (at a constant ligand concentration) was really obtained at $I = 1$ mol $l^{-1}$ (but not in other systems under investigation.) At $I = 4$ mol $l^{-1}$ poorly pronounced splitting of the signal was

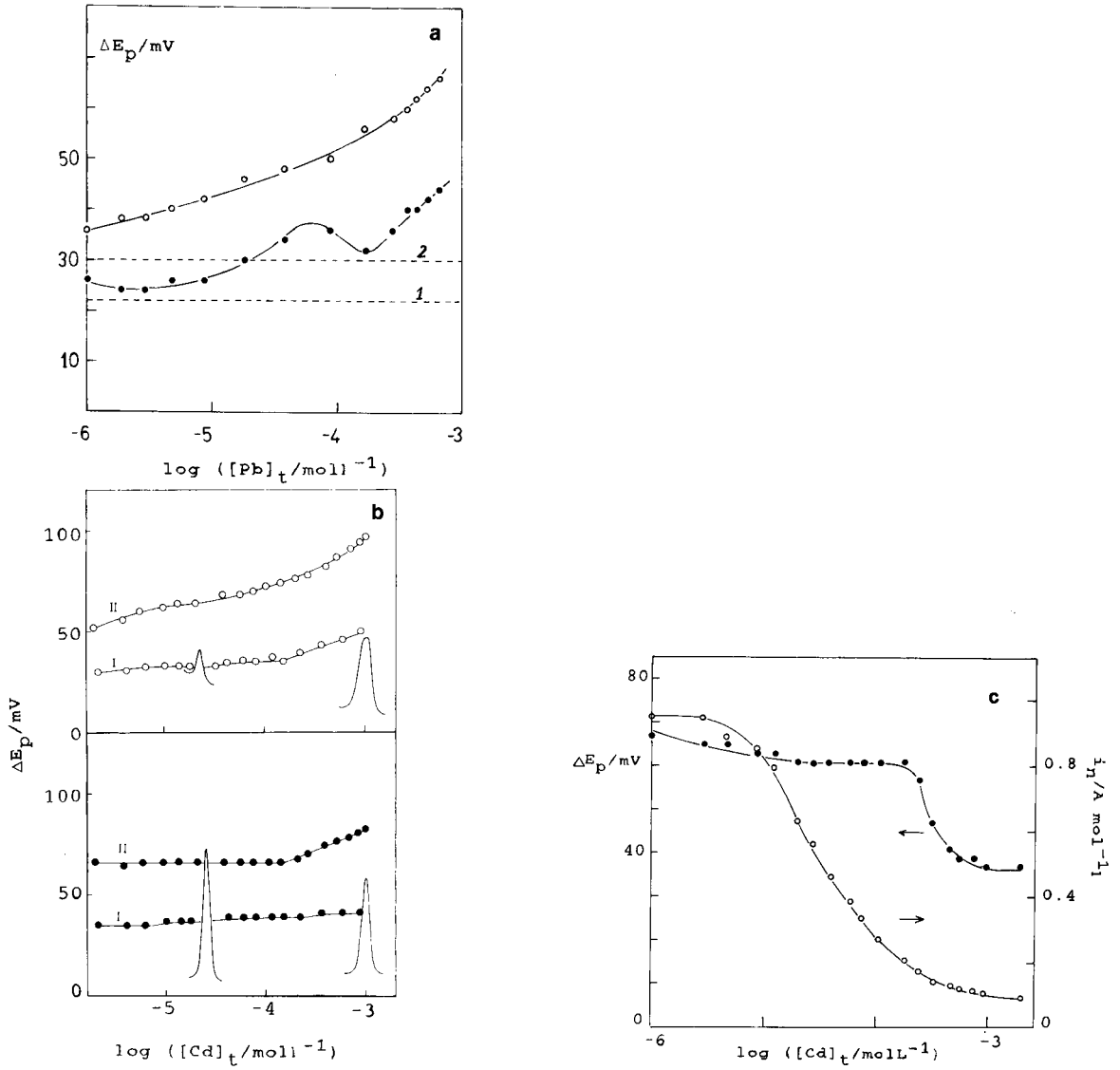


Fig. 5. (a) Dependence of lead(II) peak potential shift in (●) DPP and (○) SWV on the total metal concentration at $[Br^-] = 0.10$ mol $l^{-1}$. Expected $\Delta E_p$ is given by the dashed line, calculated from (1) Vierling's results [32] or (2) critical values [16] of stability constants. $I = 4$ mol $l^{-1}$. Initial potential $E_i = -0.20$ V. (b) Dependence of cadmium(II) peak potential shift in (●) DPP and (○) SWV on the total metal concentration at $[Br^-]$ = (I) 0.10 or (II) 0.25 mol $l^{-1}$. The change in the peak shape is also shown. $I = 4$ mol $l^{-1}$. (c) (●) Dependence of cadmium(II) peak potential shift in SWV on the total metal concentration at $[I^-] = 0.059$ mol $l^{-1}$. (○) Change in the normalized peak current ($i_n = i_p/[Cd]_t$). $I = 1$ mol $l^{-1}$. $E_i = -0.35$ V.

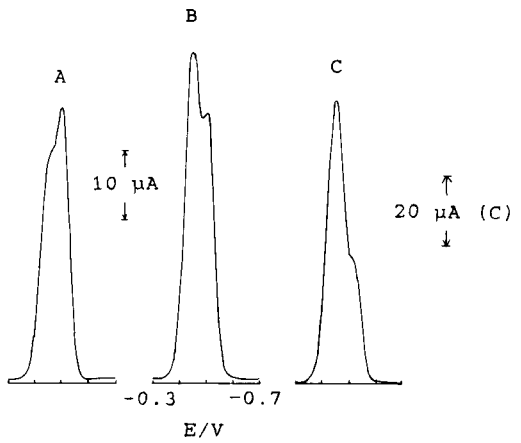


Fig. 6. Shape of cadmium(II) SVW signal recorded at $I = 4$ mol $l^{-1}$, $[I^-] = 0.012$ mol $l^{-1}$. $[Cd]_t$ = (A) $2.02 \times 10^{-4}$, (B) $3.98 \times 10^{-4}$ and (C) $7.86 \times 10^{-4}$ mol $l^{-1}$.

obtained instead (Fig. 6), which could not be used for the determination of stability constants from the shift of the main wave. Perhaps some method that improves the separation of two close processes could be applied. This problem will, however, be treated elsewhere in more detail.

*Determination of stability constants*

In a diffusion-controlled process the half-wave or peak potential shift will be linearly dependent on log[L] if only one complex is formed or if other coordination species are virtually absent over a relatively wide ligand concentration range. In such a case the composition of the given $ML_p$ species and its formation constant can be calculated by applying Lingane's method [29], i.e., from the equation

$$\Delta E_{1/2} = (2.303RT/nF) \log \beta_p [L]^p \quad (1)$$

where $\Delta E_{1/2}$ denotes the difference between the half-wave potentials measured in a non-complexing medium and in a ligand-containing solution. Adsorption of a complex species can also produce a linear dependence [14]. Such a straight line usually has a slope that corresponds to the "predominance" of $ML_2$ or $ML_3$. However, the stability constant calculated from the intercept with the ordinate is completely different from the value obtained by any other experimental technique not influenced by adsorption. For example, in the $Cd^{2+}$–$I^-$ system ($I = 1$ mol $l^{-1}$) (Fig. 3a), the slope equals 61 mV per decade but $\beta_2$ calculated from the intercept (log $\beta_2 = 5.1$) exceeds the generally accepted value (log $\beta_2 = 3.2$ [16]) by about two orders of magnitude. In $Pb^{2+}$–$I^-$ at $I = 6$ mol $l^{-1}$ even two flat segments with slopes of 58 and 87 mV per decade were obtained by SWV (Fig. 7a). Although the literature values for $\beta_2$ and $\beta_3$ corresponding to this ionic strength are not available, they can be predicted by extrapolation of $\beta_p$ vs. $I^{1/2}$ curves (Fig. 7b). Again, the experimentally obtained log $\beta_2 = 7.8$ and log $\beta_3 = 9.6$ are much higher (by 3–4 orders of magnitude) than expected. Consequently, anion-induced adsorption produces linear parts of $\Delta E_p$ vs. log [L] curve which cannot be used for the determination of individual stability constants. However, it does not mean that all flat segments should be ignored. During the study of cadmium complexation in iodide solutions ($I = 4$ mol $l^{-1}$) a linear part of the curve for log $[I^-] = -0.04$–$0.6$ has a slope of 120 mV per decade (Fig. 7a). The overall concentration constant log $\beta_4 = 7.16$, calculated from the intercept of this straight line with the ordinate, does not seem to be influenced by adsorption. It is significantly lower than the only value of $\beta_4$ (log $\beta_4 = 8.20$) that could be found in the literature for this ionic strength [3], but fits well with the log $\beta_4$ vs. $I^{1/2}$ curve if only the critically assessed values [16] are taken into account.

When several metal complexes are present in the same ligand concentration range, the half-wave or peak potential shift, not influenced by adsorption, is given [1] by

$$\Delta E_{1/2} = (2.303RT/nF) \times \log\left(1 + \beta_1[L] + \beta_2[L]^2 + \ldots \beta_N[L]^N\right) \quad (2)$$

assuming that the diffusion coefficients are the same. In such a case a set of stability constants can be obtained by a curve-fitting method [30]. From Eqn. 2 it follows that a polynomial which optimally fits the experimental results should be found, the degree of which gives the number of complexes while the coefficients correspond to the overall formation constants. For obvious rea-

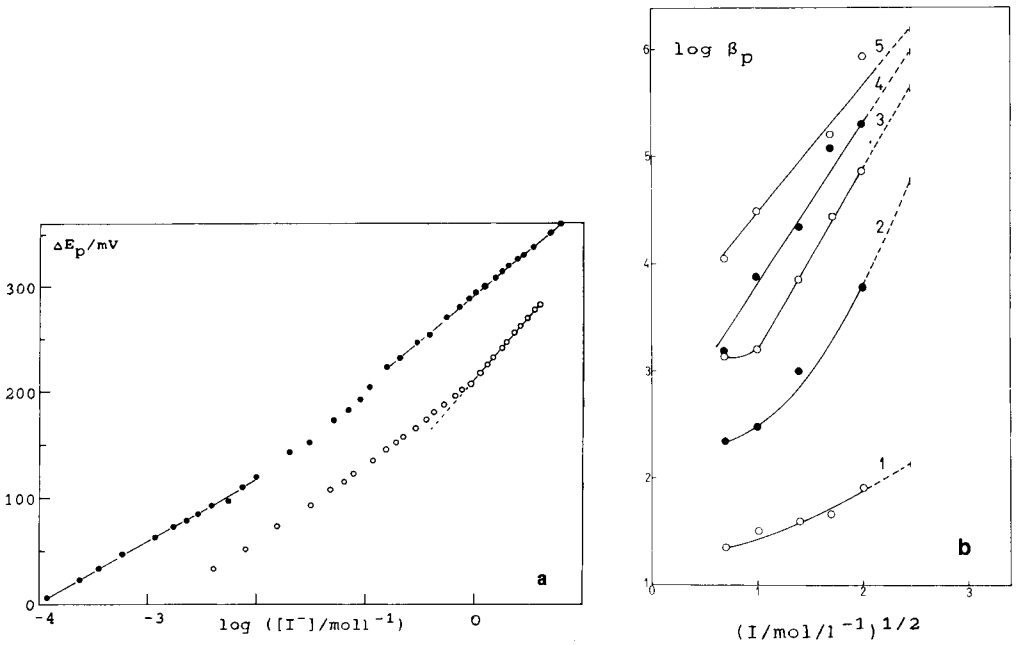


Fig. 7. (a) SWV peak potential shift in iodide solutions of (●) lead(II) and (○) cadmium(II). $[Pb]_t = 5 \times 10^{-5}$ mol $l^{-1}$, $[Cd]_t = 1.8 \times 10^{-5}$ mol $l^{-1}$. $I$ = (●) 6 or (○) 4 mol $l^{-1}$. $E_i$ = (●) −0.80 or (○) −0.40 V. Only the points relevant for the present discussion are connected with lines. (b) Dependence of the formation constants [3] on the square root from the ionic strength for different $PbI_p$ complexes ($p$ = 1–5).

sons, all $\beta_p$ values should be positive whereas between two functions with positive coefficients one with better variance of fit should be chosen. A coefficient with a confidence interval greater than the coefficient itself cannot be taken as significantly different from zero. The values presented in Table 1 (except $\beta_4$ in the $Cd^{2+}$–$I^-$ system) were calculated using a computer program [30] in which the polarographic results were numerically processed by two methods: the weight

TABLE 1

Stability constants of halide complexes determined by polarographic/voltammetric methods ($I$ = 4 mol $l^{-1}$)

| Complex | log $\beta_1$ | log $\beta_2$ | log $\beta_3$ | log $\beta_4$ | Reference |
|---|---|---|---|---|---|
| $PbCl_p$ [a] | 1.28 ± 0.05 | 2.03 ± 0.06 | 2.40 ± 0.04 | 1.57 ± 0.09 | This work |
| | 1.34 ± 0.02 | 2.06 ± 0.02 | 2.40 ± 0.04 | 1.90 ± 0.12 | 34 |
| | 1.23 ± 0.08 | 1.8 ± 0.2 | 2.2 ± 0.2 | 1.4 ± 0.2 | 35 |
| $CdCl_p$ [a] | 1.73 ± 0.04 | 2.3 ± 0.1 | 3.16 ± 0.04 | 2.5 ± 0.1 | 36 |
| | 1.77 ± 0.02 | 2.56 ± 0.05 | 3.19 ± 0.07 | 2.5 ± 0.1 | 37 |
| | 1.66 ± 0.1 | 2.4 ± 0.1 | 2.8 ± 0.3 | 2.2 ± 0.3 | 16 |
| $CdBr_p$ [b] | 1.76 ± 0.04 | 2.6 ± 0.1 | 3.5 ± 0.1 | 4.22 ± 0.06 | 25 |
| $CdI_p$ [c] | | | | 7.16 | This work |

[a] Measured in $LiClO_4$–LiCl mixtures by SWV at pH 2. $[Pb]_t = 5 \times 10^{-5}$ mol $l^{-1}$. [b] Measured in $NaClO_4$–NaBr mixtures by DPP at pH 2. $[Cd]_t = 5 \times 10^{-5}$ mol $l^{-1}$. [c] Measured in $NaClO_4$–NaI mixtures by SWV at pH 3. $[Cd]_t = 1.8 \times 10^{-5}$ mol $l^{-1}$.

method described by Momoki et al. [31] and the Gauss iterative method (also known as the Gauss–Newton or Newton–Raphson method). The former method was used for finding the initial values of the coefficients, which in the next step were introduced into the other method in order to obtain the final results.

In comparison with the value that results from Eqn. 2, half-wave or peak potential shifts influenced by adsorption are additionally increased but not to the same extent for all ligand concentrations (Fig. 3b). That is the reason why the whole ligand concentration range cannot be described by a polynomial of which all coefficients are positive. In order words, ligand-induced adsorption of dissolved metal not only gives too high stability constants but may also cause the appearance of insignificant or even negative values, i.e., values without any physical meaning.

At first glance it is not clear why a significantly increased apparent formation constant of one complex species should influence the other values. For instance, it can be calculated that the already mentioned $\log \beta_2 = 5.2$ in the $Cd^{2+}$–$I^-$ system ($I = 1$ mol $l^{-1}$), if introduced into Eqn. 2, produces peak potential shifts composed of only two contributions, i.e., from $CdI_2$ and $CdI_4^{2-}$. Two other species ($CdI^+$ and $CdI_3^-$) are virtually lost. If the values of the expected $\Delta E_p$ (based on the high $\beta_2$) are calculated for a wide iodide concentration range taking into account all four complexes or only the second and the fourth, they never differ by more than 1.3 mV from each other. As the accuracy of the peak potential reading is, in modern sampling techniques, governed by the applied scan increment which is, depending on the type of instrument, 1–2 mV, it becomes obvious why ligand–induced adsorption causes the appearance of insignificant stability constants. The stepwise complexes preceding and following the surface-active complex are simply lost because their contribution to the total peak potential shift is masked by small experimental errors. This type of result was obtained when investigating the $Cd^{2+}$–$I^-$ and $Pb^{2+}$–$Br^-$ systems. However, in the latter case adsorption does not seem to be the only problem, as pointed out by Vierling [32] and discussed by Ferri et al. [33].

Real experiments cannot be described using the approach given by Montemayor and Fatas [11]. According to them, $(\beta_p)_{\text{apparent}} = \beta_p T_c$, i.e., all polarographically determined stability constants should be divided by a correction factor to obtain the true values. Hence the net half-wave potential shift is given by:

$$\Delta E_{1/2} = (2.303RT/nF) \times \log\left(\beta_0 T_c + \beta_1 T_c[L] + \ldots \beta_N T_c[L]^N\right) \quad (3)$$

This means that the $\Delta E_{1/2}$ vs. $\log [L]$ curve, when influenced by adsorption, will shift towards higher values but retain its form. This would also mean that at zero ligand concentration $\Delta E_{1/2} = (2.303RT/nF) \log \beta_0 T_c$ should be positive taking into account that $\beta_0 = 1$ and $T_c > 1$. This is difficult to accept. In reality, however, only one complex species is surface active or at least the adsorbability of the different complexes differs significantly. Hence the adsorption effects are not equally pronounced at all ligand concentrations, i.e., not all $\beta_p$ values are affected in the same way. In fact, half-wave or peak potentials will be nearly "normal" outside the ligand concentration range in which the surface-active complex forms a significant fraction of the total metal, as predicted [14] and confirmed in the mentioned experiments with cadmium(II) in iodide media (Figs. 3B and 7A).

Table 1 gives the systems in which the complexation constants were successfully determined at $I = 4$ mol $l^{-1}$ by means of polarographic/voltammetric techniques. For chloride complexes of lead(II) and cadmium(II), the values obtained in this way are in good agreement with literature data. For the cadmium(II)–bromide system other results for the chosen ionic strength are not available but all values ($\beta_1$–$\beta_4$) determined by DPP seem to fit well with the $\log \beta_p$ vs. $\log I^{1/2}$ diagram [25].

The question arises of whether corrections for the change in the peak height on going from a non-complexing medium to ligand solutions are to be applied [22]. One should keep in mind that the DeFord–Hume equation [1] was derived for d.c. polarography in which the change in the wave

height is a consequence of the changed diffusion coefficient. In DPP and SWV, however, the increased peak current can appear because of adsorption [38,39], being from less than 100% (DPP) to more than tenfold (SWV). Its introduction into Eqn. 2 would lead to more erroneous results than leaving it out, especially when a relatively low $\Delta E_p$ value is accompanied by pronounced peak height enhancement. Additionally, for the same level of dissolved ligand, the ratio of currents depends on the total metal concentration because the current concentration relationship is not the same in pure perchlorate medium and in solutions that contain an adsorbable ligand (Fig. 5C). In fact, corresponding expressions for the peak potential shift influenced by adsorption are lacking. According to the principle cited by Crow [40], "no correction is better than a badly made one".

Finally, the question arises of the optimum measuring procedure for determining the stability constants influenced by ligand–induced adsorption. As a first step, the ligand concentration range in which pronounced adsorption effects appear should be determined. For this purpose SWV measurements at not too a high metal concentration level over a wide ligand concentration range at a constant ionic strength can be performed. In an $i_p$ vs. log[L] diagram, a bell-shaped curve will generally be obtained assuming that the adsorption of dissolved metal is really significant. In the second state, the ligand concentration which corresponds to the maximum current enhancement should be applied in the determination of the dependence of the peak potential on the total metal concentration. It is useful to perform this kind of measurement with several techniques of different sensitivity to adsorption. If $\Delta E_p$ increased continuously with increasing $[M]_t$ a low metal concentration and a slow experimental technique can be recommended. In the other two, previously mentioned, situations a high metal concentration that corresponds to the second "plateau" (Fig. 5c) should be applied if possible. Additionally, an attempt to follow the shift of the diffusion signal with increasing metal concentration can also be made if more or less pronounced splitting of the peak occurs. In such cases, combination with a procedure that improves the separation of two close signals seems promising, but has not yet been applied.

*Conclusion*

As a result of anion-induced adsorption, polarographically determined formation constants of metal complexes can differ significantly from corresponding potentiometric values. By a proper choice of exprimental conditions (total metal concentration, "speed" of the method, etc.) this difference can be decreased to such an extent that, at least in some instances, acceptable values are obtained.

This study is a contribution to the joint project "Environmental Research in Aquatic Systems" of the Institute for Applied Physical Chemistry, Research Centre (KFA), Jülich, and the Centre for Marine Research Zagreb, Rudjer Bošković Institute, Zagreb. Financial support from the International Bureau of KFA, Jülich, is gratefully acknowledged. This study was partially supported by the Ministry of Science, Technology and Informatics of the Republic of Croatia.

REFERENCES

1 D. DeFord and D.N. Hume, J. Am. Chem. Soc., 73 (1951) 5321.
2 L.G. Sillen and A.E. Martell, Stability Constants of Metal-Ion Complexes, Chemical Society, London, 1964.
3 E. Högfeldt, Stability Constants of Metal-Ion Complexes, Part A: Inorganic Ligands, Pergamon, Oxford, 1982.
4 A.M. Bond and G. Hefter, J. Electroanal. Chem., 31 (1971) 477.
5 A.M. Bond and G. Hefter, J. Electroanal. Chem., 42 (1973) 1.
6 A.M. Bond and G. Hefter, J. Electroanal. Chem., 68 (1976) 203.
7 D. Barclay and F.C. Anson, J. Electroanal. Chem., 28 (1970) 71.
8 M. Sluyters-Rehbach, S. Gonzales and J.H. Sluyters, J. Electroanal. Chem., 51 (1974) 405.
9 M. Sluyters-Rehbach and J.H. Sluyters, J. Electroanal. Chem., 65 (1975) 831.
10 Ya.I. Turyan, Zh. Obshch. Khim., 53 (1983) 2314.
11 M.C. Montemayor and E. Fatas, J. Electroanal. Chem., 246 (1988) 271.
12 M. Lovrić, Anal. Chim. Acta, 218 (1989) 7.
13 Ya.I. Turyan, Elektrokhimiya, 26 (1990) 1182.

14 M. Lovrić and M. Zelić, J. Electroanal. Chem., 319 (1991) 315.
15 E. Fatas-Lahoz, M. Sluyters-Rehbach and J.H. Sluyters, J. Electroanal. Chem., 136 (1982) 59.
16 R.M. Smith and A.E. Martell, Critical Stability Constants, Vol. 4: Inorganic Complexes, Plenum, New York, 1976.
17 P. Kivalo, Suom. Kem. B, 29 (1956) 8.
18 E. Malyszko and Z.Galus, Rocz. Chem., 46 (1972) 2291.
19 H.L. Jindal, K. Matsuda and R. Tamamushi, J. Electroanal. Chem., 90 (1978) 185.
20 J. Galvez, M.L. Alcaraz and S.-M. Park, J. Electroanal. Chem., 263 (1989) 293.
21 M. Lovrić and Š. Komorsky-Lovrić, J. Electroanal. Chem., 248 (1988) 239.
22 E. Casassas and C. Ariño, J. Electroanal. Chem., 213 (1986) 235.
23 I. Pižeta, M. Lovrić, M. Zelić and M. Branica, J. Electroanal. Chem., 318 (1991) 25.
24 M. Zelić and M. Branica, J. Electroanal. Chem., 309 (1991) 227.
25 M. Zelić and M. Branica, Anal. Chim. Acta, 262 (1992) 129.
26 F.C. Anson and D.J. Barclay, Anal. Chem., 40 (1968) 1791.
27 J.B. Flanagan, K. Takahashi and F.C. Anson, J. Electroanal. Chem., 81 (1977) 261.
28 M. Zelić and M. Lovrić, Electrochim. Acta, 35 (1990) 1701.
29 D.C. Crow, Polarography of Metal Complexes, Academic, London, 1969.
30 D. Pižeta, I. Pižeta and M. Branica, in Z. Haznadar (Ed.), Proceedings of the IXth International Symposium on Computer Aided Design and Computer Aided Manufacturing, Faculty of Electrical Engineering, University of Zagreb, Zagreb, 1987, p. 291.
31 K. Momoki, H. Sato and H. Ogawa, Anal. Chem., 39 (1967) 1072.
32 F. Vierling, Bull. Soc. Chim. Fr., 1972, 2557.
33 D. Ferri, F. Salvatore and E. Vasca, J. Coord. Chem., 20 (1989) 11.
34 A. Fedorov, L.P. Shishin, S.G. Lichacheva, A.V. Fedorova and V.E. Mironov, Zh. Neorg. Khim., 17 (1972) 79.
35 R.M. Smith and A.E. Martell, Critical Stability Constants, Vol. 6, Second Supplement, Plenum, New York, 1989.
36 M. Branica, I. Pižeta, G. Branica-Jurković and M. Zelić, Mar. Chem., 28 (1989) 227.
37 V.E. Mironov, F.Ya. Kul'ba and V.A. Nazarov, Zh. Neorg. Khim., 8 (1963) 916.
38 F.C. Anson, J.B. Flanagan, K. Takahashi and A. Yamada, J. Electroanal. Chem., 67 (1976) 253.
39 M. Lovrić and M. Branica, J. Electroanal. Chem., 226 (1987) 239.
40 D.R. Crow, Talanta, 33 (1986) 553.

*Analytica Chimica Acta*, 268 (1992) 285–292
Elsevier Science Publishers B.V., Amsterdam



# Simultaneous determination of nitrate and chloride by means of flow-injection amperometry at the membrane-stabilized water/nitrobenzene interface [1]

Stefan Wilke, Halka Franzke and Helmut Müller

*Technische Hochschule "Carl Schorlemmer" Leuna-Merseburg, Fachbereich Chemie, O-4200 Merseburg (Germany)*

(Received 13th May 1992)

**Abstract**

An amperometric flow-through electrode based on ion transfer across the interface of two immiscible electrolyte solutions was developed. A hydrophilic cellulose membrane was utilized to stabilize the interface between the flowing aqueous solution and the stationary organic phase. The detector developed was applied in a flow-injection system for the simultaneous determination of nitrate and chloride in river water. Advantage was taken of the potential-dependent response of the amperometric detector and the sufficiently separated half-wave potentials of the transfer of nitrate and chloride across the interface. The results obtained in the amperometric determination of nitrate agreed well with those from ion chromatographic measurements. Because of the comparatively poor selectivity of the detector for chloride, the results of the amperometric determination of chloride can be used only when the chloride concentration of the sample is sufficiently high.

*Keywords:* Amperometry; Flow injection; Chloride; Liquid/liquid interface; Nitrate

Most voltammetric methods are based on charge-transfer processes at electron conductor/ion conductor (electrolyte solution) interfaces. Oxidation or reduction processes at the interface are responsible for the generation or consumption of the electrons crossing the interface of the electrode. Another type of polarizable electrode is the interface between two immiscible electrolyte solutions (oil/water interface). When the organic and the aqueous solution contains a hydrophobic and a hydrophilic supporting electrolyte, respectively, the interface is polarized within a potential window which is limited by the transfer of the ions of the supporting electrolyte across the interface. The transfer of less hydrophobic or hydrophilic ions can be studied experimentally by ordinary voltammetric methods when two reference and two auxiliary electrodes are immersed in the two phases. The potential difference across the oil/water interface is measured by means of two reference electrodes, while the current is fed to the system by two auxiliary electrodes (Fig. 1).

Electrochemical studies over the last 20 years on ion transfer across the polarized oil/water interface have shown that this interface can be employed for the voltammetric and amperometric determination of ions as an alternative to the common potentiometric method at zero current (for reviews, see [1–3]). Amperometric (or voltammetric) methods have the principal advantage that the electrical current signal is directly

*Correspondence to:* S. Wilke, Technische Hochschule "Carl Schorlemmer" Leuna-Merseburg, Fachbereich Chemie, O-4200 Merseburg (Germany).

[1] Herrn Prof. Dr. G. Werner (Universität Leipzig, Fachbereich Chemie) zum 60. Geburtstag gewidmet.

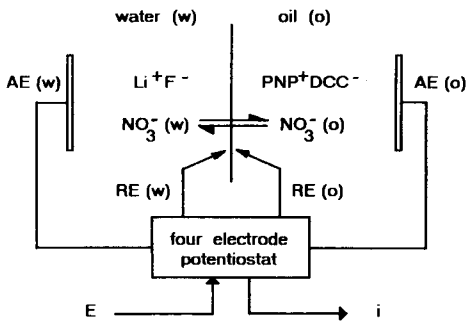


Fig. 1. Scheme of the four-electrode system for the investigation of ion transfer across the oil/water interface.

proportional to the concentration, and that the selectivity of the detector can be varied by means of a change in the electrode potential.

The problems connected with the analytical application of the oil/water interface as a voltammetric sensor are similiar to those known from the employment of liquid-state ion-selective electrodes (ISEs). In both instances it is necessary to overcome the mechanical instability of the oil/water interface. The two most promising approaches so far utilized in the construction of voltammetric sensors are well known methods used in the construction of liquid-state ISEs. The stabilization of the organic phase by gel formation with PVC has been described [4] and employed for the development of voltammetric and amperometric sensors. Their applicability in flow-injection analysis (FIA) and liquid chromatography [5,6] has been shown.

A second possibility for stabilizing the liquid/liquid interface is to insert a porous membrane between the two liquid phases. The membrane is then filled with either the organic or the aqueous solution, depending on the nature of the membrane, and the actual oil/water interface is then formed by interfacial tension at the pores of the membrane. This method was first used for constructing liquid-state ISEs [7] and was shown to be well suited for voltammetric studies of ion transfer across oil/water interfaces [8]. A wall-jet detector with a hydrophobic membrane filter has proved useful for the determination of common inorganic ions by FIA [9]. Hydrophilic dialysis membranes have been used, e.g., for the determination of ammonia [10] and for the simultaneous determination of $Na^+$ and $K^+$ in foodstuffs [11]. In comparison with hydrophobic membranes, hydrophilic cellulose membranes have the advantage that the sensors are easy to prepare and handle [11,12], the loss of nitrobenzene due to its solubility in the aqueous phase is very low [12] and the current signal is nearly independent of the flow (or stirring) rate [8,12].

It will be shown in this paper that the oil/water interface stabilized by a hydrophilic cellulose membrane can be applied for the simultaneous amperometric determination of nitrate and chloride using FIA when special conditions concerning the concentrations of this two ions are fulfilled. The common method of potentiometric determination of nitrate employing liquid-state ISEs takes advantage of the fact that nitrate is usually the most hydrophobic ion in natural waters (apart from usually negligible traces of more hydrophobic ions such as iodide, thiocyanate or anionic surfactants). However, a chloride concentration exceeding that of nitrate in the sample results in a systematic error in the nitrate determination. The nitrate concentration obtained would be too high. A high concentration of chloride in the sample would also interfere in amperometry, as the current measured in amperometry is the sum of the partial currents of the particular ionic species in the sample. This can be expressed as

$$i = \Sigma S_j c_j \qquad (1)$$

where $S_j$ is the partial sensitivity of the method to an ion $j$ of concentration $c_j$, and also holds in FIA, provided that the concentration signal entering the detector is sufficiently slow in comparison with the dynamic response of the detector [9].

The partial sensitivities, and consequently the partial currents, are independent of each other in amperometry. Thus, when the concentration of chloride is known from another measurement, the amount of the interfering influence being described by the term $S_{Cl^-}c_{Cl^-}$ could easily be corrected. In this work, however, advantage has been taken of the potential-dependent response

of the amperometric detector, which is given by

$$i_j = i_{j,\mathrm{lim}} / \left\{1 + \exp\left[ z_j F (E_{1/2,j} - E)/RT \right]\right\} \quad (2)$$

where $i_{j,\mathrm{lim}}$ and $E_{1/2}$ are the limiting diffusion current and the half-wave potential of the ion $j$, respectively, $E$ is the potential difference between the reference electrodes in the aqueous and the organic phase and all other symbols have their usual meanings. As the half-wave potentials of nitrate and chloride are reasonably well separated, both ions can be determined simultaneously from two measurements at different electrode potentials, $E_1$ and $E_2$. The corresponding peak currents, $i_1$ and $i_2$, are described by the two linear equations

$$i_1 = a_1 c(\mathrm{NO_3^-}) + b_1 c(\mathrm{Cl^-}) \text{ (at potential } E_1) \quad (3)$$

and

$$i_2 = a_2 c(\mathrm{NO_3^-}) + b_2 c(\mathrm{Cl^-}) \text{ (at potential } E_2) \quad (4)$$

where $a$ and $b$ are the partial sensitivities or, in other words, the slopes of the linear calibration graphs for $\mathrm{NO_3^-}$ and $\mathrm{Cl^-}$, respectively. The equations for the calculation of the concentrations of nitrate and chloride are obtained by solving the system of Eqns. 3 and 4:

$$[\mathrm{NO_3^-}] = (i_2 b_1/b_2 - i_1)/(a_2 b_1/b_2 - a_1) \quad (5)$$

$$[\mathrm{Cl^-}] = (i_2 a_1/a_2 - i_1)/(b_2 a_1/a_2 - b_1) \quad (6)$$

## EXPERIMENTAL

The scheme of the flow-injection system is shown in Fig. 2. A 16-$\mu$l volume of the sample solution was injected into the carrier stream (water) and then mixed with the supporting electrolyte solution (10 mM aqueous $Na_2SO_4$) in order to obtain a constant concentration of the supporting electrolyte in the detector. The flow-rate of both streams (1 ml/min in each instance) was adjusted by the hydrostatic pressure due to the height difference of the tanks and the detector. The inner diameter of the tubes between the tanks and the injector and between the injection valve and the detector was 1.0 and 0.5 mm, respectively. A specially made injection valve was used. A hydrophilic membrane filter of regenerated cellulose (RC 58, Schleicher & Schuell) was used to stabilize the interface between the aqueous solution and the nitrobenzene phase in the cell. The size of the pores was reported to be 0.2 $\mu$m.

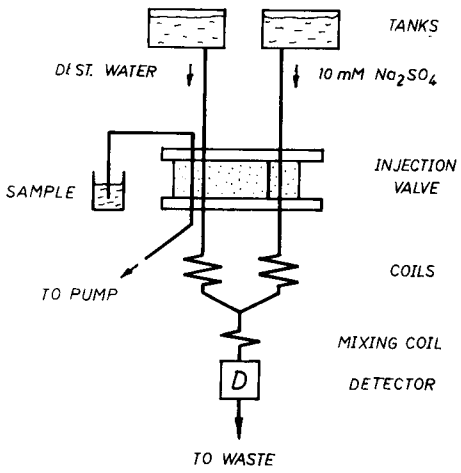


Fig. 2. Scheme of the flow-injection system. Length of the mixing tube, 13 cm; length of the coiled tubes between injector and T-piece, 50 cm; inner diameter of the tubes, 0.5 mm; sample volume injected, 16 $\mu$l.

The membrane was allowed to swell in distilled water for 15 min before the preparation of the electrode. The thickness of the swollen membrane was measured using a micrometer screw and was found to be $120 \pm 5$ $\mu$m. Because the wet membrane was elastic, it could be fixed easily at the lower orifice (3 mm i.d.) of the membrane holder, which was made of PTFE (Fig. 3). The area of the interface was 0.07 $cm^2$. The cell was filled with about 70 $\mu$l of a 10 mM solution of the organic supporting electrolyte, $\mu$-nitrido-bis(triphenylphosphorus) dicarbollylcobaltate (PNPDCC) [9], in nitrobenzene. Two silver wires in the organic phase served as reference and auxiliary electrodes, respectively, while in the aqueous phase a silver/silver chloride electrode and the cell body (stainless steel) were used as reference and auxiliary electrodes, respectively. The potential of the reference system prepared on different days was about $160 \pm 60$ mV. De-

spite the difficulty of reproducing the potential difference of different electrode couples, each of these reference systems was stable within ±5 mV over 24 h when the electrodes were allowed to stabilize for about 24 h after preparation. The electrodes were connected with the four-electrode potentiostat described previously [13]. No compensation of the *IR* drop was applied because of the low cell current. The output signal of the potentiostat was filtered by a Sallen–Key low-pass filter of second order ($\tau = 3$ s, Bessel) before it was fed to the *y–t* recorder (TZ 4100; Laboratórní Přístroje, Prague).

Comparative determinations of nitrate were made using a DX 100 ion chromatograph (Dionex) with an Ion Pac AS4A column following a standard procedure.

All samples were filtered through a paper filter. To avoid contamination of the chromatographic column, organic compounds were removed by a sample clean-up (adsorbent polymer). After filtration, samples were pumped at 1 ml/min through a column (20 cm × 0.5 mm i.d.) filled with a 50 + 50 mixture of polyamide 6 powder and a styrene-based adsorbent polymer (Y 77; Chemie AG, Bitterfeld).

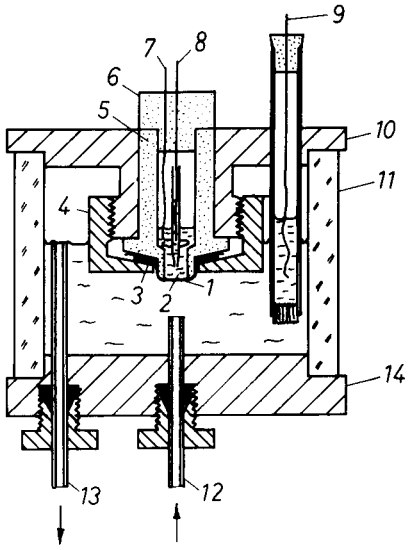


Fig. 3. Wall-jet electrochemical cell. (1) Cellulose membrane; (2) organic phase; (3) PTFE ring; (4) screw-cap; (5) PTFE bush; (6) stopper; (7) auxiliary and (8) reference electrode of the organic phase (silver wires); (9) reference electrode of the aqueous phase (Ag/AgCl); (10) electrode body which serves as aqueous auxiliary electrode; (11) glass cylinder; (12) jet inlet and (13) outlet (steel capillaries); (14) base.

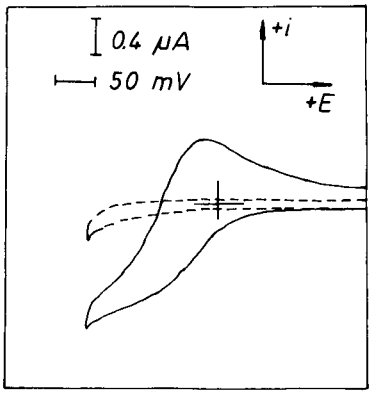


Fig. 4. Hydrodynamic voltammogram of nitrate transfer across the water/nitrobenzene interface stabilized by a hydrophilic cellulose membrane. Potential sweep rate, 20 mV $s^{-1}$; organic electrolyte, 10 mM PNPDCC in nitrobenzene; flowing aqueous electrolyte, 10 mM $Na_2SO_4$ (dashed line) + 0.5 mM $KNO_3$ in water.

All aqueous solutions were prepared from redistilled water and analytical-reagent grade reagents. Nitrobenzene "for synthesis" was shaken three times with 5 M sulphuric acid and then washed ten times with distilled water to the point of neutral reaction before use. Measurements were carried out at laboratory temperature (25 ± 2°C).

## RESULTS AND DISCUSSION

Figure 4 shows a cyclic voltammogram of nitrate ion transfer under the condition of a flowing aqueous solution containing 0.5 mM $KNO_3$ and 10 mM $Na_2SO_4$. The cathodic wave corresponds to the transfer of nitrate from water to nitrobenzene. The presence of a limiting diffusion current indicates a constant thickness of the diffusion layer on the aqueous side of the electrode surface and is attributed to the hydrophilic membrane [8]. From the equation of the limiting diffusion current in the steady state,

$$i_{d,lim} = zFADc/l \quad (7)$$

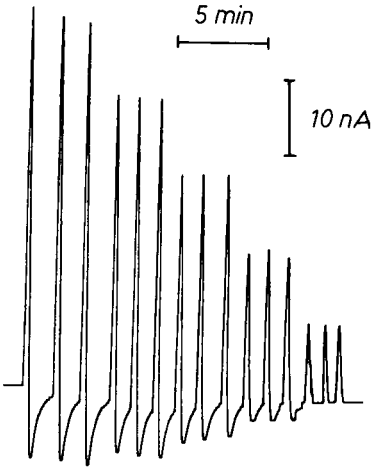


Fig. 5. Recorded current signals (triplets) of aqueous standard solutions containing 1.0, 0.8, 0.6, 0.4 and 0.2 mM $KNO_3$ (from left to right). Electrolytes: 10 mM PNPDCC in nitrobenzene and 5 mM $Na_2SO_4$ in the aqueous carrier solution.

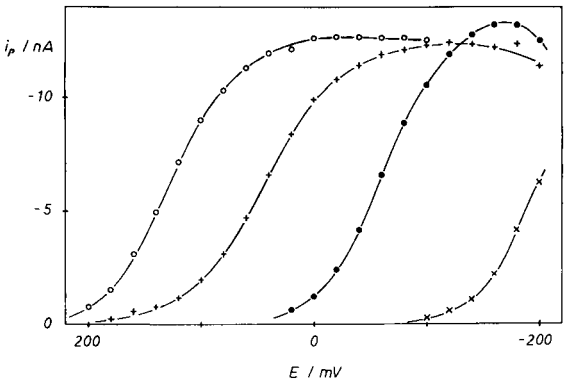


Fig. 6. Dependence of the peak height of several anions on the applied potential difference. ○ = $ClO_4^-$; + = $SCN^-$; ● = $NO_3^-$; × = $Cl^-$. All other conditions as in Fig. 5. Concentration of the anions: 0.1 mM.

where $l$ is the thickness of the membrane, the diffusion coefficient of nitrate in the membrane was calculated to be $3.8 \times 10^{-6}$ $cm^2$ $s^{-1}$ (in water: $1.9 \times 10^{-5}$ $cm^2$ $s^{-1}$).

Typical FIA signals obtained for nitrate standards of different concentrations are shown in Fig. 5. The first part of the peak represents the cathodic current due to the transfer of nitrate from water to nitrobenzene. The cathodic peak is followed by a smaller and broader anodic peak due to the reversed transfer of nitrate ions from nitrobenzene to water when the sample plug from the injection valve has passed the surface of the membrane. This anodic back-peak appears only when the electrode potential is smaller than or about equal to the half-wave potential of the anion considered. When the electrode potential is sufficiently negative, the partition equilibrium of the nitrate ions is mainly on the organic side. As the nitrate ions remain virtually completely in the organic phase, no anodic current can be observed. An anodic current following the ordinary cathodic signal has a cleaning effect on the organic phase. On the other hand, the sample frequency is decreased. However, 30 injections per hour were possible even when this phenomenon was observed. The dispersion of the sample in the FIA system was determined to be 19.

The dependence of the peak current on the electrode potential is shown in Fig. 6. The half-wave potentials of the ions studied by flow-injection amperometry are listed in Table 1. All values were related to the half-wave potential of perchlorate to eliminate systematic deviations stemming from the use of different reference electrodes. The values obtained with the RC 58 hy-

TABLE 1

Half-wave potentials related to the half-wave potential of perchlorate for different membranes and anions

| Conditions [a] | $E_{1/2} - E_{1/2}(ClO_4^-)$ (mV) | | | | | | | |
|---|---|---|---|---|---|---|---|---|
| | $ClO_4^-$ | $SCN^-$ | $I^-$ | $NO_3^-$ | $Br^-$ | $NO_2^-$ | $HCO_3^-$ | $Cl^-$ |
| A | 0 | −80 | −129 | −180 | −244 | – | – | −330 |
| B | 0 | −82 | −118 | −186 | −242 | −272 | −314 | −321 |
| C | 0 | −84 | −117 | −190 | −240 | – | – | −320 |

[a] A = RC 58 hyrophilic membrane filter (this work); B = PT 150 hydrophilic dialysis membrane [12]; C = hydrophobic membrane [9].

drophilic cellulose membrane agree well with those reported [9] for a hydrophobic membrane and a hydrophilic dialysis membrane. The error in the measurement of the half-wave potentials is about $\pm 10$ mV in each instance so that no significant differences in the half-wave potentials are observed when different membranes are considered. Obviously, the selectivity behaviour of the detector is not affected by the supporting membrane employed for the anions investigated.

The selectivity sequence follows the Hofmeister series or, in other words, the standard Gibbs energy of partition of the different ionic species. In contrast to potentiometric sensors with liquid-state membranes, the selectivity of the detector can be varied by varying the electrode potential applied. This is of use when more than one component has to be determined. The simultaneous determination of nitrate and chloride based on measurements at two different potentials was possible because these two ions have sufficiently separated half-wave potentials ($\Delta E_{1/2} \approx 140$ mV).

Figure 7 shows calibration graphs for nitrate and chloride for $E_1$ and $E_2$. The electrode potentials $E_1$ and $E_2$ were chosen so that the ratio of the sensitivities for the two ions differs considerably on changing between $E_1$ and $E_2$. $E_1$ was made approximately equal to the half-wave potential of nitrate. This choice was a compromise between selectivity and sensitivity to nitrate. The partial sensitivities obtained from the slopes of the calibration graphs were $a_1 = 40.1\ \mu A\ l\ mol^{-1}$ and $b_1 = 0.245\ \mu A\ l\ mol^{-1}$ for nitrate and chloride, respectively (the intercepts of the calibration graphs are zero in each instance, as virtually no blank peak was observed in the range of concentrations investigated). This means that the detector is nitrate selective with a selectivity ratio $a_1/b_1 = 164$. Both the analytical significance and the value of the inverse ratio ($b_1/a_1 = 0.0061$) are

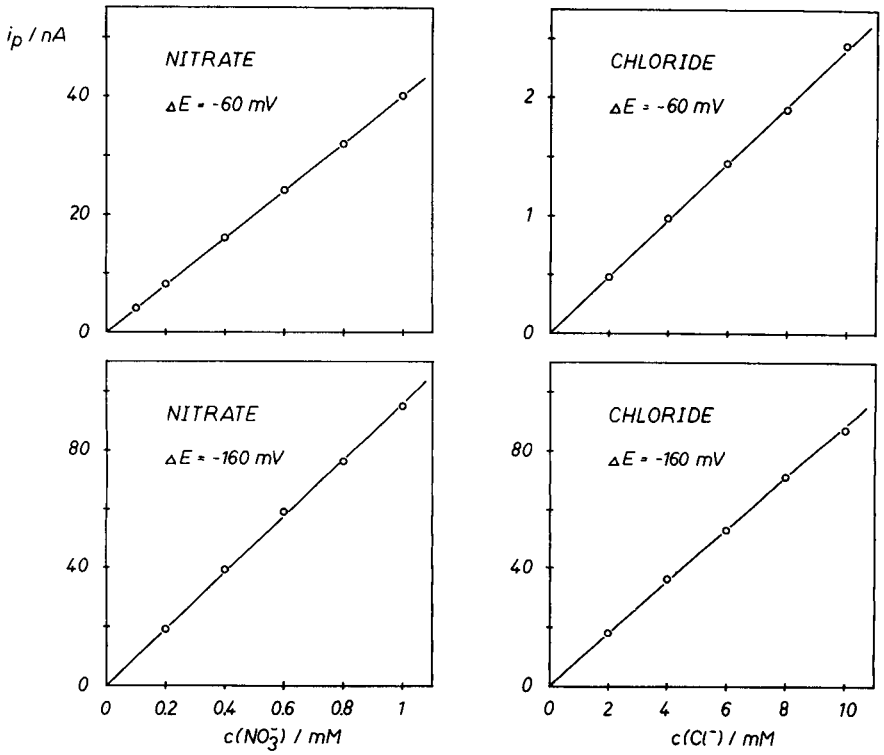


Fig. 7. Calibration graphs for nitrate and chloride at $E_1 = -60$ mV and $E_2 = -160$ mV. All other conditions as in Fig. 5.

comparable to the selectivity coefficient of liquid-state nitrate-selective electrodes [14].

$E_2$ was 100 mV more negative than $E_1$. The partial sensitivities were now $a_2 = 96.0$ $\mu$A l mol$^{-1}$ and $b_2 = 8.86$ $\mu$A l mol$^{-1}$. Therefore, on changing from $E_1$ to $E_2$, the chloride signal increased by a factor of about 30, whereas the nitrate signal only doubled as the limiting diffusion current was reached. Hence current measurement at $E_2$ is essential for the determination of the chloride concentration employing the Eqns. 5 and 6. Although more negative potentials $E_2$ give an improved selectivity for chloride, they were not applied in order to avoid precipitation at the membrane/nitrobenzene interface and within the membrane owing to too large base currents.

The method developed was used to determine nitrate and chloride in river waters (Saale and others). The samples were, in part, contaminated by industrial and domestic waste waters. The chloride level of the Saale river was about 300 mg $Cl^-$ l$^{-1}$ whereas the nitrate level was only between 20 and 25 mg $NO_3^-$ l$^{-1}$.

First, standards and samples were measured at $E_1$. This procedure was then repeated at $E_2$. The results obtained using Eqns. 5 and 6 are plotted against ion chromatographic and argentometric (Mohr's method with $K_2CrO_4$ as end-point indicator) data in Fig. 8. A satisfactory correlation is observed for nitrate (Fig. 8a). The mean relative deviation between the data obtained by the different methods is about 10%. For chloride (Fig. 8b), a correlation can also be observed. The mean relative deviation between the results of the two different methods of about 15%, but at a minimum $\pm 30$ mg $Cl^-$ l$^{-1}$, is fairly high. It must be assumed that this large error, which does not meet the usual analytical requirements, at low chloride concentrations is due to the insufficient selectivity for chloride at the potential $E_2$. The ratio $b_2/a_2 = 0.092$ indicates that the detector is about eleven times more sensitive to nitrate than to chloride at $E_2$. To obtain a ratio of at least 0.5, the potential needs to be made more negative by about 40 mV, so that it equals the half-wave potential of chloride.

Pulsed amperometry [11] could be utilized for detection at extremely negative potentials without the formation of disturbing precipitates or emulsions. Further reductions in the error of the results for chloride determination demand im-

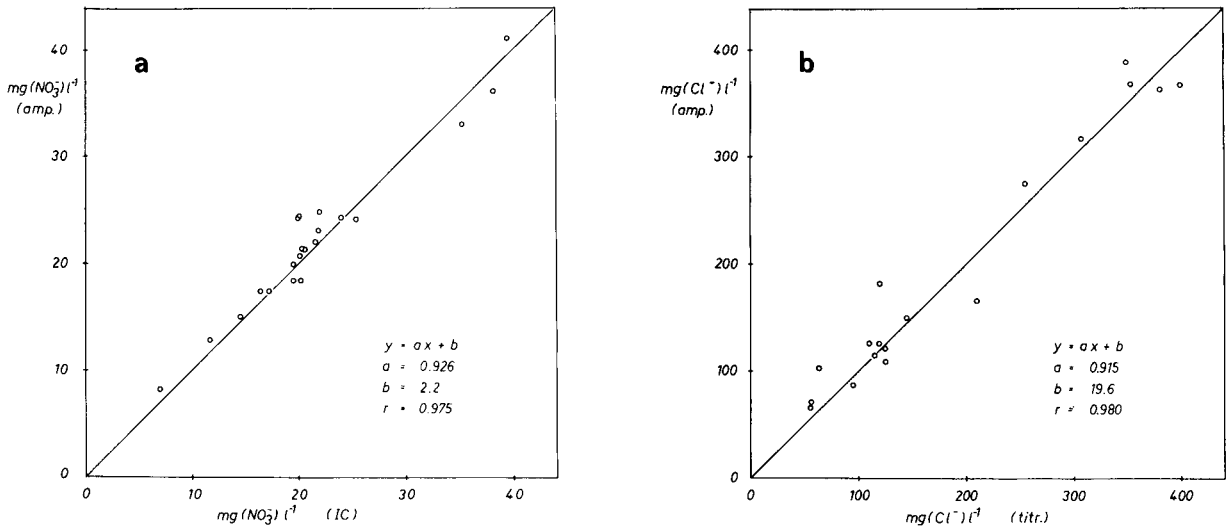


Fig. 8. Comparison of amperometric results with ion chromatographic and argentometric data for (a) nitrate and (b) chloride, respectively. The diagonal lines are of slope unity and represent the ideal relationship.

proved reproducibility of all data entering Eqn. 6, by application, for example, of an automated flow-injection system.

The lifetime of the electrode was about 2 months. After this time, the membrane had to be exchanged to avoid rupture (accompanied by leakage of nitrobenzene). The loss of nitrobenzene due to diffusion across the cellulose membrane into the aqueous phase was much lower than for hydrophobic membranes. The hydrophilic cellulose membrane can be assumed to be not very permeable to nitrobenzene dissolved in water.

Water samples and the argentometrically determined values of their chloride concentration were kindly supplied by Dr. Steinleitner, Staatliches Umweltamt, Halle. The financial support by the Deutsche Forschungsgemeinschaft is gratefully acknowledged.

REFERENCES

1 M. Senda, T. Kakiuchi and T. Osakai, Electrochim. Acta, 36 (1991) 253.
2 E. Wang and Z. Sun, Trends Anal. Chem., 7 (1988) 39.
3 J. Koryta, Electrochim. Acta, 33 (1988) 189.
4 T. Osakai, T. Kakutani and M. Senda, Bunseki Kagaku, 33 (1984) E371.
5 V. Mareček, H. Jänchenova, M.P. Colombini and P. Papoff, J. Electroanal. Chem., 217 (1987) 213.
6 E. Wang and H. Ji, Electroanalysis, 1 (1989) 751.
7 J.W. Ross, Science, 156 (1967) 1378.
8 B. Hundhammer, S.K. Dhawan, A. Bekele and H.J. Seidlitz, J. Electroanal. Chem., 217 (1987) 253.
9 B. Hundhammer and St. Wilke, J. Electroanal. Chem., 266 (1989) 133.
10 Y. Yamamoto, T. Nuno, T. Osakai and M. Senda, Bunseki Kagaku, 38 (1989) 589.
11 Y. Yamamoto, T. Osakai and M. Senda, Bunseki Kagaku, 39 (1990) 655.
12 St. Wilke and D.T. Mai, unpublished results.
13 St. Wilke, J. Electroanal. Chem., 301 (1991) 67.
14 J. Koryta and K. Stulik, Ion-Selective Electrodes, Cambridge University Press, Cambridge, 2nd edn., 1983.

*Analytica Chimica Acta*, 268 (1992) 293–299
Elsevier Science Publishers B.V., Amsterdam



# Adsorption voltammetry of the copper–4-[(4-diethylamino-2-hydroxyphenyl)azo]-5-hydroxynaphthalene-2,7-disulphonic acid (Beryllon III) system

Jingzhong Zhao and Dezhi Sun

*Department of Chemistry, Liaocheng Teachers' College, Liaocheng, Shandong (China)*

Wenrui Jin

*Department of Chemistry, Shandong University, Jinan 250100, Shandong (China)*

(Received 9th September 1991; revised manuscript received 29th April 1992)

**Abstract**

A sensitive adsorptive voltammetric procedure for the determination of trace copper, based on the adsorption characteristics of the copper(II) complex with Beryllon III at a hanging mercury drop electrode (HMDE), is described. The results show that the best base solution consists of 0.02 mol $l^{-1}$ acetic acid, 0.005 mol $l^{-1}$ sodium acetate and $1 \times 10^{-6}$ mol $l^{-1}$ Beryllon III. The limit of detection and the linear range of the derivative linear sweep adsorption voltammetric method are $5 \times 10^{-10}$ and $1 \times 10^{-9}$–$2 \times 10^{-7}$ mol $l^{-1}$, respectively. The method was applied to samples of digested human hair and to distilled water. The electrochemical behaviour of the copper complex with Beryllon III at the HMDE was also investigated in this medium. Adsorption phenomena were observed. The mechanism of the electrode reaction was found to be reduction of the copper complex adsorbed on the surface of the electrode by a totally irreversible charge transfer to metal amalgam.

*Keywords:* Stripping voltammetry; Copper; Hair

Copper is an important trace and environmental element and a common method for its determination is anodic stripping voltammetry. Since its anodic peak is near the oxidation peak of mercury, linear sweep anodic stripping voltammetry (LSASV) of copper is not very sensitive. Experimental results show that in a suitable supporting electrolyte (0.01 mol $l^{-1}$ $HClO_4$), the detection limit of LSASV is $6 \times 10^{-9}$ mol $l^{-1}$ when using a hanging mercury drop electrode (HMDE). Another disadvantage of LSASV for the determination of copper is the interference from other metal ions, in particular Zn(II), due to the formation of intermetallic compounds in amalgams.

Adsorption voltammetry is well suited to the determination of trace amounts of organic compounds and inorganic ions through their complexes [1,2]. For copper(II) ion, the ligands used include $CSN^-$ [3], catechol [4,5], 8-hydroxyquinoline [6] and thiourea [7]. Usually, the limit of detection of these methods is reported to be $10^{-8}$–$10^{-9}$ mol $l^{-1}$. Of these methods, the adsorption voltammetry of the copper(II)–catechol system is the most sensitive and the limit of

*Correspondence to:* Wenrui Jin, Department of Chemistry, Shandong University, Jinan 250100, Shandong (China).

detection is as low as $6 \times 10^{-11}$ mol $l^{-1}$ for a preconcentration time, $t_a$, of 3 min. However, the disadvantage of using catechol to determine copper lies in its susceptibility to oxidation by dissolved oxygen [5]. A stock solution needs to be prepared freshly every day.

In this work, an adsorption–voltammetric method for trace and ultra-trace measurements of copper was developed. The method relies on the effective interfacial accumulation of the copper(II) complex with 4-[(4-diethylamino-2-hydroxyphenyl)azo]-5-hydroxynaphthalene-2,7-disulphonic acid (Beryllon III) on a hanging mercury drop electrode (HMDE), the adsorbed complex then being reduced. The stock solution of Beryllon III can be used for 1 month at room temperature. Another advantage of the proposed method is the absence of the usual metal ion interferences for samples of tap water and biological substances. The limit of detection and the linear range of the derivative linear sweep adsorption voltammetry are $5 \times 10^{-10}$ and $1 \times 10^{-9}$–$2 \times 10^{-7}$ mol $l^{-1}$, respectively. The method has been used for the determination of trace amounts of copper in human hair.

The electrochemical reduction mechanism of the Cu(II)–Beryllon III system was investigated. It was found that the Cu(II) central ion in the complex adsorbed on the surface of the electrode is irreversibly reduced and that the product formed is the copper amalgam.

## EXPERIMENTAL

### *Apparatus*

A voltammetric analyser (Model 79-1, Jinan Fourth Radio Factory) coupled with an $X$–$Y$ recorder (Model 3086-11, Yokogawa Hokuskin) was used in connection with a cell, using potentiostatic control of the electrode potential by means of a three-electrode system, which consisted of an HMDE (Model SH-84, Department of Chemistry, Shandong University) with an area of 3.15 $mm^2$ as the working electrode, a platinum plate as the counter electrode and a saturated calomel electrode (SCE) as the reference electrode, connected to the analyte via a salt bridge filled with 0.02 mol $l^{-1}$ acetic acid (HOAc)–0.005 mol $l^{-1}$ sodium acetate (NaOAc). In the preconcentration step, the solution was stirred with a PTFE-covered stirring bar, rotated by a magnetic stirrer (Model 78-1, Nanhui Telecommunication Equipment Factory). pH was measured with a pH meter (Model pHs-2, Shanghai Analytical Instrument Factory).

### *Reagents and solutions*

Analytical-reagent grade chemicals were used and all solutions were prepared with triply distilled water. A $1 \times 10^{-2}$ mol $l^{-1}$ stock standard solution of Cu(II) was prepared by dissolving the appropriate amount of metallic copper in 1 + 1 $HNO_3$. After the solution had been evaporated to dryness on a sand-bath, 6.5 ml of $H_2SO_4$ were added and the solution was heated in a sand-bath until white fumes appeared. The solution was transferred to a 1000-ml volumetric flask. Working standard solutions were obtained by diluting this stock standard solution with water. A $1 \times 10^{-3}$ mol $l^{-1}$ stock standard solution of Beryllon III was prepared by dissolving an appropriate amount of Beryllon III in water.

### *Procedure*

The supporting electrolyte was 0.02 mol $l^{-1}$ HOAc–0.005 mol $l^{-1}$ NaOAc. The solution was deaerated for 15 min with pure nitrogen. The measurements were made after a preconcentration step, in which the solution was usually stirred for a certain time, $t_a$, and a preconcentration potential, $E_a$, of 0.10 V was applied. After a rest period, $t_r$, of 15 s the response curve was recorded by scanning the potential at a scan rate of 100 mV $s^{-1}$ in the negative direction. Each measurement was performed with a fresh drop. All potentials were measured against the SCE.

## RESULTS AND DISCUSSION

### *Optimum conditions for the adsorption reduction peak of the Cu(II) complex with Beryllon III*

In HOAc–NaOAc buffer solution, the reduction peak of Cu(II) appears in the voltammogram at 0.01 V (Fig. 1, curve 1) and the reduction peak

of Beryllon III appears in the adsorption voltammogram at −0.23 V (Fig. 1, curve 2). In the presence of both Cu(II) and Beryllon III, a very sensitive and well defined peak appears at a potential between +0.01 and −0.23 V after preaccumulation (Fig. 1, curve 3). It is obvious that the sensitive peak at −0.08 V results from the Cu(II) complex with Beryllon III.

It was found experimentally that the optimum concentration of supporting electrolyte was 0.02 mol $l^{-1}$ HOAc–0.005 mol $l^{-1}$ NaOAc. The peak current increased with increasing concentration of Beryllon III up to $4 \times 10^{-7}$ mol $l^{-1}$ and did not change in the concentration range $4 \times 10^{-7}$–$1.2 \times 10^{-6}$ mol $l^{-1}$. When the concentration of Beryllon III was $> 1.2 \times 10^{-6}$ mol $l^{-1}$, the peak current decreased. In subsequent experiments, $1 \times 10^{-6}$ mol $l^{-1}$ Beryllon III was adopted.

*Adsorptivity of the Cu(II) complex with Beryllon III*

Typical adsorption voltammograms for different preconcentration times, $t_a$, are shown in Fig.

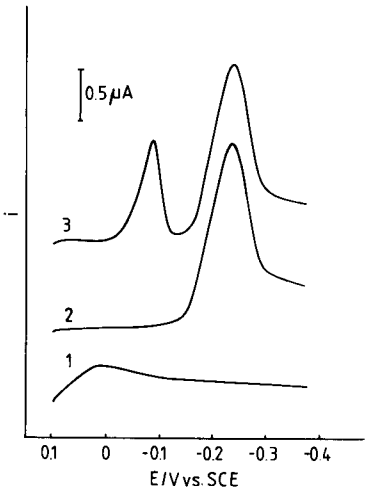


Fig. 1. Typical voltammogram of Cu(II) and typical reduction voltammograms of adsorbed Beryllon III and adsorbed Cu(II) complex with Beryllon III. (1) $5 \times 10^{-6}$ mol $l^{-1}$ Cu(II); (2) $4 \times 10^{-7}$ mol $l^{-1}$ Beryllon III; (3) $4 \times 10^{-7}$ mol $l^{-1}$ Beryllon III and $4 \times 10^{-7}$ mol $l^{-1}$ Cu(II), Supporting electrolyte, 0.02 mol $l^{-1}$ HOAc–0.005 mol $l^{-1}$ NaOAc; $E_a = 0.10$ V; $t_a = 3$ min; $t_r = 15$ s; $v = 100$ mV $s^{-1}$; HMDE area, $A = 3.15$ $mm^2$; $T = 18$°C.

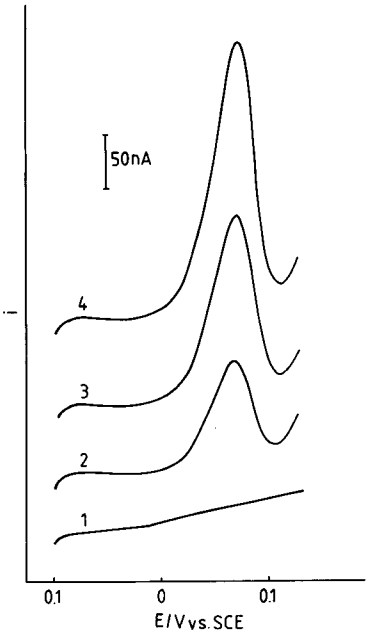


Fig. 2. Linear sweep voltammograms for the reduction of adsorbed Cu(II) complex with Beryllon III for different preconcentration times, $t_a$: (1) 0; (2) 60; (3) 120; (4) 180 s. $5 \times 10^{-8}$ mol $l^{-1}$ Cu(II), $1 \times 10^{-6}$ mol $l^{-1}$ Beryllon III. Other conditions as in Fig. 1.

2. The half-width of the reduction peak of the complex is small (47 mV). The peak current, $i_p$, increases on extending $t_a$, and $i_p$ varies linearly with the potential scan rate, $v$. From the logarithmic plot of $i_p$ vs. $v$, a slope of 0.98 is obtained. Over a relatively long $t_a$, adsorption equilibria are established. If the concentration of the complex in the bulk of solution is increased, a constant peak current is attained (Fig. 3). These results are characteristic for the reaction of adsorbed reactants on an electrode [8–10].

*Electrode process*

The overall electrode process in adsorption voltammetry can be divided into three steps: homogeneous reaction in the bulk of the solution, adsorption accumulation and reduction of the adsorbed reactant.

*Homogeneous reaction in the bulk of the solution.* The composition of the complex in the solution was measured to be 1 : 1 by using spectropho-

tometry. The most important reaction in the bulk of the solution involves the following equilibrium:

$$Cu(II) + L \rightleftharpoons Cu(II)L \quad (1)$$

where L is Beryllon III.

*Adsorption accumulation.* The adsorption of Cu(II)L on a mercury electrode proceeds in this medium only when an external potential is applied to the working electrode. The peak current depends on the preconcentration potential, $E_a$. The relationship between $i_p$ and $E_a$ is shown in Fig. 4. Obviously, the adsorption is strongest for a preconcentration potential between 0.01 and 0.24 V. Using the method described previously [11], the composition of the electroactive complex on the surface of the electrode is also 1:1. This indicates that the complex in the bulk of the solution and the complex adsorbed on the surface of the electrode have the same composition. Hence, the adsorption process can expressed as follows:

$$Cu(II)L + Hg \rightleftharpoons Cu(II)L(ads)Hg \quad (2)$$

*Reduction of the adsorbed reactant.* In order to obtain some information on the reactants and products, electrolysis was used. The working electrode was a mercury pool electrode with an average geometric area of 3 $cm^2$. An electrolysis potential of −0.15 V was applied. With increasing electrolysis time, the peak current of the reduction of the Cu(II) complex decreased to zero. After the peak current of the reduction of the complex had dropped to zero, a defined amount of $Cu^{2+}$ was added to the cell. By using linear sweep adsorption voltammetry, the peak corresponding to the reduction of the adsorbed Cu(II) complex, Cu(II)L(ads)(Hg), was obtained again. It is evident that it is Cu(II) in the complex adsorbed on the surface of the mercury electrode that is reduced. Figure 5 shows the adsorption voltammogram at different concentrations of Cu(II) ($c_{Cu(II)}$) and a constant concentration of Beryllon III ($c_{Beryllon\ III}$). The peak current of the reduction of adsorbed Cu(II)L increases when $c_{Cu(II)}$ increases, but the peak current of the adsorption reduction of adsorbed Beryllon III remains constant, even when the ratio $c_{Cu(II)}$: $c_{Beryllon\ III} = 12.5:1$. This suggests that the other product of the reduction of adsorbed Cu(II)L is Beryllon III which is still adsorbed on the surface of the electrode.

From the asymmetric shape of the reduction peak of adsorbed Cu(II)L and the fact that the position of the peak on the potential axis shifts in the negative direction with increasing scan rate and because a small broad anodic peak corresponding to the cathodic peak of the reduction of the Cu(II) complex adsorbed appears in cyclic

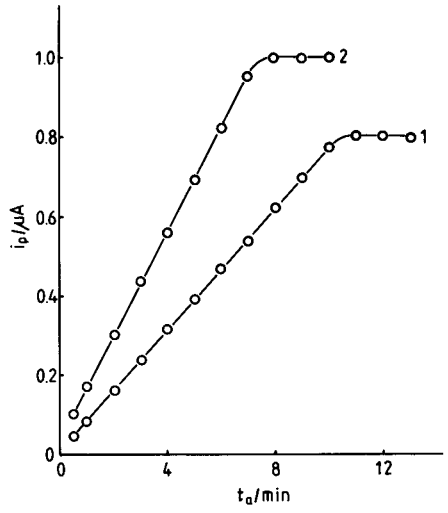


Fig. 3. Dependence of the peak current of reduction of the adsorbed Cu(II) complex with Beryllon III on the preconcentration time at different concentrations of Cu(II), $c_{Cu(II)}$: (1) $5\times10^{-8}$; (2) $1\times10^{-7}$ mol $l^{-1}$. Other conditions as in Fig. 2.

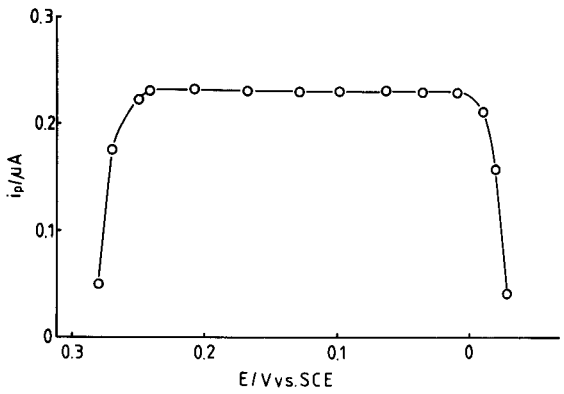


Fig. 4. Dependence of the peak current of the reduction of the adsorbed Cu(II) complex with Beryllon III on the preconcentration potential. $t_a$ = 3 min. Other conditions as in Fig. 2.

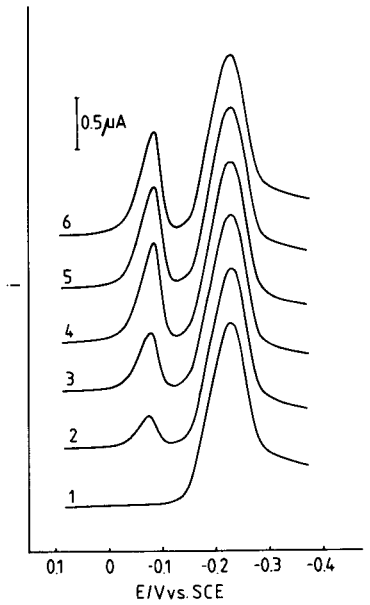


Fig. 5. Linear sweep voltammograms for the reduction of adsorbed Cu(II)L at different concentrations of Cu(II), $c_{Cu(II)}$: (1) 0; (2) $5\times10^{-8}$; (3) $10\times10^{-8}$; (4) $50\times10^{-8}$; (5) $100\times10^{-8}$; (6) $500\times10^{-8}$ mol $l^{-1}$. $4\times10^{-7}$ mol $l^{-1}$ Beryllon III; $t_a = 180$ s. Other conditions as in Fig. 2.

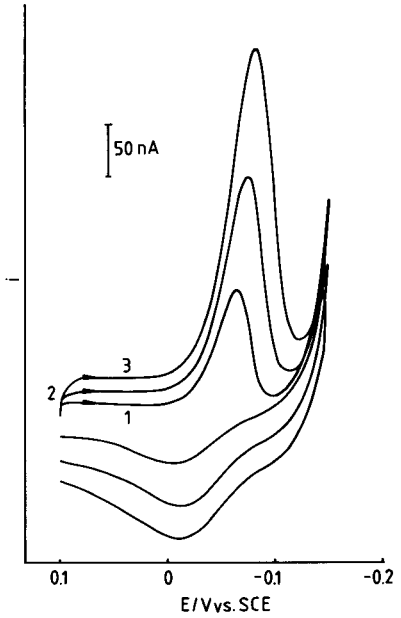


Fig. 6. Cyclic voltammograms of the adsorbed Cu(II) complex with Beryllon III at different scan rates, $v$: (1) 40; (2) 80; (3) 120 mV $s^{-1}$. $t_a = 180$ s. Other conditions as in Fig. 2.

adsorption voltammogram (Fig. 6), it can be concluded that the interfacial electrochemical reduction of adsorbed Cu(II)L is a totally irreversible process [9]. In summary, the interfacial reaction can be expressed as follows:

$$Cu(II)L(ads)(Hg) + 2e^- \rightarrow Cu(0)(Hg) + L(ads) \quad (3)$$

Comparing the cyclic voltammetric curves of adsorbed Cu(II)L shown in Fig. 6 with those of $Cu^{2+}$ and Beryllon III shown in Fig. 7, it is evident that the product of the oxidation of Cu(0)(Hg) in the presence of Beryllon III is different from the product of the oxidation of Cu(0)(Hg) in the absence of Beryllon III and the product of the oxidation of Beryllon III. Probably the product is still the Cu(II) complex with Beryllon III.

*Analytical application*

Figure 8 shows the logarithmic relationship between the derivative peak height of the reduc-

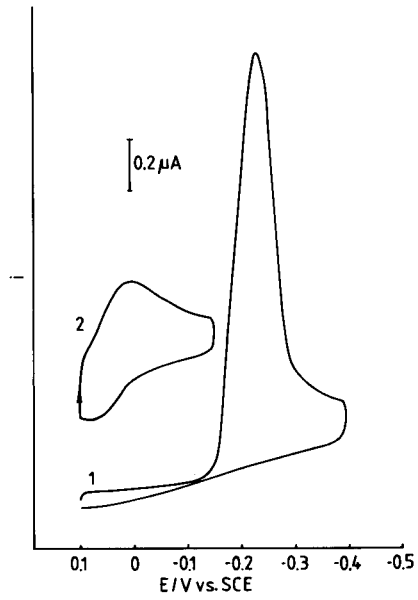


Fig. 7. Cyclic voltammograms of adsorbed Beryllon III and $Cu^{2+}$. (1) $1\times10^{-6}$ mol $l^{-1}$ Beryllon III; (2) $5\times10^{-6}$ mol $l^{-1}$ $Cu^{2+}$. Other conditions as in Fig. 6.

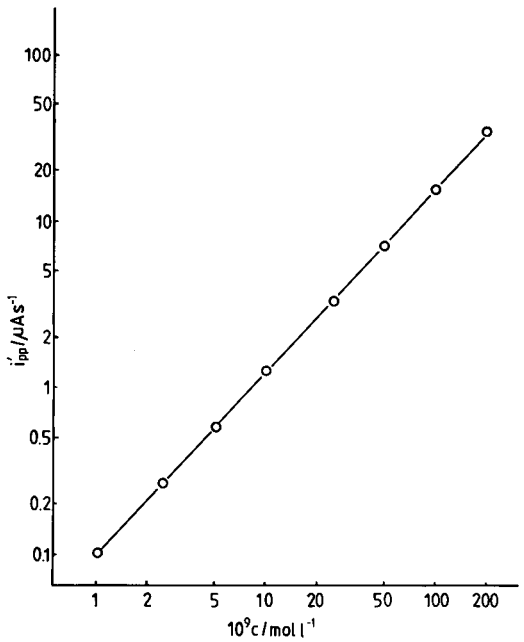


Fig. 8. Logarithmic relationship between the derivative peak height and the analytical bulk concentration of Cu(II). Conditions as in Fig. 7.

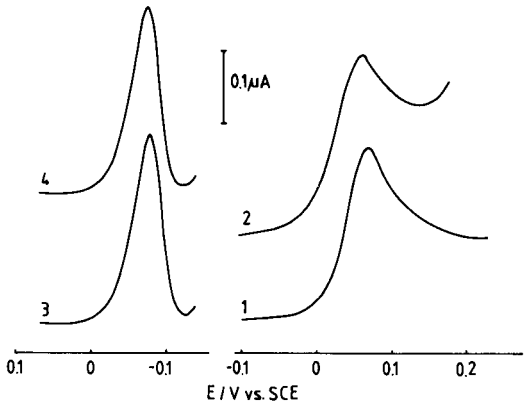


Fig. 9. Comparison between anodic stripping voltammograms of copper and adsorption voltammograms of the reduction of the Cu(II) complex with Beryllon III adsorbed without and with Zn(II). (1) $3\times10^{-7}$ mol $l^{-1}$ $Cu^{2+}$, 0.01 mol $l^{-1}$ $HClO_4$, $E_a = -0.90$ V; (2) (1) $+6\times10^{-5}$ mol $l^{-1}$ $Zn^{2+}$; (3) $5\times10^{-8}$ mol $l^{-1}$ Cu(II), $1\times10^{-6}$ mol $l^{-1}$ Beryllon III, 0.02 mol $l^{-1}$ HOAc–0.005 mol $l^{-1}$ NaOAc; (4) (3) $1\times10^{-5}$ mol $l^{-1}$ $Zn^{2+}$. $E_a = +0.10$ V. Other experimental conditions as in Fig. 1.

tion of adsorbed Cu(II)L and the analytical bulk concentration of Cu(II). A linear relationship holds between the logarithm of the derivative peak height and concentration in the range $1\times10^{-9}$–$2\times10^{-7}$ mol Cu(II) $l^{-1}$. The limit of detection of the method is $5\times10^{-10}$ mol $l^{-1}$.

The interference of Zn(II) with Cu(II) is a problem in anodic stripping voltammetry owing to the formation of an intermetallic compound in the mercury (Fig. 9, curves 1 and 2). In the adsorption voltammetry of copper, as stated above, a 200-fold excess of Zn(II) does not interfere with the reduction peak of the Cu(II) complex with Beryllon III adsorbed on the surface of the HMDE (Fig. 9, curves 3 and 4).

Experimental results show that a 100-fold excess of Ni(II), Bi(III), Co(II) and Mn(II), a 200-fold excess of Zn(II), Cd(II), Sb(II), Pb(II), As(V), Mg(II) and Fe(III) and large amounts of Ca(II), Ba(II), Al(III), Na(I), K(I), $SO_4^{2-}$, $PO_4^{3-}$, $Cl^-$ and $NO_3^-$ do not interfere in the determination of Cu(II). In normal biological samples, Cu(II) can be determined directly after digestion.

Distilled water can also be analysed directly. Samples of human hair can be analysed after digestion (according to Jin et al. [12]) prior to the adsorption voltammetric determination. Typical results determined by adsorption voltammetry

TABLE 1

Results of the determination of copper in samples of human hair and water

| Sample | Content determined by AV ($\mu g\ g^{-1}$) | Average value found by AV ($\mu g\ g^{-1}$) | Average value found by AAS ($\mu g\ g^{-1}$) |
|---|---|---|---|
| Hair A | 7.6, 7.8, 7.9 | 7.8 | 7.9 |
| Hair B | 10.3, 10.5, 10.4 | 10.5 | 10.6 |
| Hair C | 8.4, 8.6, 8.3 | 8.4 | 8.6 |
| Distilled water | 0.0050, 0.0051, 0.0051 | 0.0051 | 0.0053 |
| Doubly distilled water | 0.0014, 0.0015, 0.0014 | 0.0014 | 0.0015 |

(AV) are summarized in Table 1. The results from the determination of Cu(II) by AV are in agreement with the data obtained by atomic absorption spectrometry (AAS). The recoveries of spiked copper were 96–101%.

REFERENCES

1 J. Wang, Am. Lab., 17 (5) (1985) 41.
2 R. Kalvoda and M. Kopanica, Pure Appl. Chem., 61 (1) (1989) 97.
3 R. Kalvoda, Anal. Chim. Acta, 138 (1982) 11.
4 N.K. Lam, R. Kalvoda and M. Kopanica, Anal. Chim. Acta, 154 (1983) 79.
5 C.M.G. van den Berg, Anal. Chim. Acta, 164 (1984) 195.
6 C.M.G. van den Berg, Anal. Chim. Acta, 215 (1986) 111.
7 Ch. Yarnitzky and R. Schreiber-Stanger, J. Electroanal. Chem., 214 (1986) 65.
8 R. Kalvoda, W. Anstine and M. Heyrovsky, Anal. Chim. Acta, 50 (1970) 93.
9 E. Laviron, J. Electroanal. Chem., 52 (1974) 355.
10 A.P. Brown and F.C. Anson, Anal. Chem., 49 (1977) 1589.
11 J.-Z. Zhao and W.-R. Jin, J. Electroanal. Chem., 267 (1989) 271.
12 W.-R. Jin, S.-Q. Wen, H.-T. You and Y. Ji, Fenxi Huanxue, 13 (1985) 296.

*Analytica Chimica Acta*, 268 (1992) 301–306
Elsevier Science Publishers B.V., Amsterdam



# Linear potential sweep adsorption voltammetry for a reversible interfacial reaction: comparison of conventional and derivative measuring techniques

Wenrui Jin, He Cui and Shuren Wang

*Department of Chemistry, Shandong University, Jinan 250100, Shandong (China)*

(Received 18th December 1991; revised manuscript received 22nd May 1992)

**Abstract**

Equations for the peak current and the peak-to-peak distances of the 0.5th-, 1st-, 1.5th-, 2nd- and 2.5th-order derivatives of current with respect to time in linear potential sweep adsorption voltammetry were evaluated for a reversible interfacial reaction. The limits of detection of the method and its derivative technique were analysed theoretically. It is concluded that $10^{-10}$ mol $l^{-1}$ of substance can be determined using conventional linear potential sweep adsorption voltammetry. The limit of detection of derivative adsorption voltammetry may be at least one order of magnitude lower.

*Keywords:* Stripping voltammetry; Voltammetry; Adsorption; Derivative current; Reversible interfacial reaction

Adsorption voltammetry is a relatively new and very sensitive method suitable for the ultra-trace determination of organic compounds and inorganic ions through their complexes [1,2]. The analyte is first preconcentrated by adsorption on a working electrode. One of the most common measuring techniques used is linear potential sweep adsorption voltammetry. Ions or compounds at concentrations as low as $10^{-11}$ mol $l^{-1}$ can be detected. In this laboratory, adsorption voltammetry of electroactive and -inactive ions of metal and non-metal elements has been studied with a conventional electrode and with an ultramicroelectrode. Also, the theoretical background of the amount adsorbed in the preconcentration step and the techniques of integer and half-integer derivative linear potential sweep voltammetry have been investigated [3–25]. At least one order of magnitude decrease in the limit of detection was observed when the integer and half-integer derivative technique was used.

In this paper, the theory of linear potential sweep adsorption voltammetry, including the integer and half-integer derivative technique and the sensitivity of this method, will be discussed. The experimental dependence of the maximum values for different order derivative curves of the current with respect to potential on the experimental parameters were measured for the reversible reaction of 5-[(5′-bromo-2′-pyridyl)azo]-2,4-diaminotoluene (5-Br-PADAT) adsorbed on the surface of a hanging mercury drop electrode (HMDE).

*Correspondence to:* Wenrui Jin, Department of Chemistry, Shandong University, Jinan 250100, Shandong (China).

## EXPERIMENTAL

### *Apparatus*

A voltammetric analyser (Model 83-2.5, Ningde Analytical Instruments) coupled with an *X–Y* recorder (Model $LZ_3$-100, Shanghai Dahua In-

strument Factory) was used in connection with a cell, using potentiostatic control of the electrode potential by means of a three-electrode system, which consisted of an HMDE (Model SH-84, Department of Chemistry, Shandong University) as the counter electrode and a saturated calomel electrode (SCE) as the reference electrode, connected to the experimental solution via a salt bridge filled with $1 \times 10^{-3}$ mol $l^{-1}$ NaOH. In the preconcentration step, the solution was stirred with a PTFE-covered stirring bar, rotated by a magnetic stirrer.

*Reagents and solutions*

A $1 \times 10^{-3}$ mol $l^{-1}$ stock solution of 5-Br-PADAT (Institute of Tianjing Chemical Reagents, Tianjing) was prepared by dissolving an appropriate amount in 95% ethanol and dilute solutions were prepared by serial dilution with water.

Analytical-reagent grade chemicals were used and all solutions were prepared using triply distilled water.

*Procedure*

The supporting electrolyte was $1 \times 10^{-3}$ mol $l^{-1}$ NaOH. The solution containing 5-Br-PADAT was deaerated for 20 min with pure nitrogen. The measurements were carried out after a preconcentration step, in which the solution was usually stirred for a certain time, $t_a$, and a preconcentration potential, $E_a$, of $-0.61$ V (vs. SCE) was applied. After a rest period, $t_r$, of 30 s, the response curve was recorded by scanning the potential in the negative direction. Each measurement was done with a fresh drop. All potentials were measured vs. SCE.

## RESULTS AND DISCUSSION

*Theory*

In a previous paper [26], the general derivative equation of the current with respect to time for a reversible interfacial reaction was investigated and expressed as

$$d^a i_r/dt^a = \left(n^{(a+2)}F^{(a+2)}/R^{(a+1)}T^{(a+1)}\right)Av^{(a+1)} \times \Gamma\, d^{(a+0.5)}P(\sigma_r t)/d(\sigma_r t)^{(a+0.5)} \quad (1)$$

where $a$ is an integer or half-integer, $A$ is the area of the electrode (in $cm^2$), $v$ is the potential scan rate (in V $s^{-1}$), $\Gamma$ is the interfacial concentration of the adsorbed species, $n$, $F$, $R$ and $T$ have their usual meanings, $P(\sigma_r t)$ is a function of $\sigma_r t$, $t$ is the time measured from the beginning of the potential scan (in s) and

$$\sigma_r = nFv/RT \quad (2)$$

In adsorption voltammetry, $\Gamma$ is the amount accumulated by adsorption in the preconcentration step. It may be written as [23]

$$\Gamma = \left[kD^{2/3}\nu^{-1/6}\omega_0^{1/2}t_a + f(t_r)\right]c = \left[Kt_a + f(t_r)\right]c \quad (3)$$

where $D$ and $c$ are the diffusion coefficient (in $cm^2$ $s^{-1}$) and the bulk concentration (in mol $cm^{-3}$) of the species, respectively, $\nu$ is the kinematic viscosity (in $cm^2$ $s^{-1}$), $t_a$ is the preconcentration time (in s) in a stirred solution with angular velocity $\omega_0$ (in rad $s^{-1}$), $k$ is a constant and $f(t_r)$ is a function of $D$, $\nu$, $\omega_0$ and the rest period, $t_r$. By substituting the maximum of $d^{(a+0.5)}P(\sigma_r t)/d(\sigma_r t)^{(a+0.5)}$ shown in [25] and Eqn. 3 in Eqn. 1, the peak current and the maximum peak-to-peak values of the different order derivatives can be obtained. These are

$$i_{p,r} = 0.25(n^2F^2/RT)Avc\left[Kt + f(t_r)\right] \quad (4)$$

$$e_{pp,r} = \left(d^{0.5}i_r/dt^{0.5}\right)_{p1} - \left(d^{0.5}i_r/dt^{0.5}\right)_{p2} = 0.212\left(n^{2.5}F^{2.5}/R^{1.5}T^{1.5}\right) \times Av^{1.5}c\left[Kt_a + f(t_r)\right] \quad (5)$$

$$i'_{pp,r} = \left(di_r/dt\right)_{p1} - \left(di_r/dt\right)_{p2} = 0.192\left(n^3F^3/R^2T^2\right)Av^2c\left[Kt_a + f(t_r)\right] \quad (6)$$

$$e'_{pp,r} = \left(d^{1.5}i_r/dt^{1.5}\right)_{p1} - \left(d^{1.5}i_r/dt^{1.5}\right)_{p2} = 0.179\left(n^{3.5}F^{3.5}/R^{2.5}T^{2.5}\right) \times Av^{2.5}c\left[Kt_a + f(t_r)\right] \quad (7)$$

$$i''_{pp,r} = \left(d^2i_r/dt^2\right)_{p1} - \left(d^2i_r/dt^2\right)_{p2} = 0.167\left(n^4F^4/R^3T^3\right)Av^3c\left[Kt_a + f(t_r)\right] \quad (8)$$

$$e''_{pp,r} = \left(d^{2.5}i_r/dt^{2.5}\right)_{p2} - \left(d^{2.5}i_r/dt^{2.5}\right)_{p3} = 0.208\left(n^{4.5}F^{4.5}/R^{3.5}T^{3.5}\right) \times Av^{3.5}c\left[Kt_a + f(t_r)\right] \quad (9)$$

where the subscripts p1, p2 and p3 are the numbers of the peaks; when $t_a > 120$ s and $t_r < 15$ s, $f(t_r)$ can be neglected [23].

The ratios of $e_{pp,r}$, $i''_{pp,r}$, $e'_{pp,r}$, $i''_{pp,r}$ and $e''_{pp,r}$ to $i_{p,r}$ for different scan rates are summarized in Table 1. It can be seen that with integer and the half-integer derivative techiques higher signals can be obtained than with conventional linear potential sweep voltammetry for a reversible interfacial reaction, in particular at faster potential scan rates, higher order derivatives and higher values of $n$.

*Verification*

In a previous paper [26], the dependences of $i_{p,r}$, $e_{pp,r}$, $i'_{pp,r}$, $e'_{pp,r}$, $i''_{pp,r}$ and $e''_{pp,r}$ on $A$ and $v$ were verified for the reduction of 5-Br-PADAT adsorbed in NaOH. The dependences of $i_{p,r}$, $e_{pp,r}$, $i'_{pp,r}$, $e'_{pp,r}$, $i''_{pp,r}$ and $e''_{pp,r}$ on $t_a$ and $c$, which were calculated from $i$–$E$ curves by means of a computer using the procedure described previously [26] are tested in Figs. 1 and 2. In both figures, the linearity is satisfactory. The experimental ratios of $e_{pp,r}$, $i'_{pp,r}$, $e'_{pp,r}$, $i''_{pp,r}$ and $e''_{pp,r}$ to $i_{p,r}$ for the 5-Br-PADAT system at different scan rates are summarized in Table 2. The effect of the signal enhancement is very evident for higher order derivatives and faster scan rates.

*Limit of detection*

Although the signal of $e_{pp,r}$, $i'_{pp,r}$, $e'_{pp,r}$, $i''_{pp,r}$, and $e''_{pp,r}$ is higher than $i_{p,r}$, the limit of detection of a method is determined by the signal-to-noise ratio. In linear potential sweep voltammetry, the noise depends on the capacity current (the primary background interference):

$$i_c = AC_d v \tag{10}$$

where $C_d$ is the differential double-layer capacity per unit area.

The first and second derivatives of $i_c$ with respect to time are

$$i'_c = di_c/dt = Av(dC_d/dt)$$
$$= Av(dC_d/dE)(dE/dt) = Av^2(dC_d/dE) \tag{11}$$

$$i''_c = d^2i_c/dt^2 = Av(d^2C_d/dt^2)$$
$$= Av^3(d^2C_d/dE^2) \tag{12}$$

when the scan rate and the area of the electrode are constant.

Ordinarily, the differential double-layer capacity is a constant or changes only slowly with potential compared with the faradaic current. When the differential double-layer capacity is a constant, its derivative, $dC_d/dt$, is zero; when the differential double-layer capacity varies linearly with potential, the second derivative is zero. The corresponding capacitive contribution to the derivative signal is reduced to zero under these conditions.

According to Riemann and Liouville (see [27]), the 0.5th-order integral of the capacity, $m_c$, is defined by

$$m_c = d^{-0.5}i_c/dt^{-0.5} = 1/\sqrt{\pi}\int_0^t i_c(\lambda)/\sqrt{t-\lambda}\,d\lambda \tag{13}$$

TABLE 1

Ratios of $e_{pp,r}$, $i'_{pp,r}$, $e'_{pp,r}$, $i''_{pp,r}$ and $e''_{pp,r}$ to $i_{p,r}$ at different scan rates ($T = 298$ K)

| Ratio | $v$ (mV s$^{-1}$) | | | | | | | | |
|---|---|---|---|---|---|---|---|---|---|
| | 40 | | | 100 | | | 1000 | | |
| | $n=1$ | $n=2$ | $n=3$ | $n=1$ | $n=2$ | $n=3$ | $n=1$ | $n=2$ | $n=3$ |
| $e_{pp,r}/i_{p,r}$ (s$^{-0.5}$) | 1.06 | 1.50 | 1.83 | 1.67 | 2.37 | 2.90 | 5.29 | 7.48 | 9.17 |
| $i'_{pp,r}/i_{p,r}$ (s$^{-1}$) | 1.20 | 2.39 | 3.59 | 2.99 | 5.98 | 8.97 | 29.9 | 59.8 | 89.7 |
| $e'_{pp,r}/i_{p,r}$ (s$^{-1.5}$) | 1.38 | 3.92 | 7.17 | 5.47 | 15.5 | 28.4 | 173 | 489 | 899 |
| $i''_{pp,r}/i_{p,r}$ (s$^{-2}$) | 1.62 | 6.47 | 14.6 | 10.1 | 40.5 | 91.0 | 1012 | 4046 | 9104 |
| $e''_{pp,r}/i_{p,r}$ (s$^{-2.5}$) | 2.49 | 14.1 | 38.8 | 24.6 | 139 | 383 | 7770 | 43956 | 121130 |

where $\lambda$ is a dummy variable of the integral and $d^{-0.5}/dt^{-0.5}$ denotes the 0.5th-order integrating operator with respect to time.

Differentiation of Eqn. 13 with respect to $t$ gives

$$e_c = d^{0.5}i_c/dt^{0.5} = dm_c/dt = (A/\sqrt{\pi})C_d\upsilon t^{-0.5} \quad (14)$$

$$e'_c = d^{1.5}i_c/dt^{1.5} = de_c/dt = -(1/2)(A/\sqrt{\pi})C_d\upsilon t^{-1.5} \quad (15)$$

$$e''_c = d^{2.5}i_c/dt^{2.5} = de'_c/dt = (3/4)(A/\sqrt{\pi})C_d\upsilon t^{-2.5} \quad (16)$$

where $e_c$, $e'_c$ and $e''_c$ denote the 0.5th-, 1.5th- and 2.5th-order derivative of the capacity current, respectively.

The ratio of faradaic to capacitive current for any-order derivative linear potential sweep adsorption voltammetry of a reversible interfacial reaction may be expressed by the following equations:

$$i_{p,r}/i_{p,c} = 0.25(n^2F^2/RT)c[Kt_a + f(t_r)]/C_d \quad (17)$$

$$e_{pp,r}/e_{pp,c} = 0.375(n^{2.5}F^{2.5}/R^{1.5}T^{1.5})c[Kt_a + f(t_r)] / C_d\left[(E_i - E_{p,1})^{-1.5} - (E_i - E_{p,2})^{-0.5}\right] \quad (18)$$

$$i'_{pp,r}/i'_{pp,c} \to \infty \quad (19)$$

$$e'_{pp,r}/e'_{pp,c} = 0.630(n^{3.5}F^{3.5}/R^{2.5}T^{2.5})c[Kt_a + f(t_r)] / C_d\left[(E_i - E_{p,1})^{-1.5} - (E_i - E_{p,2})^{-1.5}\right] \quad (20)$$

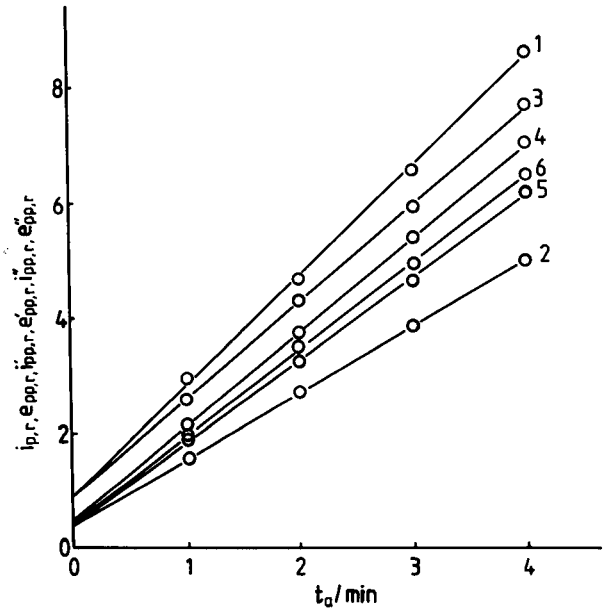


Fig. 1. Dependences of $i_{p,r}$, $e_{pp,r}$, $i'_{pp,r}$, $e'_{pp,r}$, $i''_{pp,r}$ and $e''_{pp,r}$ on the preconcentration time. ($t_a$) (1) $10^7$ $i_{p,r}$ (A) vs. $t_{ai}$; (2) $2.5\times10^6$ $e_{pp,r}$ (A $s^{-0.5}$) vs. $t_a$; (3) $2\times10^6$ $i'_{pp,r}$ (A $s^{-1}$) vs. $t_a$; (4) $5\times10^5$ $e'_{pp,r}$ (A $s^{-1.5}$) vs. $t_a$; (5) $2\times10^5$ $i''_{pp,r}$ (A $s^{-2}$) vs. $t_a$; (6) $5\times10^4$ $e''_{pp,r}$ (A $s^{-2.5}$) vs. $t_a$. $1\times10^{-3}$ mol $l^{-1}$ NaOH, $4\times10^{-8}$ mol $l^{-1}$ 5-Br-PADAT, $t_r = 30$ s, $A = 1.92$ mm$^2$, $\upsilon = 100$ mV $s^{-1}$, $T = 298$ K.

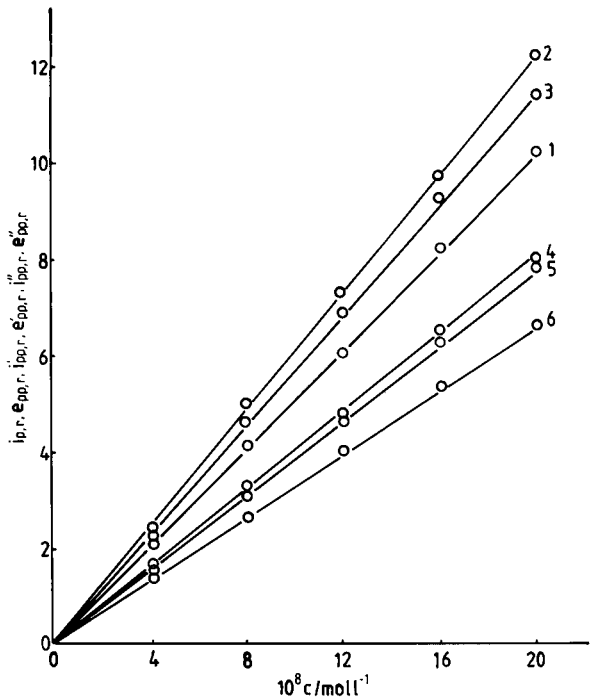


Fig. 2. Dependences of $i_{p,r}$, $e_{pp,r}$, $i'_{pp,r}$, $e'_{pp,r}$, $i''_{pp,r}$ and $e''_{pp,r}$ on the concentration of 5-Br-PADAT ($c$). (1) $10^7$ $i_{p,r}$ (A) vs. $c$; (2) $5\times10^8$ $e_{pp,r}$ (A $s^{-0.5}$) vs. $c$; (3) $2\times10^6$ $i'_{pp,r}$ (A $s^{-1}$) vs. $c$; (4) $5\times10^5$ $e'_{pp,r}$ (A $s^{-1.5}$) vs. $c$; (5) $2\times10^5$ $i''_{pp,r}$ (A $s^{-2}$) vs. $c$; (6) $5\times10^4$ $e''_{pp,r}$ (A $s^{-2.5}$) vs. $c$. $t_a = 1$ min; other experimental conditions as in Fig. 1.

TABLE 2

Experimental ratios of $e_{pp,r}$, $i'_{pp,r}$, $e'_{pp,r}$, $i''_{pp,r}$ and $e''_{pp,r}$ to $i_{p,r}$ at different scan rates ($t_a = 1$ min; other conditions as in Fig. 1)

| Ratio | v(mV $s^{-1}$) | | | |
|---|---|---|---|---|
| | 60 | 80 | 100 | 120 |
| $e_{pp,r}/i_{p,r}$ ($s^{-0.5}$) | 1.68 | 2.12 | 2.39 | 2.61 |
| $i'_{pp,r}/i_{p,r}$ ($s^{-1}$) | 3.65 | 4.87 | 6.08 | 7.30 |
| $e'_{pp,r}/i_{p,r}$ ($s^{-1.5}$) | 7.25 | 11.2 | 14.1 | 18.8 |
| $i''_{pp,r}/i_{p,r}$ ($s^{-2}$) | 20.6 | 32.3 | 51.0 | 62.7 |
| $e''_{pp,r}/i_{p,r}$ ($s^{-2.5}$) | 40.6 | 75.0 | 120 | 174 |

$$i''_{pp,r}/i''_{pp,c} \rightarrow \infty \quad (21)$$

$$e''_{pp,r}/e''_{pp,c} = 0.214(n^{4.5}F^{4.5}/R^{3.5}T^{3.5})c[Kt_a + f(t_r)] / C_d\left[(E_i - E_{p,2})^{-2.5} - (E_i - E_{p,3})^{-2.5}\right] \quad (22)$$

where $E_i$ is the initial potential, $E_{p,1}$, $E_{p,2}$ and $E_{p,3}$ denote the potentials of the first, second and third peak on their derivative voltammograms, respectively, $i_{p,c}$ is the capacity current at the peak of the faradaic voltammogram, and $e_{pp,c}$, $i'_{pp,c}$, $e'_{pp,c}$, $i''_{pp,c}$ and $e''_{pp,c}$ are the differences between two values of $e_c$, two values of $i'_c$, two values of $e'_c$, two values of $i''_c$ and two values of $e''_c$ at two neighbouring peaks on the faradaic derivative plots of current with respect to time, respectively.

Equations 17–22 show that (i) the ratio of faradaic to capacitive current cannot be improved by an increase in the electrode area or the scan rate for the conventional and derivative techniques, but the sensitivity can be enhanced by an extension of the preconcentration time and an increase in the stirring rate concerning $K$ in these equations; (ii) the higher the derivative order, the more sensitive the method is with the half-integer derivative techniques; and (iii) the first- and second-order derivative technique gives the highest ratio because the first- and second-order derivatives of the capacity current approach zero.

TABLE 3

Theoretical limits of detection of the conventional, 0.5th-, 1.5th- and 2.5th-order derivative techniques for a reversible reaction of species adsorbed at different preconcentration times

| Limit of detection (mol $l^{-1}$) | $t_a$ (min) | | | |
|---|---|---|---|---|
| | 2 | 3 | 6 | 10 |
| $10^{10}\ c_{i,r}$ | 5.3 | 3.5 | 1.8 | 1.1 |
| $10^{12}\ c_{e,r}$ | 4.9 | 3.3 | 1.6 | 0.98 |
| $10^{13}\ c_{e',r}$ | 2.5 | 1.7 | 0.83 | 0.50 |
| $10^{14}\ c_{e'',r}$ | 2.0 | 1.3 | 0.66 | 0.40 |

When the faradaic to capacitive current ratio is taken equal to 1 as the standard for determining the limit of detection and $K = 1 \times 10^{-2}$ cm $s^{-1}$, $(E_i - E_{p,1}) = 0.3$ V for the curves of the 0.5th- and 1.5th-order derivative of current vs. $E$, $(E_i - E_{p,2}) = 0.3$ V for the curve of the 2.5th-order derivative of current vs. $E$, $n = 2$, $T = 298$ $K$ and $C_d = 40$ $\mu$ F $cm^{-2}$ are taken, the limits of detection calculated from Eqns. 17, 18, 20 and 22 for the conventional, 0.5th-, 1.5th- and 2.5th-order techniques, $c_{i,r}$, $c_{e,r}$, $c_{e',r}$ and $c_{e'',r}$ are listed in

TABLE 4

Experimental limits of detection for different systems for the conventional and different derivative techniques

| System [a] | Limit of detection (mol $l^{-1}$) | | | |
|---|---|---|---|---|
| | Conventional | 1st-derivative | 1.5th-derivative | 2.5th-derivative |
| Bi (III)–5-Br-PADAP [b] | $2 \times 10^{-10}$ | $7.5 \times 10^{-11}$ | | |
| 5-Br-PADAT [b] | $7.5 \times 10^{-10}$ | $5 \times 10^{-10}$ | $4 \times 10^{-10}$ | $1 \times 10^{-10}$ |
| Co (II)–5-Br-PADAP [c] | $1 \times 10^{-9}$ | | $1.5 \times 10^{-10}$ | |
| V(V)–5-Br-PADAP [c] | $5 \times 10^{-10}$ | | $2.5 \times 10^{-11}$ | $2.5 \times 10^{-11}$ |
| Nb (V)–5-Br-PADAP [c] | $9 \times 10^{-10}$ | $5 \times 10^{-11}$ | | |
| Fe (III)–5-Br-PADAP [c] | | $7.5 \times 10^{-11}$ | $1 \times 10^{-10}$ | $5 \times 10^{-11}$ |

[a] 5-Br-PADAP = 2-[(5′-bromo-2′-pyridyl)azo]-5-diethylaminophenol; 5-Br-PADAT = 5-[5′-bromo-2′-pyridyl)azo]-2,4-diaminotoluene. [b] Reversible interfacial reaction. [c] Totally irreversible interfacial reaction.

Table 3. The theoretical limit of detection of conventional linear potential sweep adsorption voltammetry may be as low as $10^{-10}$ mol $l^{-1}$ which has been demonstrated expeimentally with many systems reported in the literature. Although theoretically with the 0.5th-, 1.5th- and 2.5th-order derivative technique one can determine $10^{-12}$–$10^{-15}$ mol $l^{-1}$ of substance and with the 1st- and 2nd-order derivative method the limits should be even lower than with the half-integer derivative technique, only concentrations larger than $10^{-11}$–$10^{-12}$ mol $l^{-1}$ can be detected experimentally, because of the noise from the instrument and the variations in the interferences from other chemicals (such as other surface-active species, oxygen and impurities in the sample solution and the product of decomposition of the substance being determined) and the instability of the species detected. Nevertheless, the derivative technique is still very attractive for ultra-trace analysis.

Comparing Eqns. 4–9 with the corresponding equations for a totally irreversible interfacial reaction [28], it is found that the form of the corresponding expressions is the same except for the coefficients, which vary between 0.736 and 0.493. This means that the limits of detection of linear potential sweep adsorption voltammetry for both interfacial reactions are nearly the same or at least of the same order of magnitude. Table 4 shows the limits of detection of different systems determined in this laboratory for conventional and different order derivative techniques in linear potential sweep adsorption voltammetry. It can be seen that the limit of detection of the derivative technique can be at least one order of magnitude lower than that of the conventional method.

REFERENCES

1 J. Wang, Am. Lab., 17 (5) (1985) 41.
2 R. Kalvoda and M. Kopanica, Pure Appl. Chem., 61 (1989) 97.
3 W.-R. Jin and K. Liu, Acta Chim. Sin., 43 (1985) 923.
4 W.-R. Jin and W. Jiang, Chin. J. Appl. Chem., 2 (2) (1985) 1.
5 L.-Z. Wang, W.-R. Jin, R.-L. Chen and C.-D. Feng, Chem. J. Chin. Univ., 6 (1985) 691.
6 S.-Q. Wen, R.-L. Chen, W.-R. Jin and H. Zhai, Metall. Anal. (China), 6 (2) (1986) 38.
7 W.-R. Jin and Y.-C. Hou, Fenxi Huaxue, 15 (1987) 1057.
8 J.-Z. Zhao and W.-R. Jin, J. Electroanal. Chem, 256 (1988) 181.
9 W.-R. Jin and Y.-B. Ren, Chin. J. Appl. Chem., 5 (2) (1988) 93.
10 W.-R. Jin, Y.-B. Ren and H. Xu, Acta Chim. Sin., 47 (1989) 385.
11 W.-R. Jin, Q.-F. Yang, G.-X. Mai, S.-R. Wang and J.M. Lu, Fenxi Huaxue, 17 (1989) 294.
12 J.-Z. Zhao and W.-R. Jin, J. Electroanal. Chem., 267 (1989) 271.
13 S.-L. Shi, J.-Y. Wang, W.-R. Jin and J.-M. Lu, Fenxi Huaxue, 17 (1989) 1085.
14 W.-R. Jin, J.-F. Wang, X.-L. Zhang and S.-R. Wang, J. Electroanal. Chem., 281 (1990) 21.
15 W.-R. Jin and X.-X. Li, Anal. Chim. Acta, 236 (1990) 453.
16 W.-R. Jin, S.-L. Shi and J.-Y. Wang, J. Electroanal. Chem., 291 (1990) 41.
17 J.-M. Lu, W.-R. Jin, S.-Y. Wang and T.-L. Sun, J. Electroanal. Chem., 291 (1990) 49.
18 J.-Y. Wang, C.-L. Sun and W.-R. Jin, J. Electroanal. Chem., 291 (1990) 59.
19 J.-M. Lu, W.-R. Jin and S.-Y. Wang, Anal. Chim. Acta, 238 (1990) 375.
20 W.-R. Jin, K. Jiao and H. Metzner, Electroanalysis, in press.
21 C.-L. Sun, J.-Y. Wang, W. Hu, X.-X. Mao and W.-R. Jin, J. Electroanal. Chem., 306 (1991) 251.
22 W.-R. Jin, Y.-C. Hou, C.-T. Yan, J.-Y. Wang and C.-L. Sun, Electroanalysis, 4 (1992) 233.
23 W.-R. Jin, Y.-C. Hou, C.-T. Yan, J.-Y. Wang and C.-L. Sun, Electroanalysis, 4 (1992) 239.
24 W.-R. Jin and J.-X. Peng, J. Electroanal. Chem., in press.
25 L.-J. Qu, L.-C. Chen and W.-R. Jin, Fenxi Huaxue, 19 (1991) 83.
26 W.-R. Jin, H. Cui and S.-R. Wang, J. Electroanal. Chem., 297 (1991) 37.
27 M. Riesz, Acta Math., 81 (1949) 1.
28 W.-R. Jin, H. Cui, L.-X. Zhu and S.-R. Wang, J. Electroanal. Chem., in press.

*Analytica Chimica Acta*, 268 (1992) 307–309
Elsevier Science Publishers B.V., Amsterdam



# A study of the prospects for a ciprofloxacin PVC coated wire ion-selective electrode based on 4-quinolones

H. Avsec and S. Gomišček

*Department of Chemistry and Chemical Technology, University of Ljubljana, 61000 Ljubljana (Slovenia)*

(Received 6th February 1992; revised manuscript received 18th May 1992)

**Abstract**

A potentiometric sensor system characterized by a membrane, based on a molecular dispersion of certain 4-quinolones and dioctylphthalate as a plasticizing solvent mediator in an inert poly(vinyl chloride) (PVC) support, is assessed for the selectivity towards ciprofloxacin (CF) ions. The electrodes which respond to CF ions have been prepared by coating a silver wire conductor with the PVC based film. The preferred system with norfloxacin in the membrane shows a linear response with a Nernstian slope of 54–62 mV/pCF over the range of $1 \times 10^{-4}$ to $1 \times 10^{-2}$ M solution of CF. The electrode exhibits good selectivity with respect to inorganic ions of biological importance. CF can be determined successfully in its pure solutions and in some pharmaceutical preparations using the standard addition technique.

*Keywords:* Ion-selective electrodes; PVC coated wire electrodes; 4-Quinolones

Ciprofloxacin (CF), (1-cyclopropyl-6-fluoro-1,4-dihydro-4-oxo-7-(1-piperazinyl)-3-quinolone-carboxylic acid) is an antibacterial agent of the 4-quinolone group with a broad spectrum of activity against Gram-positive and Gram-negative bacteria [1]. For its determination different methods can be used, e.g., chromatographic methods, differential pulse polarography and cathodic stripping voltammetry [2–6]. Although potentiometry using a suitable indicator electrode is nowadays widely used in analytical chemistry there are no data about 4-quinolone ion-selective electrodes (ISEs).

Most of the commercially available electrodes are rather bulky and expensive. The electrodes in which the metal conductor is in contact with a slightly soluble salt of the metal – 2nd order electrodes or solid ISEs – can be accepted as the precursors of coated wire ISEs (CW-ISEs). They are prepared by the incorporation of a slightly soluble salt in the polymer matrix and by coating the wire support with a mixture containing the active substance, a softener and poly(vinyl chloride) [7–11].

The aim of this paper is to report on the preparation and the performance characteristics of CW-ISEs sensitive to ciprofloxacin and to other 4-quinolones.

*Correspondence to:* H. Avsec, Department of Chemistry and Chemical Technology, University of Ljubljana, 61000 Ljubljana (Slovenia).

## EXPERIMENTAL

### *Apparatus*

Potential measurements were made using an MA 5740 Iskra pH meter equipped with an MA 9150 Iskra (Ljubljana) printer. The CW-ISEs already described and the Orion 90–09 saturated calomel electrode were used as indicator and

reference electrodes, respectively. All measurements were performed while the solution was constantly being stirred with a magnetic strirrer.

*Reagents*

All chemicals were of analytical reagent grade purity. Demineralized (Milli-Q, Millipore, Bedford, MA) water was used.

Ciprofloxacin was obtained in the form of Testsubstanz Ciprofloxacin, Bayer, Leverkusen, and 500 mg tablets (Cenin® 500) from Bayer Pharma, Ljubljana.

*Preparation of electrodes*

A silver wire, 3 cm × 1 mm o.d., was fastened with epoxy resin to a glass tube (7 mm o.d.) in such a way that the wire protruded 5 mm from the bottom of the tube. The wire was first cleaned, polished and electrolytically coated with AgCl and then with the PVC mixture [12]. This was prepared by dissolving 28.1 wt.% PVC and 63.1 wt.% dioctylphthalate as plasticizer in 3 ml of tetrahydrofuran. 100 mg of electroactive substance was added to this mixture. This suspension was warmed in a drying apparatus at 60°C for 20 min. In order to coat the wire with the suspension, the exposed portion of wire was carefully immersed in the suspension, and was allowed to form a thin film by drying overnight on air. Finally the electrode was conditioned by soaking in $1 \times 10^{-3}$ M ciprofloxacin solution for approximately one hour before being used. It may be stored dry, but should be preconditioned again before re-use.

As the active substances were used 4-quinolone, ciprofloxacin (CF), pefloxacin (PF), norfloxacin (NF) or the ciprofloxacin–tetraphenyl borate ion pair (CF–TPB). A precipitate of CF–TPB was prepared by mixing aqueous solutions containing equimolar amounts of sodium tetraphenylborate and ciprofloxacin and subsequently filtering, washing with water, and drying at room temperature.

*Potentiometric determination of ciprofloxacin*

The performance of the electrodes was investigated by measuring the e.m.f. values in concentrations of ciprofloxacin between $1 \times 10^{-2}$–$1 \times 10^{-5}$ M (50-ml beaker). The solution was stirred during the measurement. Potentials were recorded when stable readings were obtained (normally within 30 s) and the calibration graph was constructed. The same procedure was applied for the determination of CF in the sample solutions.

## RESULTS AND DISCUSSION

The response characteristics of the 4-quinolone electrodes under investigation are given in Table 1. The results indicate that the electrodes show a Nernstian response for ciprofloxacin over a relatively large concentration range. The detection limits and the range of linearity are similar for all the electrodes investigated whereas the absolute values of the potentials differ for particular electrodes. The response time of the electrodes was tested by measuring the time required for the electrode to attain a steady potential after successive immersions in ciprofloxacin solutions each having a 10-fold higher concentration. The measurements for norfloxacin and ciprofloxacin–tetraphenylborate electrodes are characterized by a fast and stable response within 20–30 s for

TABLE 1

Response characteristics of 4-quinolone CW-ISEs

| Parameter | Electrodes | | | |
|---|---|---|---|---|
| | CF | CF–TPB | NF | PF |
| Slope (mV/pCF) | 50 | 52–54 | 54–62 | 50 |
| Linear range (M) | $1 \times 10^{-2}$–$1 \times 10^{-4}$ | | $1 \times 10^{-2}$–$1 \times 10^{-4}$ | |
| Detection limit (M) | $5 \times 10^{-5}$ | $7.9 \times 10^{-5}$ | $5 \times 10^{-5}$ | $5 \times 10^{-5}$ |
| Response time (min) | 2–5 | 0.5–2 | 0.5–2 | 2–5 |

TABLE 2

Selectivity coefficients (log $k_{AB}^{pot}$) of ciprofloxacin CW-ISEs based on 4-quinolones

| Interferent, B | Added as | log $k_{A,B}$ | | |
|---|---|---|---|---|
| | | PF | CF–TPB | NF |
| $CH_3COO^-$ | $CH_3COOK$ | −0.46 | −0.61 | −0.66 |
| $CH_3COO^-$ | $CH_3COONa$ | −0.53 | −0.73 | −0.64 |
| $Cl^-$ | NaCl | −0.14 | −0.18 | −0.16 |
| $Cl^-$ | KCl | −0.15 | −0.18 | −0.17 |
| Cefotaxime | Na salt | −0.98 | −0.79 | −0.89 |
| Penicillin G | Na salt | −0.97 | −0.62 | −0.73 |
| Ampicillin | Na salt | −0.81 | −0.62 | −0.68 |
| Amoxicillin | – | – | – | −0.93 |
| Ceftriaxone | – | – | – | −0.70 |
| Cefoxitin | – | – | – | −0.60 |
| Methicillin | – | – | – | −0.55 |

solutions of more than $1 \times 10^{-3}$ M and 0.5–2 min for solutions of less than $1 \times 10^{-3}$ M.

The performance of norfloxacin and ciprofloxacin–tetraphenylborate electrodes did not change over two months, whereas the lifetime of the ciprofloxacin and the pefloxacin electrodes was shorter (about one week).

The effect of pH ($1 \times 10^{-3}$ M ciprofloxacin solution) on the electrode potential was investigated by observing the changes in the potential readings with pH of the solution after the addition of small volumes of HCl and/or NaOH (0.1 M or 1 M). The investigated electrode (norfloxacin) gave a useful pH range from 4.5 to 7.0. In alkaline media the measurements were hindered owing to the formation of a precipitate in the test solutions. The influence of some inorganic anions and antibiotics on the potentials obtained was investigated, and the selectivity coefficients $k_{AB}^{pot}$ were determined by the separate solution technique and equal concentrations of participants [13]. The values given in Table 2 were obtained using the equation

$$\log k_{AB}^{pot} = (E_1 - E_2)/S + \log[A] - \log[B^z]^{1/z}$$

where $E_1$ is the potential of the electrode in the ciprofloxacin (A) solution ($1 \times 10^{-3}$ M) and $E_2$ is the potential in a solution containing the interferent (B) ion ($1 \times 10^{-3}$ M).

The results obtained clearly show that 4-quinolone electrodes do not show high selectivity for the investigated species. It can also be seen that the investigated 4-quinolones interfere with each other. However, all the 4-quinolone electrodes proved to be useful in the potentiometric determination of ciprofloxacin in pure solutions or in pharmaceuticals using the standard addition technique for the evaluation. The ingredients in the tablets do not interfere. Cenin® 500 tablets (ca. 780 mg) for oral application containing 582 mg CF · HCl, i.e., 500 mg CF/tablet were used in the recovery study. The content of CF in the tablet was determined using the calibration graph obtained with the "Testsubstanz". The mean value (± standard deviation) obtained was 500.1 ± 0.8 mg CF/tablet ($n = 9$). Thus, the relative standard deviation was found to be 0.16%.

The material is based on work supported by the US Fund for Scientific and Technological Cooperation, in cooperation with the National Institute of Standards and Technology, Gaithersburg, MD, under Grant NIST-JF-848.

REFERENCES

1 V.T. Andriole, The Quinolones, Academic Press, London, 1988.
2 G.J. Krol, A.J. Noe and D. Beermann, J. Liquid Chromatogr., 9 (1986) 2897.
3 B. Joos, B. Ledergerger, M. Flepp, J.D. Bettex, R. Luthy and W. Siegenthaler, Antimicrob. Agents Chemother., 27 (1985) 353.
4 J.M. Brogard, F. Jehl, H. Monteil, M. Adloff, J.F. Blickle and P. Levy, Antimicrob. Agents Chemother., 28 (1985) 311.
5 A. Veber, M. Veber, F. Kozjek and S. Gomiscek, Acta Pharm. Yug., 30 (1989) 321.
6 L. Tekstor, M. Veber, M. Marolt-Gomiscek and S. Gomiscek, Vestn. Slov. Kem. Drus., 36 (1989) 25.
7 R.M. Cattrall and H. Freiser, Anal. Chem., 43 (1971) 1905.
8 H. Hirata and K. Date, Talanta, 17 (1970) 883.
9 H. James, G. Carmack and H. Freiser, Anal. Chem., 44 (1972) 856.
10 A.F. Shoukry and S.S. Badawy, Microchem. J., 36 (1987) 107.
11 C.R. Martin and H. Freiser, J. Chem. Educ., 57 (1980) 512.
12 H. Avsec and S. Gomiscek, Vestn. Slov. Kem. Drus., 37 (1990) 299.
13 K. Srinivasan and G.A. Rechnitz, Anal. Chem., 41 (1969) 1203.

*Analytica Chimica Acta*, 268 (1992) 311–314
Elsevier Science Publishers B.V., Amsterdam



# Piezoelectric determination of traces of thiourea

S.Z. Yao, F.J. He and L.H. Nie

*New Material Research Institute, Department of Chemical Engineering, Hunan University, 410082 Changsha (China)*

(Received 14th October, 1991; revised manuscript received 14th April 1992)

**Abstract**

A method was developed for the determination of thiourea based on the reaction of the latter with a solution of iodine in carbon tetrachloride at pH 7, followed by measuring the frequency change of a gold-plated piezoelectric crystal caused by the unreacted iodine. The frequency change is proportional to thiourea concentration over the range $1 \times 10^{-7}$–$6 \times 10^{-6}$ mol $l^{-1}$ (7.6–457 ng $ml^{-1}$). The relative standard deviation was 1.4% for six measurements of $6 \times 10^{-7}$ mol $l^{-1}$ (46 ng $ml^{-1}$) thiourea.

*Keywords:* Piezoelectric sensing; Thiourea

Thiourea has found many applications in medicine, industry and chemistry. Various methods have been proposed for the determination of thiourea, such as titrimetry with haloamines [1], potassium dichromate [2], Masson and Race reagent [3] or iodine [4], Raman spectrometry [5], stripping voltammetry [6], ion-selective electrode potentiometry [7] and spectrophotometry [8]. However, most of these methods are either insensitive, tedious or require special instrumentation. The piezoelectric detector has the advantage of being highly sensitive and has found a number of applications in chemical analysis [9–12]. In this paper, a very sensitive and simple method for the determination of ultra-traces of thiourea in solution by using a piezoelectric detector is suggested.

## EXPERIMENTAL

### *Apparatus and reagents*

The complete assembly of the equipment is outlined in Fig. 1. AT-cut, 9-MHz quartz crystals (12.5 mm diameter) with a gold-plated electrode (6 mm diameter) on each side were prepared as follows. The surface of the commercial quartz crystal with silver-plated electrodes was cleaned with fine emery paper and washed with water and acetone. It was then immersed in a gold-plating bath of pH 9.5 containing 12 g $l^{-1}$ $K_6[Au(SO_3)_2$ HY] (Y = EDTA) and plated using a 1 A $dm^{-2}$ current density for 10 s, then at 0.1 A $dm^{-2}$ for 3 min [13]. A gold layer corresponding to a decrease of 25–45 kHz in oscillation frequency of the crystal was obtained. The crystal was connected to an integrated circuit oscillator built in this laboratory [14] supplied by a d.c. voltage

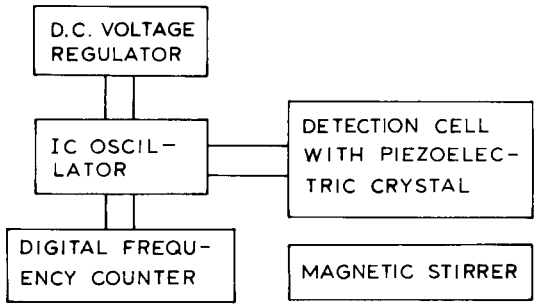


Fig. 1. Block diagram of the experimental assembly.

*Correspondence to:* S.Z. Yao, New Material Research Institute, Department of Chemical Engineering, Hunan University, 410082 Changsha (China).

regulator. The frequency change was monitored by a digital counter. A detection cell with a magnetic stirrer was used.

All chemicals were of analytical-reagent grade and doubly distilled water was used for rinsing and the preparation of solutions.

A stock solution of thiourea (4 mmol $l^{-1}$) was prepared and used within 1 week. Solutions of lower concentration were prepared by appropriate dilution. Iodine solution in carbon tetrachloride (1.2 mmol $l^{-1}$) was prepared weekly and kept in an amber-coloured glass flask, from which 12 or 24 $\mu$mol $l^{-1}$ iodine solution was prepared daily by dilution with carbon tetrachloride. Buffer solutions were prepared by mixing a 0.2 mol $l^{-1}$ solution of disodium hydrogenphosphate and a 0.1 mol $l^{-1}$ solution of citric acid [15].

*Standard procedure*

Transfer 100 $\mu$l of sample solution with a microsyringe into a 60-ml separating funnel containing 10 ml of buffer solution. Add 10 ml of 12 (or 24) $\mu$mol $l^{-1}$ iodine solution in carbon tetrachloride. After shaking for 10 min and phase separation, transfer the organic layer into the measuring cell with the piezoelectric crystal detector and turn on the magnetic stirrer. After exactly 5 min, remove the crystal and record the frequency shift ($F$) after drying. Repeat the procedure with a blank and record the frequency shift ($F_0$). Plot the frequency change, $\Delta F = F_0 - F$, against thiourea concentration to give a calibration graph.

## RESULTS AND DISCUSSION

*Factors affecting thiourea determination*

*pH.* The effect of solution pH on thiourea determination was investigated in order to establish the most appropriate working pH. The frequency change was not affected by solution pH within the range of 6.4–8.0. At pH values outside this range, the frequency change decreases (Fig. 2). In this work, pH 7 was used.

*Reaction time.* The reaction between the analyte and the oxidant proceeds heterogeneously with continuous shaking of the two immisible

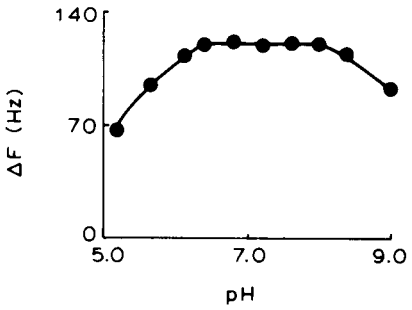


Fig. 2. Dependence of frequency change of the piezoelectric detector on pH. Concentration of thiourea, $5\times10^{-7}$ mol $l^{-1}$.

phases. After the analyte in the aqueous phase has been completely consumed by the oxidant, the unreacted iodine is measured with the piezoelectric monitor. Therefore, it is necessary to study the influence of the reaction time on the determination. It was found that the appropriate reaction time is 10 min; a shorter time resulted in a smaller frequency change and a longer reaction time exhibited no increase in frequency change.

*Amounts of reactants.* To examine the effect of iodine concentration on the determination of thiourea, various amounts of iodine were added to thiourea solutions of different concentration, and their effect on the thiourea determination was tested. The results showed that the required amount of iodine depends on the concentration of the analyte and when the iodine concentration exceeds six times the thiourea concentration, there was no significant influence.

According to Amin [4], iodine reacts with thiourea according to the reaction

$$CS(NH_2)_2 + 4I_2 + 6H_2O \rightarrow (NH_4)_2SO_4 + 8HI + CO_2$$

Hence a 1.5-fold stoichiometric amount of the oxidant is required for the heterogeneous reaction to proceed quantitatively under the aforementioned experimental condition.

*Organic solvent.* Instead of carbon tetrachloride, other non-polar organic solvents can also be used, e.g., chloroform or heptane. However, carbon tetrachloride gave the highest sensitivity in the determination of thiourea. In ethers, such as

diethyl or diisopropyl ether, the frequency change is low. Acetone and ethanol cannot be used.

Experiments with various aqueous solution to organic phase volume ratios demonstrated that the results of thiourea determination were not affected by the volume ratio of aqueous solution to carbon tetrachloride solution in the tested range of 1:2–2:1 with a constant carbon tetrachloride volume of 10 ml. Larger ratios caused low results. No increase in frequency change was observed when repeated extraction was carried out. For example, twice repeated 10-min extractions each with 5 ml of carbon tetrachloride gave nearly the same frequency change as when one 10-min extraction with 10 ml of carbon tetrachloride was made.

*Interferences, regeneration and lifetime of the monitor*

To investigate interferences, various ions were added to an $8 \times 10^{-7}$ mol $l^{-1}$ thiourea solution, and their effects on the thiourea determination were tested. Differences in frequency change of more than 5% were considered to result from interferences. No significant interferences were caused by benzoate, acetate, carbonate, phosphate, nitrate, sulphate, bromide, chloride, cadmium, zinc, calcium, cobalt, copper, nickel, aluminium and magnesium ions at a 150-fold mole ratio to thiourea or urea and formate at a 50-fold mole ratio to thiourea. Sulphite causes a positive interference when its mole ratio to thiourea is greater than 1.2:1, as it undergoes oxidation in the presence of an excess of iodine.

The gold electrode of the piezoelectric crystal after measurement is cleaned with a cotton swab impregnated with ammonia solution (1 + 8) or a 1.25% solution of sodium thiosulphate to dissolve the adsorbed iodine species. After being washed with water, it is washed with acetone and dried, and is then ready for the next measurement. To regenerate the piezoelectric monitor, other solutions can also be used, such as sodium hydrogensulphite or sodium carbonate solutions. Sodium hydroxide solution cannot be used because of its etching effect on the quartz crystal after prolonged contact, resulting in an increase in the oscillation frequency.

The piezoelectric detector with gold-plated electrodes is advantageous over the silver-plated type in that it gives a longer lifetime and can be used not less than 270 cycles. For a $5 \times 10^{-7}$ mol $l^{-1}$ solution of thiourea, the frequency change after the 3rd, 50th, 100th and 260th measurements were 115, 117, 115 and 109 Hz, respectively.

*Calibration, reproducibility and analytical application*

The calibration graph of frequency change versus thiourea concentration for a 5-min adsorption time was linear over the range $1 \times 10^{-7}$–$6 \times 10^{-6}$ mol $l^{-1}$ (7.6–457 ng $ml^{-1}$) and is described by the regression equation

$$[\text{thiourea}] = (0.04523\Delta F - 0.2737) \times 10^{-7} \text{ mol } l^{-1}$$

or

$$[\text{thiourea}] = (0.3443\Delta F - 2.0834) \text{ ng ml}^{-1}$$

TABLE 1

Determination of thiourea

| Parameter | Thiourea added ($10^{-7}$ mol $l^{-1}$) | | | | | | | |
|---|---|---|---|---|---|---|---|---|
| | 3.00 | 5.00 | 7.00 | 9.00 | 15.0 | 25.0 | 35.0 | 50.0 |
| Frequency change (Hz) | 74.6 | 120 | 159 | 205 | 327 | 543 | 789 | 1089 |
| Thiourea found [a] ($10^{-7}$ mol $l^{-1}$) | 3.10 | 5.17 | 6.91 | 9.00 | 14.5 | 24.3 | 35.4 | 49.0 |
| Recovery (%) | 103 | 103 | 98.5 | 100 | 96.5 | 97.5 | 101 | 98.0 |

[a] Averages of three measurements.

where $\Delta F$ is measured in Hz. The regression coefficient is 0.998. The standard deviation was 2 Hz (1.4%) for six determinations of $6 \times 10^{-7}$ mol $l^{-1}$ (46 ng $ml^{-1}$) thiourea. For lower thiourea concentrations, a longer adsorption time is suggested, e.g., 10 min for $10^{-8}$ mol $l^{-1}$.

To test the method, sample solutions containing thiourea at $1 \times 10^{-7}$–$5 \times 10^{-6}$ mol $l^{-1}$ (7.6–380 ng $ml^{-1}$) were analysed using the proposed procedure. The results are given in Table 1.

*Adsorption mechanism*

Cyclic voltammetry and x-ray photoelectron spectroscopy (XPS) have been used to elucidate the adsorption mechanism of iodine on the gold-plated crystal. For all the electrodes, with different amounts of adsorbed iodine species, the peak potentials on the voltammograms approximate to that of the iodine–iodide couple. The binding energies on their XPS spectra are nearly the same as those for free iodine, 618.3 eV ($3d_{5/2}$ level) and 629.7 eV ($3d_{3/2}$ level). Hence it can be concluded that the iodine species absorbed on the gold-plated electrodes of the piezoelectric crystal is simply $I_2$. Further evidence for this is the phenomenon that the surface of the crystal electrode is red (when a small amount of iodine is adsorbed) or dark red (when a large amount of iodine is absorbed), which implies the existence of free iodine on the electrode surface.

The authors thank the Natural Science Fund and the State Education Commission Fund of the People's Republic of China for financial assistance.

REFERENCES

1 C.P.K. Paillai and P. Indrasema, Talanta, 27 (1980) 751.
2 J.K. Puri, V.K. Vats and V. Sharma, Indian J. Chem., Sect. A, 25 (1986) 565.
3 A. Srivastava and S. Bose, J. Indian Chem. Soc., 62 (1985) 546.
4 D. Amin, Analyst, 110 (1985) 215.
5 H.J. Bowley, E.A. Crathorne and D.L. Gerrard, Analyst, 111 (1986) 539.
6 K.R. Xiu, Y.E. Liu and S.J. Chen, Huanjing Kexue, 7 (1987) 61.
7 P. Sharma and M. Singh, J. Electrochem. Soc. India, 34 (1985) 6.
8 C.S.P. Sastry, P. Satyanarayana and M.K. Tummuru, Indian J. Chem., Sect. A, 24 (1985) 258.
9 J.F. Alder and J.J. McCallum, Analyst, 108 (1983) 1169.
10 S.Z. Yao, Z.H. Mo and L.H. Nie, Anal. Chim. Acta, 215 (1988) 79.
11 L.H. Nie, B. Chen and S.Z. Yao, Acta Pharm. Sin., 21 (1986) 605.
12 S.Z. Yao, L.H. Nie and Z.H. Mo, Anal. Chim. Acta, 217 (1989) 327.
13 S.Z. Yao, Z.Q. Zhu and M. Nie, Diandu ju Huanbao, 7 (1987) 9.
14 S.Z. Yao and Z.H. Mo, Anal. Chim. Acta, 193 (1987) 97.
15 J.A. Dean (Ed.), Lange's Handbook of Chemistry, McGraw-Hill, New York, 12th edn., 1979, pp. 5–81, 82.

*Analytica Chimica Acta*, 268 (1992) 315–321
Elsevier Science Publishers B.V., Amsterdam



# Modified electrical heating system for hydride generation atomic absorption spectrometry and elaboration of a digestion method for the determination of arsenic and selenium in biological materials

Daniel Mayer, Sabine Haubenwallner and Walter Kosmus

*Institute for Analytical Chemistry, Karl-Franzens University, Universitätsplatz 1, 8010 Graz (Austria)*

Wolfgang Beyer

*Institute for Medicinal Chemistry, Karl-Franzens University, Harrachgasse 21, 8010 Graz (Austria)*

(Received 25th March 1992; revised manuscript received 19th May 1992)

**Abstract**

A modified electrical heating system for hydride generation atomic absorption spectrometry has been designed. The heating block permits a rapid and convenient change of the quartz tube in order to clean and condition its surface. Frequent conditioning guarantees high and constant measurement sensitivity. Further, an inexpensive and simple microwave digestion procedure has been developed. The methods were tested by analysing reference materials and proved to be appropriate for trace concentrations of arsenic and selenium.

*Keywords:* Atomic absorption spectrometry; Arsenic; Hydride generation; Microwave digestion; Selenium

The important trace elements arsenic and selenium act in different biological cycles. Selenium is essential for the human organism. It is an integral part of the enzyme glutathione peroxidase, which protects cell membranes from lipid peroxidation and radicals [1,2] and, in consequence of this function, plays an important role in immune defence [3]. Additionally, selenium is utilized for therapeutic purposes in numerous diseases, e.g., acute pancreatitis [4], and has demonstrated anticarcinogenic effects in numerous cases [5–10]. Arsenic is known for its interactions with selenium [11]. Moreover, it catalyses glutathione biosynthesis [12] and may be important for arginine, membrane phospholipid and zinc metabolism [13]. Hence, although arsenic has not been identified as an essential trace element in man, it seems to have some biological importance, and interest in and research on its functions are increasing.

Selenium and arsenic concentrations in human tissues are very low. Analytical methods reaching detection limits of 1 ng absolute or even below are necessary to establish "normal values" for the human organism or to define arsenic and selenium deficiency or intoxication. Further, the determination of arsenic and selenium, especially when present in trace concentrations, has become very important in many fields such as metallurgy, toxicology and environmental control. One of the

*Correspondence to:* W. Kosmus, Institute for Analytical Chemistry, Karl Franzens University, Universitätsplatz 1, 8010 Graz (Austria).

most suitable methods meeting highest requirements is hydride generation atomic absorption spectrometry (AAS).

The hydride generation technique is based on the volatilization of the element as a gaseous, covalent hydride by adding a reducing agent (sodium tetrahydroborate) to an acidified sample solution. The element hydride is transported to an electrically or flame-heated quartz tube placed in the optical axis of the AAS apparatus, where atomization occurs and the atomic absorption is measured. The main advantages of the hydride generation technique are low detection limits element separation from the bulk matrix and, for very low concentrations, the enrichment of the analyte element, e.g., in a cold trap or in a graphite furnace [14,15]. The separation of the hydrides leads to a substantial decrease in interferences compared with flame or graphite furnace AAS. As only the analyte and almost no interfering elements or substances reach the measuring cell, usually no background correction is required [16–18].

A comparison between the two atomization methods reveals that electrical heating is preferable to the flame method not only because of its operating almost free from interferences, but also because the electrothermal hydride technique is clean and the temperature inside the measuring chamber is constant and exactly adjustable for different elements, resulting in well defined and therefore reproducible conditions inside the atomization chamber. Another advantage of low-voltage electrical heating systems is their cheap and safe operation. Finally, they are much easier to handle as for instance, no change of gas supply is necessary.

## THEORETICAL

### *Sensitivity-determining parameters*

The sensitivity of the hydride technique depends on the following factors: cell temperature [19]; purge time [19]; gas flow [18,20,21]; concentration of the reducing agent [18]; speed of the reduction step [17]; sample volume [17]; acidity of the sample solution [18,22,23]; valence state of the analyte element [17,18,24,25]; interferences [23,26–28]; and condition of the cell surface [19,29].

### *Atomization of the hydrides*

The atomization of the free element hydrides in a heated quartz tube must be due to their collisions with free hydrogen radicals and the following reaction mechanism seems to be the most likely [19]:

$$MH_x + H^{\cdot} \rightarrow MH_{x-1} + H_2$$

$$\vdots$$

$$MH + H^{\cdot} \rightarrow M^{\cdot} + H_2$$

The hydrogen radicals are generated according to the reaction suggested by Dědina and Rubeška [30] for the fuel-rich hydrogen–oxygen flame. As shown by Welz and Melcher [28], this mechanism should also be valid for electrically heated systems:

$$H^{\cdot} + O_2 \rightarrow OH^{\cdot} + O^{\cdot}$$

$$O^{\cdot} + H_2 \rightarrow OH^{\cdot} + H^{\cdot}$$

$$OH^{\cdot} + H_3 \rightarrow H_2O + H^{\cdot}$$

In addition, this reaction mechanism explains the influence of the purge time and of the oxygen concentration in the quartz tube on the measuring sensitivity. As the concentration of oxygen and, in consequence, the $H^{\cdot}$ radical concentration in the cuvette decrease with increasing purge time, the atomization of the element hydride does not occur completely when the purge time is too long.

### *Influence of the quartz surface on hydride atomization*

Whereas most of the parameters mentioned above may be optimized without difficulty, one problem remains. It is evident and well documented that frequently used quartz cells are contaminated with sample components or excess sample concentrations of hydride-forming elements may form a layer on the cuvette surface even after only one measurement. Contaminations cause signal depressions and peak broadening, leading to a decrease in sensitivity. This

effect has been mentioned and explained by numerous investigators [19,29]. The contaminants are burnt into the surface, forming a kind of catalytic film which accelerates radical recombination and therefore reduces the concentration of H· radicals within the cuvette. Therefore, as the equilibrium concentration of the H· radicals which is required for the atomization of the gaseous hydrides is disturbed, a significant signal depression and lower sensitivity, respectively, are the consequence. In order to maintain the highest sensitivity, it is necessary frequently to remove contaminants from the quartz tube. Different cuvette treatments have been suggested [19,29,31]. Cleaning and conditioning procedures may include acid treatments or sandblasting to increase the surface area. Rinsing in 40% hydrofluoric acid for ca. 15 min has proved to be the most effective cuvette treatment procedure resulting in optimum sensitivity.

Further, the vitreous silica phase can be considered for the active surface catalysing the hydride atomization [32]. Heating quartz at high temperatures leads to the formation of the high-temperature phase $\beta$-cristobalite, which hinders hydride atomization. This sensitivity-reducing phase may be present even on new quartz cuvettes and can also be removed with the HF cuvette treatment [33,34]. Another conditioning procedure is to keep the temperature of the cell at about 1000°C for a few hours in order to anneal the quartz tube (the annealing temperature of clear fused quartz is 1080°C) after having exposed it to a dilute hydrofluoric acid solution. The annealing process removes any kind of residual mechanical stresses and prevents the formation of $\beta$-cristobalite [34].

## EXPERIMENTAL

The measuring cells of commercially available hydride systems are usually heated with the AAS burner flame. Only very few electrically heated systems are offered. Mostly they consist of a closed block, equipped with a T-shaped quartz tube. Laboratory-constructed hydride systems are normally made by winding a heating-wire around the quartz tube and isolating it twice with asbestos or quartz tape and an outer jacket, e.g., made of ceramic [34,35].

All cleaning and conditioning procedures mentioned above require a heating system that permits a rapid convenient cuvette change without the use of special tools or the necessity to call for a service engineer. Further, a heating device reaching temperatures up to 1100°C is desirable to allow the annealing of the quartz tube without time-consuming dismantling procedures. With one exception, none of the hydride systems constructed so far offers the possibility of keeping a high sensitivity by replacing, cleaning or conditioning the quartz tubes, as they cannot be removed from the heating block. Moreover, the thin and fragile wire of laboratory-constructed heating units easily breaks or burns out when heated too long at high temperatures.

These difficulties motivated us to develop an electric heating system that is not affected by any of the problems mentioned above. Our specially designed heating block, equipped with a T-shaped quartz tube, with both ends open, can easily be opened and closed and is convenient to handle and to work with. The heating is supplied by a continuously variable low-voltage transformer guaranteeing optimum atomization temperatures for each element being determined. For hydride generation we adapted a mercury cold vapour device. The heating block is mounted on the burner head of the AAS instrument and can be adjusted exactly in the optical axis.

### *Apparatus*

The system was developed by using a Hitachi Model Z-6100 atomic absorption spectrometer under the manufacturer's recommended conditions. Cathodeon hollow-cathode lamps were used. Cell surface temperatures were determined with Technotherm 9400 detector. The entire hydride system was constructed in the laboratory and allowed the free selection of time and temperature parameters. A schematic diagram of the system is shown in Fig. 1.

### *Chemicals*

Analytical-reagent grade reagents (Merck Suprapur) were used through. Argon (Air Liq-

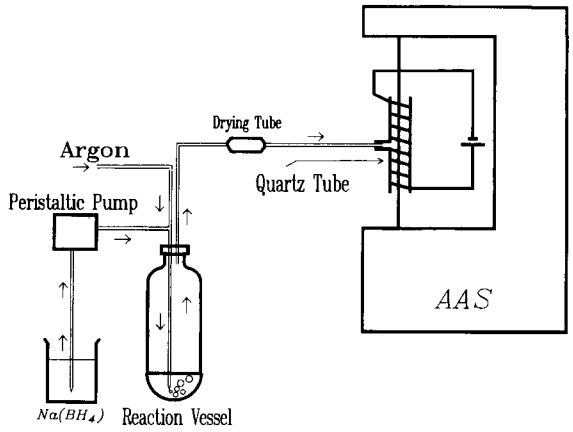


Fig. 1. Schematic diagram of the hydride generation system.

uide, quality N 50) was 99.999% pure. Sodium tetrahydroborate solution was prepared by dissolution of sodium tetrahydroborate powder (Merck) in 1% NaOH solution to a final concentration of 3% (w/v). The solution was filtered through a folded filter-paper and could be used for 4 days when stored at 4°C. Arsenic and selenium working solutions (1 mg $l^{-1}$) were prepared immediately before use by dilution of Merck Titrisol stock solutions (1 g $l^{-1}$) in 1.5% HCl.

*Cleaning*

PTFE digestion tubes and glass flasks were filled with 1 M HCl and soaked for 10 h, then 2 ml of sodium tetrahydroborate solution were added while purging with argon to remove the generated hydrides. All laboratory ware was cleaned by rinsing three times with 1.5% HCl followed by washing three times with deionized water and drying.

*Digestion procedure*

In order to check the hydride system for proper working and reproducibility, the arsenic and selenium concentrations of organic reference materials were determined. Arsenic and selenium are prone to volatility losses during wet digestion, particularly of difficult matrices, hence the elaboration of dependable ashing methods presents a permanent challenge. Even the results of highly qualified laboratories participating in a certification programme presented in a recent paper [35] showed a remarkable diversity only for these two elements, and microwave digestion proved to provide the most dependable and reproducible results.

Microwave digestion is the method of choice for the mineralization of organic and biological matrices without the use of hazardous perchloric acid. It reduces the sample preparation time significantly, resulting in a high sample throughput. Commercially available digestion devices are very expensive but, apart from their safety arrangements, their functioning is similar to that of household microwave ovens. Although our laboratory is equipped with a modern microwave digestion system, an inexpensive and yet efficient method to decompose organic matrices for arsenic and selenium determination was developed. A household microwave oven (maximum power 650 W) was adapted with the following alterations: a plastic turntable that accepted 12 digestion vessels and rotated at 6 rpm was installed; the oven was evacuated by an exhaust, directing to a fume-hood; and 50-ml PTFE centrifuge tubes (Oak Ridge No. 3114) were prepared by heating them at a constant temperature of 200°C for 96 h. This "annealing" of the PTFE [36] resulted in an improved pressure resistance of the vessels, making them more suitable for closed digestion procedures, which are necessary to avoid loss of volatile arsenic and selenium.

Samples of 5 × 1 ml of serum (Seronorm™, Batch No. 116) and 5 × ca. 200 mg of NIST SRM 1577a Bovine Liver were digested using the following procedure. For predigestion, 7.5 ml of $HNO_3$ (sub-boiled distilled) and 2.5 ml of $H_2SO_4$ (Merck Suprapur, 96%) were added to the samples, which were allowed to react at room temperature (RT) until vigorous starting reactions ceased (ca. 1 h). The tubes were placed into a water-bath and heated at 90°C for 30 min, closed tightly and heated at 90°C for 30 minutes, then cooled to RT, opened to release the pressure and closed again. For microwave digestion, the tubes were placed into the microwave oven and each heating step was followed by cooling to RT, pressure release and careful capping before the next heating as follows. The tubes were heated for 4 min at 100 W, cooled to RT and the pressure was

released, followed by heating for 6 min at 325 W, cooling, pressure release, adding 100 $\mu$l of $H_2O_2$, heating for 6 min at 325 W, cooling, pressure release, heating for 6 min at 455 W, cooling, pressure release, heating for 6 min at 650 W, cooling, adding 200 $\mu$l of $H_2O_2$, placing the opened tubes in a water-bath and heating for 1 h at 90°C.

Finally, the clear digestion solutions (ca. 5 ml) were transferred into glass flasks and made up to a final volume of 10 ml. With this digestion procedure no loss of volatile arsenic and selenium occurred and although it needed more attention and manual operations compared with automated microwave digestion devices, the simple and inexpensive equipment made it a suitable method for organic sample preparation.

*Determination of arsenic and selenium*

Aliquots of 1 ml were used for analysis. The sample solution was transferred into the reaction vessel and 10 ml of deionized water and 4 ml of 32% HCl were added before measurement. The reaction vessel was connected to the hydride system and purged for 45 s, then the reducing agent was added by means of a peristaltic pump and, after passing a drying tube filled with $CaCl_2$, the generated element hydride was purged into the atomization and measuring cell. The atomic absorption signal was measured and recorded. To obtain maximum peak heights, the optimum temperature for both elements first had to be determined, as it may vary with the measuring conditions. Some workers have observed that mixing small amounts of oxygen or air with the purge gas stream reduced the influence of the cell temperature on the measurement sensitivity, especially for arsenic [19,29]. With the present heating system, the optimum atomization temperatures for both elements were determined without the presence of oxygen or air. It was found that 1100°C for arsenic and 750°C for selenium produced the highest sensitivity.

The temperature dependence of the atomization signal for both arsenic(III) and selenium(IV) in aqueous solutions is shown in Fig. 2. The results clearly demonstrate that the sensitivity of the arsenic determination reaches a maximum at

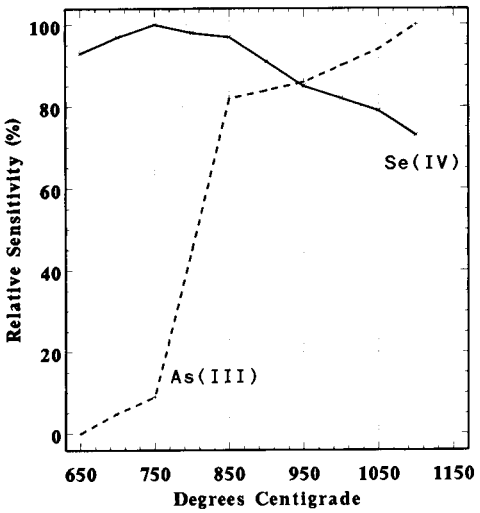


Fig. 2. Relative sensitivity of the absorbance for Se(IV) and As(III) as different temperatures.

1100°C and perhaps could even be increased slightly at higher temperatures, whereas the maximum sensitivity for selenium determination appears between 750 and 850°C. This again emphasizes the importance of adjusting the correct and optimized temperature for each element. Only electrically heated atomization cells offer this possibility; the temperature of a gaseous flame cannot be regulated properly.

The calibration graphs established with aqueous solutions were linear within the range 0.5–100 ng absolute for both arsenic and selenium.

The standard measuring conditions for the AAS instrument were as follows: source, hollow-cathode lamp; lamp current, As 13 mA, Se 8 mA; lines, As 193.7 nm, Se 196.0 nm; measurement mode, AAS (conc.); signal mode, sample; calculation mode, peak height; calculation time 20 s; delay time, 5 s; and time constant 0.05 s. Those for the hydride system were as follows: purge gas, argon; purge time, 45 s; flow-rate, 400 ml $min^{-1}$; $NaBH_4$ addition, 30 s; total volume of added $NaBH_4$, 3.0 ml; total volume, 15 ml; and temperature, As 1100°C, Se 750°C.

## RESULTS AND DISCUSSION

The sensitivity of arsenic and selenium determinations could be increased considerably by

rinsing the quartz cell with 40% hydrofluoric acid for about 15 min. Figure 3 shows the peaks of the atomization signals for 5 ng of arsenic (A) before and (B) after cuvette conditioning. A clearly improved performance, with an increased peak height and a narrower shape, can be observed. The cuvette treatment had to be repeated after ca. 100 measurements in order to maintain the high sensitivity. The same cuvette has been used for 2 years without any decrease in sensitivity. Additionally, it was possible to demonstrate the importance of optimum atomization temperatures for different elements to obtain the maximum atomization signals without the necessity for mixing oxygen or air with the purge gas stream. In further studies it is intended to define proper decomposition temperatures for all hydride-forming elements.

The accuracy of the method was evaluated by analysing standard reference materials, five samples of NIST SRM 1577a Bovine Liver for arsenic and five samples of Seronorm Trace Element Serum (batch No. 116) for selenium. Three determinations were performed for each sample. Reagent blanks were processed with the samples. The detection limit of the method for both elements (three times the standard deviation of the blank) was 0.3 ng absolute in a 15-ml sample volume or 0.02 $\mu g\ l^{-1}$. The results are summarized in Table 1. These results, obtained by calculation of blank-corrected data, and recovery studies (Table 2) performed simultaneously, illustrate the high precision and reproducibility of the proposed digestion and analysis method. The application of recommended reduction procedures prior to hydride generation for As(V) and Se(VI) [37,38] showed no differences in the results compared with untreated samples. As no interference effects could be observed, the standard addition method was not required.

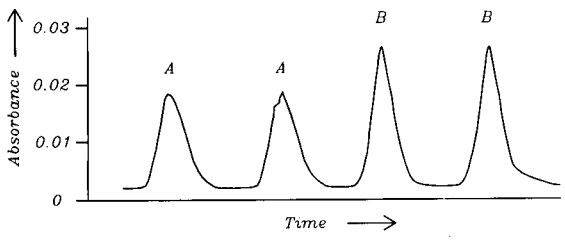


Fig. 3. Absorption peaks for 5 ng of As (A) before and (B) after cuvette conditioning.

TABLE 1

Analysis of NIST SRM 1577a Bovine Liver for As and Seronorm Trace Element Serum (batch No. 116) for Se, based on generation of hydrides from 1-ml sample volumes

| As in bovine liver ($ng\ g^{-1}$) [a] | Se in blood serum ($ng\ ml^{-1}$) [b] |
|---|---|
| 43.5 ± 2.1 | 100.4 ± 5.2 |
| 46.1 ± 2.4 | 94.2 ± 3.6 |
| 47.3 ± 3.2 | 103.1 ± 3.1 |
| 50.3 ± 2.8 | 95.7 ± 4.4 |
| 48.9 ± 2.3 | 105.5 ± 5.0 |

[a] Certified content 47 ± 6 ng $g^{-1}$. [b] Certified content 100 ± 6 ng $ml^{-1}$.

The measuring sensitivity of the hydride generation technique depends strongly on the atomization temperature and the state of the cuvette surface, where atomization of the element hydride occurs. In order to maintain the quartz surface in an optimum state, it is essential to use a system that permits periodic cuvette treatment. Neither laboratory-made heating blocks nor commercially available electrically heated hydride systems offer this possibility and once the tube is covered with contaminants the entire heating unit has to be disassembled in order to clean the cuvette. With the present heating block, however, this problem has been solved and cleaning or conditioning procedures can be done easily and quickly, guaranteeing precise analytical results for long periods of time. Optimum decomposition temperatures for different element hydrides can

TABLE 2

As(III) and Se(IV) recoveries

| As(III) | | | Se(IV) | | |
|---|---|---|---|---|---|
| Added (ng) | Found (ng) | Recovery (%) | Added (ng) | Found (ng) | Recovery (%) |
| 5 | 5.2 | 104 | 10 | 9.7 | 97.0 |
| 5 | 5.4 | 108 | 10 | 9.5 | 95.0 |
| 5 | 4.8 | 96 | 30 | 33.0 | 110.0 |
| 10 | 9.1 | 91 | 30 | 28.4 | 94.7 |
| 10 | 10.5 | 105 | 50 | 49.6 | 99.2 |
| 10 | 9.7 | 97 | 50 | 48.3 | 96.6 |

be adjusted exactly with the continuously variable low-voltage transformer. Another advantage of this system is its inexpensive and safe operation. It is easy to combine with any available classical hydride generation system, especially the recently developed flow injection–hydride generation systems. As it can be heated to 1100°C, periodic annealing of the quartz tube is possible, even during the operation of an autosampler. Other determination methods such as the mercury cold vapour technique can be performed without changing the equipment. Finally, the simple fitting of the block on the burner head also permits an easy change to flame measurement.

Further, it has been demonstrated that microwave digestion of organic samples can be performed quickly and reliably without the use of expensive microwave dissolution systems. Only a few modifications turned a simple household microwave oven into a proper working digestion system. It may be applied for routine application to digest any kind of biological sample. With these improvements in the hydride generation technique and microwave digestion, simple and cheap analytical tools to determine essential trace elements at very low concentrations have been developed.

More detailed information and technical descriptions are available on request from the authors.

The authors thank Siegfried Schwab for helpful suggestions and technical assistance.

REFERENCES

1 W. Hartfiel and W. Schulte, Akt. Ernährungsmed., 13 (1988) 77.
2 G. Ohlenschläger, paper presented at Biosynposia Symposium, Stuttgart, 1988.
3 A. Peretz, paper presented at Biosynposia Symposium, Stuttgart, 1988.
4 T. Zimmermann, paper presented at IVth Stuttgarter Mineralstoffsymposium, Stuttgart, 1991.
5 C. Ip, Ann. Clin. Res., 18 (1986) 22.
6 R. Shamberger, J. Natl. Cancer Inst., 44 (1970) 931.
7 G.N. Schrauzer, Bioinorg. Chem., 9 (1978) 245.
8 G.N. Schrauzer, Münch. Med. Wochenschr., 43 (1985) 731.
9 Ch. Witting, U. Witting and V. Krieg, Cancer Res. Clin. Oncol., 104 (1982) 109.
10 M. Marshall, Cancer Lett., 7 (1979) 331.
11 M. El-Bagiarmi, H. Ganther and M. Sunde, Rev. Toxicol. Environ. Sci., 8 (1980) 585.
12 D.V. Frost, in M. Anke, H.J. Schneider and Ch. Brückner (Eds.), Proceedings des 3. Spurenelement Symposiums, Arsen, Jena, 1980.
13 F.H. Nielsen and E.O. Uthus, in E. Frieden (Ed.), Biochemistry of the Essential Trace Elements, Plenum, New York, 1984, p. 319.
14 M.O. Andreae, J.F. Asmode, P. Foster and L. Van't Dack, Anal. Chem., 53 (1981) 1766.
15 S.N. Willie, R.E. Sturgeon and S.S. Berman, Anal. Chem., 58 (1986) 1140.
16 B. Welz, Atomic Absorption Spectrometry, VCH, Weinheim, 1985, p. 69.
17 D. Siemer, P. Koteel and V. Jariwala, Anal. Chem., 48 (1976) 836.
18 K.C. Thompson and D.R. Thomerson, Analyst, 99 (1974) 595.
19 B. Welz and M. Melcher, Analyst, 108 (1983) 213.
20 F.D. Pierce, T.C. Lamoreaux, H.R. Brown and R.S. Fraser, Appl. Spectrosc., 30 (1976) 38.
21 P. Vian and G.R. Wood, Talanta, 23 (1976) 89.
22 T. Tsuda, M. Wada, S. Aoki and Y. Matsuit, J. Assoc. Off. Anal. Chem., 71 (1988) 373.
23 B. Welz and M. Melcher, Wasser, 59 (1982) 407.
24 M. Melcher and B. Welz, Applied Atomic Absorption Spectroscopy, Bodenseewerk Perkin-Elmer, Überlingen, 1980, p. 22.
25 H.W. Sinemus, M. Melcher and B. Welz, At. Spectrosc., 2 (1981) 81.
26 F.D. Pierce and H.R. Brown, Anal. Chem., 48 (1976) 693.
27 M. Verlinden and H. Deelstra, Fresenius' Z. Anal. Chem., 296 (1979) 253.
28 B. Welz and M. Melcher, Anal. Chim. Acta, 131 (1981) 17.
29 B. Welz and M. Melcher, Applied Atomic Absorption Spectroscopy, Bodenseewerk Perkin-Elmer, Überlingen, 1983, p. 32.
30 J. Dědina and I. Rubeška, Spectrochim. Acta, Part B, 35 (1980) 119.
31 W.H. Evans, F.J. Jackson and D. Dellar, Analyst, 104 (1979) 16.
32 M. Verlinden, Anal. Chim. Acta, 140 (1982) 229.
33 D.B. Hartfield, Anal. Chem., 59 (1987) 1887.
34 R.C. Chu, G.P. Barron and A.W. Baumgarner, Anal. Chem., 44 (1972) 1476.
35 S. Caroli, E. Beccaloni, L. Fornarelli, P. Delle Femmine, M. Mancini, M. Gallorini and Gy. Zaray, Acta Chim. Hung., 128 (1991) 507.
36 H.M. Kingston and L.B. Jassie, Anal. Chem., 58 (1986) 2534.
37 R. Glaubig and S. Goldberg, Soil Sci. Soc. Am. J., 52 (1988) 536.
38 B. Welz and M. Melcher, Wasser, 62 (1984) 137.

*Analytica Chimica Acta*, 268 (1992) 323–329
Elsevier Science Publishers B.V., Amsterdam



# Efficiency and mechanism of macroporous poly(vinylthiopropionamide) chelating resin for adsorbing and separating noble metal ions and determination by atomic spectrometry

Zhixing Su, Xijun Chang, Keli Xu, Xingyin Luo and Guangyao Zhan

*Department of Chemistry, Lanzhou University, Lanzhou 730000, Gansu (China)*

(Received 25th November 1991; revised manuscript received 2nd April 1992)

**Abstract**

A macroporous poly(vinylthiopropionamide) chelating resin was synthesized from spherical poly(vinyl chloride) resin particles and used for the enrichment and separation of trace noble metal ions. Trace Au(III), Pt(IV) and Pd(II) in sample solutions can be enriched quantitatively in the range 5 M HCl–pH 9 with recoveries $> 96\%$, and the recovery of trace Ir(IV) at pH 1–9 was $> 93\%$; however, the adsorption of Rh(III) and Ru(III) at pH 3–6 was $< 16\%$. When Au, Pt, Pd and Ir ions were adsorbed by the resin at a flow-rate of 4 ml $min^{-1}$, the recoveries of Au, Pt, Pd eluted with 6% thiourea–1 M HCl and Ir with 6 M HCl were $> 96\%$. The adsorption capacity of the resin was 978 mg $g^{-1}$ for Au, 288 mg $g^{-1}$ for Pt, 455 mg $g^{-1}$ for Pd and 10 mg $g^{-1}$ for Ir. When the resin was reused ten times, the recoveries of the above ions on enrichment were still $> 92\%$ and a 100-fold excess of other ions caused little interference in the determination of the ions. The eluted ions were determined by inductively coupled plasma atomic emission spectrometry (ICP-AES). The lowest concentrations determined were 0.040 $\mu g$ $ml^{-1}$ for Au, Pt and Pd and 0.020 $\mu g$ $ml^{-1}$ for Ir. The contents of Au and Ir in non-ferrous metals determined by preconcentration followed by Zeeman-effect atomic absorption spectrometry or ICP-AES were in good agreement with the certified values. The structures of the resin, investigated by Fourier transform IR spectrometry and electron spectroscopy revealed that Au, Pt and Pd ions were chelated mainly with the thioketo form of the thiopropionamide group in the resin, forming a quadridentate chelate.

*Keywords:* Atomic emission spectrometry; Inductively coupled plasma spectrometry; Sample preparation; Chelating resins; Gold; Iridium; Palladium; Platinum; Preconcentration

The preconcentration and separation of noble metal ions by ion-exchange [1–6] and reversed-phase extraction chromatography [7–15] have been reported. However, the selectivity of the former for noble metal ion adsorption was not good and showed a low adsorption capacity and the latter procedure was time consuming and inconvenient. A series of spherical macroporous polystyrene chelating resins can selectively adsorb noble metal ions [16–23], but their synthesis generally requires chloromethylation, which is problematic. We have synthesized macroporous poly(vinylethylenediamine), poly(vinyldiethylenetriamine), poly(vinylpropionamide oxime) and poly(vinylamidine thiocyanatothiourea) chelating resins by using spherical poly(vinyl chloride) resin (PVC), and used them succesfully for adsorbing and separating trace elements from various matrices [24–28].

*Correspondence to:* Xijun Chang, Department of Chemistry, Lanzhou University, Lanzhou 730000, Gansu (China).

In this paper, after a poly(vinylcyanoethyl) resin had been synthesized from PVC [27], a macroporous poly(vinylthiopropionamide) chelating resin (PVTPA) was synthesized there from and used to enrich and separate noble metal ions from non-ferrous matrices. Inductively coupled plasma atomic emission spectrometry (ICP-AES) was used to investigate the efficiency of the resin for noble metal ion adsorption, e.g., the acidity, the flow-rate, the regeneration, the capacity, the precision, the interference of other ions and the conditions of desorbing these ions from the collector were studied. Zeeman-effect atomic absorption spectrometry (Z-AAS) was used to detect the ions separated by the resin from real samples containing non-ferrous matrices with reliable results. Fourier transform (FT) IR spectrometry and electron spectroscopy were used to study the structures of the resin and a chelating mechanism was elucidated.

## EXPERIMENTAL

### *Instruments and apparatus*

An ICP/6500 inductively coupled plasma spectrometer (Perkin-Elmer), a Z 180-80 polarized Zeeman-effect atomic absorption spectrometer (Hitachi), a Model 170-SX FT-IR spectrometer (Nicolet), a Model PHI-550 multi-functional electron spectrometer (Perkin-Elmer), a Model 1106 elemental analyzer (Carlo Erba) and a four-necked flask for synthesizing the chelating resin were used. The adsorption column was a glass tube (12 cm × 0.5 cm i.d.; 0.15 cm i.d. at the lower end) containing 0.2 g of chelating resin, immersed in high-purity water overnight, and into which a small pad of absorbent cotton-wool was introduced beforehand.

### *Reagents and standards*

High-purity reagents were used in all experiments. Stock solutions of 1 mg $ml^{-1}$ Au, Pt, Pd and Ir were prepared by dissolving spectroscopically pure $HAuCl_4 \cdot 4H_2O$, $(NH_4)_2PtCl_6$, $PdCl_2$ and $(NH_4)_2IrCl_6$ in dilute HCl. They were diluted and mixed to give stock standard solutions of 8–40 $\mu g$ $ml^{-1}$ of Au, Pt and Pd and 4–40 $\mu g$ $ml^{-1}$ of Ir (1 M HCl).

### *Synthesis of chelating resin*

According to previous work [27], a poly(vinylcyanoethyl) resin (PVCE) containing 16.03% N was synthesized by the reaction of spherical PVC resin particles with ethylenediamine and cyanoethylene. PVCE (10 g), thioacetamide (25 g) and dimethylformamide (DMF) (30 ml) were mixed in a four-necked flask. Dry hydrogen chloride gas was passed into the flask and refluxed for 4 h at 118°C. The resin was then washed with 0.2 M NaOH, distilled water and 5% HCl in that order until $S^{2-}$ was no longer detected. Finally, the resin was extracted for 4 h with acetone and high-purity water and dried under IR radiation. Thus, a macroporous PVTPA chelating resin was obtained with the possible structure shown:

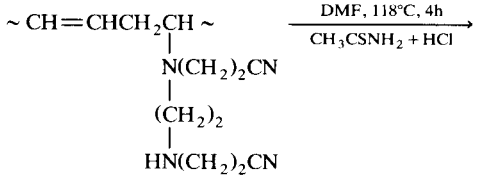


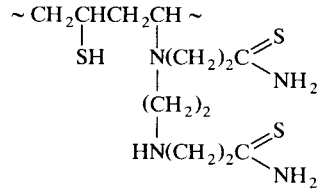


The contents of sulphur and nitrogen in the PVTPA resin measured with the elemental analyser were 15.2% and 12.6%, respectively. The average pore diameter and pore volume of the PVTPA resin determined by the mercury intrusion method [29] were 6.5 $\mu m$ and 0.514 $cm^3$ $g^{-1}$, respectively, and the specific suface area measured by the BET method [29] was 5.9 $m^2$ $g^{-1}$. The experiments showed that the PVTPA chelating resin was not dissolved in general organic solvents, its functional–analytical group was not destroyed at 140°C and the sulphur contents of the resin kept unused for 1 year or reused ten times were 15.01% and 14.8%, respectively.

*Analytical procedure*

Standard solution of Au, Pt, Pd and Ir or real sample solutions of non-ferrous matrices were prepared in clean vessels (200–500-ml samples). Subsequently, the samples were adjusted to the appropriate acidity or pH with HCl or Clark–Lubs buffer solution and were passed through the columns at controlled flow-rates (e.g., 3–4 ml $min^{-1}$). After elution of Au, Pt and Pd from the columns with 10 ml of mixed 6% thiourea–1 M HCl, and of Ir with 6 M HCl, Au, Pt, Pd and Ir in the eluates were determined by use of the ICP 6500 instrument (forward power 1100 W; viewing height 17 mm; argon plasma gas flow-rate 14 l $min^{-1}$, argon auxiliary gas flow-rate 0.4 l $min^{-1}$, argon nebulizer gas flow-rate 1.0 l $min^{-1}$; wavelengths, Au 201.200, Pt 214.423, Pd 229.651 and Ir 224.268 nm).

*Procedure for mineral sample analysis*

A 0.5-g amount of mineral sample was placed in a PTFE autoclave and 6 ml of concentrated $HNO_3$ and 2 ml of concentrated HF were added. The sealed sample was heated for 4 h in a thermostat at 270°C and was transferred on to a sand-bath. After the remainder of the HF had volatilized at a lower temperature, the sample was dissolved in 2 M HCl in a clean vessel. According to the above analytical procedure, the sample solution with non-ferrous matrices was enriched by the PVTPA resin and eluted from the column, and the noble metal ions in the eluate were detected by use of the Model 180-80 Z-AAS instrument (lamp current, Au 10.0, Pt 12.5, Pd 10.0 and Ir 12.5 mA; wavelengths, Au 242.795, Pt 265.945, Pd 247.642 and Ir 254.397 nm).

## RESULTS

*Influence of acidity on adsorption*

Figure 1 shows the effects of pH and acidity for adsorption of Au, Pt and Pd (0.040 $\mu g\ ml^{-1}$) and Ir (0.020 $\mu g\ ml^{-1}$) ions. The recoveries of trace Au, Pt and Pd in the range of 5 M HCl–pH 9 were > 96% and the recovery of trace Ir between pH 1 and 9 was > 93%. However, the

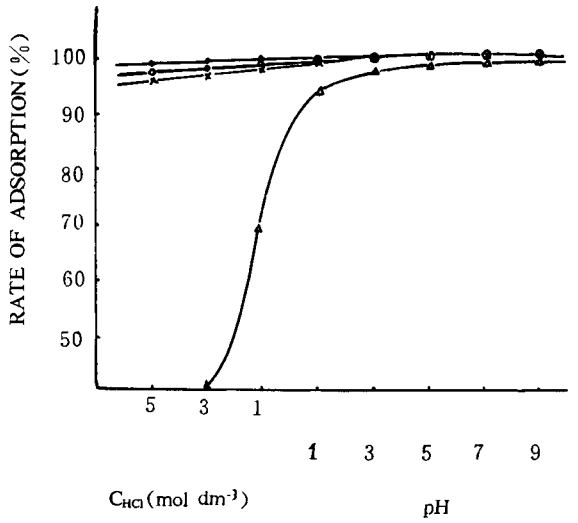


Fig. 1. Effect of acidity and pH on Au, Pt, Pd and Ir adsorption by the PVTPA resin. • = Au; × = Pt; ○ = Pd; △ = Ir.

recoveries for Rh(III), Ru(III) (0.20 $\mu g\ ml^{-1}$) at pH 3–6 were only 16%. Other ions [Cu(II), Zn(II), Cd(II), Ni(II), Co(II), Fe(III), Al(III), Ca(II), Mg(II), V(V), Cr(III), Mo(VI), Mn(II), Ga(III), In(III), Sb(III) and Pb(II)] were not adsorbed at pH ⩽ 3. Therefore, Au, Pt, Pd and Ir ions can be separated quantitatively from such ions by means of PVTPA resin by adsorption at PH ⩽ 3.

*Influence of flow-rate*

Figure 2 shows the recoveries of Au, Pt and Pd (in 1–2 M HCl medium) and Ir (at pH 2–3) at

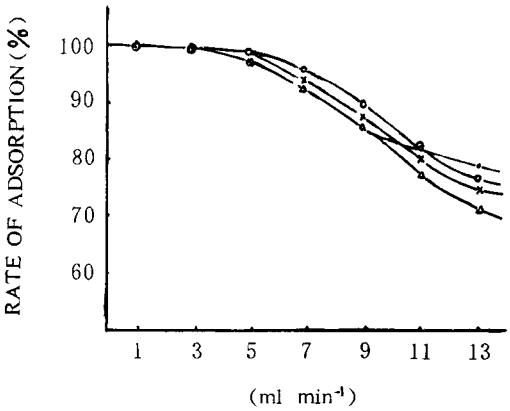


Fig. 2. Effect of flow-rate on Au, Pt, Pd and Ir enrichment. Symbols as in Fig. 1.

TABLE 1

Interference of other ions (10 $\mu$g ml$^{-1}$) on Au, Pt, Pd and Ir enrichment (recovery, %)

| Ions [a] | Cu(II) | Zn(II) | Ni(II) | Co(II) | Fe(III) | Al(III) | Ca(II) | Mg(II) |
|---|---|---|---|---|---|---|---|---|
| Au | 98.0 | 100 | 100 | 96.0 | 97.0 | 99.0 | 100 | 100 |
| Pt | 90.0 | 91.0 | 93.0 | 90.0 | 93.0 | 94.0 | 92.0 | 95.0 |
| Pd | 94.0 | 96.0 | 95.0 | 96.0 | 97.0 | 97.0 | 94.0 | 96.0 |
| Ir | 93.0 | 95.0 | 94.0 | 92.0 | 93.0 | 96.0 | 95.0 | 98.0 |

[a] The concentrations of Au, Pt and Pd ions were 80 ng ml$^{-1}$ and Ir ion 40 ng ml$^{-1}$.

different flow-rates. Obviously, trace Au, Pt and Pd (0.080 $\mu$g ml$^{-1}$) and Ir (0.040 $\mu$g ml$^{-1}$) ions can be enriched quantitatively at flow-rates $\leqslant 5$ ml min$^{-1}$ with the recoveries $\geqslant 96\%$.

*Desorption conditions*

Figure 3 shows the recoveries of Au, Pt and Pd ions (0.20 $\mu$g ml$^{-1}$) desorbed with 10 ml of different concentrations of thiourea in 1 M HCl from the columns and that of Ir ion (0.20 $\mu$g ml$^{-1}$) eluted with 10 ml of HCl of various concentrations from the resin (desorbing velocity 3 ml min$^{-1}$). Evidently, Au, Pt and Pd can be desorbed quantitatively by 10 ml of 6% thiourea–1 M HCl and Ir was eluted easily with 10 ml of 6 M HCl from the columns with recoveries > 96%.

*Interference of other ions*

Table 1 shows the effects of other ions on the adsorption of Au, Pt and Pd (0.080 $\mu$g ml$^{-1}$) and Ir (0.040 $\mu$g ml$^{-1}$) by PVTPA resin. It is clear that a 100-fold excess of foreign ions caused virtually no interference with the analytes.

*Adsorption capacity and regeneration*

A 0.1-g portion of PVTPA resin was placed in each of four conical flasks. A stock solution of Au, Pt, Pd and Ir was added to each flask and diluted to an equal volume, e.g., 100 ml (Au 1, Pt 0.3, Pd 0.5 and Ir 0.02 mg ml$^{-1}$). Their acidity was adjusted to 1–2 M HCl for Au, Pt and Pd and to pH 2–3 for Ir, shaking the mixtures on a vibrator. The concentrations of the above ions in the solution were measured by ICP-AES until equilibrium was reached. Thus, a statistically saturated adsorption capacity of the resin could be calculated to be 978 mg g$^{-1}$ for Au, 288 mg g$^{-1}$ for Pt, 455 mg g$^{-1}$ for Pd and 10 mg g$^{-1}$ for Ir. When Au, Pt and Pd (0.040 $\mu$g ml$^{-1}$) and Ir (0.020 $\mu$g ml$^{-1}$) ions in solutions containing other cations at the concentrations given in Table 1 were enriched repeatedly ten times with PVTPA resin according to the analytical procedure, the recoveries of these ions still were > 92%.

*Precision and accuracy*

Applying the above-selected conditions, trace Au, Pt and Pd (0.040 $\mu$g ml$^{-1}$) and Ir (0.020 $\mu$g ml$^{-1}$) ions added to each of seven portions of solutions of other ions as described in Table 1 were enriched simultaneously with PVTPA resin and were desorbed and determined. Their recoveries were > 97% and the relative standard deviations (R.S.D) were 2.5% for Au, 3.4% for Pt,

TABLE 2

Analytical results for real samples of non-ferrous smelter samples

| Element | Sample 1 [a] | | | Sample 2 [b] | | |
|---|---|---|---|---|---|---|
| | Found ± S.D. (ng ml$^{-1}$) | Given (ng ml$^{-1}$) | R.S.D. (%) | Found ± S.D. (ng g$^{-1}$) | Given (ng g$^{-1}$) | R.S.D. (%) |
| Au | – | – | – | 86.9 ± 1.6 | 86.7 | 1.9 |
| Ir | 24.1 ± 0.3 | 24.4 | 1.3 | – | – | – |

[a] Solution sample from a non-ferrous smelter was measured five times by ICP-AES in combination with a column procedure.
[b] Mineral sample from a smelter was measured five times by Z-AAS in combination with a column procedure.

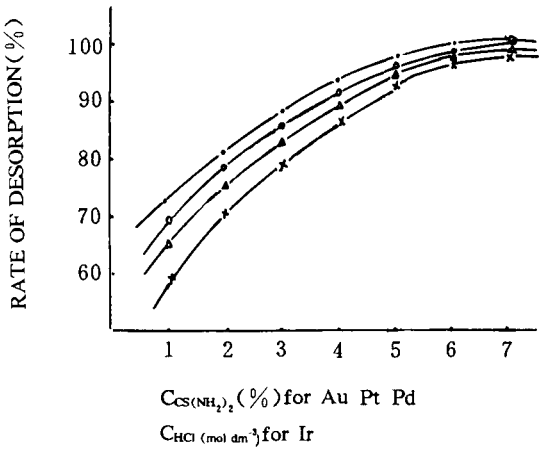


Fig. 3. Recovery of Au, Pt and Pd desorbed by thiourea and Ir eluted with HCl from a PVTPA column. Symbols as in Fig. 1.

2.8% for Pd and 4.2% for Ir, as measured by ICP-AES. The analytical results for a real sample solution and a mineral sample from a non-ferrous smelter based on a column procedure, given in Table 2, showed that the concentrations of Au and Ir in the real samples measured by the proposed procedure agreed closely with the data given by the smelter operator.

## DISCUSSION

Figure 4 shows the IR spectra of PVTPA resin alone and saturated with Au, Pt and Pd ions. According to other workers [30,31], the peaks in Figure 4 (1) can be analysed as follows: 3383 $cm^{-1}$, $\nu$(N–H); 2924 $cm^{-1}$, $\nu$(C–H); 2590 $cm^{-1}$, $\nu$(S–H); 1629 $cm^{-1}$, $\delta(NH_2)$ and $\nu$(C=C); 1429 $cm^{-1}$, $\delta$(C–H); 1372 $cm^{-1}$, $\nu$(C–N) of $CSNH_2$; 1295 $cm^{-1}$, $\nu$(C–N) and $\delta$(NH); 1224 $cm^{-1}$, $\nu$(C=S); 1038 $cm^{-1}$, $\nu$(C–N); 772 $cm^{-1}$, $\delta$(N–H) and $\nu$(C–Cl) (remaining 1% of Cl). On comparing traces 2, 3 and 4 with 1 in Fig. 4, it can be seen that the peak at 1224 $cm^{-1}$ of $\nu$(C=S) was displaced 15–17 $cm^{-1}$ towards lower wavenumbers after Au, Pt and Pd ions had been adsorbed by PVTPA resin. This was because of coordination of the lone-pair electron of the sulphur in C=S with the vacant orbital of Au, Pt or Pd ion [32]. However, the peak at 3383 $cm^{-1}$ of $\nu$(N–H) was displaced 20–29 $cm^{-1}$ towards higher frequency, which was due to the coordination of the lone-pair electron of the nitrogen in N–H with each ion [30]. The appearance of the peak at 876 $cm^{-1}$ of $\nu$(C=S) [32] resulted from the coordination of sulphur with Pt and Pd, transforming the imine-thiol (HN=CSH) form to the thioketo form ($H_2NC$=S) [33]. The new peak near 320 $cm^{-1}$ also resulted from the combination of Au, Pt and Pd with sulphur, nitrogen and chlorine [34,35]. Accordingly, the chelate structure formed from PVTPA resin with Au, Pt or Pd (M) ions may be written as

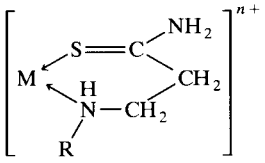


Figures 5 and 6 show parts of the electron spectra of PVTPA resin saturated with Au, Pt

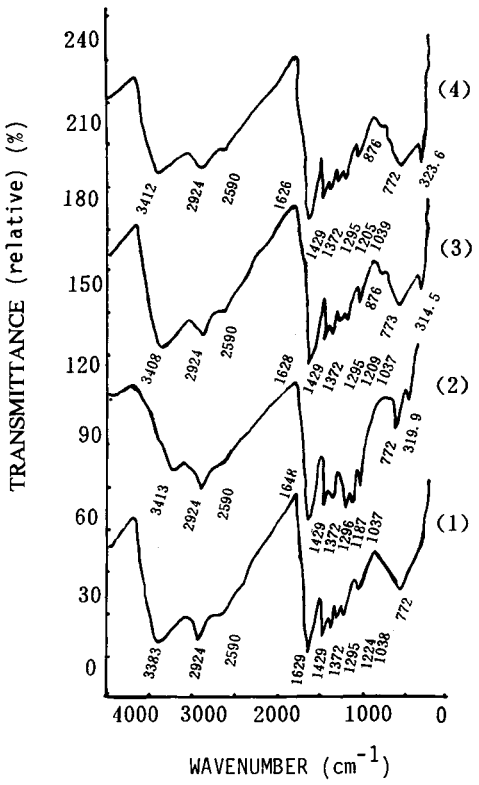


Fig. 4. IR spectra: (1) chelating resin; (2) with adsorbed Au; (3) with adsorbed Pt; (4) with adsorbed Pd.

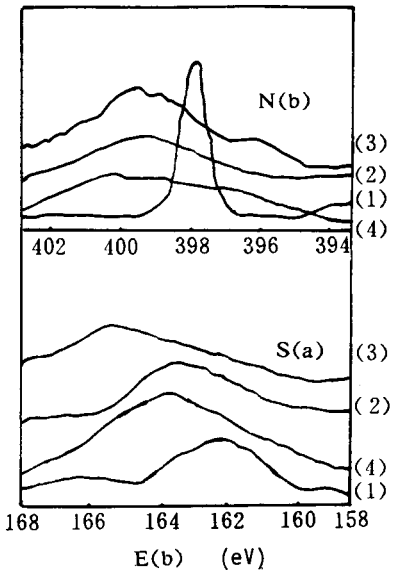


Fig. 5. Parts of ESCA scanning pattern of (a) S and (b) N: (1) chelating resin; (2) with adsorbed Au; (3) with adsorbed Pt; (4) with adsorbed Pd.

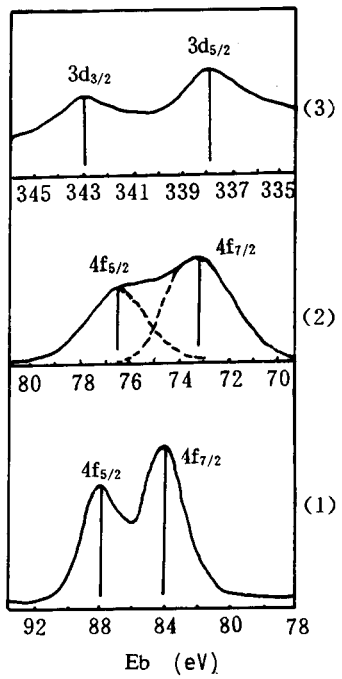


Fig. 6. Parts of ESCA scanning pattern of PVTPA resin after adsorbing (1) Au, (2) Pt and (3) Pd.

and Pd and the chemical displacement values (changed values of inner electronic binding energy, $E_b$) are given in Table 3. The results can be discussed as follows.

After Au, Pt and Pd ions had been adsorbed by the PVTPA resin, the $E_b$ values of the S(2p) orbit of the sulphur atom were increased by 1.6–3.4 eV, the M–S bond formation weakening the shielding effect of the S(2p) orbit, resulting in a decrease in the electronic cloud density around the sulphur nucleus. Moreover, the $E_b$ values of the N(1s) orbit of the nitrogen atom were increased by 1.6–2.3 eV as a result of the coordination of the nitrogen atom in N–H with Au, Pt and Pd ions.

The two sharp peaks that correspond with the $4f_{5/2}$ and $4f_{7/2}$ energy states after Au ion adsorption on the PVTPA resin arise from partial reduction of Au(III) to Au(0) [36,37] by the thiol form of the resin.

After Pt(IV) ion had been adsorbed by the PVTPA resin, the $E_b$ value (73.4 eV) of one of the two overlapping peaks that corresponds to the $4f_{7/2}$ state was in good agreement with the $E_b$ value (72.0–74.0 eV) of the Pt(II) complex given in [38]. The result revealed also that the thiol function reduced some Pt(IV) to Pt(II) prior to chelate formation [39]. Similarly, two peaks were separated by 4.9 eV (correlated with $3d_{3/2}$ and $3d_{5/2}$ energy states) after Pd(II) adsorption and chelation [39].

On the basis of the above discussion, the structure of the chelates of Pt(II) and Pd(II) with PVTPA resin can be expressed as follows (where M = Pt or Pd):

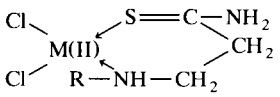


The mechanism of chelation of Au(III) and Pt(IV) with PVTPA resin requires further study because of the complicated structures.

## *Conclusion*

A macroporous PVTPA chelating resin was synthesized in a simple manner and shows good chemical and mechanical stability. Separation of Au, Pt, Pd and Ir ions from other ions can be

TABLE 3

Inner electronic binding energy ($E_b$) of the elements in PVTPA resin before and after adsorbing Au, Pt and Pd

| Atom (electronic orbit) | $E_b$(eV) | | | |
|---|---|---|---|---|
| | PVTPA | PVTPA –Au | PVTPA –Pt | PVTPA –Pd |
| C(1 s orbit) | 284.6 | 284.6 | 284.6 | 284.6 |
| N(1 s orbit) | 397.9 | 399.5 | 399.7 | 400.2 |
| S(2 p orbit) | 161.8 | 163.4 | 165.2 | 163.8 |
| Metal ion (bonding orbital) | – | 84.2 | 73.4 | 337.9 |
| | – | 87.9 | 76.7 | 343.0 |

achieved by applying a reliable column procedure. The proposed procedure reveals considerable advantages in convenient operation, low interferences, large adsorption capacity, high selectivity and good precision and accuracy for Au, Pt, Pd and Ir. Pt(II) and Pd(II) chelate via the sulphur and nitrogen atoms of the thioketo form of the PVTPA functional groups.

The authors express appreciation to Miss Min Sun and Mr. Xi-bai Zhao for their help with the experimental work.

REFERENCES

1 W.M. Macnevin and E.S. Mckay, Anal. Chem., 29 (1957) 1220.
2 E. Blasius and D. Rexin, Fresenius' Z. Anal. Chem., 179 (1961) 105.
3 J.G. Sen Gupta and F.E. Beamish, Am. Mineral., 18 (1963) 379.
4 L.N. Moskvin and B.K. Preobrazhenskii, Radiokhimiya, 6 (1964) 237.
5 J. Korkisch and H. Klakl, Talanta, 15 (1968) 339.
6 K. Brajter, K. Kleyny and Z. Vorbrodt, Talanta, 27 (1980) 433.
7 C. Pohlanadt and T.W. Steele, Talanta, 19 (1972) 839.
8 T. Braun and A.B. Farag, Anal. Chim. Acta, 65 (1973) 115.
9 G.A. Kanert and A. Chow, Anal. Chim. Acta, 69 (1974) 355.
10 K. Brajter and K. Slonawska, Talanta, 30 (1983) 471.
11 G.-M. Bao and W.-T. Gan, Fenxi Huaxue, 6 (1978) 428.
12 X.-E. Yu and S.-F. Li, Fenxi Huaxue, 9 (1981) 432.
13 L.-Y. Li and X.-W. Xu, Huaxue Shiji, 5 (1983) 205.
14 L.-Y. Li, X.-W. Xu and Y.-M. Sun, Huaxue Shiji, 5 (1983) 367.
15 I. Markova, Fresenius' Z. Anal. Chem., 332 (1988) 11.
16 G. Koster and G. Schmuckler, Anal. Chim. Acta, 38 (1967) 179.
17 G.V. Myasoedova, I.I. Antokol, L.I. Bolshakova, F.I. Danilova, I.A. Fedotova, E.B. Varshl, E.E. Rakovskii and S.B. Savvin, Zh. Anal. Khim., 37 (1982) 1837.
18 G.V. Myasoedova, I.I. Antokolskaya and S.B. Savvin, Talanta, 32 (1985) 1105.
19 S. Siddhanta and H.R. Das, Talanta, 32 (1985) 457.
20 X. Lin, W.-Z. Chen, G.-J. Hao, Y.-Z. Yang and B.-L. He, Ion Exchange Adsorption, 2 (1986) 1.
21 S.-T. Wang, W.-Z. Chen and B.-L. He, Chem. J. Chin. Univ., 8 (1987) 81.
22 L.-Y. Li, Y.-Q. Zhou, Z. Yin and S.-T. Wang, Fenxi Huaxue, 15 (1987) 297.
23 N.M. Kuz'min and V.Z. Krasil'shchick, Zh. Anal. Khim., 43 (1988) 1349.
24 X.-J. Chang, Z.-X. Su, G.-Y. Zhan and X.-Y. Luo, Acta Chim. Sin., 48 (1990) 157.
25 X.-J. Chang, Y.-F. Li, X.-Y. Luo, G.-Y. Zhan and Z.-X. Su, Anal. Chim. Acta, 245 (1991) 13.
26 X.-J. Chang, X.-Y. Luo and Z.-X. Su, Chem. J. Chin. Univ., 9 (1988) 574.
27 Z.-X. Su, D.-R. Cao and Z.-C. Zhang, Ion Exchange Adsorption, 4 (1988) 454.
28 Z.-X. Su, X.-J. Chang, G.-Y. Zhang and X.-Y. Luo, Microchem. J., 44 (1991) 78.
29 B.-L. He and Z.-Q. Shi, Ion Exchange Adsorption, 3 (1987) 44.
30 Q.-N. Dong, IR Spectral Methods, Publishing House of Chemical Industry, Beijing, 1979, pp. 104–196.
31 M. Hironori and E. Hiroaki, Anal. Chim. Acta, 162 (1984) 339.
32 H.G.R. Burns, Inorg. Chem., 7 (1968) 278.
33 S.K. Sengupta, S.K. Sahni and R.N. Kapoor, Acta Chim. Acad. Sci. Hung., 104 (1980) 89.
34 J.R. Allkins and P.J. Hendra, J. Chem. Soc. A, 8 (1967) 1325.
35 K. Nakmoto, IR and Raman Spectroscopy of Inorganic and Coordination Compounds, translated by D.-R. Huang and R.-Q. Wang, Publishing House of Chemical Industry, Beijing, 1986, pp. 350–361.
36 G. Johansson, J. Hedman, A. Berndtsson, M. Klasson and R. Nidlsson, J. Electron Spectrosc., 2 (1973) 295.
37 J.C. Fuggle, E. Kallne, L.M. Watson and D.J. Fabian, Phys. Rev. B, 16 (1977) 750.
38 J. Escard, B. Pontvianne and J.P. Contour, J. Electron Spectrosc., 6 (1975) 17.
39 V.I. Nefedov, I.A. Zakharova, I.I. Mioseev, M.A. Poraikoshits, M.N. Vorgaftik and A.P. Belov, Zh. Neorg. Khim., 18 (1973) 3264.

*Analytica Chimica Acta*, 268 (1992) 331–345
Elsevier Science Publishers B.V., Amsterdam



# Effects of pH, temperature and reaction products on the performance of an immobilized creatininase–creatinase–sarcosine oxidase enzyme system for creatinine determination

Henning Sakslund and Ole Hammerich

*Department of Chemistry, The H.C. Ørsted Institute, University of Copenhagen, Universitetsparken 5, DK-2100 Copenhagen Ø (Denmark)*

(Received 18th March 1992)

**Abstract**

The effects of pH, temperature ($t$) and reaction products on the performance of enzyme reactors containing immobilized creatininase (CA), creatinase (CI) and sarcosine oxidase (SO) for the determination of creatinine were studied by flow-injection analysis with amperometric detection of the resulting hydrogen peroxide. The optimum performance of the coupled enzyme system was found at pH 7.7 and 25°C. Some of the CI and SO activity was lost irreversibly at $t \geqslant 30$°C. In contrast, the activity of CA increased reversibly with $t$ up to at least 40°C. The effects of the reaction products on the enzyme activities were examined. Glycine caused the CA activity to increase and the SO activity to decrease, whereas the CI activity was unaffected by this compound. Sarcosine caused a decrease in the CI activity. The activities of all three enzymes were insensitive towards the presence of formaldehyde and urea and so was the activity of SO in the presence of creatine and hydrogen peroxide. The fraction, $\alpha$, of the injected creatinine (or creatine) equilibrated by the CA reactor is introduced as a quantitative measure of the CA activity, and was between 10 and 72% depending on the enzyme loading. The unused immobilized enzymes were found to maintain their activity for at least 6 months. When in heavy daily use, CA and SO lost ca. 25% of the activity over a period of 20–30 days, whereas the activity of CI was found to be essentially unchanged.

*Keywords:* Enzymatic methods; Flow injection; Creatinine

Creatinine is the final product of creatine metabolism in mammals [1,2]. The daily creatinine production rate, which amounts to ca. 2% of the whole body creatine, is only slightly affected by factors such as sepsis, trauma, fever, the state of hydration or dietary changes, and for this reason the creatinine clearance has become of clinical importance as a valuable index of the renal glomerular filtration rate [1,2]. The reference ranges for serum/plasma creatinine and urine creatinine are 35–140 $\mu$M and 71–265 $\mu$mol $d^{-1}$ $kg^{-1}$, respectively [3,4], but during kidney dysfunction or muscle disorder the creatinine concentration in serum/plasma may rise to values higher than 1000 $\mu$M [5].

The creatinine concentration is still often determined by the Jaffe reaction [6,7], in which creatinine by virtue of the active methylene group reacts with alkaline sodium picrate to give a red–yellow complex. However, the Jaffe reaction possesses a number of analytical shortcomings resulting in inaccurate determination of creatinine, a major problem being that alkaline picrate is not specific towards creatinine but reacts with a

*Correspondence to:* O. Hammerich, Department of Chemistry, H.C. Ørsted Institute, University of Copenhagen, Universitetsparken 5, DK-2100 Copenhagen Ø (Denmark).

variety of other substrates having active methylene groups [1,8]. In addition, the interference from numerous compounds present or potentially present in serum/plasma and urine has been reported [1,9]. This has stimulated attempts to convert creatinine enzymatically to products that may be detected either spectrophotometrically or electrochemically [1,10,11].

One promising strategy involves the application of the three-enzyme system creatininase (CA)–creatinase (CI)–sarcosine oxidase (SO) by which creatinine is converted into hydrogen peroxide as shown in Fig. 1.

The serum/plasma concentration of creatine, the product of the first enzymatic conversion, is usually in the range 26–100 $\mu$M [4], but may, as creatinine, rise to more than 1000 $\mu$M under pathological conditions [5]. For this reason it is necessary either to remove creatine before the measurements are made or simultaneously to determine the creatine concentration in the sample. The detection of the resulting hydrogen peroxide is typically carried out by linking the enzyme system to a mixture of 4-aminophenazone and 2,4,6-tribromo-3-hydroxybenzoic acid, which in the presence of a fourth enzyme, peroxidase, results in the formation of a benzoquinone imine dye that may be detected spectrophotometrically [12–17]. Although a detection system based on these principles is commercially available (Boehringer), it appears to be too expensive and impractical for routine use because of the many reagents and the long time required [1]. A useful alternative may be a detection system in which the enzymes are immobilized and incorporated in a flow system.

There are only a few reports concerning the detection of creatinine by an immobilized CA–CI–SO enzyme system [18–21]. Successful attempts have been made to use the CA–CI–SO system in membrane electrodes with amperometric detection of either oxygen [18] or hydrogen peroxide [19,20]. In a different approach, the enzyme system was immobilized on controlled-pore glass (CPG) for the application in a flow-injection analysis (FIA) system [21]. The hydrogen peroxide concentration was determined by chemiluminescence resulting from the reaction with an alkaline reagent containing luminol and hexacyanoferrate(III). The creatinine detection limit

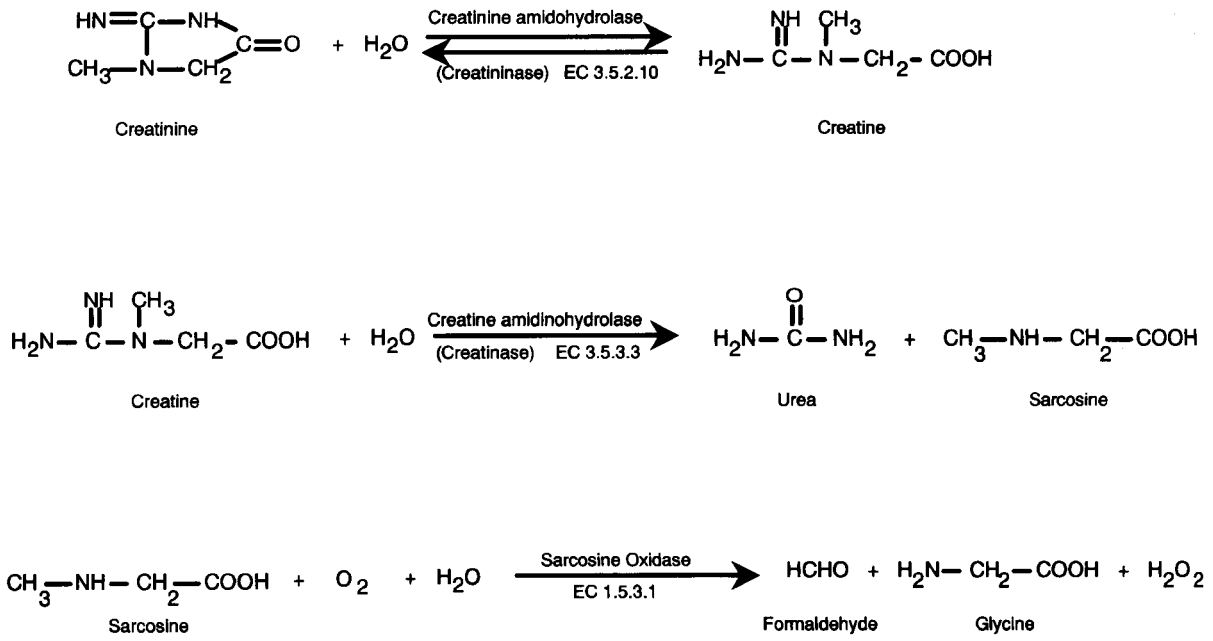


Fig. 1. Reaction scheme for the enzymatic determination of creatinine and creatine.

was reported to be 300 $\mu$M, which is above the clinical reference range (see above).

In order to develop further an immobilized CA–CI–SO system with amperometric detection of hydrogen peroxide, a study was initiated aimed at the evaluation of the effects of different parameters such as pH, temperature and reaction products on the performance of the enzyme system. This part of the experimental work was done using FIA with three successive reactors containing the enzymes separately. With this set-up it was possible to collect data for the single enzymes and to investigate the response of the overall enzyme system. Another FIA system capable of monitoring creatinine in the clinical useful concentration range was made by coimmobilization of the enzymes. This may be a useful alternative to the FIA systems using the traditional Jaffe reaction [22–24] or the four-enzyme method based on the conversion of creatinine to creatine phosphate with the consumption of reduced nicotinamide adenine dinucleotide, the decrease of which may be monitored spectrophotometrically [25].

## EXPERIMENTAL

### *Enzymes and chemicals*

The following enzymes and reagents were purchased from Sigma and were used as received: creatinine amidohydrolase (creatininase, E.C. 3.5.2.10, Cat. No. C-7399, lot 20H0349, from *Flavobacterium* sp.), creatine amidinohydrolase (creatinase, E.C. 3.5.3.3, Cat. No. C-7024, lot 64F06401, from *Flavobacterium* sp.), sarcosine oxidase (E.C. 1.5.3.1, Cat. No. S-7759, lot 89F1059, from *Corynebacterium* sp.), creatinine (C-4255), creatine (C-0780), sarcosine (S-9881), urea (U-5128), formalin (F-1635) (37% aqueous solution containing 10–15% methanol as a stabilizing reagent), glycine (G-7126), FAD (F-6625) and sodium phosphate (S-0876). Hydrogen peroxide was obtained from Merck (Perhydrol) as a 30% aqueous solution the actual concentration of which was determined regularly by titration with potassium permanganate solution. The concentration of the latter was determined by titration with sodium oxalate. All other chemicals were of analytical reagent grade. Redistilled water was used throughout.

Solutions of creatinine or creatine equilibrate slowly on standing. Therefore, fresh standard solutions of creatinine and creatine were prepared every second day.

### *Immobilization of enzymes*

The enzymes were immobilized on controlled-pore glass, CPG-10 (average pore size 700 Å, particle size 75–125 $\mu$m; Serva, Cat. No. 44771) by modification of a method described by Weetall [26]. The glass was cleaned by covering the particles with concentrated nitric acid for 2 h, then washed thoroughly with water on a G3 glass filter and finally dried at 95°C for 45 min and at 200°C for 6 h. The cleaned glass (1 g) was silanized by adding 50 ml of 10% (v/v) 3-aminopropyltriethoxysilane in toluene followed by heating at 100°C for 50 min. After washing on a G3 glass filter with 100 ml of toluene and 250 ml of 99.5% ethanol, the silanized glass was air dried at room temperature for 15 min and then dried at 120°C overnight. A small amount of the glass was treated with 3 drops of 3% 2,4,6-trinitrobenzenesulphonic acid in 1 ml of borax buffer, which gave rise to an orange colour indicating successful silanization. The silanized glass (1 g) was activated by adding 10 g of 2.5% (v/v) glutaraldehyde–0.1 M phosphate buffer (pH 7.0). The reaction was allowed to take place for 105 min, the first 35 min under reduced pressure in order to remove air from the glass pores. The pink glass so obtained was washed with 500 ml of water on a G3 glass filter. The enzymes to be immobilized were dissolved in 3.0 ml of 0.1 M phosphate buffer (pH 7.0) and added to the activated glass. The ratio of the weight of enzyme to weight of activated glass was 1 : 10, except for the CA reactor (see below). The mixture was allowed to react under reduced pressure for 60 min at room temperature and then stored overnight in a refrigerator. During this process the colour changed to pale violet. Amounts of 200 U (0.7143 mg) of CA, 200 U (23.81 mg) of CI and 100 U (22.73 mg) of SO were used during the experiment in which the enzymes were immobilized separately. For the

CA reactor, a ratio of weight of enzyme to weight of activated glass of 1:10 would result in only 7 mg of activated glass. This was found to be an uncomfortably small amount and instead 200 mg were used. The immobilization yields were 52%, 52% and 72%, respectively, as estimated from the absorbances at 280 nm of the enzyme solutions before and after immobilization. For the trienzyme reactor 300 U (1.0714 mg) of CA, 300 U (23.81 mg) of CI, and 100 U (22.73 mg) of SO were coimmobilized, and for the CI–SO bienzyme reactor the same amounts of CI and SO as for the trienzyme reactor were used. The total immobilization yields were 88% and 78%, respectively. Glutaraldehyde of grade 2 was used when the enzymes were immobilized separately and glutaraldehyde of grade 1 was used during the coimmobilization.

The immobilized enzymes were packed in separate pumping tubes (1.42 mm i.d., 100 $\mu$l volume). When not in use, the enzyme preparations were stored in phosphate buffer (pH 7.7) at 4°C.

*Flow-injection system*

The flow-injection manifold shown in Fig. 2A was used during the work with the separately immobilized enzymes and that in Fig. 2B for work with the coimmobilized enzyme systems. In both instances the manifold included a peristaltic pump (Ismatec, Type MS-REGLO), a six-port injection valve (Omnifit, Cat. No. 1106) with a 50 $\mu$l injection loop, two-shift valves (Omnifit, Cat. No. 1109) and a laboratory-made electrochemical cell connected to a potentiostat (Tacussel, Type PRG-DEL) equipped with a potentiometric recorder (Radiometer, REC 62 Servograph). The electrochemical cell was of the wall-jet type constructed after a design used by Moges and Johansson [27]. The working electrode was made from platinum and had a surface area of 0.79 mm$^2$. The auxiliary electrode was a platinum wire and a saturated calomel electrode (SCE) (Radiometer K401) served as the reference electrode. The working potential was +650 mV vs. SCE. The distance between the working electrode and the inlet channel was 0.5 mm. The components of the manifolds were connected by Microline tubing (0.51 mm i.d.) (Cole-Parmer) and the distances between the injection port and the first enzyme reactor and between the enzyme reactors were kept as short as possible in order to minimize sample dispersion. For the single-enzyme reac-

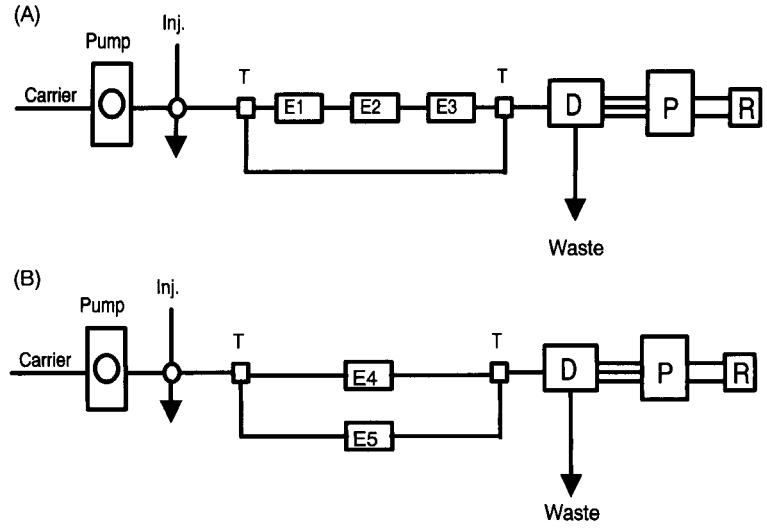


Fig. 2. FIA manifolds used during the work with (A) separately immobilized enzymes and (B) coimmobilized enzymes. T, shift valve; D, electrochemical wall-jet detector; P, three-electrode potentiostat; R, recorder; E1–E5, enzyme reactors containing immobilized CA (E1), CI (E2), SO (E3), coimmobilized CA, CI and SO (E4) and coimmobilized CI and SO (E5).

tors the dispersion coefficients [28] in the presence of three, two, one and no reactors in the flow stream were 7.0, 5.3, 3.6 and 1.8, respectively. For the bienzyme and trienzyme reactors the dispersion coefficients were 3.6 and 3.7, respectively. The carrier stream was a 0.1 M sodium phosphate buffer (pH 7.7). Deaeration was carried out by subjecting the buffer solution to aspirator vacuum. The samples to be injected were diluted to the desired concentration with this carrier in all instances. All measurements were made at room temperature if not stated otherwise.

When temperatures different from room temperature were needed, a mixing coil (1 m) was inserted in front of the enzyme reactors and the mixing coil and the reactors were then placed in a thermostated water-bath. The mixing coil ensured that the temperature of the carrier had acquired the temperature of the water-bath when reaching the enzymes. Another mixing coil (1 m) was inserted behind the reactors and placed in a separate water-bath held at room temperature to ensure that the temperature of the carrier was always the same when reaching the detector.

*Detector current*

The rate of the electrochemical oxidation of hydrogen peroxide, and hence the detector current, depend on the cell voltage, pH and temperature and may also be affected by the composition of the solution flowing through the cell. Except for the cell voltage, which was kept constant during the experiments, the pH, temperature and solution composition varied, and this had to be taken into account when the effects of these parameters on the performance of the enzyme reactors were examined.

In the experiments in which the temperature of the enzyme reactors was varied, the problem was easily solved by maintaining the detector at constant temperature (see above). In all other instances the effect of the reaction conditions on the efficiency of the hydrogen peroxide oxidation was monitored in separate experiments with standard solutions of hydrogen peroxide added to the substrate solutions. In these experiments the solutions bypassed the enzyme reactors. The hydrogen peroxide signal was found to be affected only by pH and the presence of formaldehyde. In those two instances the detector current observed for the substrate in question was normalized by the peak currents observed for the hydrogen peroxide solutions.

As discussed in detail later, the reactors were not operated under equilibrium conditions (CA) or with complete substrate conversion (CI and SO) and the detector current therefore depended also on the conversion efficiencies for the single enzymes. These were monitored throughout the experiments under steady-state conditions by injecting equivalent amounts of the corresponding substrates and, in separate experiments, hydrogen peroxide bypassing the enzyme reactors. The volume of the injection loop during these measurements was 2 ml in all instances. The results are given in the captions to the figures.

## RESULTS AND DISCUSSION

*Introductory studies*

Initially the specificity of the immobilized enzymes towards non-complementary substrates was investigated. The experiments showed that the reaction products urea, formaldehyde, glycine and hydrogen peroxide did not act as substrates for any of the enzymes and that the conversion of creatinine, creatine and sarcosine were catalysed only by the enzymes expected from the reaction scheme in Fig. 1. In addition, it was found that hydrogen peroxide was the only species in the reaction scheme that was electroactive at the applied working potential (+650 mV vs. SCE).

The effect of pH on the enzyme activity was studied in the range 6.8–8.8. Each time the pH of the carrier solution was changed the enzyme reactors were exposed to the new conditions for 30 min before any measurements were made. The results are summarized in Fig. 3.

It is seen that the activity of SO varies only slightly with pH in the range 7.6–8.2 with a maximum located at pH 7.8. This is similar to results reported for the same enzyme in solution, both SO isolated from *Corynebacterium* sp. [29]

and from other bacterial sources [30–32]. The two-reactor CI–SO enzyme system had its maximum rate at pH 8.0 and for the three-reactor CA–CI–SO system at pH 7.7, located in a pH range, 7.6–8.1, in which the activity hardly changed. We are not aware of solution studies of CA and CI isolated from *Flavobacterium* sp., but our results agree well with those reported for CA [33–36] and CI [37–39] of different origins. For both enzymes an activity maximum close to pH 8.0 and a pH range of 7.5–8.5 with nearly unchanged enzyme activity were found. It is concluded that the immobilization had only a minor effect, if any, on the pH–activity profiles for the enzymes involved in this study.

Previously, Petersson et al. [21] reported an activity maximum at pH 8.5 for a CA–CI–SO system in which the enzymes were immobilized individually, but contained in the same reactor. The enzyme activity was found to be notably reduced at both sides of the maximum with relative activities close to 60% and pH 8.2 and 8.8, respectively. The reason for this behaviour was not discussed.

All further experiments were done at pH 7.7.

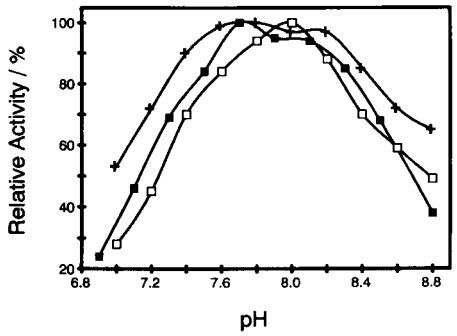


Fig. 3. Effect of pH on the relative enzymatic activity of (+) SO, (□) CI–SO and (■) CA–CI–SO. For SO: 100 μM sarcosine injected; detector current calibrated with 10 and 20 μM hydrogen peroxide; flow-rate, 1.0 ml $min^{-1}$. For CI–SO: 1 mM creatine injected; detector current calibrated with 10 and 15 μM hydrogen peroxide; flow-rate, 0.66 ml $min^{-1}$. For CA–CI–SO: 1 mM creatinine injected; detector current calibrated with 15 μM hydrogen peroxide; flow-rate, 0.40 ml $min^{-1}$.

TABLE 1

Creatinine calibration data for a three-reactor CA–CI–SO enzyme system with a lightly loaded CA reactor [a]

| Creatinine (μM) | Creatine (μM) | Detector current (nA) | | |
|---|---|---|---|---|
| 0 | 0 | 0 | | |
| 25 | 0 | 0.24 | Slope | 0.00892 |
| 50 | 0 | 0.45 | Intercept | 0.0080 |
| 75 | 0 | 0.69 | *r* | 0.9996 |
| 100 | 0 | 0.89 | | |
| 150 | 0 | 1.32 | | |
| 200 | 0 | 1.71 | | |
| 300 | 0 | 2.42 | | |
| 400 | 0 | 3.26 | | |
| 0 | 5 | 0.69 | | |
| 25 | 5 | 0.91 | Slope | 0.00816 |
| 50 | 5 | 1.11 | Intercept | 0.698 |
| 75 | 5 | 1.31 | *r* | 0.9998 |
| 100 | 5 | 1.51 | | |
| 150 | 5 | 1.91 | | |
| 200 | 5 | 2.34 | | |
| 300 | 5 | 3.16 | | |
| 400 | 5 | 4.04 | | |

[a] The steady-state conversion efficiencies were 9% (CA), 49% (CI) and 70% (SO); flow-rate, 0.40 ml $min^{-1}$.

*Interconversion of creatinine and creatine catalysed by CA*

Two typical sets of calibration data for the three-reactor system are given in Tables 1 and 2. The creatinine calibration graph (Table 1) is almost linear up to 400 μM, both for injection of creatinine alone and for creatinine coinjected with 5 μM creatine.

The data in Table 1, which refer to a lightly loaded CA reactor, show that the detector current observed for injection of a 25 μM creatinine solution was 0.24 nA, corresponding to 0.0096 nA l $\mu mol^{-1}$, whereas that for a 5 μM creatine solution was 0.69 nA, corresponding to 0.138 nA l $\mu mol^{-1}$. For a more heavily loaded CA reactor (Table 2) the sensitivities were 0.0205 nA l $\mu mol^{-1}$ (creatinine) and 0.0455 nA l $\mu mol^{-1}$ (creatine). Hence it appears that the sensitivity is much smaller for creatinine than for creatine, indicating, as discussed in more detail below, that the CA reactors did not work under equilibrium conditions in the two sets of experiments.

TABLE 2

Creatine calibration data for a three-reactor CA–CI–SO enzyme system with a moderately loaded CA reactor [a]

| Creatinine (μM) | Creatine (μM) | Detector current (nA) | | |
|---|---|---|---|---|
| 0 | 0 | 0 | | |
| 0 | 200 | 9.1 | Slope | 0.0435 |
| 0 | 400 | 18.5 | Intercept | 0.380 |
| 0 | 600 | 26.5 | $r$ | 0.9995 |
| 0 | 800 | 34.8 | | |
| 0 | 1000 | 42.5 | | |
| 100 | 0 | 2.05 | | |
| 100 | 200 | 11.4 | Slope | 0.0433 |
| 100 | 400 | 20.7 | Intercept | 2.57 |
| 100 | 600 | 28.5 | $r$ | 0.9993 |
| 100 | 800 | 36.8 | | |
| 100 | 1000 | 45.0 | | |

[a] The steady-state conversion efficiencies were 49% (CA), 36% (CI) and 68% (SO); flow-rate, 0.40 ml $min^{-1}$.

For a CA reactor operated under equilibrium conditions the system is described by Eqns. 1 and 2 from which an expression, Eqn. 3, for the detector current is easily derived:

$$K = [\text{creatine}]_{eq}/[\text{creatinine}]_{eq} \quad (1)$$

$$C^0_{\text{creatinine}} + C^0_{\text{creatine}} = [\text{creatinine}]_{eq} + [\text{creatine}]_{eq} \quad (2)$$

$$i = \text{constant}[K/(1+K)](C^0_{\text{creatinine}} + C^0_{\text{creatine}}) \quad (3)$$

In Eqns. 1–3, $K$ is the equilibrium constant (ca. 1.3 at pH $\geqslant$ 7 [34]) and $[\text{creatinine}]_{eq}$ and $[\text{creatine}]_{eq}$ are the equilibrium concentrations of the two substrates; $C^0_{\text{creatinine}}$ and $C^0_{\text{creatine}}$ are the concentrations of the creatinine and creatine solutions injected (one of which may be zero corresponding to a solution of only creatinine or creatine), $i$ is the detector current and the constant is a sensitivity factor depending on experimental parameters such as the conversion efficiencies of the CI and SO reactors, the flow-rate, the dispersion coefficient and the flow pattern in the electrochemical detector.

From Eqn. 3, it is seen that under equilibrium conditions the same sensitivity is expected for creatinine ($C^0_{\text{creatine}} = 0$), creatine ($C^0_{\text{creatinine}} = 0$) or a mixture of both and that a plot of $i$ vs. $C^0_{\text{creatinine}} + C^0_{\text{creatine}}$ defines a straight line with a slope of constant $\times K/(1+K)$. Although the data in Tables 1 and 2 were not originally recorded for testing whether equilibrium prevails in the CA reactor, the different sensitivities observed are sufficient, however, to allow for the conclusion that the outlets of the CA reactors are not equilibrium mixtures of creatinine and creatine under the experimental conditions. In addition, it is noticed that the ratio of the creatine to creatinine sensitivity for the lightly loaded reactor, approximately 14, is much higher than the corresponding ratio, 2.2, for the more heavily loaded reactor indicating, as expected, that a much higher fraction of the substrate was equilibrated by the more heavily loaded reactor.

Further insight into this problem was gained by introduction of a parameter, $\alpha$, representing the fraction of the injected substrate that has been equilibrated by passing through the CA reactor. Thus, $\alpha = 0$ corresponds to the no-reaction case and $\alpha = 1$ to the situation in which the reactor outlet is an equilibrium mixture. This leads to Eqns. 4–6, which together with Eqn. 1 result in Eqn. 7 for the detector current.

$$C^0_{\text{creatinine}} + C^0_{\text{creatine}} = [\text{creatinine}] + [\text{creatine}] \quad (4)$$

$$C^0_{\text{creatinine}} - \alpha(C^0_{\text{creatinine}} - [\text{creatinine}]_{eq}) = [\text{creatinine}] \quad (5)$$

$$C^0_{\text{creatine}} - \alpha(C^0_{\text{creatine}} - [\text{creatine}]_{eq}) = [\text{creatine}] \quad (6)$$

$$i = \text{constant}\left[\left(\frac{\alpha K}{1+K}\right)C^0_{\text{creatinine}} + \left(\frac{1-\alpha+K}{1+K}\right)C^0_{\text{creatine}}\right] \quad (7)$$

In Eqns. 4–6, [creatinine] and [creatine] represent the creatinine and creatine concentrations at the outlet of the CA reactor, which in this case are different from $[\text{creatinine}]_{eq}$ and $[\text{creatine}]_{eq}$.

From Eqn. 7, it is seen that a plot of $i$ vs. $C^0_{\text{creatinine}}$ at constant $C^0_{\text{creatine}}$ defines a straight line with a slope of constant $\times \alpha K/(1+K)$ and an intercept of constant$[(1-\alpha+K)/(1+$

$K)]C^0_{creatine}$. With $K = 1.3$ [34], the data given in Table 1 for $C^0_{creatine} = 5$ $\mu$M resulted in $\alpha = 0.10$ and constant = 0.147 nA l $\mu$mol$^{-1}$, showing that only 10% of the substrate passing the CA reactor was equilibrated. Analogously, a plot of $i$ vs. $C^0_{creatine}$ at constant $C^0_{creatinine}$ defines a straight line with a slope of constant$[(1 - \alpha + K)/(1 + K)]$ and an intercept of constant $\times$ $\alpha K/(1 + K)C^0_{creatinine}$, which for the data in Table 2 at $C^0_{creatinine} = 100$ $\mu$M results in $\alpha = 0.72$ and constant = 0.063 nA l $\mu$mol$^{-1}$. The corresponding conversion efficiencies are easily obtained from $\alpha$ as $\alpha K/(1 + K)$, resulting in the values 0.056 ($\alpha$ = 0.10) and 0.41 ($\alpha = 0.72$). These are both significantly smaller than the steady-state values of 0.09 and 0.49, respectively (Tables 1 and 2). The lower values observed for the single-injection experiments are probably caused by the dispersion associated with this mode of operation. However, a more complete interpretation of these figures requires a detailed analysis of the interplay between the enzyme activities and the mass transport patterns in the reactors, which is beyond the scope of this paper.

Even for the more heavily loaded reactor (Table 2) the conversion is smaller than that observed by Moges and Johansson [25], who reported that a CA reactor similar to that used in this study could be operated under equilibrium conditions corresponding to $\alpha = 1$. However, examination of the experimental details shows that in addition to a lower flow-rate, these authors used a reactor with a higher CA loading than we did, which appears to be the major factor responsible for the observed difference in behaviour. However, as FIA was only used in this work owing to its convenience in systematic studies of the performance of enzyme reactors, further efforts to attempt equilibrium conditions in the CA reactor were not made.

*Activities of single-enzyme reactors*

In order to separate the effects of different experimental factors, such as temperature or the reaction products formed during the conversion of creatinine to hydrogen peroxide, the activities of the single-enzyme reactors were determined as follows. For the effect of temperature, the activity of the SO reactor was first investigated by injection of solutions of sarcosine (100 $\mu$M). With this result at hand, the activity of the CI reactor could be obtained from the results obtained by injection of creatine solutions (100 $\mu$M) into the coupled CI–SO reactor system, which again provided for the determination of the CA reactor activity from results obtained by injection of creatinine solutions (100 $\mu$M) into the three-reactor CA–CI–SO system. When the effects of reaction product were tested, solutions with different concentrations of the compound in question were coinjected with either sarcosine, creatine or creatinine (100 $\mu$M in each instance). The highest concentration was chosen expecting the worst possible case, that is, a blood sample containing a pathological level of the particular compound. The dispersion coefficients were taken into account in the estimates of the maximum concentrations.

*Effect of the temperature on CA, CI and SO*

The dependence of the enzyme activity on the temperature for the enzyme reactors in series and for the single reactors is shown in Fig. 4. Both of the coupled enzyme systems show the maximum

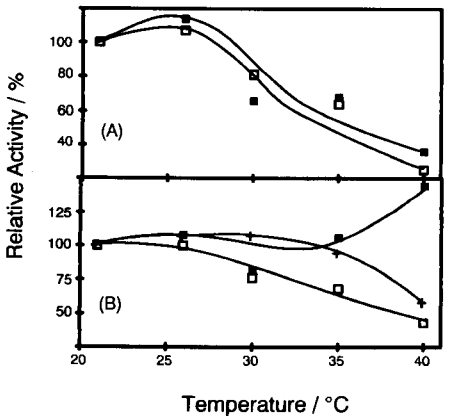


Fig. 4. Effect of temperature on the relative enzymatic activity of (A) the coupled enzyme systems (□) CI–SO and (■) CA–CI–SO and (B) the single enzymes (+) SO, (□) CI and (■) CA. 100 $\mu$M substrate injected; flow-rate, 0.40 ml min$^{-1}$; conversion efficiencies determined at the end of the experiment, CA 32%, CI 17% and SO 15%.

activity close to 25°C, with only a small temperature dependence in the range 21–27°C (Fig. 4A). At temperatures higher than ca. 27°C the activity was observed to decrease with increasing temperature and was reduced to ca. 30% of the original activity at 40°C.

Essentially the same temperature dependence was observed for the activity of immobilized CI (Fig. 4B). This parallels the behaviour of CI in solution for which the maximum activity was found [38] at a slightly higher temperature, 30°C, followed by a significant decrease in activity in passing from 30 to 40°C [38,40]. It should be mentioned, however, that the solution data refer to CI isolated from other bacteria than *Flavobacterium* sp. For SO we found that the activity was essentially independent of the temperature in the range 21–35°C with the maximum located between 26 and 30°C. This is slightly lower than the maximum at 37°C reported for the soluble enzyme [29]. The decrease in activity at higher temperatures followed also in this instance the behaviour of the enzyme in solution [29,31,32]. Our results for the immobilized enzymes show that the loss of activity at higher temperatures is irreversible for both CI and SO.

In contrast to CI and SO, CA exhibited increasing activity with increasing temperature, the highest activity being found at the maximum temperature used, 40°C. This behaviour parallels that for solution CA (from bacterial species other than *Flavobacterium* sp.), which has been reported to be stable even at temperatures close to 60°C [34,35]. The changes in the CA activity with temperature were found to be reversible.

Overall it appears that the temperature–activity relationship of the immobilized enzymes is very similar to that observed for the enzymes in solution.

*Effect of glycine on CA, CI and SO*

The overall activity of the three-reactor system was increased significantly by the presence of glycine, in particular at low concentrations, as shown in Fig. 5A. The reference range in plasma is 100–600 $\mu$M [3], but it was observed that a glycine concentration as small as 10 $\mu$M caused a measurable increase in activity.

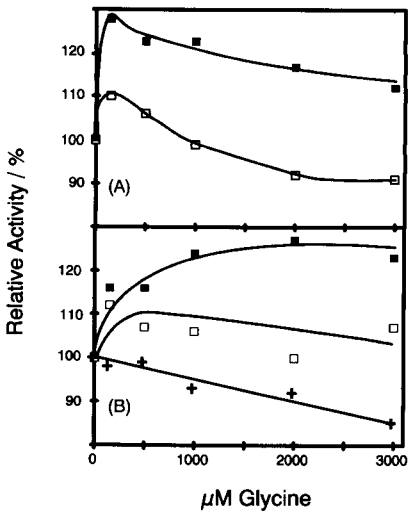


Fig. 5. Effect of glycine on the relative enzymatic activity of (A) the coupled enzyme systems (□) CI–SO and (■) CA–CI–SO and (B) the single enzymes (+) SO, (□) CI and (■) CA. Coinjection of glycine and 100 $\mu$M substrate; flow-rate, 0.40 ml $min^{-1}$; conversion efficiencies determined at the end of the experiment, CA 55%, CI 30% and SO 12%.

The results in Fig. 5B show that the overall effect of increasing the glycine concentrations is the result of an increasing activity of CA accompanied by a decreasing activity of SO. The activity of CI was found to be essentially independent of the presence of glycine. The observation that conversion of sarcosine by SO is inhibited by the presence of glycine may at first not seem surprising, as glycine is a product of this conversion (see Fig. 1). However, the result of a solution study [41] of SO, also from *Corynebacterium* sp., indicated that glycine at concentrations up to 200 mM did not show any significant inhibitory effect on the enzyme activity. We are not able to explain this difference. Moreover, the loss of activity we found was irreversible, which seems to indicate that the effect of glycine under our experimental conditions cannot be explained solely as the result of an increasing rate of the back reaction for the SO-catalysed process. The inhibitory effect of glycine is not expected to cause serious problems in the clinical use of the system, as the normal levels of creatinine and creatine

will result in glycine concentrations much below 1000 $\mu$M.

The increased activity of CA in the presence of glycine was found to be reversible.

*Effect of formaldehyde (and methanol) on CA, CI and SO*

Commercial aqueous formalin solutions contain up to 10–15% of methanol as a stabilizer. For the solution used in this work the methanol content was determined by gas chromatography to be 10.5%. Therefore, in order to separate the possible effects of formaldehyde and methanol, measurements were made with both the formalin solution and, in a separate experiment, methanol.

The results for the formalin solution are presented in Fig. 6 and it is seen that the overall reduction observed for the activity of the coupled enzyme systems (Fig. 6A) is related to both CA and CI, whereas the SO activity was essentially unaffected by the formalin solution (Fig. 6B).

Essentially the same results were obtained with pure methanol (Fig. 7A and B), which is not a substrate for any of the enzymes.

In both instances the loss in activity for CI was reversible whereas that for CA was irreversible.

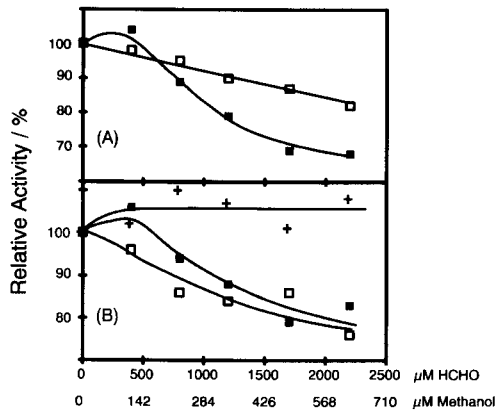


Fig. 6. Effect of a formalin solution stabilized by methanol on the relative enzymatic activity of (A) the coupled enzyme systems (□) CI–SO and (■) CA–CI–SO and (B) the single enzymes (+) SO, (□) CI and (■) CA. Coinjection of formalin and 100 $\mu$M substrate; detector current normalized by 25 and 50 $\mu$M hydrogen peroxide solutions; flow-rate, 0.40 ml $min^{-1}$; conversion efficiencies determined at the end of the experiment, CA 52%, CI 30% and SO 43%.

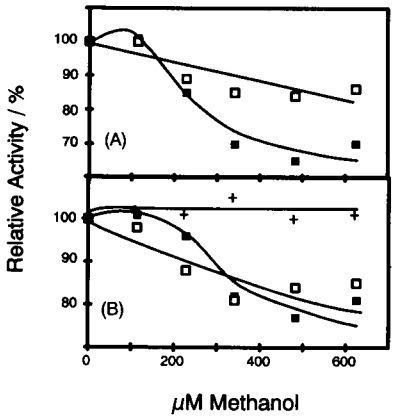


Fig. 7. Effect of methanol on the relative enzymatic activity of (A) the coupled enzyme systems (□) CI–SO and (■) CA–CI–SO and (B) the single enzymes (+) SO, (□) CI and (■) CA. Coinjection of methanol and 100 $\mu$M substrate; flow-rate, 0.40 ml $min^{-1}$; conversion efficiencies determined at the end of the experiment, CA 40%, CI 30% and SO 43%.

Overall the results suggest that the effect observed for the formalin solution may be caused solely by the presence of methanol in the formalin solutions. Hence it appears that formaldehyde in itself has only a small effect, if any, on the activity of the enzymes.

The concentration of methanol in whole blood is below 50 $\mu$M [4] and, accordingly, the inhibitory effect of this compound is expected to be of only minor importance in practical applications of the detection system.

*Effect of urea on CA, CI and SO*

The reference range for urea in serum/plasma is 2.2–9.8 mM [3] and no effect on the enzyme activities was observed at concentrations up to 12 mM. This is in agreement with results reported for CI and SO in solution [42].

*Effect of creatine on SO*

Creatine up to 1.0 mM did not show any measurable effect on SO, in agreement with solution studies [30,43] of the same enzyme, although from a different bacterium.

*Effect of sarcosine on CA and CI*

As sarcosine is a reaction product from the CI reactor, the possible effect of this compound has

to be determined by difference measurements. However, the detector current resulting from injection of 100 $\mu$M creatinine solutions was usually much smaller than that related to the injection of sarcosine solutions, and for this reason the effect of sarcosine on CA could not be investigated. When sarcosine was coinjected with creatine, reliable measurements could only be obtained for sarcosine concentrations up to 200 $\mu$M. The results showed that the presence of sarcosine caused a reversible decrease in the activity of the CI reactor, in agreement with solution studies of CI (not from *Flavobacterium* sp.) [37]. The effect of sarcosine is not expected to cause problems in a clinical application of the three-enzyme system as its plasma concentration differs appreciably from zero only in rare instances (e.g., hypersarcosinaemia) [44].

*Effect of hydrogen peroxide on SO*

For the same reasons as given above for sarcosine, the effect of hydrogen peroxide could only be studied for the SO reactor and the results demonstrated that hydrogen peroxide does not affect the activity of SO. The concentration of hydrogen peroxide in plasma is generally believed to be close to zero, but recently an average plasma concentration of $34 \pm 18$ $\mu$M was reported [45]. As a consequence of this, the creatine values determined by techniques based on the detection of hydrogen peroxide may be slightly overestimated. However, as creatinine in real samples has to be determined by a difference measurement, the effect of hydrogen peroxide cancels.

*Coimmobilized enzyme reactors*

The work presented so far demonstrates that the effects of the reaction products inevitably formed during the enzymatic conversion of creatinine to hydrogen peroxide are indeed small. However, the separation of the three enzymes in separate reactors, or membranes, is inconvenient in practical work and for this reason a series of additional experiments were carried out with reactors containing coimmobilized enzyme systems.

One way of applying the three-enzyme system as a part of a FIA system would be to include a separate CA reactor in series with a reactor containing coimmobilized CI and SO. The total concentration of creatinine and creatine could then be determined by passing the test solution through both reactors and creatine alone by excluding the CA reactor. The creatinine level would then result as the difference between these two measurements. However, this strategy would not be applicable to enzyme electrodes and for this reason it was decided instead to use one reactor containing coimmobilized CA, CI and SO for the determination of the total concentration of creatinine and creatine and another reactor containing only coimmobilized CI and SO for the determination of the creatine concentration.

Common to both methods is that it must be assumed that the interconversion of creatinine and creatine is sufficiently slow that this process does not effect the concentrations in the absence of CA. This is indeed the case. The uncatalysed equilibration in water has been reported to take more than 1000 h [46] and even in urine the hydrolysis of creatinine is sufficiently slow to be without importance in practical work [47].

The two reactors were introduced into the FIA system as shown in Fig. 2B.

*Calibration for creatine and creatinine*

The calibration graphs for creatinine and creatine obtained by using the CA–CI–SO and CI–SO

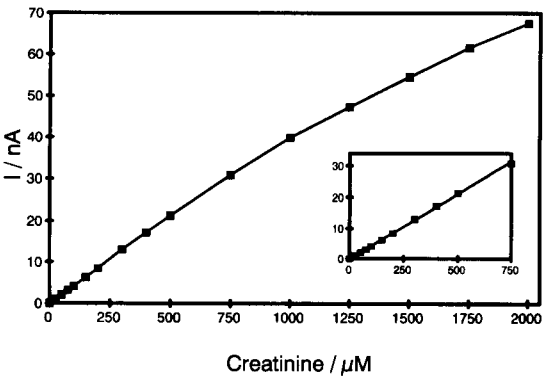


Fig. 8. Creatinine calibration graph. Flow-rate, 0.35 ml min$^{-1}$; conversion efficiencies, CA 21%, CI 51% and SO 70%. The calibration graph may be approximated as $i = -5.92 \times 10^{-6} (C^0_{\text{creatinine}})^2 + 0.0456 C^0_{\text{creatinine}} - 0.232$; $r = 0.9999$. The inset shows the linear range of the graph for which $i = (0.0431 \pm 0.0003) C^0_{\text{creatinine}} - (0.140 \pm 0.064)$; $n = 9$, $r = 0.9999$.

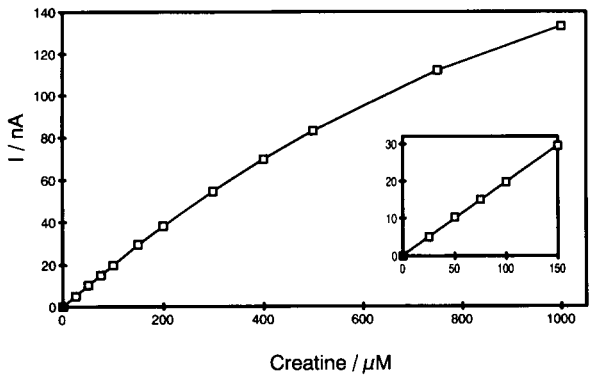


Fig. 9. Creatine calibration graph. Flow-rate, 0.35 ml $min^{-1}$; conversion efficiencies, CI 47% and SO 72%. The calibration graph may be approximated as $i = -6.80 \times 10^{-5} (C^0_{creatine})^2 + 0.200 C^0_{creatine} + 0.372$; $r = 0.9999$. The inset shows the linear range of the graph, for which $i = (0.195 \pm 0.002) C^0_{creatine} + (0.311 \pm 0.155)$; $n = 5$, $r = 0.9999$.

enzyme reactors, respectively, are shown in Figs. 8 and 9. The creatinine calibration graph is linear ($r = 0.9999$) in the concentration range 25–700 $\mu$M and that for creatine is linear in the range 25–150 $\mu$M (the linear ranges are shown in Figs. 8 and 9 as insets and the relationships between $i$ and $C^0_{substrate}$ valid within these ranges are given in the captions). The linear ranges cover fully the reference ranges of creatinine (35–140 $\mu$M) and creatine (26–100 $\mu$M) in serum or plasma [3,4] and for creatinine also most of the range for abnormal levels. The detection limits are 9.0 $\mu$M for creatinine and 2.8 $\mu$M for creatine, determined from the calibration graph as the sum of a blank signal and 3.28 standard deviations of the blank corresponding to the 95% confidence interval.

It is of interest that the upper limit of the linear range for creatinine is nearly five times that for creatine, in spite of the fact that the steady-state conversion efficiencies for CI and SO are virtually identical for the two- and three-enzyme reactors. In addition, it is seen that the calibration slope for creatinine, that is, the sensitivity, is only one fifth of that for creatine. These observations are probably connected with the moderate steady-state conversion efficiency (21%) for CA in the three-enzyme reactor. A consequence of this is that the CI–SO system of the three-enzyme reactor on injection of a creatinine solution will experience a creatine concentration that is only one fifth of that experienced by the two-enzyme reactor on injection of the same volume of an equimolar creatine solution. Hence, it appears that the narrower linear range observed for creatine is the result of saturation of the CI–SO system. This again means that the upper limit of the linear range for creatinine may be pushed to even higher concentrations than 700 $\mu$M by application of a three-enzyme reactor with an even smaller steady-state conversion efficiency than 21%. However, this improvement of the linear response range will be paid for by a lower sensitivity of the system.

Concentrations above the two upper limits may still be determined with high precision by incorporating the non-linear part of the calibration graphs. Equations that approximate the entire curves are given in the captions of the figures.

*Effect of flow-rate*

The conversion efficiencies as determined by the steady-state method varied qualitatively with the flow-rate, as expected. The results are shown in Fig. 10, from which it is seen that the conversion efficiencies increase with decreasing flow-

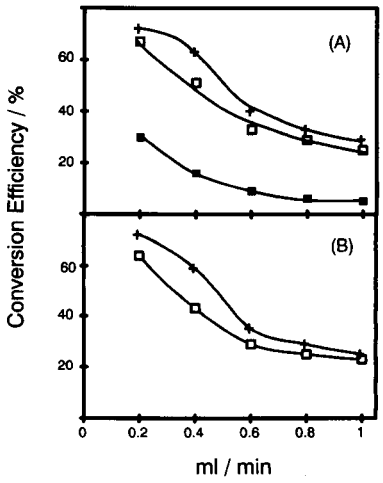


Fig. 10. Conversion efficiency of the single enzymes (+) SO, (□) CI and (■) CA for (A) the CA–CI–SO reactor and (B) the CI–SO reactor as function of flow-rate. 100 $\mu$M substrate injected.

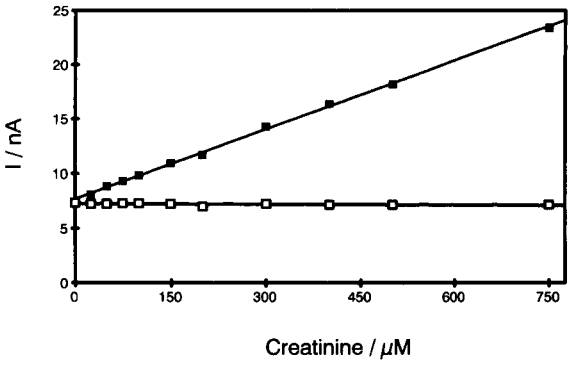


Fig. 11. Standard additions of creatinine to 50 μM creatine (■), for solution passing the CA–CI–SO reactor, $i = (0.0212 \pm 0.0003) C^0_{\text{creatinine}} + (7.68 \pm 0.08)$, $n = 11$, $r = 0.9993$, and (□) for solution passing the CI–SO reactor. Flow-rate, 0.35 ml $\text{min}^{-1}$; conversion efficiencies for the CA–CI–SO reactor, CA 16%, CI 52% and SO 63%, and for the CI–SO reactor, CI 43% and SO 59%.

rate, but 100% conversion was not observed for any of the enzymes, even at the lowest flow-rates applied.

*Standard addition graphs and standard deviations*

Graphs for standard addition of creatinine to creatine and for creatine to creatinine are shown in Figs. 11 and 12, respectively. For the two-enzyme CI–SO reactor the graph for addition of creatinine (Fig. 11, □) is completely flat, confirming that creatinine is not converted into creatine to any significant extent in the absence of CA.

The two lines in Fig. 12 are almost parallel. The difference in intercepts is 2.08 nA, corresponding to a creatinine sensitivity of 0.0208 nA l $\mu\text{mol}^{-1}$. This compares favourably with the value of 0.0212 nA l $\mu\text{mol}^{-1}$ obtained as the slope of the standard addition graph for creatinine (Fig. 11, ■).

The standard deviation for 25 injections of 100 μM creatinine was 0.6% and that for 100 μM creatine was 0.9%, with a sample throughput of 24 $\text{h}^{-1}$.

*Stability of immobilized enzymes*

Unused CPG-immobilized enzymes were stored in 0.1 M phosphate buffer (pH 7.7) at 4°C, protected by Parafilm. After 6 months the activity of each enzyme was essentially the same as for the freshly made enzyme preparations.

When in use, the stabilities of the coimmobilized enzymes were still found to be satisfactory. The data given in Fig. 13 show that the activity of CI was essentially unchanged after a period of 66 days, whereas the activities of CA and SO de-

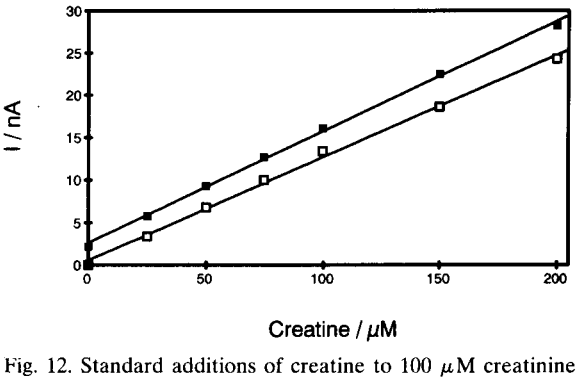


Fig. 12. Standard additions of creatine to 100 μM creatinine for (■) solution passing the CA–CI–SO reactor, $i = (0.131 \pm 0.002) C^0_{\text{creatine}} + (2.64 \pm 0.25)$, $n = 7$, $r = 0.9992$, and (□) for solution passing the CI–SO reactor, $i = (0.121 \pm 0.003) C^0_{\text{creatine}} + (0.559 \pm 0.317)$, $n = 7$, $r = 0.9985$. Flow rate, 0.35 ml $\text{min}^{-1}$; conversion efficiencies for the CA–CI–SO reactor, CA 16%, CI 52% and SO 63%, and for the CI–SO reactor, CI 43% and SO 59%.

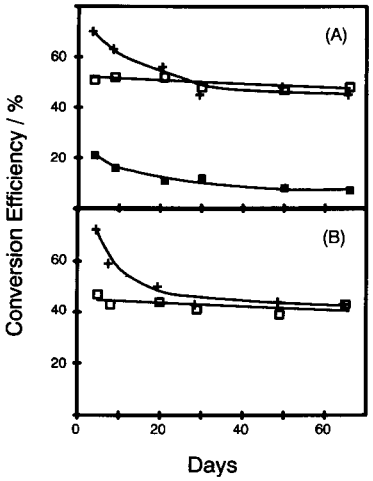


Fig. 13. Stability of the single enzymes (+) SO, (□) CI and (■) CA for (A) the CA–CI–SO reactor and (B) the CI–SO reactor as measured by the conversion efficiency as a function of time. 100 μM substrate injected; flow-rate, 0.40 ml $\text{min}^{-1}$.

creased slowly during the first 20–30 days, after which they remained essentially constant. The enzyme reactors were used frequently for the first 2 weeks and thereafter only occasionally. The reduced activity of CA and SO was attributed to denaturation and/or irreversible chemical transformation.

*Effect of FAD on SO*

Sarcosine oxidase differs from most other flavoproteins by having two differently bound flavin adenine dinucleotide (FAD) units [48], one covalently and the other non-covalently bound [29]. It has been suggested [49,50] that sarcosine is oxidized at the site of the non-covalently bound FAD, which then serves to transport the electrons to the site of the covalently bound FAD where oxygen is being reduced. Hence it might be envisaged that the decrease in activity with time of immobilized SO (Fig. 13) is related to the loss of non-covalently bound FAD and if so that the SO activity may be fully or partly regained by exposing the reactor to FAD. In order to test this hypothesis, a heavily used SO reactor, the conversion efficiency of which had eventually dropped to 14%, was allowed to stand for 24 h at 6°C in the presence of a solution containing 60 mM FAD. However, no effect could be detected as the result of the treatment. Treatment for longer times was not attempted. Even if an appreciable improvement in the reactor conditions were to have been observed, the regeneration times would probably be too long to be of practical importance.

We express our gratitude to Professor Gillis Johansson (University of Lund) for many helpful discussions, for preprints of Refs. 25 and 27 and for his kind hospitality during the stay of H.S. in Lund. Parts of the instrumentation were generously provided by Radiometer A/S.

REFERENCES

1 K. Spencer, Ann. Clin. Biochem., 23 (1986) 1.
2 S. Narayanan and H.D. Appleton, Clin. Chem., 26 (1980) 1119.
3 H. Olesen, K. Kjeldsen and I. Ibsen, Klinisk-Kemisk Kompendium, F.A.D.L.s Forlag, Copenhagen, 1979.
4 N.W. Tietz (Ed.), Textbook of Clinical Chemistry, Saunders, Philadelphia, 1st edn., 1986, pp. 1810–1857.
5 S.F. Sena, D. Syed and R.B. McComb, Clin. Chem., 34 (1988) 594.
6 M. Jaffe, Z. Physiol. Chem., 10 (1886) 391.
7 R.L. Murray, in L.A. Kaplan and A.J. Pesce (Eds.), Clinical Chemistry: Theory, Analysis and Correlation, Mosby, St. Louis, MO, 1984, pp. 1247–1253.
8 N. Tryding and K.-A. Roos, Drug Interferences and Drug Effects in Clinical Chemistry, Apoteksbolaget, Stockholm, 5th edn., 1989.
9 J. Rogulski and A. Pacanis, Dev. Clin. Biochem. 2 (1980) 134.
10 H. Wisser and E. Knoll, Internist, 28 (1987) 123.
11 A.W. Wahlefeld and J. Siedel, in H.U. Bergmeyer (Ed.), Methods of Enzymatic Analysis, VCH, Weinheim, 3rd edn., 1985, pp. 488–507.
12 B.L. Bacon and H.L. Pardue, Clin. Chem., 37 (1991) 1338.
13 V.K. Nguyen, C.-M. Wolff, J.L. Seris and J.-P. Schwing, Analysis, 18 (1990) 582.
14 B. Lindbàck and A. Bergman, Clin. Chem., 35 (1989) 835.
15 M.P Goren, S. Osborne and R.K. Wright, Clin. Chem., 32 (1986) 548.
16 W.G. Guder, G.E. Hoffmann, A. Hubbuch, W.A. Poppe, J. Siedel and C.P. Price, J. Clin. Chem. Clin. Biochem., 24 (1986) 889.
17 P. Fossati, L. Prencipe and G. Berti, Clin. Chem., 29 (1983) 1494.
18 V.K. Nguyen, C.-M. Wolff, J.L. Seris and J.-P. Schwing, Anal. Chem., 63 (1991) 611.
19 J. Motonaka, H. Takabayashi, S. Ikeda and N. Tanaka, Anal. Lett., 23 (1990) 1981.
20 T. Tsuchida and K. Yoda, Clin. Chem., 29 (1983) 51.
21 B.A. Petersson, E.H. Hansen and J. Růžička, Anal. Lett., 19 (1986) 649.
22 M.C. Gutierrez, A. Gomez-Hens and D. Perez-Bendito, Fresenius' Z. Anal. Chem., 335 (1989) 576.
23 B. Xia and S. Liu, Fenxi Huaxue, 16 (1988) 1116; Chem. Abstr., 110 (1991) 208746v.
24 J.F. van Staden, Fresenius' Z. Anal. Chem., 315 (1983) 141.
25 G. Moges and G. Johansson, Talanta, submitted for publication.
26 H.H. Weetall, Methods Enzymol. 44 (1976) 140.
27 G. Moges and G. Johansson, Anal. Chim. Acta, in press.
28 J. Růžička and E.H. Hansen, Flow Injection Analysis, Wiley, New York, 2nd edn., 1988, pp. 23–26.
29 M. Suzuki, J. Biochem., 89 (1981) 599.
30 Y. Inouye, M. Nishimura, Y. Matsuda, H. Hoshika, H. Iwasaki, K. Hujimura, K. Asano and S. Nakamura, Chem. Pharm. Bull., 35 (1987) 4194.
31 S. Ogushi, K. Nagao, S. Emi, M. Ando and D. Tsuru, Chem. Pharm. Bull., 36 (1988) 1445.
32 N. Mori, M. Sano, Y. Tani and H. Yamada, Agric. Biol. Chem., 44 (1980) 1391.

33 M. Suzuki, Jpn. Kokai, 7834983; Chem. Abstr., 89 (1978) 40883j.
34 K. Rikitake, I. Oka, M. Ando, T. Yoshimoto and D. Tsuru, J. Biochem., 86 (1979) 1109.
35 W.J. Donnelly and D.B. Johnson, Int. J. Biochem, 8 (1977) 11.
36 Y. Inouye, Y. Matsuda, T. Naid, S. Arai, Y. Hashimoto, K. Asano, M. Ozaki and S. Nakamura, Chem. Pharm. Bull., 34 (1986) 269.
37 M. Coll, S.H. Knof, Y. Ohga, A. Messerschmidt, R. Huber, H. Moellering, L. Rüssmann and G. Schumacher, J. Mol. Biol., 214 (1990) 597.
38 T. Yoshimoto, I. Oka and D. Tsuru, Arch. Biochem. Biophys., 177 (1976) 508.
39 Y. Matsuda, N. Wakamatsu, Y. Inouye, S. Uede, Y. Hashimoto, K. Asano and S. Nakamura, Chem. Pharm. Bull., 34 (1986) 2155.
40 A. Kaplan and D. Naugler, Mol. Cell. Biochem., 3 (1974) 9.
41 S. Hayashi, M. Suzuki and S. Nakamura, Biochim. Biophys. Acta, 742 (1983) 630.
42 A.M. Buysse, J.R. Delanghe, M.L.D. Buyzere, A.M.D. Moll, K.D. Scheerder and L. Noens, Clin. Chim. Acta, 187 (1990) 155.
43 Y. Matsuda, H. Hoshika, Y. Inouye, S. Ikuta, K. Matsuura and S. Nakamura, Chem. Pharm. Bull., 35 (1987) 711.
44 T. Gerritsen and H.A. Waisman, N. Engl. J. Med., 275 (1966) 66.
45 S.D. Varma and P.S. Devamanoharan, Free Radical Res. Commun., 14 (1991) 125.
46 G. Edgar and H.E. Shiver, J. Am. Chem. Soc., 47 (1925) 1179.
47 T.J. Miller, Anal. Lett., 24 (1991) 1779.
48 H.-D. Zeller, R. Hille and M.S. Jorns, Biochemistry, 28 (1989) 5145.
49 K. Kvalnes-Krick and M.S. Jorns, Biochemistry, 25 (1986) 6061.
50 M.S. Jorns, Biochemistry, 24 (1985) 3189.

*Analytica Chimica Acta*, 268 (1992) 347–350
Elsevier Science Publishers B.V., Amsterdam



# Acetylcholine biosensor involving entrapment of two enzymes. Optimization of operational and storage conditions

R. Rouillon, N. Mionetto and J.-L. Marty

*Groupe d'Etudes et de Recherches Appliquées Pluridisciplinaires, UA CNRS 461, Université de Perpignan, Centre de Phytopharmacie, 52 Avenue de Villeneuve, 66860 Perpignan (France)*

(Received 2nd April 1992; revised manuscript received 14th May 1992)

**Abstract**

A bi-enzymatic sensor for the determination of acetylcholine was prepared by co-entrapment of acetylcholinesterase and choline oxidase in poly(vinyl alcohol) bearing styrylpyridinium groups. The measurements were based on the detection of enzymatically liberated hydrogen peroxide. The best conditions of use are pH 8, 30°C and a buffer concentration higher than 0.05 M. The storage stability in a dry state is excellent.

*Keywords:* Biosensors; Enzymatic methods; Acetylcholine

The determination of acetylcholine is of interest for analytical and clinical purposes. An enzymatic sensor, based on an immobilized enzyme in close proximity to an amperometric transducer, can be an excellent tool for this objective. The detection of acetylcholine is based on the following reactions:

$$\text{acetylcholine} + H_2O \xrightarrow{\text{acetylcholine esterase}} \text{choline} + \text{acetic acid} \quad (1)$$

$$\text{choline} + 2O_2 + H_2O \xrightarrow{\text{choline oxidase}} \text{betaïne} + 2H_2O_2 \quad (2)$$

Different possibilities have been explored: acetylcholinesterase and choline oxidase packed separately [1,2], both enzymes co-immobilized [3,4] or free acetylcholinesterase added to the buffer with immobilized choline oxidase [5]. A great deal of information is available on immobilization techniques [6] and techniques for the detection of acetylcholine have been reviewed [3,7].

This laboratory is investigating physical entrapment of enzymes using poly(vinyl alcohol) bearing styrylpyridinium groups (PVA-SbQ), developed by Ichimura [8] in order to achieve an easily handled, cheap and disposable membrane with high activity and stability. The objective of this work was to investigate the optimum conditions for the detection of acetylcholine using co-entrapment of choline oxidase and acetylcholinesterase.

*Correspondence to*: J.-L. Marty, Groupe d'Etudes et de Recherches Appliquées Pluridisciplinaires, UA CNRS 461, Université de Perpignan, Centre de Phytopharmacie, 52 Avenue de Villeneuve, 66860 Perpignan (France).

## EXPERIMENTAL

### *Reagents*

Choline oxidase (E.C. 1.1.3.17, 10 U $mg^{-1}$ from *Alcaligenes* sp.), acetylcholine esterase (E.C.

3.1.1.7, 1000 U $mg^{-1}$ from electric eel), acetylcholine chloride and cellulose nitrate membranes were purchased from Sigma. Poly(vinyl alcohol) with styrylpyridinium groups (PVA-SbQ: degree of polymerization 1700, degree of saponification 88, SbQ content 1.3 mol%, solid content 11%, pH 7) was kindly provided by Toyo Gosei (Tokyo). All others chemicals were of analytical-reagent grade. All solutions were prepared in distilled water.

*Preparation of enzyme membrane*

50 U of choline oxidase, 10 U of acetylcholinesterase or 50 U of choline oxidase and 10 U of acetylcholinesterase dissolved in 0.2 ml of distilled water were added to 1 g of an 11% solution of PVA-SbQ. The mixture was spread on a cellulose nitrate membrane (diameter 3 mm, thickness 20 $\mu$m, pore diameter 0.2 $\mu$m). Before polymerization, the gel was homogenized on a mechanical shaker for 30 min at room temperature in the dark. The air-dried membrane was exposed to UV radiation for 3 h and stored at 4°C.

*Instrumentation and procedure*

The amperometric transducer Glu 1 (Solea-Tacussel, Villeurbanne, France) consisted of a platinum anode at a potential fixed at +650 mV with respect to an Ag/AgCl reference electrode and was plugged into a PRGE polarograph (Solea-Tacussel). The enzymatic membrane was maintained in contact with the platinum tip by a screw-cap on the 180 cm × 12 mm o.d. plastic tube containing the electrodes. The amperometric measurement of $H_2O_2$ was performed according to the following reaction:

$$H_2O_2 \xrightarrow{\text{Pt anode}} O_2 + 2H^+ + 2e^-$$

The sensor was immersed in 10 ml of phosphate buffer. The temperature was maintained with a thermostated water circulation bath. When the current of the sensor became constant, an appropriate volume of choline or acetylcholine solution was injected into the jacketed vessel. The current increased rapidly and reached a steady state.

## RESULTS AND DISCUSSION

The assay of acetylcholine depends on the activities of choline oxidase and acetylcholinesterase (reactions 1 and 2). The performance of the choline oxidase is the limiting factor because its specific activity is very much lower than the activity of commercially available acetylcholinesterase.

*Effect of pH*

Immobilized choline oxidase showed a broad pH optimum between 7 and 9 (Fig. 1a). Acetylcholinesterase immobilized using Ellman's technique [9] had an optimum pH at 8–8.5 (Fig. 1b). Using co-immobilized acetylcholinesterase and choline oxidase with hydrogen peroxide detection, the enzyme electrode sensitivity increased from 9 mA l $mol^{-1}$ at pH 6.5 to 67 mA l $mol^{-1}$ at pH 8.5, then decreased slightly (Fig. 1c). As pH 8 is at pH 6.5 to 67 mA l $mol^{-1}$ at pH 8.5, then decreased slightly (Fig. 1c). As pH 8 is the best operating pH for choline oxidation [7], further experiments were carried out at this pH.

*Effect of temperature*

The response of the sensor increased with increasing temperature in the range 20–30°C, was nearly constant between 30 and 40°C and de-

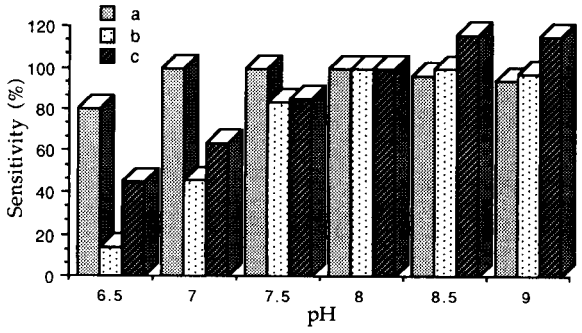


Fig. 1. Effect of pH on the sensitivity of immobilized enzymes. (a) Immobilized choline oxidase, amperometric detection; (b) immobilized acetylcholinesterase, activity detected with a spectrophotometric technique; (c) acetylcholinesterase and choline oxidase co-entrapped, amperometric detection. Sensitivity is given relative to the value at pH 8.0. Conditions of amperometric detection: 5 mM acetylcholine or choline as substrate; temperature, 30°C; 0.05 M phosphate buffer between pH 6.0 and 8.5 and 0.2 M carbonate buffer for pH 9.0.

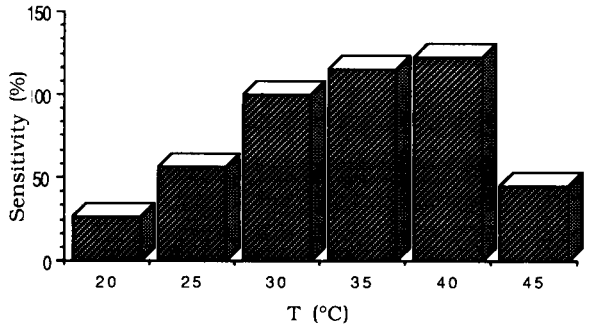


Fig. 2. Effect of temperature on the sensitivity of the acetylcholine biosensor. 5 mM acetylcholine as substrate in 0.05 M phosphate buffer (pH 8.0). Sensitivity is given relative to the value at 30°C.

creased considerably at 45°C (Fig. 2). The activity of the membrane enzyme after incubation in working buffer for 6 h was also studied. The sensitivity increased between 20 and 30°C and decreased above 30°C. The temperature selected for further experiments was 30°C.

*Effect of buffer concentration*

Figure 3 shows the effect of buffer concentration on the response in phosphate buffer (pH 8). The variation of pH due to the liberation of $H^+$ was too high in weakly buffered solutions (0.01 M). It is necessary to use buffer concentrations higher than 0.05 M.

*Dynamic range*

A linear calibration graph was obtained up to $5 \times 10^{-3}$ M in 0.05 M phosphate buffer (pH 8).

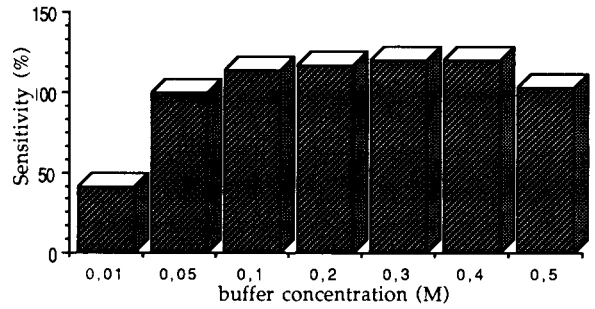


Fig. 3. Effect of buffer concentration on the sensitivity of the acetylcholine biosensor. 5 mM acetylcholine as substrate in phosphate buffer (pH 8.0); temperature, 30°C. Sensitivity is given relative to the value with 0.05 M buffer.

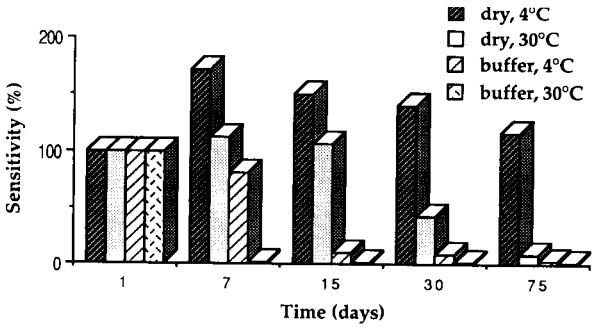


Fig. 4. Effect of storage conditions on the stability of the biosensor. Measurements were carried out with 5 mM acetylcholine as substrate in 0.05 M phosphate buffer (pH 8.0). Sensitivity is given relative to the value at day one.

The detection limit (2 × background noise) for acetylcholine was $1 \times 10^{-5}$ M.

*Operational stability*

In a typical experiment, the operational stability was tested over a 6-h period under the optimum conditions defined above. After five assays, the loss of activity was 11% and after ten assays the membrane had retained 75% of its initial sensitivity.

*Storage stability*

The long-term stability of the acetylcholine electrode was examined. The biosensor was stored in a dry state or in 0.05 M phosphate buffer pH 8 at 4 or 30°C. The results are shown in Fig. 4. The decrease in sensitivity was considerable if the enzyme membranes were placed in the working buffer. When the enzymes membranes were stored in a dry state at 4°C, the sensitivity increased during the first week and was stable for more than 3 months.

*Conclusion*

Several papers have been published on the co-immobilization of choline oxidase and acetylcholinesterase for the detection of acetylcholine. The immobilization procedure used here with co-entrapment of the two enzymes is easy and needs mild conditions. The results are as good as those obtained by other workers [4,5] using the same type of detection (hydrogen peroxide) and

better than those obtained by groups using oxygen detection [9] or potentiometric detection with only acetylcholinesterase [10]. Many enzyme membranes have been produced for the determination of various substrates. The advantages of the present system are the ease of preparing the membrane and its very good storage stability in a dry state.

REFERENCES

1 M. Masoom, Anal. Chim. Acta, 214 (1988) 173.
2 J. Ricny, J. Coupek and S. Tucek, Anal. Biochem., 176 (1989) 221.
3 R.M. Morelis and P. Coulet, Anal. Chim. Acta, 231 (1990) 27.
4 M. Mascini and D. Moscone, Anal. Chim. Acta, 179 (1986) 439.
5 T. Yao, Anal. Chim. Acta, 153 (1983) 153.
6 L. Goldstein and G. Manecke, in L.B. Wingard, E. Katchalski-Katzir and L. Goldstein (Eds.), Applied Biochemistry and Bioengineering, Vol. 1, Academic, New York, 1976, p. 23–110.
7 J.-L. Marty, K. Sode and I. Karube, Anal. Chim. Acta, 228 (1990) 49.
8 K.J. Ichimura, J. Polym. Sci., 22 (1984) 2817.
9 G.L. Ellman, K.D. Courtey, V. Andres and R.M. Featherstone, Biochem. Pharmacol., 7 (1961) 88.
10 C. Tran Minh, P.C. Pandey and S. Kumaran, Biosensors Bioelectron., 5 (1990) 461.

*Analytica Chimica Acta*, 268 (1992) 351–355
Elsevier Science Publishers B.V., Amsterdam



# Spectrophotometric determination of traces of iron using a poly(vinyl chloride) membrane containing bathophenanthroline

Takashi Saito

*Department of Chemical Technology, Kanagawa Institute of Technology, 1030, Shimoogino, Atsugi, Kanagawa 243-02 (Japan)*

(Received 20th February 1992; revised manuscript received 18th May 1992)

**Abstract**

A sensitive and simple spectrophotometric method for the determination of traces of iron using a poly(vinyl chloride) (PVC) membrane containing 4,7-diphenyl-1,10-phenanthroline (bathophenanthroline) and *o*-nitrophenyl octyl ether (*o*-NPOE) was developed. To a 5-ml water sample containing iron, 0.5 ml of $6.5 \times 10^{-2}$ M hydroxylammonium sulphate, $1.3 \times 10^{-2}$ M potassium iodide, and acetic acid–sodium acetate buffer solution (pH 5.0) were added. A sheet of PVC membrane consisting of 1.0 wt.% bathophenanthroline and 64.8 wt.% *o*-NPOE was then placed in the sample solution and stirred with a magnetic stirrer at 60°C. After stirring for a fixed time, the absorbance of the red membrane was measured at 538 nm using a spectrophotometer. The iron concentration in the sample solution was calculated using a calibration graph. The detectable concentration of iron was in the range $6.80 \times 10^{-7}$–$4.29 \times 10^{-5}$ M. Seven repeated measurements with $2.15 \times 10^{-5}$ M iron under the same conditions gave an average, relative standard deviation and repeatability for the absorbances of the membranes of 0.180, 4.3% and 0.0215, respectively.

*Keywords:* UV–Visible spectrophotometry; Bathophenanthroline; Iron; Poly(vinyl chloride) membrane

Some years ago a spectrophotometric method for the determination of trace components in an aqueous solution using a polymer membrane (film) was described [1]. A method using a solid phase such as a membrane as the extraction medium possesses many advantages over conventional liquid–liquid extraction in spectrophotometry: trace components at the $\mu g\ l^{-1}$ level can be determined with high sensitivity because the targeted component is concentrated in a small membrane sheet; by using a membrane incorporating a ligand exhibiting a high reactivity to the targeted component, selective detection of the component can be accomplished; solid-phase extraction is an economical method using only a small amount of extraction solvent and ligand; if the complex formed in the membrane possesses absorption in the visible region, the visible determination of the targeted component can be carried out directly; and the coloured membrane can be stored for a long period of time.

Regarding the application of solid-phase extraction spectrophotometry, methods for the determination of alkylbenzene sulphonates have been reported using a polyurethane foam [2] and poly(vinyl chloride) (PVC) [3] as adsorbents. Spectrophotometric methods for iron(III) [4] and aluminium(III) [5] have also been investigated using a PVC membrane.

For these studies, the spectrophotometric measurement of analyte species is based on the colour of the solid phase formed as a result of

*Correspondence to:* T. Saito, Department of Chemical Technology, Kanagawa Institute of Technology, 1030, Shimoogino, Atsugi, Kanagawa 243-02 (Japan).

ion-pair adsorption of an anionic metal chelate with the crystal violet cation. However, none of the solid phases already mentioned possesses selectivity for the targeted component. By using a polymer membrane which incorporates a chelating reagent with a high reactivity towards the analyte species, these species can be determined with high selectivity. Therefore, no preparative procedures for the separation from other coexisting substances are required. As an example, a spectrophotometric method for traces of copper(II) with a concentration of the order of $10^{-7}$–$10^{-5}$ M has been developed using a PVC membrane containing 4,7-diphenyl-2,9-dimethyl-1,10-phenanthroline (bathocuproine) [6].

In this study, a method for determining total iron, i.e., iron(II) and (III), was investigated using a PVC membrane that included a chelate reagent, 4,7-diphenyl-1,10-phenanthroline (bathophenanthroline), and was found to possess high selectivity and sensitivity towards iron(II).

## PRINCIPLE: MECHANISM OF COLOURING OF THE MEMBRANE

The colouring mechanism of the PVC membrane shown in Fig. 1 was assumed. Iron(II) in the sample solution, which possesses a coordination number of six, is trapped by the bathophenanthroline (B), which is a bidentate ligand, at the PVC membrane surface, and forms a positively charged complex ion ($[Fe \cdot B_3]^{2+}$) with a molar ratio of 1:3. The iron(II) complex ion consists of a regular octahedral structure. Further, the complex ion forms an ion pair with two iodide ions to produce a neutral complex $[Fe^{2+} \cdot 3B \cdot 2I^-]$ at the above membrane surface, which diffuses into the membrane. The molar ratio of iron(II), bathophenanthroline and iodide ion for the iron(II) coordinate complex is 1:3:2. The formation of its complex is expressed by

$$Fe^{2+} + 3B + 2I^- = [FeB_3I_2]$$

The colour of the PVC membrane changed from colourless to red when the iron(II) complex was formed at the membrane surface. The colour intensity of the membrane depends on the concentration of the iron(II)–bathophenanthroline complex, i.e., iron(II). Accordingly, by measuring the absorbance of the red membrane at 538 nm, which is the maximum absorption wavelength of the complex, using a spectrophotometer, the iron in a sample solution can be determined from a calibration graph.

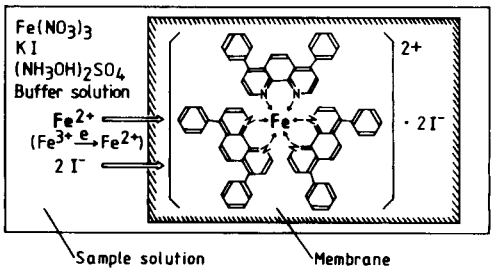


Fig. 1. Extraction mechanism of iron(II) into the PVC membrane containing bathophenanthroline.

## EXPERIMENTAL

### *Reagents and instruments*

Bathophenanthroline, used as a chelate reagent, was of analytical-reagent grade from Dojindo Labs. PVC ($n = 1100$), iron(III) nitrate, potassium iodide, hydroxylammonium sulphate, acetic acid, sodium acetate and tetrahydrofuran (THF) were supplied by Wako. *o*-Nitrophenyl octyl ether (*o*-NPOE) was supplied by Dojindo Labs.

The absorbance of the PVC membrane was measured using a Shimadzu Model UV-150-02 spectrophotometer with a minimum absorbance of 0.0001. For atomic absorption spectrometry, a Shimadzu Model AA-680 instrument was used.

### *Preparation of PVC membrane*

A 0.0242-g amount of bathophenanthroline, 1.622 g of *o*-NPOE as a plasticizer and 0.8561 g of PVC were placed in a 100-ml beaker. The contents of the bathophenanthroline, *o*-NPOE and PVC were 1.0, 64.8 and 34.2 wt%, respectively. THF (25 ml) was then slowly added to the membrane sample with stirring. After the solid had dissolved, the solution was cast in a flat Petri dish with a diameter of 147 mm and stored until

the THF had completely evaporated. The PVC membrane obtained was flexible and had a light yellow colour due to the colour of *o*-NPOE. The PVC membrane was cut into pieces of $5 \times 30$ mm. The thickness of the membrane was 0.150 mm. The volumes of the membranes which were applied in the experiments were $(2.25 \pm 0.056) \times 10^{-2}$ cm$^3$.

*Procedure*

A 5-ml volume of an aqueous solution containing iron was placed in a 30-ml glass sample tube with a PTFE stirring rod (20 mm × 7 mm diameter) and then 0.5 ml of $6.5 \times 10^{-2}$ M hydroxylammonium sulphate, $1.3 \times 10^{-2}$ M potassium iodide and acetic acid–sodium acetate buffer solution (pH 5.0) were added.

A sheet of PVC membrane was placed in the sample solution and stirred with a magnetic stirrer (150 rpm) at 60°C. After stirring for a fixed time (normally 50 min), the membrane was removed from the solution and rinsed with a small amount of water, then wiped to remove any water droplets. The membrane was then put on a glass plate and set in the spectrophotometer holder. The absorbance of the coloured membrane was measured at 538 nm. The same procedure was also carried out with 5 ml of distilled, deionized water in place of the sample solution as a blank test for the reagents used. The iron concentration was calculated from a calibration graph.

## RESULTS AND DISCUSSION

*Effect of temperature*

Figure 2 shows the change in membrane absorbance as a function of time at different temperatures with an iron concentration of $1.07 \times 10^{-5}$ M. The membrane absorbance increased with time and temperature. Although the colouring of membrane took place near room temperature, the absorbance was low and it is not possible to determine traces of iron. Accordingly, a higher temperature is required for a rapid and sensitive analysis. When the temperature was increased to more than 70°C, however, membrane absorbance increased continuously with time. It is suggested that the increasing membrane absorbance is due to the shrinkage of the membrane with time because of the elution of the extracting solvent, *o*-NPOE, from the PVC membrane. A temperature of 60°C was adopted in subsequent experiments.

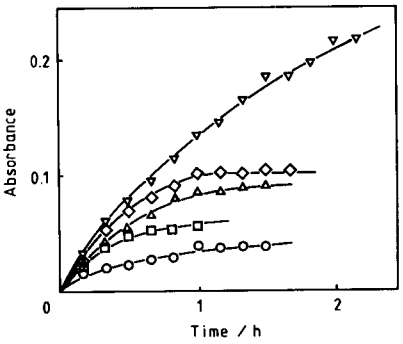


Fig. 2. Effect of temperature on the colouring of the membrane: (○) 30; (□) 40; (△) 50; (◇) 60; (▽) 70°C.

*Effect of counter anion species*

The effect of anion species that form ion pairs with the positively charged iron(II)–bathophenanthroline complex ions was tested, and the results are shown in Fig. 3. $Cl^-$, $Br^-$, $I^-$, $ClO_4^-$ and picrate ions were compared at a concentration of $1.3 \times 10^{-2}$ M.

The colour intensity of the membrane was found to decrease in the order $I^- > ClO_4^-$ > picrate > $Br^-$, $Cl^-$. When $Cl^-$ or $Br^-$ was added as a counter ion, the colouring rate of the membrane was lower than that for the system without a counter ion. For this reason, it was assumed

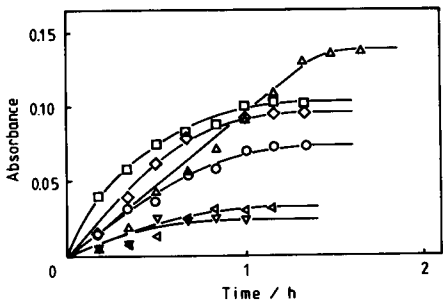


Fig. 3. Effect of counter-ion species on the colouring of the membrane: (▽) $Cl^-$; (◁) $Br^-$; (□) $I^-$; (◇) $ClO_4^-$; (△) picrate ion; (○) no counter ion.

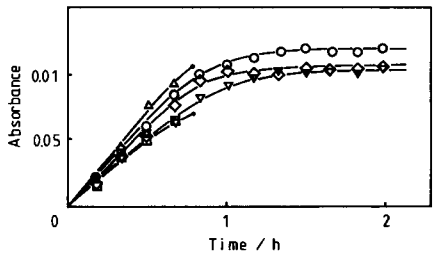


Fig. 4. Effect of pH on the colouring of the membrane. (□) pH 3.5; (△) pH 4.1; (○) pH 5.0; (◇) pH 5.9; (▽) pH 7.0.

that the trapping of iron(II) in the membrane by bathophenanthroline is prevented because of the formation of a halogen–iron(II) complex ion with high hydrophilicity in the aqueous solution. On the other hand, the use of $I^-$ or $ClO_4^-$, which have a higher lipophilicity than $Cl^-$ and $Br^-$, gave a high colour intensity for the membrane. It is suggested that their lipophilic anions act as the driving force for the formation of iron(II)–bathophenanthroline–anion complexes in the membrane.

*Effect of pH*

The most suitable pH value for the formation of the iron(II)–bathophenanthroline chelate compound is in the range 4–6 [7–11]. The effect of pH on the colour changes of the membrane was examined (Fig. 4). At lower pH values the absorbance of the membrane increased. However, at pH 4.1, the colour of the sample solution became red when the solution was stirred for 45 min after starting the experiment. Further, at pH 3.5, red precipitates were generated in the sample solution, which increased with time. Because the solubility of the ligand in water increased with increasing acidity of the sample solution, it is assumed that the iron(II) in the aqueous solution and the bathophenanthroline, which eluted into the aqueous solution from the PVC membrane, formed complexes. In this study, a buffer solution of pH 5.0 was adopted.

*Relationship between iron(II) concentration and membrane absorbance*

The time course of membrane absorbance versus iron(II) concentration is shown in Fig. 5, with initial concentrations of $I^-$ of $1 \times 10^{-3}$ M and iron(II) from $2.1 \times 10^{-6}$ to $4.3 \times 10^{-5}$ M.

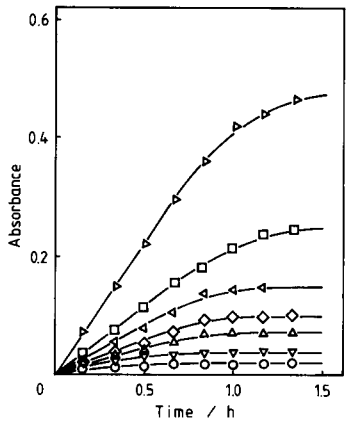


Fig. 5. Relationship between the iron(II) concentration and membrane absorbance. Iron concentration: (○) $2.1 \times 10^{-6}$; (▽) $4.3 \times 10^{-6}$; (△) $8.6 \times 10^{-6}$; (◇) $1.1 \times 10^{-5}$; (◁) $1.7 \times 10^{-5}$; (□) $2.1 \times 10^{-5}$; (▷) $4.3 \times 10^{-5}$ M.

When the iron(II) solution containing a membrane was stirred for 50–60 min, the absorbance of the membrane, i.e., the amount of iron(II) complex in the membrane, became constant. It is assumed that all the iron(II) in the solution was trapped in the membrane because no iron(II) was detected by atomic absorption spectrometry in the solution after stirring for 60 min. However, the colour intensity of the membrane increased with increase of iron(II) concentration. The membrane absorbance after stirring for 50 min was proportional to the initial concentration of iron(II). The calibration graph can be expressed by

$$A = 8.60 \times 10^3[Fe^{2+}]$$

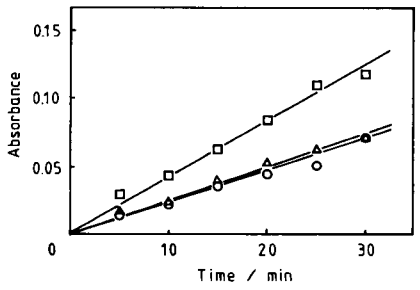


Fig. 6. Effect of $5.0 \times 10^{-6}$ M copper(I) coexisting in $1.0 \times 10^{-5}$ M iron(II) solution. (○) Iron(II) sample; (□) Iron(II) sample containing copper(I); (△) Iron(II) sample containing copper(I) and $5 \times 10^{-5}$ M bathocuproine disulphonic acid disodium salt.

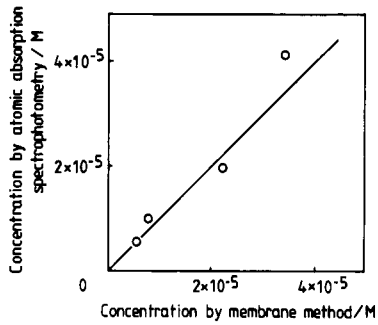


Fig. 7. Correlation of iron(II) concentrations measured by spectrophotometry using a PVC membrane as described here and by atomic absorption spectrometry.

where $A$ is the absorbance of the membrane, and $[Fe^{2+}]$ is the concentration of iron(II) (M). In the range of the already given concentrations, it is expected that the diffusion rate of iron(II) to the membrane interface from the solution was rate determining.

The expected upper limit for the concentration of iron to be measured with the PVC membrane used in this study was $4.29 \times 10^{-5}$ M when 5 ml of sample solution were analysed. This was calculated from the amount of bathophenanthroline ($6.43 \times 10^{-7}$ mol) contained in the membrane, assuming that 3 mol of the ligand reacted with 1 mol of iron(II). The limit of detection for iron, expressed as the concentration equivalent to three times the standard deviation of the blank value of membrane absorbance, is $6.80 \times 10^{-7}$ M. Further, the average, the relative standard deviation and the repeatability, $r$, for the absorbances of the membranes were $0.180 \pm 0.0077$, 4.3% and 0.0215, respectively, from seven repeated measurements with $2.15 \times 10^{-5}$ M iron under the same conditions.

*Interference by metal ions*

Zinc(II), cadmium(II), cobalt(II), nickel(II), aluminium(III) and lead(II) did not interfere in the determination of iron. However, when copper(II) was added at an equimolar concentration to an aqueous solution containing $1.07 \times 10^{-5}$ M iron, a ca. 1.8-fold increase in the absorbance of the membrane occurred, as shown in Fig. 6. Because the colour of the membrane was light brown, it is assumed that a copper(I)–bathophenanthroline chelate compound was formed in the membrane. To eliminate this positive interference by copper(I), bathocuproine sulphonic acid disodium salt was added to the solution as a masking agent. When it was added in greater than a tenfold molar excess over copper(I) the interference of copper(I) was effectively masked.

*Correlation of iron concentrations*

The correlation between the values of iron(II) determined by spectrophotometry using a PVC membrane as proposed here and those obtained by atomic absorption spectrometry was investigated. Four samples containing iron(II) were analyzed by both methods. The results are shown in Fig. 7; the slope of the line is 1.10 and the correlation coefficient is 0.9952.

*Application*

The proposed method was applied to the determination of iron in two water samples, the results being $4.9 \times 10^{-6}$ and $1.4 \times 10^{-5}$ M. The iron in the former sample could not be determined directly using atomic absorption spectrometry without preconcentration of the sample because its concentration was below the detection limit.

REFERENCES

1 Z. Adam and W.E. Hornby, Talanta, 31 (1984) 863.
2 T. Tanaka, K. Hiiro and A. Kawahara, Bunseki Kagaku, 22 (1973) 523.
3 T. Tanaka, K. Hiiro and A. Kawahara, Bunseki Kagaku, 23 (1974) 650.
4 E. Kaneko, H. Tanno and T. Yotsuyanagi, Mikrochim. Acta, I (1991) 37.
5 E. Kaneko, H. Tanno and T. Yotsuyanagi, Mikrochim. Acta, III (1988) 333.
6 T. Saito, Bunseki Kagaku, 40 (1991) 227.
7 M. Miyamoto, Bunseki Kagaku, 9 (1960) 753.
8 A.R. Gahler, R.M. Hamner and R.C. Shubert, Anal. Chem., 33 (1961) 1937.
9 R.E. Peterson, Anal. Chem. 25 (1953) 1337.
10 R.P. Hair and E.J. Newman, Analyst, 89 (1964) 42.
11 D.J.B. Galliford and E.J. Newman, Analyst, 87 (1961) 68.

*Analytica Chimica Acta*, 268 (1992) 357–359
Elsevier Science Publishers B.V., Amsterdam



# Acid decomposition procedure for the spectrophotometric determination of silica in rocks and minerals at room temperature

C.R.M. Rao, G.S. Reddi and T.A.S. Rao

*Chemical Laboratory, Geological Survey of India, Madras 600 032 (India)*

(Received 20th March 1992; revised manuscript received 19th May 1992)

**Abstract**

An acid decomposition procedure at room temperature for the spectrophotometric determination of silica in rocks and minerals is described. The sample solution is prepared by treatment with hydrofluoric acid and aqua regia at room temperature. Unreacted fluoride ions are complexed with boric acid and the silica is determined by the molybdenum blue method. Accurate values were obtained for a number of international reference standards. The entire procedure is carried out at room temperature. Only plastic ware is used for the decomposition of the samples. The method is thus ideal for large batch analyses.

*Keywords:* Sample preparation; UV–Visible spectrophotometry; Acid decomposition; Geological materials; Minerals; Rocks; Silica

Most spectrophotometric methods for the determination of silica in rocks and minerals utilize fusion with alkali metal carbonates or peroxides for the sample decomposition. Some methods also involve decomposition with hydrofluoric acid in closed vessels at elevated temperature to bring the silica into a soluble form [1,2]. The different stages of these procedures need considerable care to prevent loss of analyte. In this work studies were made of the suitability of a solution of a rock sample obtained by hydrofluoric acid and aqua regia decomposition at room temperature, as described previously [3,4], for the spectrophotometric determination of silica by the molybdenum blue method. It was observed that the excess of hydrofluoric acid after complexation with boric acid does not interfere in the colour development and accurate results for silica were obtained. The spectrophotometric measurements were made at 650 nm [5].

The accuracy of the method was established by analysing international standards. The reproducibility of the $SiO_2$ values obtained by the suggested method was determined by taking two samples containing 49.1 and 78.7% of $SiO_2$. Plastic ware was used for the decomposition stage. This method involves fewer stages in sample decomposition than other methods and is considered ideal for batch analyses of large numbers of rock samples.

*Correspondence to:* C.R.M. Rao, Chemical Laboratory, Geological Survey of India, Madras 600 032 (India).

## EXPERIMENTAL

### *Apparatus and reagents*

Polyethylene bottles of 100-ml capacity with screw-caps were used. Analytical-reagent grade chemicals were used throughout.

Ammonium molybdate reagent was prepared by dissolving 10 g of ammonium molybdate in 100 ml of 1 M ammonia solution and adding 20 ml of HCl (1 + 1) with stirring. The reducing solution was prepared by dissolving 0.7 g of anhydrous sodium sulphite and 0.15 g of 1-amino-2-naphthol-4-sulphonic acid in 10 ml of water. Separately, 9 g of sodium or potassium metabisulphite were dissolved in 90 ml of water and the two solutions were mixed. Other reagents were 10% aqueous oxalic acid, 40% hydrofluoric acid, boric acid and aqua regia.

*Procedure*

A 0.1-g amount of each of the powdered rock test samples ( < 250 mesh) and two in-house standard rock samples of known silica content (AMDEL 24412, basalt, 45.05% $SiO_2$; AMDEL 24415, rhyolite, 72.10% $SiO_2$) were weighed into polyethylene bottles. A blank was also run simultaneously. A 2-ml volume of aqua regia and 6 ml of hydrofluoric acid were added and the capped bottles were allowed to stand at room temperature for 24 h. The contents of the bottles were diluted with 20 ml of demineralized water, then 5.6 g of boric acid were added and the contents of the bottles were transferred quantitatively into 100-ml volumetric flasks, diluted to volume with water and shaken thoroughly until a clear solution was obtained.

A 1-ml volume of the sample solution was pipetted into a 100-ml volumetric flask (for samples containing less $SiO_2$, e.g., limestone, bauxite, large aliquots of sample solution were taken with corresponding addition of blank solution to the in-house standards to maintain the same pH and salt content) and 15 ml of demineralized water and 2 ml of ammonium molybdate solution were added and mixed and the flask was left aside for 10 min. To the mixture 5 ml of 10% oxalic acid solution and 2 ml of the reducing solution were added and the solution was diluted to 100 ml with demineralized water. After 1 h the absorbance values of the test samples were determined at 650 nm and compared with those of the in-house standard rock samples and the $SiO_2$ values for the test samples were calculated.

A typical analysis of a sample containing 50.04% of $SiO_2$ gave, for the suggested amount of sample and solution, an absorbance reading of 0.58. The test samples were also analysed for their $SiO_2$ contents using the conventional gravimetric method [6].

TABLE 1

Comparison of results obtained with the proposed method and with the conventional gravimetric method [6]

| Test sample | $SiO_2$ (%) [a] | |
|---|---|---|
| | Proposed method | Conventional method |
| Ultrabasic rock | 40.25 | 39.91 |
| Basalt | 51.37 | 51.64 |
| Granite | 67.52 | 67.88 |
| Granite | 75.66 | 75.23 |

[a] Each value is an average of three determinations.

## RESULTS AND DISCUSSION

The results obtained by the proposed acid decomposition method and conventional gravimetric methods are in good agreement (Table 1). Following the suggested method, eight independent determinations were made on two samples containing 49.1 and 78.7% of $SiO_2$. The precision was good (Table 2). Further, a number of international standards were analysed by the proposed method and the results obtained compared

TABLE 2

Reproducibility of results for silica obtained by the proposed method

| Determination No. | $SiO_2$ (%) | |
|---|---|---|
| | Basalt sample | Granite sample |
| 1 | 48.15 | 77.97 |
| 2 | 49.00 | 78.85 |
| 3 | 48.58 | 77.97 |
| 4 | 50.28 | 79.74 |
| 5 | 49.86 | 79.74 |
| 6 | 49.43 | 78.85 |
| 7 | 48.75 | 78.41 |
| 8 | 49.34 | 78.15 |
| S.D. | 0.697 | 0.723 |
| R.S.D. (%) | 1.417 | 0.918 |

TABLE 3

Silica contents of standard reference samples determined by the proposed method

| Sample | Type | $SiO_2$ (%) | |
|---|---|---|---|
| | | Proposed method | Certified value |
| NBS 143 | Argillaceous limestone | 6.71 | 6.84 |
| NBS 104C | Bauxite | 6.58 | 6.81 |
| FeR 1 | Irone ore | 16.59 | 16.90 |
| MRG 1 | Ultrabasic rock | 39.61 | 39.32 |
| BCS 315 | Clay | 51.60 | 51.24 |
| W 1 | Basalt | 52.58 | 52.72 |
| GH | Granite | 75.37 | 75.85 |
| In-house standard (AMDEL 24413) | Granite | 65.42 | 65.75 |
| In-house standard (AMDEL 24419) | Basalt | 51.37 | 51.00 |

favourably with the certified values (Table 3), demonstrating the efficacy of the method for the determination of silica. The decomposition method described was also found to be suitable for the determination of silica in iron ore, bauxite limestone and related materials.

The use of plastic ware and the avoidance of heating at any stage render the method rapid and adaptable for large batch analyses. An advantage of the method is the limited personal attention required at the decomposition stage, which decreases the likelihood of errors.

The authors thank Sri C.R. Narayanan, Director, Geological Survey of India, for helpful suggestions and the Australian Mineral Development Laboratories (AMDEL), Adelaide, for providing the standards.

REFERENCES

1 W.M. Johnson and J.A. Maxwell, Rock and Mineral Analysis, Wiley, New York, 1981.
2 T. Suzuki and M. Sensui, Anal. Chim. Acta, 245 (1991) 43.
3 C.R.M. Rao and G.S. Reddi, Anal. Chim. Acta, 237 (1990) 251.
4 G.S. Reddi, C.R.M. Rao, T.A.S. Rao and H.S. Muralidhar, Anal. Chim. Acta, 251 (1991) 205.
5 P.G. Jeffery, Chemical Methods of Rock Analysis, Pergamon, Oxford, 1970, p. 397.
6 W.F. Hillebrand and G.E.F. Lundell, Applied Inorganic Analysis, Wiley, London, 1953, p. 793.

*Analytica Chimica Acta*, 268 (1992) 361–363
Elsevier Science Publishers B.V., Amsterdam



# BOOK REVIEWS

Satinder Ahuja, *Trace and Ultratrace Analysis by HPLC*, Wiley-Interscience, New York, 1992 (ISBN 0-471-51419-5). xi + 419 pp. Price £59.00.

This text seeks to provide a discussion of high-performance liquid chromatography (HPLC) in terms of its application to analyses at the trace ($\mu g\ g^{-1}$) and ultratrace ($< \mu g\ g^{-1}$) levels. Some introductory comments on the problems of these analyses, together with some typical examples are provided in Ch. 1. Chapter 2 addresses theoretical considerations, whilst some aspects of HPLC instrumentation are covered in the following two chapters. Sample preparation methods are treated in Ch. 5 and procedures for method development are covered in Ch. 6. Methods for optimizing selectivity (Ch. 7) and detectability (Ch. 8) are then discussed, with the remainder of the book (some 110 pp.) being devoted to the use of HPLC in the analysis of pharmaceuticals, foods, environmental samples and cosmetics.

The book is written in a narrative style and contains relatively few illustrations and diagrams for a work of its length. I was left wondering about the real purpose of this text. The choice of material is fairly general and does not represent a full treatment of those aspects of HPLC methodology of particular relevance to trace and ultratrace analysis. For example, on-line preconcentration methods are covered very superficially, despite their importance to the subject. The depth of treatment varies considerably between topics and there is a tendency in places for the level of detail in both theory and discussion to become excessive. The utility of the extensive applications chapter is somewhat diminished by the rather scant index (7 pp.).

I consider that this book may appeal to those needing a general overview of HPLC, but it does not provide a great deal of specialist information for readers seeking guidance and methodology for trace and ultratrace analysis.

Paul R. Haddad

E. Smolková-Keulemansová and L. Feltl, *Analysis of Substances in the Gaseous Phase* (*Wilson & Wilson's Comprehensive Analytical Chemistry*, Vol. XXVIII, Series Editor G. Svehla), Elsevier, Amsterdam, 1991 (ISBN 0-444-89122-6). xiv + 480 pp. Price US$205.00/Dfl.400.00.

As the Series Editor points out in his preface, the subject of gas analysis is a somewhat neglected field, but has experienced a considerable revival due to interest in environmental measurement of gases. Given this comment by the Series Editor it is sad that the book does not make any real contribution to meeting the need for books on the analytical chemistry of atmospheric trace gases. The book is strong on basic principles, starting with the history of gas analysis, going through the gas laws and dealing with the fundamentals of many of the traditional methods. It is, however, very weak on up-to-date applications and instrumentation. For example, the Orsat apparatus is described in considerable detail, and the nitric oxide plus ozone chemiluminescence procedure is described but without discussion of the instrumentation. However, more modern methods like the nitrogen dioxide luminol method for trace analysis of $NO_2$ does not receive a mention, nor does the diffusion tube procedure for analysis of this and other gases. Almost 50% of the book deals with gas chromatography and whilst this deals in detail with theory, only 14 pages are devoted to the applications of gas chromatography, and of these, only two are on gas analysis. The book finishes with a bibliography citing a rather small number of papers, many of them from the 1960s and 70s as well as company

literature, much of which is at least 10 years old. There are no references cited in the text itself. Regrettably this is a book which could, and should, have been written about 20 years ago. Whilst good on theory it does not describe the applications of the 1990s; it will be of value to those looking for traditional methods, but not to those seeking the most up-to-date applications and methods.

Roy M. Harrison

R.J.H. Clark and R.E. Hester (Eds.), *Spectroscopy of Advanced Materials*, Wiley, Chichester, 1991 (ISBN 0-471-92981-6). xv + 405 pp. Price £115.

This book is volume 19 in the *Advances in Spectroscopy* series and contains 6 chapters written by a grand total of 16 authors. The preface is only somewhat more than 2 pages long and is nothing more than an introduction of the authors of the different chapters followed by a 3 page survey of the SI units. The topics of the present volume deal with materials science with descriptions in the different chapters devoted to infrared and Raman spectroscopy, pulsed neutron and photoexcitation spectroscopy for the study of materials, including organic conductors, non-linear optical materials, semi- and superconductors and polyconjugated systems.

The editors are professors of chemistry at University College, London and the University of York. The authors are all carefully selected specialists from different countries with affiliations at university laboratories, specialised institutes and industrial laboratories.

Articles are well written, apparently carefully edited and nicely produced. The articles refer to an abundant set of up-to-date literature references, some of them as recent as 1990. The index, *the* weak point of many multi-authored works, is well designed and useful.

The book is intended for a rather specialised public and not at all, as is stated on the book cover, for a public of scientists and technologists, teachers and graduate and undergraduate students. Neither is it a self-contained account of technological materials and their characterization. It is rather a selection of both materials and experimental techniques. Several further volumes of this series would be needed to describe this expanding field in some detail. With these shortcomings it is a recommendable addition to the library of materials science laboratories.

F. Adams

Bruce Asamoto (Ed.), *FT-ICR/MS: Analytical Applications of Fourier Transform Ion Cyclotron Resonance Mass Spectrometry*, VCH, Weinheim, 1991 (ISBN 0-895-73767-1). xii + 306 pp. Price £47.00/DM134.00.

The editor has brought together a collection of in depth articles, by experts in the field, on the implementation of the FT-ICR/MS technique in the domain of analytical mass spectrometry. The text is divided into ten chapters, the first two being a wide ranging historical and theoretical introduction to the topic and a comprehensive description of instrumentation and design features. Subsequent chapters describe the theory and practical applications in detail of the external ion source, chemical ionisation FT/MS, laser desorption ionisation, UV laser microprobe, HPLC interfacing and the application of FT/MS to agricultural chemistry, biotechnology and the structural analysis of peptides. Extensive listings of current references are provided for each chapter. The authors have made an effort to emphasize the facets of FT/MS which provide superior data in comparison with other mass spectrometric techniques and also describe areas in which the technique may be less informative.

Practising mass spectroscopists and those considering new fields of analysis or instrumentation will welcome this comprehensive review of the most recent addition to the established techniques of mass spectrometry. Those involved in scientific education who simply wish to keep abreast of current developments will also find the volume to be a reference work of great merit, well presented and illustrated and at a price,

which by present standards, is extremely good value.

A.D. Roberts

TrAC—*Trends in Analytical Chemistry, Reference Edition 1991*, Vol. 10, Elsevier, Amsterdam (ISBN 0-444-89503-5). viii + 372 pp. Price US$311.50/ Dfl.545.00.

This volume contains all the scientific articles originally published in the monthly editions of TrAC in 1991, printed on high quality paper, and bound in hard covers. It contains a wealth of short review articles covering most of the growing areas of analytical science, as well as the various "computer corner" items, meeting reports and feature articles. These "trends" provide excellent indicators of the directions in which analytical science is advancing, supported by extensive information on these developments. As such, it will be of great value both to practising analytical scientists and to students.

Irving Sunshine (Ed.), *Recent Developments in Therapeutic Drug Monitoring and Clinical Toxicology*, Marcel Dekker, New York, 1992 (ISBN 0-8247-8586-X). xii + 791 pp. Price US$175.00 (US and Canada), US$201.25 (all other countries).

This bulky tome is a collection of manuscripts presented at the *Second International Conference on TDM-Toxicology, Barcelona*, on an unspecified date. There are 113 papers, grouped under Therapeutic Monitoring (25 papers), Pharmacology (17), Liquid Chromatographic Methods (16), Antileptics (12), Substances Subject to abuse (17), Inorganics (6) and Miscellaneous (20). There is a subject index.

G.A. Webb (Ed.), *Annual Reports on NMR Spectroscopy*, Vol. 24, Academic Press, London, 1992 (ISBN 0-12-505324-X). ix + 373 pp. Price £65.00/ US$139.00.

This volume in the long running series reflects "the protean nature of the applications of NMR". It includes solid state NMR, including imaging, studies of interfaces, measurements of intercellular ions in living systems, mercury-199 NMR and applications in coal research. As always, there is a good subject index.

B. Jezowska-Trzebiatowska, B. Kochel, J. Sławiński and W. Stręk (Eds.), *Biological Luminescence*, World Scientific, Singapore, 1990 (ISBN 981-02-0405-1). xi + 647 pp.

This book contains 44 papers in camera ready form which were presented at an International School on Biological Luminescence held in Poland in June 1989. The aim of the meeting was to promote interdisciplinary discussion on the luminescence of biosystems and included lecturers on physics, chemistry, biology, biocybenetics, medicine and environmental protection.

The presentations are categorised under the headings biophysical and biocybenetic, biological, biochemical, physico-chemical, and medical and other applications. The biochemical section discusses the properties of a range of luciferases, particularly bacterial systems, but there is very little material that is of direct analytical interest. There is also no subject index which makes it difficult for the interested non-specialist to obtain information.

This book is therefore not of particular relevance to an analytical chemistry readership.

ANALYTICA CHIMICA ACTA, VOL. 268 (1992)

# AUTHOR INDEX

# NEWS BRIEF

## Los Alamos opens analytical chemistry lab

LOS ALAMOS National Laboratory is building an automated analytical chemistry laboratory to assist researchers in tackling work in developing clean-up technologies for nuclear and chemical wastes. The volume and magnitude of chemical analysis required for understanding the clean-up requirements of dozens of contaminated federal sites, including national laboratories, is considered to be formidable. Cyberlab, the new laboratory complex being designed in Los Alamos, is expected to go a long way in addressing these complex analytical needs. Utilizing a high level of robotics and automation, the system will have interchangeable, standard laboratory modules that conduct filtering, measuring, and analytic tasks.

DOE's environmental restoration program is projected to have a workload of 10 million samples a year by 1995. At the current cost of $300 a sample, the expense would be prohibitive, so DOE has embarked on a plan to develop new technology that will dramatically cut those costs. If successful, Cyberlab could set a new industrial standard for carrying out chemical analyses.

*Source: New Technology Week, 4 May 1992*

***Readers are invited to send any news item that they would like to have considered for publication in this section to:***
***ACA Newsbrief***
***Elsevier Science Publishers***
***P.O. Box 330,***
***1000 AH Amsterdam,***
***The Netherlands***
***Fax: (+31) 20 5862 845***

## Award Symposia

THE 44th Pittsburgh Conference and Exposition will feature several technical sessions in which awards will be presented to distinguished scientists. The Award Symposia currently planned for PITTCON '93 include: Pittsburgh Spectroscopy Award (sponsored by the Spectroscopy Society of Pittsburgh), Maurice F. Hasler Award, Charles N. Reilley Award, Dal Nogare Award, Bomem-Michelson Award, Pittsburgh Analytical Chemistry Award (sponsored by the Society for Analytical Chemists of Pittsburgh), Keene P. Dimick Award, James L. Waters Symposium, and the Williams–Wright Industrial Spectroscopist Award.

# Announcements of meetings

### *WCFIA 93, WINTER CONFERENCE ON FLOW INJECTION ANALYSIS, MARATHON, FLORIDA KEYS, FL, USA, JANUARY 3–6, 1993*

Much of the progress made by FIA over the years results from better hardware designs and innovative chemical applications. WCFIA 93 is intended to meld these two important aspects of science.

WCFIA 93 will focus on industrial FIA techniques solving real world problems. New hardware as well as software-driven applications will be presented.

The three-day conference will highlight the following areas:

— Process Chemistry
— Biotechnology
— Instrument Design
— New Methods
— Atomic Spectroscopy
— Electrochemistry

The conference also offers a unique opportunity for informal exchange of information and ideas among chemists and engineers in the FIA field.

For further information, please contact: WCFIA 93, c/o Gary D. Christian, Department of Chemistry BG-10, University of Washington, Seattle, WA 98195, USA.

### *PITTCON '93. THE 44th PITTSBURGH CONFERENCE & EXPOSITION ON ANALYTICAL CHEMISTRY AND APPLIED SPECTROSCOPY, ATLANTA, GA, USA, MARCH 8–12, 1992*

The Pittsburgh Conference Committee presents PITTCON '93, March 8 to 12 in Atlanta, Georgia. The technical program features the best of new technological developments and applications in Analytical Chemistry, Spectroscopy and related sciences. Special sessions, invited symposia, contributed papers and short courses will be presented. In addition, the exposition of modern laboratory instrumentation, equipment, supplies and services will showcase the latest developments from around the world.

You are invited to submit a contributed paper for consideration as an oral presentation or as a poster. The Program Committee will review all submissions and will select those presentations that will be included in the 1993 technical program. Papers are requested in the following categories:

**Methodology**
— Atomic Spectroscopy
— Chemometrics
— Computers
— Electrochemistry
— Gas Chromatography
— Liquid Chromatography
— Magnetic Resonance
— Mass Spectroscopy
— Sample Handling/Automation
— Scanning Probe Microscopy
— Separation Sciences
— Supercritical Fluid Separations
— Thermal Analysis
— UV/VIS Absorbance/Luminescence
— Vibrational Spectroscopy
— Other

**Application**
— Basic Chemical Research
— Bioanalytical
— Clinical Toxicology
— Environmental
— Food
— Forensic
— Fuels & Energy
— Industrial Hygiene
— Instrumental Development/Improvement
— Material Characterization
— Process Chemistry
— Other

For further information, please contact: Mrs. Alma Johnson, Program Secretary, The Pittsburgh Conference, 300 Penn Center Blvd., Suite 332, Pittsburgh, PA 15235-5503, USA. Tel.: 412 825-3220.

### *5th SYMPOSIUM ON THE ANALYSIS OF STEROIDS, SZOMBATHELY, HUNGARY, MAY 3–5, 1993*

The 5th Symposium on the Analysis of Steroids is sponsored by the Analytical Division of the Chemical Section of the Hungarian Academy

of Sciences and the Chemical Works of Gedeon Richter Ltd., Budapest. Topics covered will include:

— *Environment, steroids and cancer.* Analysis of steroids and related compounds in metabolic studies.
— *Determination of steroids in biological samples.* Clinical steroid analysis. Analytical methodology for studying the biosynthesis, regulation, metabolism and receptors of steroids as well as the pharmacokinetic study of steroid drugs. Determination of steroids in samples of plant and animal origin.
— *Industrial and pharmaceutical steroid analysis.* Methods for the purity testing of steroids. Analysis of pharmaceutical dosage forms including stability assays. Analysis of the intermediates of steroid syntheses. Structure elucidation of steroids.

The scope of the symposium covers discussion of methodological problems as well as practical applications drawn from the fields of all the main steroid groups (hormones, sterols, vitamin D, bile acids, cardiac glycosides, sapogenins, alkaloids etc.).

The organizing and scientific committees comprise: S. Görög (Budapest, Chairman), P. Horváth (Budapest, Secretary), H. Adlercreutz (Helsinki), P. Arányi (Budapest), Gy. Falkay (Szeged), T. Fehér (Budapest), K. Griffiths (Cardiff), B. Herényi (Budapest), W. Hubl (Dresden), L.G. Kovács (Szombathely), A. Laukó (Budapest), T.L. Paál (Budapest), L. Stárka (Prague), and K.Sz. Szalay (Budapest).

For further information, please contact: Prof. S. Görög, c/o Chemical Works of Gedeon Richter Ltd., P.O. Box 27, H-1475 Budapest, Hungary. Phone: +36 1-1574-566; Fax: +36 1-1571-578; Telex: 22-5067 right h.

## *EUROPEAN SEMINAR ON INFRARED SPECTROSCOPY, LYON, FRANCE, JUNE 7–9, 1993*

The purpose of this seminar is to provide an overview of the technology that has been developed over the years. It will be of interest to both future and existing users of IR and Raman spectroscopy. Lectures will cover a wide range of applications. A further aim is to assemble users for an exchange of scientific ideas and for fruitful contact between academia and industry.

The scientific programme will consist of plenary lectures and contributed papers (from users and manufacturers). You are invited to submit papers for oral presentation (15 minutes including questions/discussion) or poster.

Papers should concern the following subjects: Recent applications, process and quality control or instrumental development of the infra-red technology in the field of microscopy (FTIR Raman including optical hot stage), near infra-red, hyphenated systems, photoacoustic spectroscopy and other related techniques.

The languages of the seminar will be French and English.

A poster prize is being offered to encourage authors. The posters will be judged according to their didactic character and presentation.

For further information, please contact: G. Lachenal, Université Lyon I, Laboratoire des Matériaux Plastiques et des Biomatériaux, 43 Boulevard du 11 Novembre 1918, 69622 Villeurbanne Cédex, France. Fax: +33 78 89 25 83.

## *PREP-93, 10th INTERNATIONAL SYMPOSIUM ON PREPARATIVE CHROMATOGRAPHY, ARLINGTON, VA, USA, JUNE 14–16, 1993*

PREP-93 will be held at the Key Bridge Marriott Hotel in Arlington, Virginia, which is located minutes from Washington National Airport and Georgetown. The three-day program will include invited and contributed lectures, poster presentations, an exhibit of software and technical literature, and discussion sessions.

You are invited to submit an abstract for consideration for inclusion in the program. Papers should describe original research in areas of preparative chromatography, especially:
— Theory of Non-Linear Chromatography, Overloaded Elution and Displacement Chromatography
— Kinetics of Mass Transfer at High Concentrations
— Stationary Phases
— Applications to Drugs and Specialty Chemicals
— Applications to Recombinant and Natural Proteins to Peptides, Other Biopolymers, Chiral Separations, etc.

— Optimization of Experimental Conditions
— Economics of Preparative Chromatography
— Instrumentation

The Scientific Committee welcomes suggestions for additional topics to be covered in the Symposium. The deadline for submission of abstracts is December 1, 1992. Abstracts received after this date will be considered for poster presentation.

For further information, please contact: Barr Enterprises, P.O. Box 279, Walkersville, MD 21793, USA. Tel.: 301 898-3772; Fax: 301 898-5596.

## *5th EUROPEAN CONFERENCE ON THE SPECTROSCOPY OF BIOLOGICAL MOLECULES, LOUTRAKI, GREECE, SEPTEMBER 5–10, 1993*

This international conference will focus mainly on the structure and dynamics of biological and related systems as determined from Raman and IR spectroscopic methods. However, it will also provide a critically comparative review of recent progress in this field as achieved through the application of other methods, particularly NMR, CD, optical absorption and fluorescence, X-ray crystallography and neutron scattering.

Topics to be included are: proteins — structure, conformation and dynamics — drug and metal interactions; chromophoric proteins — haem systems, rhodopsins, photosynthetic systems, etc.; enzymes — reaction kinetics and mechanism-substrate/inhibitor interactions; nucleic acids — structure, conformation and dynamics — drug and metal interactions; protein–nucleic interactions; biomembranes — lipids, organization, interactions with proteins; carbohydrates — oligo- and polysaccharides; biochemical/biotechnological applications; experimental methods, FT-Raman techniques; theoretical methods; supramolecular chemistry and molecular recognition; other topics such as environmental applications, etc. will also be considered.

The scientific programme will include invited lectures and poster sessions, with an emphasis on providing opportunities for discussion. There will be no parallel sessions. Submission of oral and poster papers is invited in all the topic areas of the conference. The organizing committee will select the oral presentations and will issue invitations in January 1993.

A major exhibition of spectroscopic instrumentation and equipment will be held in conjunction with the scientific programme.

For further details, please contact: Professor Theo Theophanides, Chairman of ECSBM '93, Department of Chemical Engineering, National Technical University of Athens, Zografou Campus, Zografou 15780, Athens, Greece. Phone: +30 1-7792438, 724227 or 7728114; Fax: +30 1-7700989.

## *APPLICATIONS OF HPLC AND CE IN THE BIOSCIENCES, VERONA AND SOAVE, ITALY, SEPTEMBER 7–10, 1993*

A three-day International Symposium on Applications of HPLC and Capillary Electrophoresis in the BioSciences, resulting from the combined 12th International Symposium on Biomedical Applications of Chromatography and Electrophoresis and the 2nd International Symposium on Applications of HPLC in Enzyme Chemistry, will be held in Verona and Soave (Italy). Organized by the Institute of Forensic Medicine of the University of Verona and the Institute of Chemistry of the University of Brescia, School of Medicine, the Symposium will focus on five areas:

— New methodological achievements in HPLC and CE applied to the biosciences
— HPLC and CE analysis of drugs and other toxic substances in biological media
— HPLC and CE in enzyme analysis
— HPLC and CE in immunochemistry and DNA analysis
— Use of bioreactors in HPLC and CE.

The selection of the invited speakers will reflect this focus. In addition to the plenary lectures, the programme will consist of oral presentations and posters. The language of the symposium will be English.

The papers presented will be published in a special issue of *Journal of Chromatography: Biomedical Applications.*

For further information, please contact: Dr. F. Tagliaro, Scientific Secretariat, c/o Istituto di Medicina Legale, Policlinico Borgo Roma, I-37134 Verona, Italy.

***HTC 3. THIRD INTERNATIONAL SYMPOSIUM ON HYPHENATED TECHNIQUES IN CHROMATOGRAPHY, ANTWERP, BELGIUM, FEBRUARY 22–25, 1994***

The symposium will cover all fundamental aspects, instrumental developments and applications of the various hyphenated chromatographic techniques, e.g. GC–GC, GC–MS, PTV–GC–MS, GC–MS–MS, GC–FTIR, GC–AED, LC–MS, LC–LC, LC–GC–MS, LC–LC–GC, LC–FIA–DAD, LC–SFC, SFC–LC, SFC–MS, SFC–FTIR, SFE–GC, SFE–LC, CZE–MS, CCC–MS, ITP–MS, etc. In parallel, all prominent manufacturers of chromatographic instruments and accessories will participate in an exhibition of their newest equipment.

The scientific programme will comprises both oral and poster presentations. The official language will be English. Papers are invited in the above and related areas.

Papers presented at the symposium will be reviewed for publication in a special volume of *Journal of Chromatography*. The deadline for the receipt of abstracts is June 30, 1993.

For further information, please contact: Royal Flemish Chemical Society (KVCV), Working Party on Chromatography, c/o Dr. R. Smits, BASF Antwerpen N.V., Central Laboratory, Scheldelaan, B-2040 Antwerp, Belgium. Phone +32 3-568.28.31; Fax: +32 3-568.32.50; Telex: 31047 basant b.

***Announcements are included free of charge. Information on planned events should be sent well in advance (preferably 6 months or more) to: ACA Newsbrief, Elsevier Science Publishers P.O. Box 330, 1000 AH Amsterdam, The Netherlands Fax: (+31) 20 5862 845***

# Calendar of forthcoming meetings

★ *indicates new or amended entry*

★ ***October 26, 1992***
***Zürich, Switzerland***
Workshop: Identity Testing in the Pharmaceutical Industry. *Contact:* Mr. Lars Fährstedt, Chairman of the Section, AB Astra, S-151 85 Södertälje, Sweden. Fax: +46 8 5532 8832.

★ ***November 2–5, 1992***
***Amsterdam, The Netherlands***
Fourier Transform Infrared (FTIR) Spectroscopy. A Four-Day Intensive Course. *Contact:* The Center for Professional Advancement, Oudezijds Voorburgwal 316A, 1012 GM Amsterdam, The Netherlands. Tax: +31 20-6202136.

***November 3–5, 1992***
***Helsinki, Finland***
KEMIA '92 Exhibition and Finnish Chemical Congress. *Contact:* Ms. Eva Kota-aho, Programme Secretary, The Association of Finnish Chemical Societies, Hietaniemenkatu 2, SF-00100 Helsinki, Finland. Tel.: +358 408-022; Fax: +358 408-780.

***November 4–5, 1992***
***Hyatt Cherry Hill Hotel, NJ, USA***
CHEMICAL SPECIALITIES USA 92 (formerly known as CHEMSPEC USA) Exhibition and Symposium. *Contact (for exhibition details):* Mike Tarrant, Exhibition Sales Director, FMJ International Publications Ltd., Queensway House, 2 Queensway, Redhill, Surrey RH1 1QS, UK. Tel.: +44 737-768611; Fax: +44 737-671685; Telex 948669 topjnl g. *Contact (for symposium details):* John Woolner, Spring Innovations Ltd., 216 Moss Lane, Bramhall, Stockport K7 1BD, UK. Tel.: +44 61 440-0082; Fax: +44 61 440-8095.

***November 4–6, 1992***
***Montreux, Switzerland***
9th Montreux Symposium on Liquid Chromatography–Mass Spectrometry (LC/MS, SFC/MS, CZE/MS, MS/MS). *Contact*: M. Frei-Häusler, IAEAC Secretariat, Postbox 46, 4123 Allschwil 2, Switzerland. Tel.: +41 61-632789; Fax: +41 61-4820805. *(Further details published in Vol. 248, No. 2).*

★ ***November 12, 1992***
***Manchester, UK***
Recent Advances and Applications of Hyphenated Techniques. *Contact:* Analytical Division, The Royal Society of Chemistry, Burlington House, Piccadilly, London W1V 0BN, UK. Tel.: +44 71-437 8656.

***November 16–17, 1992***
***Tübingen, Germany***
GC–MS in the Bioanalytical. Chromatographic–Mass Spectrometric Methods. *Contact:* Universitätsbund Tübingen, WiT - WissensTransfer, Wilhelmstrasse 5, 7400 Tübingen, Germany. Tel. +49 7071 296439.

***November 16-20, 1992***
***Somerset, NJ, USA***
Eastern Analytical Symposium and Expo. *Contact:* Mr. Badoux, c/o RWB Convention Management, 4704 Bert Drive, Monroeville, PA 15146, USA. Tel. 412 372-8965; Fax: 412 372-6748.

★ ***November 18, 1992***
***Teddington, UK***
Standardization and Nomenclature in Chromatography. *Contact:* Dr. D. Simpson, Analysis for Industry, Factories 2/3, Bosworth House, High Street, Thorpe-le-Soken, Essex CO16 0EA, UK. Tel.: +44 255-861714; Fax: +44 255-862111.

★ ***November 18–21, 1992***
***Gosen, Germany***
7th CIC Workshop: Software Development in Chemistry. *Contact:* Prof. Dr. Dieter Ziessow, 7 CIC, Iwan-N.-Stranski-Institut, Technische Universität Berlin, Strasse des 17 Juni 112, W-1000 Berlin 12, Germany. Tel.: +49 30-314 24958; Fax: +49 30-314 26602.

***November 24–27, 1992***
***Milan, Italy***
ATB '92. Advanced Technology for the Clinical Laboratory and Biotechnology. 8th European Edition of the Oak Ridge Conference. *Contact:* ATB '92 Conference, Via Carlo Farini 70, 20135 Milan, Italy. Tel.: +39 2-66802323; Fax: +39 2-6686699.

***November 29–December 2, 1992***
***Sydney, Australia***
12th International Symposium on HPLC of Proteins, Peptides and Polynucleotides. *Contact:* 12 ISPPP Secretariat, G.P.O Box 128, Sydney, NSW 2001, Australia. Tel.: +61 2 262-2277; Fax: +61 2 262-2323. *(Further details published in Vol. 264, No. 2).*

***December 1-5, 1992***
***Jakarta, Indonesia***
6th Chemical Instrumentation and Laboratory Indonesia Exhibition (CIL 92). *Contact:* Matthew Meredith, Overseas Exhibition Services Ltd., 11 Manchester Square, London W1M 5AB, UK. Tel.: +44 71-486-1951; Fax: +44 71-486-8773 or 413-8222; Telex: 24591 MONTEX G.

★ ***December 2–4, 1992***
***Amsterdam, The Netherlands***
Near Infrared Spectroscopy. A Three-Day Intensive Course. *Contact:* The Center for Professional Advancement, Oudezijds Voorburgwal 316A, 1012 GM Amsterdam, The Netherlands, Tel.: +31 20-6202136.

★ ***December 9, 1992***
***London, UK***
Key Issues in Robust Analytical Measurements. *Contact:* Analytical Division, The Royal Society of Chemistry, Burlington House, Piccadilly, London W1V 0BN, UK. Tel.: +44 71-437 8656.

★ ***December 14–16, 1992***
***Budapest, Hungary***
Budapest Chromatography Conference. *Contact:* Intercongress Ltd., Ildikó Benyhe, Dózsa György ut 84/a, H-1068 Budapest, Hungary. Tel.: +36 1-1222203; Fax: +36 1-1424118; Telex: 223955.

★ ***December 15–18, 1992***
***Loughborough, UK***
Statistics for Analytical Chemistry. Short Course. *Contact:* Mrs. S. Maddison, Department of Chemistry, Loughborough University of Technology, Loughborough, Leics. LE11 3TU, UK. Tel.: +44 509-222575; Fax: +44 509-233163.

★ ***January 3–6, 1993***
***Marathon, FL, USA***
WCFIA 93. Winter Conference on Flow Injection Analysis. *Contact:* WCFIA '93, c/o Gary D. Christian, Department of Chemistry BG-10, University of Washington, Seattle, WA 98195, USA. *(See "Announcements" for further details).*

***January 10–15, 1993***
***Granada, Spain***
1993 European Winter Conference on Plasma Spectrochemistry. *Contact:* Prof. Alfredo Sanz Medel (Chairman), Department of Physical and Analytical Chemistry, Faculty of Chemistry, University of Oviedo, C. Julian Claveria s/n, 33006 Oviedo, Spain. Tel. +34 85-103480 or 103474; Fax +34 85-237850. *(Further details published in Vol. 264, No. 2).*

***January 25-28, 1993***
***Orlando, FL, USA***
HPCE '93. Fifth International Symposium on High Performance Capillary Electrophoresis. *Contact:* Shirley E. Schlessinger, Symposium Manager, HPCE '93, Suite 1015, 400 East Randolph Drive, Chicago, IL 60601, USA. Tel.: 312 527-2011. *(Further details published in Vol. 260, No. 1).*

★ ***January 26–27, 1993***
***Houston, TX, USA***
7th International Forum on Process Analytical Chemistry: Analytical Techniques for Process Quality and Control. *Contact:* InfoScience Services Inc., Conference Division, Suite 313, 3000 Dundee Road, Northbrook, IL 60065, USA. Tel. 708 291-9161; Fax: 708 291-0097.

★ ***January 26–27, 1993***
***Houston, TX, USA***
Envirolab: The Analytical Environment. *Contact:* InfoScience Services Inc., Conference Division, Suite 313, 3000 Dundee Road, Northbrook, IL 60065, USA. Tel. 708 291-9161; Fax: 708 291-0097.

***February 9–10, 1993***
***Tokyo, Japan***
CHEMSPEC ASIA 93. Exhibition. *Contact:* Jane Malcolm-Coe, PR & Publicity Manager, FMJ International Publications Ltd., Queensway House, 2 Queensway, Redhill, Surrey RH1 1QS, UK. Tel.: +44 737-768611. Fax: +44 737-761685.

***March 8-12, 1993***
***Atlanta, GA, USA***
PITTCON '93. 44th Pittsburgh Conference and Exposition on Analytical Chemistry and Applied Spectroscopy. *Contact:* Linda S. Briggs, Pittsburgh Conference, 300 Penn Center Blvd., #332, Pittsburgh, PA 15235, USA. Tel. 412 825-3220; Fax: 412 825-3224. *(See "Announcements" for further details).*

★ ***March 19, 1993***
***Antwerp, Belgium***
Symposium on Possibilities and Limitations of Chiral Separation Techniques. *Contact:* Royal Flemish Chemical Society (KVCV), Working Part on Chromatography, c/o Dr. R. Smits, BASF Antwerpen N.V., Central Laboratory, Scheldelaan, B-2040 Antwerp, Belgium. Tel.: +32 3 568 2831; Fax: +32 3 568 3250; Telex: 31047 basant b.

★ ***April 4–7, 1993***
***Clwydd, Wales, UK***
Ion Exchange Processes. *Contact:* Haydn Hughes, Faculty of Science, The North East Wales Institute, Connah's Quay, Clwydd CH5 4BR, Wales, UK.

★ ***April 20–21, 1993***
***Pontypridd, Wales, UK***
The Interpretation of Vibrational Spectra. The Infrared and Raman Discussion Group and the University of Glamorgan Residential School. *Contact:* Mrs. Stephanie Williams, Faculty of Science and Engineering, University of Glamorgan, Pontypridd, Mid Glamorgan CF37 1DL, Wales, UK.

★ ***April 20–23, 1993***
***Brussels, Belgium***
5th European Congress on Biopharmaceutics and Pharmacokinetics. *Contact:* Mrs. F. Rey, 3/17 Avenue de l'Observatoire B-1180 Brussels, Belgium. Tel.: +32 2 375 1648; Fax: +32 2 375 3299.

★ ***May 3–5, 1993***
***Szombathely, Hungary***
5th Symposium on the Analysis of Steroids. *Contact:* Prof. S. Görög, c/o Chemical Works of Gedeon Richter Ltd., P.O. Box 27, H-1475 Budapest, Hungary. Tel.: +36 1-1574 566; Fax: +36 1-1571 578; Telex: 22-5067 richt h. *(See "Announcements" for further details).*

***May 9-14, 1993***
***Hamburg, Germany***
HPLC '93. 17th International Symposium on Column Liquid Chromatography. *Contact:* Gesellschaft Deutscher Chemiker, Abteilung Tagungen, Varrentrappstr. 40–42, D-6000 Frankfurt am Main 90, Germany. Tel.: +49 69-7917-360; Fax: +49 69-7917-475.

★ ***May 12–14, 1993***
***Paris, France***
Spectral Analysis of Complex Structures. *Contact:* Uppsala University, School of Engineering, P.O. Box 534, S-75121 Uppsala, Sweden.

***May 25–27, 1993***
***Ghent, Belgium***
Vth International Symposium on Quantitative Luminescence Spectrometry in Biomedical Sciences. *Contact:* Dr. Willy R.G. Baeyens, Symposium Chairman, University of Ghent, Pharmaceutical Institute, Harelbekestraat 72, 9000 Ghent, Belgium.

★ ***June 2–4, 1993***
***Stockholm, Sweden***
Symposium on Analysis of Peptides. *Contact:* Swedish Academy of Pharmaceutical Sciences, P.O.Box 1136, S-111 81 Stockholm, Sweden. Tel.: +46 8 245085; Fax: +46 8 205511.

★ ***June 3–4, 1993***
***Brno, Czechoslovakia***
European Conference on Analytical Chemistry and Pharmaceuticals, Chromatography and Spectroscopy, and Thermal Analysis. *Contact:* Dr. V.M. Bhatnagar, Alena Chemicals of Canada, P.O. Box 1779, Cornwall, Ont., Canada K6H 5V7. Tel.: 613 932-7702.

★ ***June 7–9, 1993***
***Lyon, France***
European Seminar on InfraRed Spectroscopy. *Contact:* G. Lachenal, Université Lyon I, Laboratoire des Matériaux Plastiques et des Biomatériaux, 69622 Villeurbanne Cédex, France. Fax: +33 78 89 25 83. *(See "Announcements" for further details).*

★ ***June 8–11, 1993***
***Egham, UK***
Seventh International LIMS Conference. *Contact:* John Boother, Programme Chairman, JB Scientific, P.O. Box 5, Riseley, Reading RG7 1YL, UK. Tel.: +44 734 883125; Fax: +44 734 885604.

★ ***June 9–12, 1993***
***Dortmund, Germany***
22nd International Roland W. Frei Memorial Symposium on Environmental Analytical Chemistry. *Contact:* Mrs. M. Frei-Hausler, P.O. Box 46, CH-4123 Allschwil 2, Switzerland. Fax: +41 61-4820805.

***June 13-17, 1993***
***Århus, Denmark***
3rd Scandinavian Symposium on Chemometrics. *Contact:* SSC3 Secretariat, Department of Chemical Technology, Danish Technological Institute, Teknologiparken, DK-8000 Århus C, Denmark. Tel.: +45 86-142400; Fax: +45 86-147445.

★ ***June 14–16, 1993***
***Arlington, VA, USA***
PREP-93, 10th International Symposium on Preparative Chromatography. *Contact:* Barr Enterprises, P.O. Box 279, Walkersville, MD 21793, USA. Tel.: 301 898-3772; Fax: 301 898-5596. *(See "Announcements" for further details).*

***June 23–24, 1993***
***Basle, Switzerland***
CHEMSPEC EUROPE 93. *Contact:* Jane Malcolm-Coe, PR & Publicity Manager, FMJ International Publications Ltd., Queensway House, 2 Queensway, Redhill, Surrey RH1 1QS, UK. Tel.: +44 737-768611. Fax: +44 737-761685.

★ ***June 27–30, 1993***
***Santa Barbara, CA, USA***
Fullerenes '93. The First International Interdisciplinary Colloquium on the Science and Technology of the Fullerenes. *Contact:* In North America: Kim Cavallero, Pergamon Seminars, 660 White Plains Road, Tarrytown, NY 10591-5153, USA. Tel.: 914 333-2550; Fax: 914 333-2468. All other countries: Gill Spear, Pergamon Seminars, c/o Elsevier Advanced Technology, Mayfield House, 256 Banbury Road, Oxford OX2 7DH, UK. Tel.: +44 865 512242; Fax: +44 865 310981.

***June 29-July 4, 1993***
***York, UK.***
XXVIII Colloquium Spectroscopicum Internationale. *Contact:* Department of Chemistry (CSI Secretariat), Loughborough University of Technology, Loughborough, Leics. LE11 3TU, UK.

***July 7–9, 1993***
***York, UK.***
Modern Ultraviolet Spectrometry. *Contact:* Dr. Tom Frost, Wellcome Founda-

tions Ltd., Dartford Hill, Dartford DA1 5AH, UK. Tel: +44 322 223-488; Fax: +44 322 289-285.

★ ***July 19–21, 1993***
***Guildford, UK***
6th Symposium on Handling of Environmental and Biological Samples in Chromatography. *Contact:* Mrs. M. Frei-Häusler, IAEAC Secretariat, Postfach 46, CH-4123 Allschwil 2, Switzerland.

***August 9–11, 1993***
***Winnipeg, Canada***
3rd Soil and Sediment Residue Analysis Workshop. International Association of Environmental Analytical Chemistry. *Contact:* Dr. G.R. Barrie Webster, Pesticide Research Laboratory, Department of Soil Science, University of Manitoba, Winnipeg, MB, Canada R3T 2N2. Tel.: (204) 474-6039; Fax: (204) 272-6019. Prof. Dr. J. Tarradella, IGE-Ecole Polytechnique, Federale de Lausanne, 1015 Lausanne, Switzerland. Tel.: +41 21 6932712; Fax: +41 21 6932727.

***August 15–20, 1993***
***Beijing, China***
34th IUPAC Congress: Chemistry for the 21st Century. *Contact:* Prof. Xinqi Song, Secretary-General of 34th IUPAC Congress, c/o Chinese Chemical Society, P.O. Box 2709, Beijing 100080, China.

***August 23–27, 1993***
***Budapest, Hungary***
9th Danube Symposium on Chromatography. *Contact:* Prof. L. Szepesy, Symposium Secretariat, Department of Chemical Technology, Technical University of Budapest, Budafoki ut 8, H-1521 Budapest, Hungary. Tel. +36 1 186-9000; Fax +36 1 181-2755; Telex 225931 muegy h. *(Further details published in Vol. 264, No. 2).*

★ ***September 5–10, 1993***
***Loutraki, Greece***
5th European Conference on the Spectroscopy of Biological Molecules. *Contact:* Professor Theo Theophanides, Chairman of ECSBM '93, Department of Chemical Engineering, National Technical University of Athens, Zografou Campus, Zografou 15780, Athens, Greece. Tel.: +30 1-7792438; Fax+ +30 1-7700989. *(See "Announcements" for further details).*

***September 5–11, 1993***
***Edinburgh, UK.***
Euroanalysis VIII. *Contact:* Miss P.E. Hutchinson, Analytical Division, The Royal Society of Chemistry, Burlington House, Piccadilly, London W1V 0BN, UK. Tel.: +44 71 437 8656; Fax: + 44 71 734 1227; Telex: 268001. *(Further details published in Vol. 252, No. 1–2).*

★ ***September 7–10, 1993***
***Verona and Soave, Italy***
Applications of HPLC and CE in the BioSciences (12th International Symposium on Biomedical Applications of Chromatography and Electrophoresis and 2nd International Symposium on the Applications of HPLC in Enzyme Chemistry). *Contact:* Dr. F. Tagliaro, Scientific Secretariat, c/o Istituto di Medicina Legale, Policlinico Borgo Roma, I-37134 Verona, Italy. *(See "Announcements" for further details).*

***September 8–10, 1993***
***Prague, Czechoslovakia***
International Association of Environmental Analytical Chemistry 4th Workshop on Chemistry and Fate of Modern Pesticides and Related Pollutants. *Contact:* Dr. J. Hajslova, Institute of Chemical Technology, Department of Food Chemistry and Analysis, Suchbatarova 5, 16628 Prague 6-Dejvice, Czechoslovakia. Fax: +42 23-114769.

★ ***November 1–4, 1993***
***Oslo, Norway***
LAB '93, Laboratory Exhibition. *Contact:* Norges Varemesse, P.O. Box 130, Skoyen, 0212 Oslo 2, Norway. Tel.: +47 2-43 90100; Fax: +47 2-43 1914.

★ ***February 22–25, 1994***
***Antwerp, Belgium***
HTC 3. Third International Symposium on Hyphenated Techniques in Chromatography. *Contact:* Royal Flemish Chemical Society (KVCV), Working Part on Chromatography, c/o Dr. R. Smits, BASF Anstwerpen N.V., Central Laboratory, Scheldelaan, B-2040 Antwerp, Belgium. Tel.: +32 3 568 2831; Fax: +32 3 568 3250; Telex: 31047 basant b. *(See "Announcements" for further details).*

★ ***February 28–March 4, 1994***
***Chicago, IL, USA***
PITTCON '94. Pittsburgh Conference on Analytical Chemistry and Applied Spectroscopy. *Contact:* Pittsburgh Conference, Suite 332, 300 Penn Center Blvd., Pittsburgh, PA 15235-9962, USA.

★ ***April 19–22, 1994***
***Munich, Germany***
ANALYTICA 94. 14th International Trade Fair for Biochemical and Instrumental Analysis with International Conference. *Contact:* Bernhard Schauder, ANALYTICA Press Office, Münchener Messe- und Ausstellungs-Gesellschaft mbh, Messegelände, Postfach 12 10 09, D-8000 Munich 12, Germany. Tel.: +49 89-51070; Fax: +49 89-5107506; Telex: 5212086 ameg d.

***May 8–13, 1994***
***Minneapolis, MN, USA***
HPLC '94. 18th International Symposium on High Performance Liquid Chromatography. *Contact:* Janet E. Cunningham, Barr Enterprises, P.O. Box 279, Walkersville, MD 21793, USA. Tel.: (301) 898-3772; Fax: (301) 898-5596.

★ ***June 19–24, 1994***
***Bournemouth, UK***
20th International Symposium on Chromatography. *Contact:* The Executive Secretary, Chromatographic Society, Suite 4, Clarendon Chambers, 32 Clarendon Street, Nottingham NG1 5JD, UK. Tel.: +44 603-500596; Fax: +44 602-500614.

★ ***September 21–23, 1994***
***Stockholm, Sweden***
5th International Symposium on Pharmaceutical and Biomedical Analysis- *Contact:* Swedish Academy of Pharmaceutical Sciences, P.O.Box 1136, S-111 81 Stockholm, Sweden. Tel.: +46 8 245085; Fax: +46 8 205511.

★ ***March 6–10, 1995***
PITTCON '95. Pittsburgh Conference on Analytical Chemistry and Applied Spectroscopy. *Contact:* Pittsburgh Conference, Suite 332, 300 Penn Center Blvd., Pittsburgh, PA 15235-9962, USA.

**PUBLICATION SCHEDULE FOR 1993**

| | S'92 | O'92 | N'92 | D'92 | J | F |
|---|---|---|---|---|---|---|
| Analytica Chimica Acta | 267/1<br>267/2 | 268/1<br>268/2 | 269/1<br>269/2 | 270/1<br>270/2 | 271/1<br>271/2 | 272/1<br>272/2 |
| Vibrational Spectroscopy | | 4/1 | | | | 4/2 |

# INFORMATION FOR AUTHORS

**Manuscripts**. The language of the journal is English. English linguistic improvement is provided as part of the normal editorial processing. Authors should submit three copies of the manuscript in clear double-spaced typing on one side of the paper only. *Vibrational Spectroscopy* also accepts papers in English only.

**Abstract**. All papers and reviews begin with an Abstract (50–250 words) which should comprise a factual account of the contents of the paper, with emphasis on new information.

**Figures**. Figures should be prepared in black waterproof drawing ink on drawing or tracing paper of the same size as that on which the manuscript is typed. One original (or sharp glossy print) and two photostat (or other) copies are required. Attention should be given to line thickness, lettering (which should be kept to a minimum) and spacing on axes of graphs, to ensure suitability for reduction in size on printing. Axes of a graph should be clearly labelled, along the axes, outside the graph itself. All figures should be numbered with Arabic numerals, and require descriptive legends which should be typed on a separate sheet of paper. Simple straight-line graphs are not acceptable, because they can readily be described in the text by means of an equation or a sentence. Claims of linearity should be supported by regression data that include slope, intercept, standard deviations of the slope and intercept, standard error and the number of data points; correlation coefficients are optional.

Photographs should be glossy prints and be as rich in contrast as possible; colour photographs cannot be accepted. Line diagrams are generally preferred to photographs of equipment.

Computer outputs for reproduction as figures must be good quality on blank paper, and should preferably be submitted as glossy prints.

**Nomenclature, abbreviations and symbols**. In general, the recommendations of the International Union of Pure and Applied Chemistry (IUPAC) should be followed, and attention should be given to the recommendations of the Analytical Chemistry Division in the journal *Pure and Applied Chemistry* (see also *IUPAC Compendium of Analytical Nomenclature, Definitive Rules*, 1987).

**References**. The references should be collected at the end of the paper, numbered in the order of their appearance in the text (*not* alphabetically) and typed on a separate sheet.

**Reprints**. Fifty reprints will be supplied free of charge. Additional reprints (minimum 100) can be ordered. An order form containing price quotations will be sent to the authors together with the proofs of their article.

**Papers dealing with vibrational spectroscopy** should be sent to: Dr J.G. Grasselli, 150 Greentree Road, Chagrin Falls, OH 44022, U.S.A. Telefax: (+1-216) 2473360 (Americas, Canada, Australia and New Zealand) or Dr J.H. van der Maas, Department of Analytical Molecule Spectrometry, Faculty of Chemistry, University of Utrecht, P.O. Box 80083, 3508 TB Utrecht, The Netherlands. Telefax: (+31-30) 518219 (all other countries).

---



0003-2670/92/$05.00



This issue is printed on acid-free paper.

PRINTED IN THE NETHERLANDS

Data Handling in Science and Technology Volume 8

# Design and Optimization in Organic Synthesis

by **R. Carlson**, Department of Organic Chemistry, Umeå University, Umeå, Sweden

This is the first general textbook on experimental design and optimization in organic synthesis. The book presents a unified methodology for carrying out systematic studies when the objective is to develop efficient and optimum synthetic methods. Strategies are included both for exploring the experimental conditions and for systematic studies of entire reaction systems (substrates, reagent(s) and solvents). The methodology is based on multivariate statistical techniques.

The following topics are treated in depth: classical two-level designs for screening experiments, gradient methods (steepest ascent, simplex methods) as well as response surface techniques for optimization, principal components analysis and PLS modelling.

The book is intended as a hands-on text for chemists and engineers engaged in developing synthetic methods in industrial research, e.g. in fine chemicals and pharmaceuticals production, as well as for advanced undergraduate students, graduate students, and researchers in an academic environment.

***Contents:***



**1992 xvi + 536 pages**

**Price: US $ 169.00 / Dfl. 330.00**

**ISBN 0-444-89201-X**

**Elsevier Science Publishers**

P.O. Box 211, 1000 AE Amsterdam, The Netherlands
P.O. Box 882, Madison Square Station, New York, NY 10159, USA